UNIVERSITY OF SOUTHAMPTON

THE TRANSCRIPTIONAL REGULATION OF THE TISSUE INHIBITOR OF METALLOPROTEINASES-1 (TIMP-1) GENE IN HEPATIC STELLATE CELLS

David Edward Smart

Doctor of Philosophy

FACULTY OF MEDICINE, HEALTH AND BIOLOGICAL SCIENCES

SCHOOL OF MEDICINE

DIVISION OF INFECTION INFLAMMATION AND REPAIR

Submitted October 2001

UNIVERSITY OF SOUTHAMPTON

ABSTRACT

FACULTY OF MEDICINE, HEALTH AND BIOLOGICAL SCIENCES
SCHOOL OF MEDICINE
DIVISION OF INFLAMMATION, INFECTION AND REPAIR

Doctor of Philosophy

THE TRANSCRIPTIONAL REGULATION OF TISSUE INHIBITOR OF METALLOPROTEINASE (TIMP-1) GENE IN HEPATIC STELLATE CELLS

By David E. Smart

The tissue inhibitor of metalloproteinase (TIMP-1) has previously been shown to be a significant pro-fibrotic mediator and is significantly increased in liver fibrosis. This increase in TIMP-1 expression leads to a shift in extracellular remodelling through a reduction in matrix degradation. Previous work has identified the activated hepatic stellate cells (HSC) as the primary source of the TIMP-1 in liver fibrosis and has also established that its increased expression is mediated at the transcriptional level.

This work has shown *in vitro* that the AP-1 site at the 5' end of the TIMP-1 minimal promoter is crucial for transcriptional activity in the HSC. Furthermore this study has established that the Jun D homodimer is the main positive regulator of AP-1 mediated TIMP-1 gene transcription. The other endogenous AP-1 proteins, Fos B and Fra 2, were shown to function as negative regulators through their formation of inhibitory heterodimers. In contrast, investigations of the IL-6 promoter indicated that it was differentially regulated from TIMP-1, although both promoters are up regulated in the activated HSC and dependent on Jun D for transcription. The IL-6 promoter activity however, was shown to be dependent on the binding of a Jun D containing dimer but not a homodimer and it was suggested that the positive transcriptional effects were mediated via another as yet undetermined site. Work in NIH3T3 fibroblasts confirmed the classical c-Jun/c-Fos regulation of TIMP-1 transcription in the fibroblast line, suggesting the Jun D mediated mechanism of TIMP-1 regulation may be HSC specific.

Investigations *in vivo* also confirmed the results of the *in vitro* studies, indicating that HSC activation was accompanied by an increase in Jun D expression and a change in its molecular weight. The change in Jun D size may further regulate gene expression, as the short form of Jun D is believed to be inactive, possessing no transactivation domain.

Through the use of a mouse model it was possible to demonstrate that Jun $D^{-/-}$ knockout mice developed significantly less fibrosis than the wild type controls following an 8week CCl_4 liver injury. Using Taqman quantitative RT PCR it was possible to demonstrate a biological mechanism for the reduced fibrosis seen in the Jun $D^{-/-}$ knockouts, as their livers contained significantly less TIMP-1 and pro-collagen 1 mRNA than the controls.

Other investigations identified that both the SP-1 and LBP-1 sites in the TIMP-1 promoter were crucial for high level transcription. Protein and supershift analysis suggested that the SP-1 binding complexes differ between the HSC and fibroblasts, implicating the interactions of SP-1 & SP-4 and SP-1 & SP-3 respectively. A single strand binding complex was also identified, binding to the first LBP-1 site of the TIMP-1 promoter, however the content and function of this complex is at present unknown.

Contents

List of Tables and Illustrations

Acknowledgments

I would like to acknowledge the following people for helping me to complete my PhD thesis:

Firstly my family, brother Mathew, sister Sarah and parents Chris and Lesley who have known me the longest and had to put up with me the most. Putting up with me will be a continuing theme throughout these acknowledgments. My father helped in particular by answering my many childhood questions concerning science and technology and when I just wanted to know what would happen if? I also have to thank my mother for her continued support, encouragement and understanding even after the infamous kitchen explosion.

I would also like to thank my fiancée Sally who has checked my spelling and grammar, reading the entire thesis more than once. Sally was also in charge of support and motivation during the write up of my PhD and hopefully she will continue to do so, especially now that I will never again make her read this thesis. Oh yes and I promise to return the favour in your chosen career of teaching.

My final thanks go to Dr Derek Mann, my supervisor as a PhD student. Derek, although a bit of a lad, got the supervision balance just about right. I would also like to thank all my other work colleagues and friends, of which there are too many to mention due to the length of time this book has taken me to write.

Dedication

I would finally like to dedicate this thesis to the memory of my Grandfather, Leslie Dodridge, who died during the three years of laboratory work that went into its production. Leslie was generous, helping others to the point where his long-term project remained unfinished. Hopefully the finishing of this project will go some way towards making up for my part in preventing him from finishing his own.

List of Abbreviations and Units

AEBSF	4-(2-Aminoethyl)benzenesulfonyl fluoride
AMP	Adenosine monophosphate
AP-1	Activator protein–1
APS	Ammonium persulfate
ARE	AU-rich element
ATF	Activating transcription factor
ATP	Adenosine triphosphate
bp	Base pairs
BSA	Bovine serum albumin
CAT	Chloramphenicol acetyl transferase
C/EBP	CCAAT enhancer binding protein
CINC	Cytokine induced neutrophil chemoattractant
CMV	Cytomegalovirus
CRE	Cyclic AMP response element
CREB	CRE-Binding protein
CREM	CRE-Modulating protein
CSF	Colony stimulating factor
CTD	Carboxy-terminal domain
DiDc	Poly-deoxyinosinic-deoxycytidylic acid
Dig A	Dignam buffer A (Dignam *et al.*, 1983)
Dig C	Dignam buffer C (Dignam *et al.*, 1983)
DNA	Deoxyribose nucleic acid
DMEM	Dulbecco modified eagle medium
DMSO	Dimethyl sulfoxide
DTT	Dithiothreitol
E-coli	*Escherichia coli*
ECM	Extracellular matrix
EDTA	Ethylenediaminetetraacetic acid
ELISA	Enzyme-linked immunosorbent assay
EMSA	Electrophoretic Mobility Shift Assay
ERK	Extracellular signal related kinase
ETS	Transcription Factor, origin avian E26 erythroblastoma virus (v-ETS, E Twenty-six specific)
FGF	Fibroblast growth factor
FOS	Transcription factor, origin Finkel, Biskis, Jenkins\Reilly murine Osteosarcoma virus
FRA	Fos related antigen
FRK	Fos regulating kinase
GAPDH	Glyceraldehyde-3-phosphate dehydrogenase
GFAP	Glial fibrillary acidic protein
HBS	Hepes buffer saline
HBSS	Hank's buffered saline solution
HBV	Hepatitis B virus
HCV	Hepatitis C virus
HDV	Hepatitis D virus
HGF	Hepatocyte growth factor
HIV	Human immunodeficiency virus
HMC	High mobility complex
HNE	4-hydroxy-2,3-nonenal
HRP	Horseradish peroxidase
HSC	Hepatic stellate cell
ICAM-1	Intracellular adhesion molecule-1
IL-6	Interleukin-6
JAB1	JUN activation domain binding protein 1

JNK	JUN N terminal kinase
JUN	Transcription factor, origin avian sarcoma virus 17 (v-Jun, Ju-nana, Japanese for 17)
Lac Z	β-Galactosidase
LB	Luria Broth, microbial growth medium
LBP-1	Leader binding protein-1
LMC	Low mobility complex
LSF	Late SV40 transcription factor
M6P/IGFIIR	Mannose 6-phosphate/ insulin like growth factor II receptor
MAPK	Mitogen activated protein kinase
MCP-1	Monocyte chemotactic protein-1
MMP	Matrix metalloproteinase
MT-MMP	Membrane type matrix metalloproteinase
mRNA	Messenger ribonucleic acid
MYB	Transcription factor, origin Myeloblastoma (v-MYB avian E26 leukaemia virus)
NACS	Sodium ion exchange resin column (supplied by GIBCO BRL)
NAD^+	Nicotinamide adenine dinucleotide
NFκB	Nuclear factor κB
NGF	Nerve growth factor
OD	Optical density
OSM	Oncostatin M
PAGE	Poly-acrylamide gel electrophoresis
PAI-1	Plasminogen activator inhibitor-1
PBL	PBLCAT3
PBS	Phosphate Buffered Saline
PCR	Polymerase chain reaction
PDGF	Platelet derived growth factor
PEA3	Polyoma enhancer site 3
PEG	Poly-Ethylene glycol
REL	Transcription Factor, origin avian Reticuloendotheliosis virus strain T
RNA	Ribonucleic acid
RSV	Rat sarcoma virus
RT PCR	Reverse transcriptase polymerase chain reaction
SD	Standard deviation
SE	Standard Error
SDS	Sodium dodecyl sulphate
αSMA	α-Smooth muscle actin
SP-1	Specificity Protein-1, Classic Krüppel like transcription factor.
SRE	Serum response element
STAT	Signal transducer and activator of transcription
SV40	Simian papovavirus
TAE	Tris acetate EDTA
TAF	TBP associated factor
TAR	Trans-activation response region
TBE	Tris boric acid EDTA buffer
TBP	TATA binding protein
TBS	Tris buffered saline
TBS-T	Tris buffered saline-tween
TE	Tris EDTA buffer
TIMP	Tissue inhibitor of metalloproteinase
TLC	Thin layer chromatography
TGFβ	Transforming growth factor-β
TEMED	N,N,N',N'-Tetramethylethylenediamine
TNFα	Tumour necrosis factor-α
TPA	12-O-Tetradecanoylphorbol-13-acetate

tPA	Tissue plasminogen activator
TRE	TPA-response element
Tris	Tris(hydroxymethyl)aminomethane
Tween 20	Polyoxyethylenesorbitan monolaurate
UK	United kingdom
uPA	Urokinase plasminogen activator
UTE-1	Upstream TIMP-1 element-1
UTR	Un-translated region
UV	Ultra Violet
WT	Wild type
YY1	Ying yang-1

Units Used in this Thesis

p	10^{-12}
n	10^{-9}
μ	10^{-6}
m	10^{-3}
c	10^{-2}
k	10^{3}
A	Ampere
BP	Base pair
Bq	Becquerel
C	Centigrade
Ci	Curie
Da	Dalton
g	Gramme or Acceleration (centripetal acceleration) as a function of gravitational acceleration ($9.8ms^2$)
l	Litre
M	Molarity
m	Meter
mol	Mole
pH	$-Log_{10}[H^+]$
U	Standard unit of enzyme activity
V	Volt
v/v	Volume/Volume (ml/100ml)
w/v	Weight/Volume (g/100ml)

Chapter 1.

General Introduction

1.1 Cirrhosis: An Overview

Cirrhosis is a pathological condition resulting from the progression of liver fibrosis and as such presents a major health care problem. Cirrhosis is at present believed to be irreversible in all but a few cases. Although the rate of fibrosis progression varies from individual to individual the prognosis is approximately 50% survival at five years from diagnosis of cirrhosis (Kumer *et al.*, 1994). The condition results in a loss of liver cells and function followed by necrosis, with the inevitable chronic liver failure and death.

Cirrhosis results in both macroscopic and microscopic changes of liver morphology. Initially in the early stages of disease there is enlargement through hyperplasia and generalised fibrosis (see Figure 1.1.1). This liver enlargement is later reversed with the cellular necrosis and contraction of fibrous scar tissue. Hyperplasia of the surviving hepatocytes leads to regenerative nodules with destruction of normal liver architecture. The vasculature of the liver is disrupted as fibrous bands obstruct portal venous radicles (see Figure 1.1.1). This causes abnormal blood flow between portal veins and hepatic arterioles resulting in portal hypertension. Portal hypertension is responsible for many of the clinical manifestations of liver cirrhosis including varices and ascites (Chandrasoma *et al.*, 1995). Oesophageal varices are the most serious of the secondary complications of cirrhosis. These occur as aneurisms of the veins at the entrance to the stomach. Varices are prone to haemorrhage following mechanical damage from food. Damage to varices also commonly occurs as a result of both chemical damage and mechanical damage through vomiting. Haemorrhage of oesophageal varices can often result in catastrophic, fatal blood loss. As a result cirrhosis patients are regularly examined and treated for their presence. Ascites is an edema associated with the accumulation of fluid in the abdominal cavity. This build up of fluid is due both to the portal hypertension and also the reduction in liver function. The reduced liver function is manifested in ascites through a decreased production of serum proteins by the liver, reducing the osmotic potential of the blood. The loss of liver function also leads to increased bleeding tendency, loss of male secondary sexual characteristics, problems with the nervous system, and encephalopathy through the build up of toxic metabolites eventually leading to coma and death (Kumer *et al.*, 1994; Chandrasoma *et al.*, 1995; Bortolotti *et al.*, 1996).

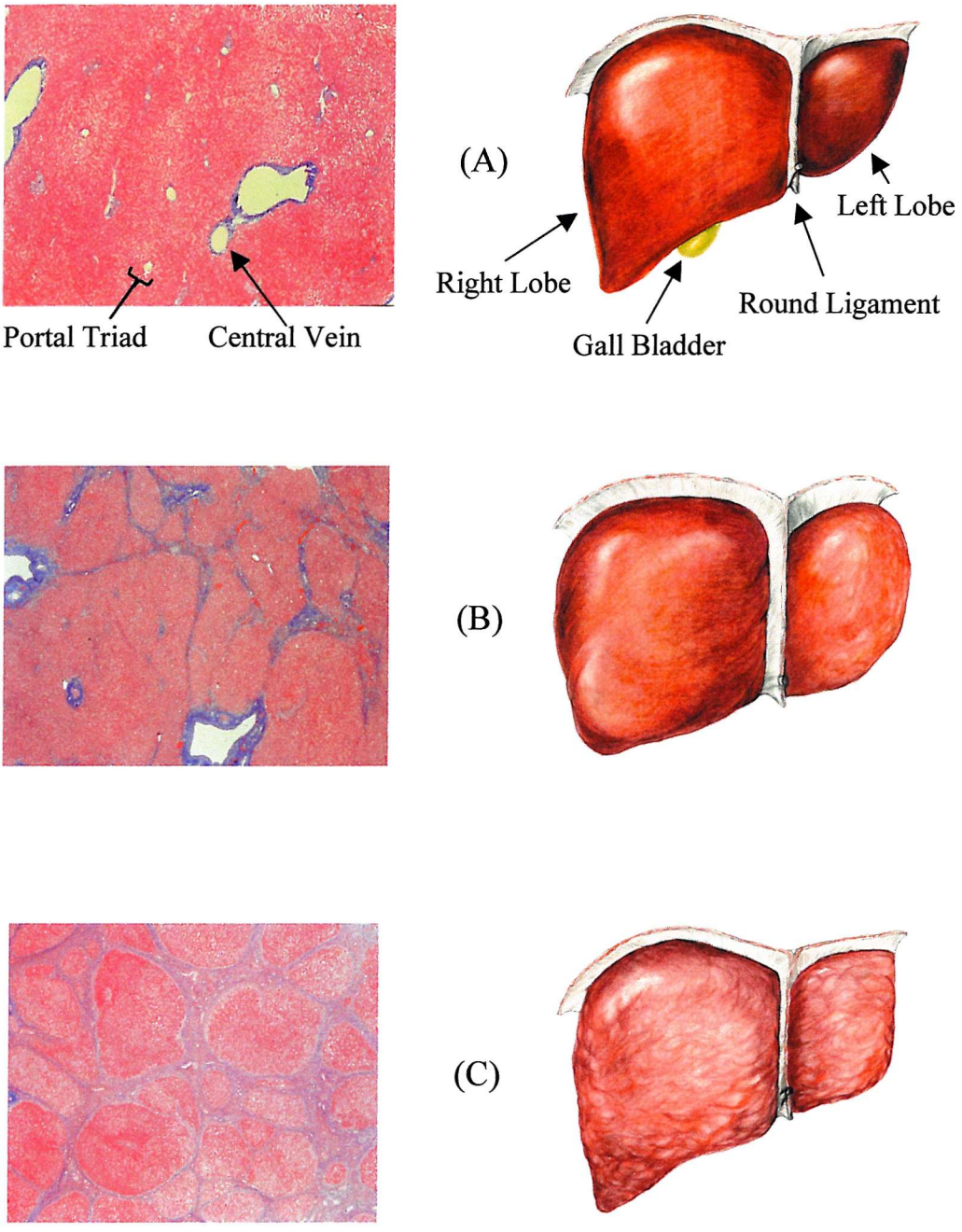

Figure 1.1.1. The progression of liver disease with chronic liver injury, at the microscopic and macroscopic level. The progression of liver disease is seen on the left microscopically, collagen appears blue. Diagrammatic macroscopic changes can be seen on the right. (A) Normal healthy liver. (B) Fibrotic liver. (C) Liver Cirrhosis. Pictures authorised by GlaxoWellcome.

1.2 The Causes of Liver Damage

Liver or hepatic fibrosis occurs in response to chronic injury. Liver insult may come in many forms including persistent viral and helminthic infections, bilary or hepatic obstruction, chemical, autoimmune and hereditary metal overload conditions. The causes of liver fibrosis vary world wide, reflecting both cultural and social differences (Chandrasoma *et al.*, 1995).

1.3 Viral Causes of Fibrosis

Fibrosis attributable to persistent viral infection is induced by the hepatitis viruses, in particular types B, C and D. Types A, E and G are not as yet a significant problem (Figure 1.3.1).

Hepatitis	
A	Fecal oral via contaminated food or water
B	Blood/body fluids and mother/child
C	Blood/body fluids and mother/child
D	Blood/body fluids and mother/child found in hepatitis B only
E	Fecal oral via contaminated water
G	Blood

Figure 1.3.1 Routes of Hepatitis virus transmission.

Hepatitis B virus (HBV) is a member of the hepadnavirus family and has a semi-double stranded DNA genome. Hepatitis B is at present the most common cause of fibrosis worldwide. The World Health Organisation estimates there to be approximately 350 million chronic HBV carriers (Purcell, 1993). Twenty five percent of chronic disease suffers are at risk of life threatening liver disease with its associated complications. In the UK the rate of infection with HBV is about 1 in 1000. There is an effective vaccine against the hepatitis B virus available, although it is only available to those in risk categories (Xu *et al.*, 1985).

The hepatitis C virus (HCV) is an enveloped virus, sharing similarities with the Flaviviruses, with a positive-strand RNA genome. Hepatitis C is rapidly taking over as the most common cause of fibrosis, especially in the developed world. It is estimated that world wide 3% of the population are infected, 200 million chronically (Mast *et al.*, 1999; Sarbah *et al.*, 2000). HCV infection occurs primarily as a result of blood to blood contact, sexual intercourse carries only a slight risk of HCV transmission (Fabris *et al.*, 1999). It is believed that between 60-90% of intravenous drug users in the United Kingdom (UK) are infected. There is however a large number of patients that have been infected as a result of transfusion with blood or blood products. In the UK screening was not performed for HCV until September 1991. Unlike HBV, hepatitis C has no available vaccine making the protection of risk groups impossible. The true scale of the HCV as a cause of cirrhosis is only beginning to come to light as chronic hepatitis C may take a number of decades to result in cirrhosis.

1.4 Chemically Induced Fibrosis

Chemically induced fibrosis is at present the primary cause of liver disease in the developed world. The chemical induction of fibrosis represents a major cultural difference between developed and developing worlds, as a major cause in the West is chronic alcoholism.

Alcoholism is believed to lead to liver damage at the site of its metabolism to Acetaldehyde or Ethanal. The metabolism of Ethanol is performed by the Nicotinamide Adenine Dinucleotide (NAD^+) dependent enzyme, Alcohol dehydrogenase. Due to its toxicity Ethanal has to be further metabolised. Metabolism of the toxic Ethanal is performed by the enzyme aldehyde dehydrogenase, which converts it to Ethanoic Acid (Acetic Acid or Acetate). This conversion is also dependent on NAD^+. The consumption of large quantities of alcohol leads to a temporary localized reduction of NAD^+ in the liver and thus leads to an accumulation of Ethanal. It is believed that it is the accumulation of Ethanal in the liver that leads to injury. The accumulation of Ethanal leads to lipid peroxidation and, through P450s, the production of protein aldehyde adducts. Antibodies to these adducts have also been identified in alcoholics with

cirrhosis, suggesting an autoimmune component of alcoholic liver disease (Niemela *et al.*, 2000; Rolla *et al.*, 2000). More recently identified, as another effect of alcohol in liver disease, is the increase in intestinal permeability. The increase in intestinal permeability allows endotoxin to enter the blood stream stimulating the liver Kupffer cells (liver macrophages) and exacerbating disease (Bautista, 2000; Mathurin *et al.*, 2000; Parlesak *et al.*, 2000; Thurman *et al.*, 2000). The role of alcohol in fibrosis is also important as it has been shown to significantly worsen the prognosis for HCV. The combination of alcohol and HCV causes both an increase in the rate of collagen deposition and hepatocyte necrosis (Degos, 1999, Tamai *et al.*, 2000). The combination of alcohol and paracetamol has been shown to result in multiplicative effects leading to observable histological damage with sub toxic doses of each component (Prescott, 2000).

Another significant cause of chemically induced injury is iron, commonly as a result of iron overload. Iron overload can result from an increased intake of iron, for example from excessive use of iron containing drugs and the use of iron cooking utensils. Alcoholic cirrhosis is often associated with iron overload due to both increased intake and absorption. Other chemical inducers of liver disease include high doses of salicylates, cytotoxic anticancer drugs, carbon tetrachloride, chloroform, halothane and isoniazid (Chandrasoma *et al.*, 1995).

1.5 Hereditary Conditions Leading to Fibrosis

Hereditary diseases also represent a significant number of the cases of liver fibrosis worldwide. These include Wilson's disease, hemochromatosis, α_1 Antitrypsin and chronic hemolytic anemias (Chandrasoma *et al.*, 1995).

Wilson's disease is a recessive autosomal disorder. It results from the normal absorption of copper but with an inability of the body to excrete excess copper in the bile leading to a toxic accumulation in the cytoplasm of the hepatocytes (Chandrasoma *et al.*, 1995; Schaefer *et al.*, 1999). Wilson's disease results in a progressive microvacuolar accumulation of lipid and focal necrosis. The disease usually presents in late childhood as a viral-like hepatitis. This hepatitis progresses without liver transplantation to fibrosis

and then cirrhosis. Wilson's disease also leads to deposition of copper throughout the body in connective tissue and the brain. Deposition of copper in the brain leads to a slow degeneration.

Primary or familial hemochromatosis is believed to be due to an increased absorption of iron resulting in elevated levels of serum iron. There is an accumulation of the excess iron in hepatocytes. This disease is an autosomal recessive disorder, in 90% of cases caused by the inheritance of two copies of a mutated gene located on chromosome 6 linked to HLA-A3. The exact cause is not known but it is believed to result in increased intestinal absorption. The increased iron saturates the capacity for protein iron storage in the form of transferrin and hemosiderin. Typically onset is at 30-40 years of age once iron-binding protein is saturated. The pathology of hemochromatosis is believed to result from the concurrent reduction of the free ferric iron, production of oxygen free radicles and subsequent production of lipid peroxides (Houglum *et al.*, 1994).

Secondary hemochromatosis is the name given to any condition that results in iron overload, as previously described, such as increased consumption or absorbance. Hereditary chronic hemolytic anemias such as β-thalassemia can also be included in the classification of secondary hemochromatosis. Hemolytic anemias result in iron overload due to the requirement for repeated blood transfusion, leading to disease through increased intake (Chandrasoma *et al.*, 1995).

There are differences in tissue morphology relating to the method of injury such as the brown hemosiderin deposits that occur in hemochromatosis, but the overall response remains the same.

1.6 The Changes in Fibrosis

Liver fibrosis is characterised by the production of a hepatic scar representing an increase in the extracellular matrix (ECM). The formation of the hepatic scar is a normal part of the healing process of the liver, however in fibrosis this system itself becomes pathological. With the development of cirrhosis the pathological scarring of the liver is

believed to be self-sustaining (Bachem *et al.*, 1992; Friedman, 1993). The scar tissue represents an increase in the deposition of fibrillary collagens concurrent with a change in the distribution and composition of the ECM. The fibrosis is characterised by an increase in collagens Type I and III as well as ECM glycoconjugates, including proteoglycans, fibronectin, and hyaluronic acid (Rojkind *et al.*, 1979; Gressner *et al.*, 1990; Friedman, 1993).

There is not only a change in the composition of the ECM in the liver but also it's distribution. In order to understand how the deposition of collagen changes in the liver it is necessary to understand the morphology of the liver. The liver is constructed in horizontal cross section (see Figure 1.6.1.A) as a number of portal triads positioned radially around the central vein. The portal triads of the liver are made up from three vessels; the terminal branchs of the hepatic artery, portal vein and the bile duct (see Figure 1.6.1.B). The terminal branches of the hepatic artery and portal vein are linked to the central vein by the hepatic sinusoidal channels. The hepatic sinusoid or sinusoidal channels are the series of capillaries radiating from the central vein (see Figure 1.6.1 A and B). Each sinusoid is surrounded by the space of Dissé, which is an ECM filled gap that separates the hepatocytes from the endothelial cells that line the sinusoidal channel (see Figure 1.6.2.). The space of Dissé is believed to be necessary for the efficient movement of metabolites to and from the hepatocytes and blood.

The changes to collagen deposition in fibrosis are initially concentrated in the subendothelial space of Dissé, forming bands of fibrosis (Minto *et al.*, 1983; Bissell *et al.*, 1987; Mak *et al.*, 1988). This subendothelial deposition of ECM is often referred to as "capillarization" (Schaffner *et al.*, 1963). In fibrosis the space of Dissé is transformed from a non-fibril forming basement-membrane-like ECM, containing collagen type IV, laminin and proteoglycans, to the fibril-forming collagens I, III. There is also an increase fibronectin (Martinez-Hernandez *et al.*, 1985; Schuppan *et al.*, 1993; Levavasseur *et al.*, 1995). The accumulation of ECM in the hepatic sinusoid is characteristic of liver fibrosis (see Figure 1.6.3). Although initially confined to the hepatic sinusoid the ECM accumulation spreads throughout the liver.

(A)

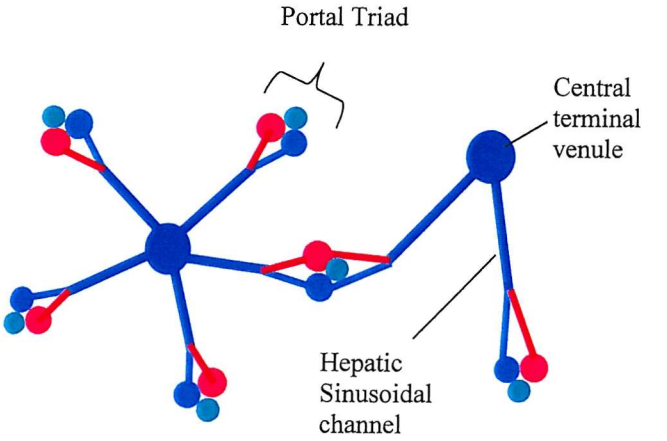

(B)

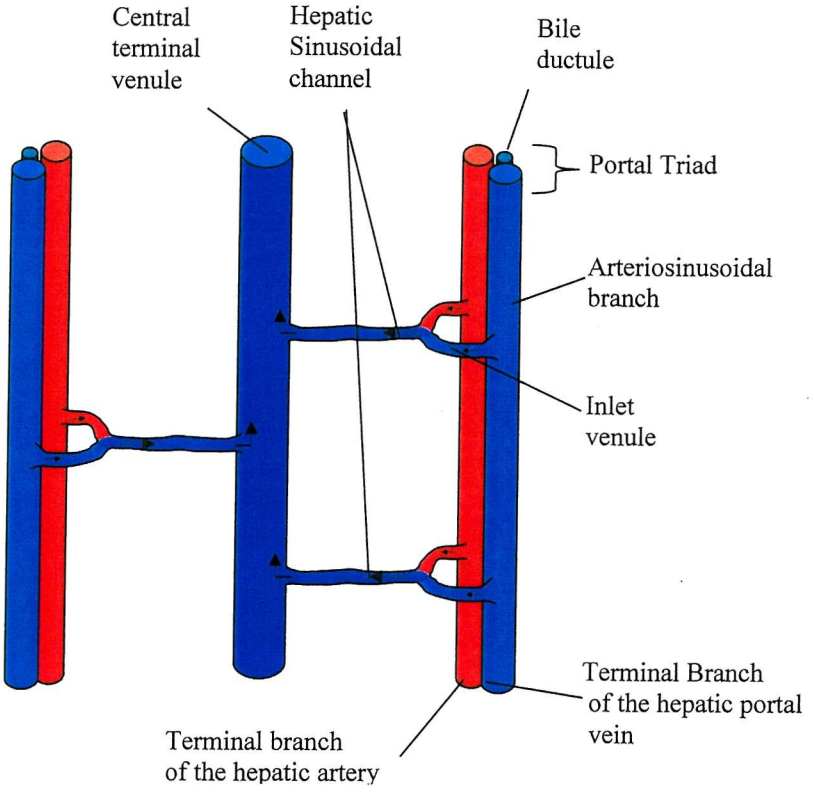

Figure 1.6.1 The hepatic microcirculation A) horizontal B) vertical section

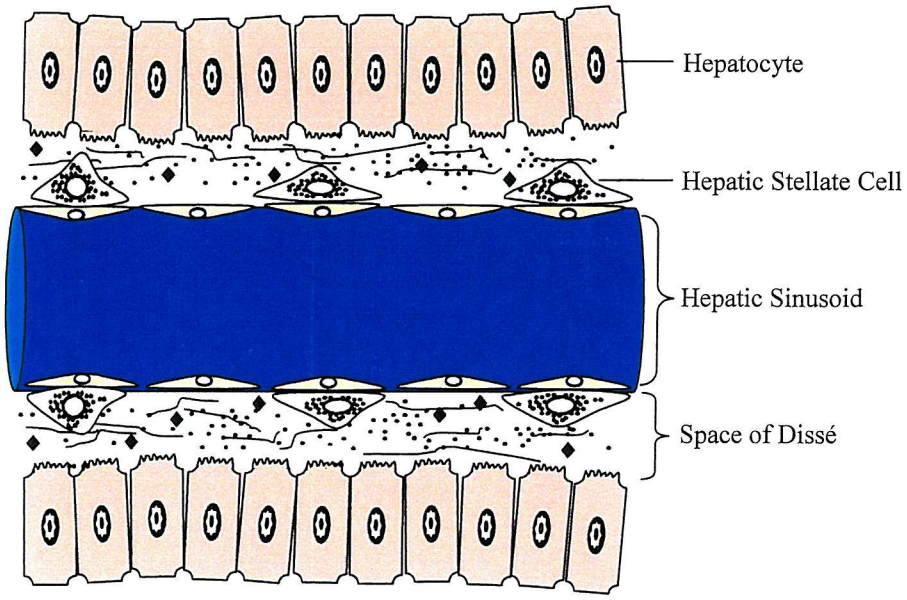

Figure 1.6.2. Microscopic architecture of the liver.

The function of the liver is not only affected by the gross deposition of collagen but also by some of the more slight modifications of ECM composition. Many of the cells of the hepatic sinusoid are adherent, responding to changes in basement type membrane. Such changes are believed to affect the function of the hepatocytes, hepatic stellate cell (HSC) and endothelial cells. Basement type membrane (collagen IV, laminin and proteoglycans) is believed to maintain the differentiated functional hepatocyte and the quiescent non-fibrogenic HSC phenotypes (see Figure 1.6.3). The ECM change affects the endothelial cells, resulting in the loss of capillary fenestration (see Figure 1.6.3). This leads to a reduction in metabolite exchange between the sinusoid and the hepatocytes. The altered rate of metabolite movement results in a subsequent reduction in liver function (Minto *et al.,* 1983; Friedman *et al.,* 1989; McGuire *et al., 1992*).

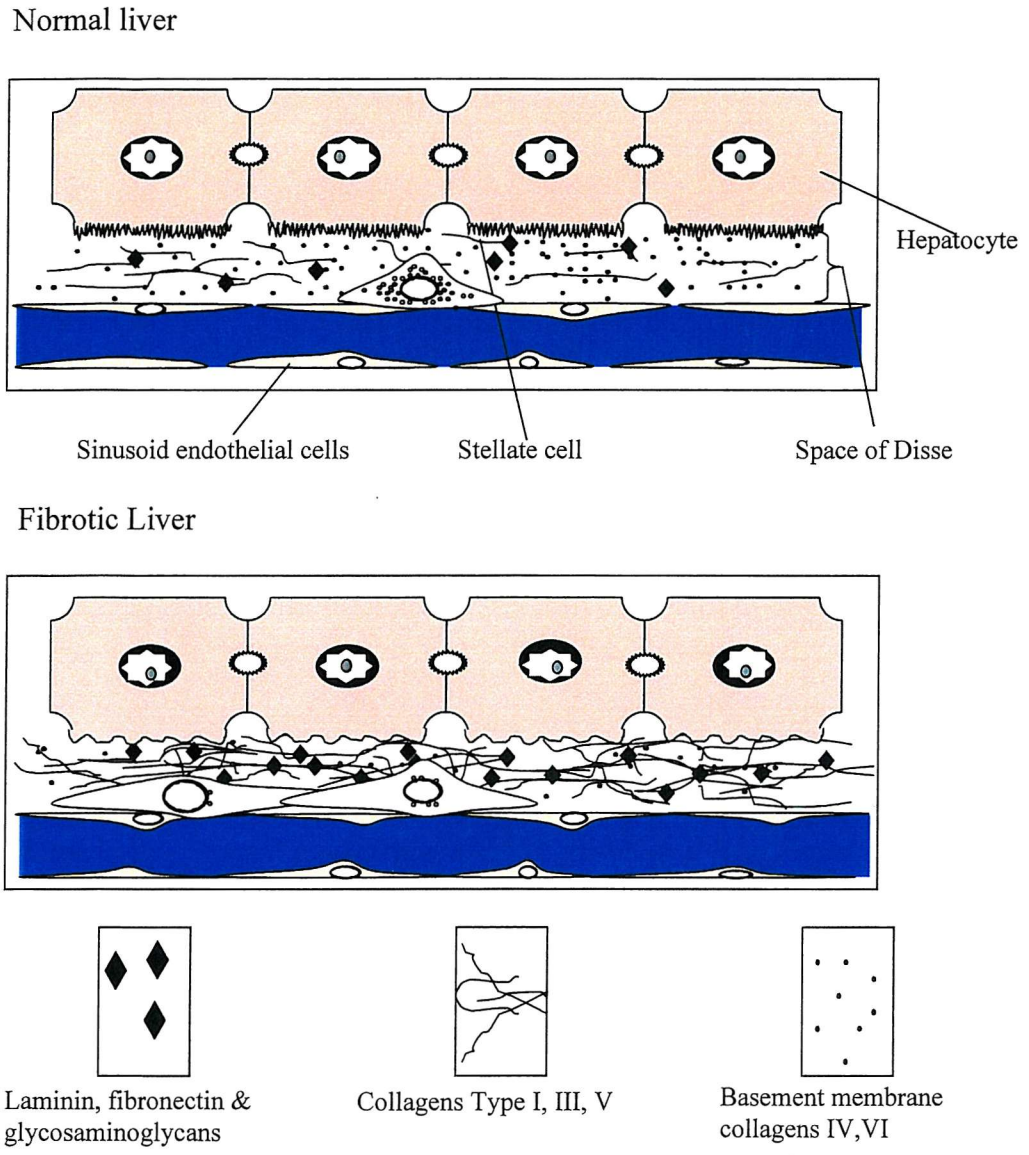

Figure 1.6.3. The microscopic changes in cellular morphology and tissue architecture with the onset of fibrosis. Changes include alterations in the ECM composition and alterations to the cells present, such as the loss of capillary fenestration, hepatocyte brush boarder and HSC retinoid droplets.

The early changes in chronic liver injury such as ECM alteration and increased deposition in the space of Dissé, led to an investigation for the effectors of fibrosis in the cells present there. The cells that make up the space of Dissé include hepatocytes, endothelial and HSC. In situ RNA studies of fibrotic liver have shown that there is no increase in ECM gene transcription in hepatocytes, a slight increase in endothelial cells and a large increase in the HSC (Milani et al., 1989).

1.7 The Hepatic Stellate Cell Undergoes a Phenotypic Change in Fibrosis

The formation of the early hepatic scar in the space of Dissé of the sinusoid highlighted the role of the HSC in liver disease. The HSC was seen as a possible source of the production of ECM in liver fibrosis through an up regulation of ECM proteins and associated mRNA. A growing consensus supports the role of the HSC in both normal ECM remodeling and pathological fibrosis in the liver (Minto *et al.*, 1983; Okanoue, *et al.*, 1983; Mak *et al.*, 1988; Martinase-Hernandez *et al.*, 1985; Milani *et al.*, 1989; Levavasseur *et al.*, 1995).

The HSC retains a number of historical aliases including Ito cell and Lipocyte. The HSCs in normal liver are believed to be rounded and contain intracellular vitamin A droplets. They make up one third of all the non-parenchymal cells of the liver, making them the primary store and point of metabolism for retinoids in the body (Friedman, 1993).

The HSC undergoes a change from the quiescent retinoid-storing cell (see Figure 1.7.1) to a proliferating myofibroblast-like cell (see Figure 1.7.2 and 1.7.3). HSC activation is observed in both human disease and also in animal-based liver injury models (Friedman, 1996). The phenotypic change in the HSC is often referred to as "activation". The HSC transformation at the level of morphology results in the loss of retinoid droplets and cell elongation (Mak *et al.*, 1988; Bachem *et al.*, 1992). As well as the morphological changes there are other phenotypic changes in the HSC that occur with activation. The phenotypic changes can be divided into four categories, these include: proliferation, contraction, ECM metabolism / fibrogenesis and chemotactant / cytokine release. The production and the roles of the cytokines will be discussed later (see Section 1.8)

The position of the HSC, encircling the sinusoid (see Figure 1.6.2) and the cytoskeletal intermediate contents of the HSC, led to their comparison with perivascular cells (Blomhoff *et al.*, 1991). Perivascular cells, or pericytes, occur in many organs, including the kidney in the form of the mesangial cells. The expression of desmin (a cytoskeletal filament intermediate) and α smooth muscle actin (αSMA) by HSC causes them to be

associated with smooth muscle cells or myofibroblast nomenclature (Nouchi *et al.*, 1991; Rockey et al., 1992). The HSC comparison with smooth muscle cells, the presence of contractile elements (ie. αSMA) and their location around blood vessels, has led to the suggestion that HSCs have a role in the control of blood flow through the sinusoid, especially during hypertension (Friedman *et al.*, 1992; Pinzani *et al.*, 1992; Rockey *et al.*, 1993; Friedman, 1993; Mallat, 1998; Rockey *et al.*, 1998; Kawada *et al.*, 1999). It has also been shown that contraction of the HSC can be induced by a number of agonists, of particular importance is endothelin-1 (Rockey *et al.*, 1998). Endothelin-1 has also been shown to increase αSMA expression in the HSC (Rockey *et al.*, 1992).

The deposition of collagen in fibrosis is consistently associated with HSC cells that have undergone a phenotypic change. Activated HSC have been shown to express a wide range of ECM proteins, both *in vivo* and *in vitro.* These include procollagens I, II, III, IV and VI. The HSC has also been shown to produce, fibronectin and to a lesser extent laminin, proteoglycans, heparan sulphate, dermatan, laminin, tenascin, decorin, biglycan, chondroitin and hyaluronic acids (Rojkind *et al.*, 1979; Friedman *et al.*, 1985; Arenson *et al.*, 1988; Maher *et al.*, 1988; Takahara *et al.*, 1988; Martinez-Hernandez *et al.*, 1989; Gressner *et al.*, 1990; Loreal *et al.*, 1992; Meyer *et al.*, 1992; Ramadori *et al.*, 1992; Schwogler *et al.*, 1992). The HSC has consequently been identified as the main producer of ECM in fibrosis (Friedman *et al.*, 1985; Milani *et al.*, 1989; Gressner *et al.*, 1990; Arenson *et al.*, 1988; Loreal *et al.*, 1991).

The activation of the HSC as a result of liver injury leads to a down regulation in interstitial collagenase / matrix metalloproteinase-1 (MMP-1) and increases in matrix type MMP (MT1-MMP) and gelatinase A (MMP-2). Stromelysin and gelatinase B (MMP-9) are also shown to be induced, but this is only transient (see Section 1.9 and 1.10) (Milani *et al.*, 1994; Vyas *et al.*, 1995; Takahara *et al.*, 1997). Crucially, with respect to fibrosis, the phenotypic change results in an increase in expression of the tissue inhibitors of metalloproteinase-1 and –2, (TIMP-1 and TIMP-2) (see Section 1.13 and 1.14). The overall result of the altered proteinase and inhibitors is degradation of the

basement membrane and accumulation of collagen types I and III. The mechanism of this outcome will be discussed later (see Section 1.15).

In order to investigate the molecular mechanisms involved in HSC activation it is necessary to use a model of fibrosis. Similar changes in cellular phenotype can be seen in fibrosis (rat and human) and *in vitro,* by culturing the HSC on uncoated tissue plastic. The culture of HSCs on plastic forms the basis of an excepted *in vitro* model of fibrosis and HSC activation (Friedman *et al.,* 1985). Recent work has validated the *in vitro* model of HSC activation using tissue culture plastic. The paper used proteomics to compare 43 proteins that were altered in HSC activation on plastic with the same proteins in cells purified from the livers of rats that had undergone an 8 week CCl_4 liver injury study (Kristensen *et al.,* 2000). The purified HSCs are initially quiescent and contain retinoid droplets cell (see Figure 1.7.1). After three days of culture the HSCs loose their retinoid droplets, rounded appearance and begin to flatten out (see Figure 1.7.2). After five days the HSCs are proliferative, beginning to express both αSMA and TIMP-1, and adopt the myofibroblast-like phenotype (see Figure 1.7.3 and 1.7.4). The expression of TIMP-1 by the HSCs is sustained throughout their culture following activation. The cultured HSCs have also been shown to secrete MMPs, including interstitial collagenase (MMP-1), gelatinase A (MMP-2) and stromelysin-1 (MMP-3) (Arthur *et al.,* 1989; Arthur *et al* 1991).

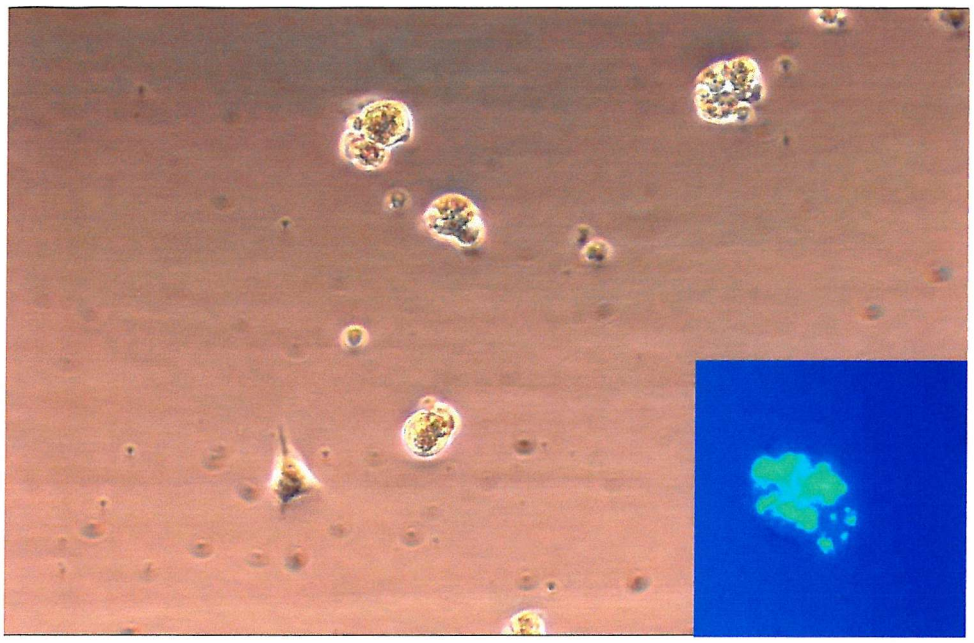

Figure 1.7.1 Quiescent rat HSC cultured on tissue culture plastic for 24 hours, following isolation. The cells are rounded and have cytoplasmic retinoid-containing lipid droplets. The cells were photographed using an inverted bright field microscope, AxioCam MR CCD camer and AxioVision 3.0 Image capture software (Carl Zeiss) 200x magnification. The inset shows the retinoid droplet florescence of a single cell using 328nm UV epifluorescence illumination and 300x magnification. Photographs taken by Author.

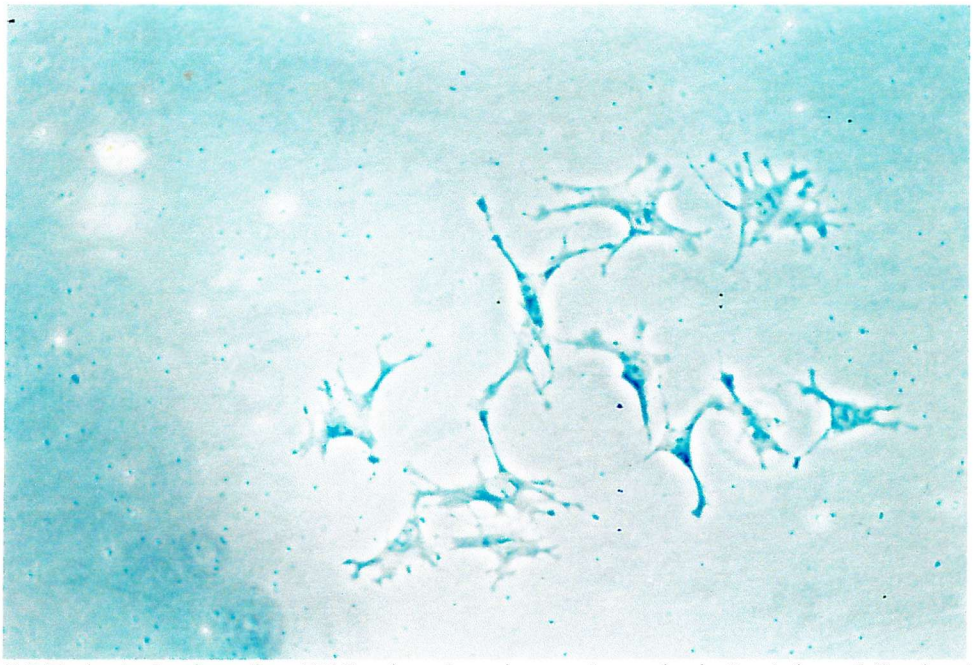

Figure 1.7.2 Early Activation of rat HSC cultured on tissue culture plastic for 4 days, following isolation. The cells have lost many of the retinoid droplets and are being to change in morphology, spreading out. Photographed using an inverted phase contrast microscope (Leica) and an automatic exposure system (Leica) at 160x magnification. Photograph taken by Author.

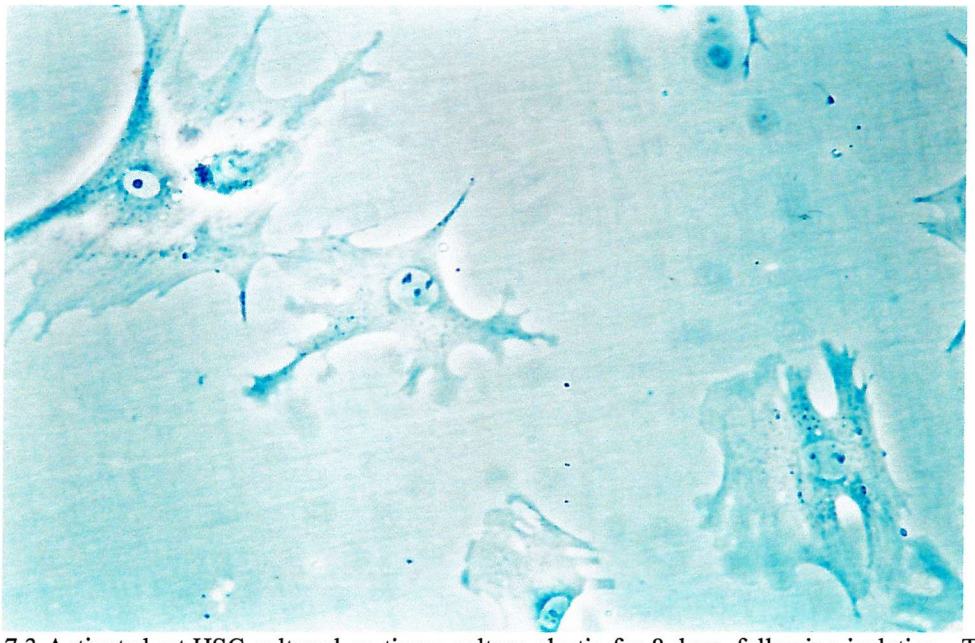

Figure 1.7.3 Activated rat HSC cultured on tissue culture plastic for 8 days, following isolation. The cells have lost most of the retinoid droplets and have changed in phenotype, adopting a flattened morphology. Photographed using an inverted phase contrast microscope (Leica) and an automatic exposure system (Leica) at 200x magnification. Photograph taken by Author.

Figure 1.7.4 αSMA staining of activated rat HSC cultured on uncoated plastic for 8 days, following isolation. The primary αSMA antibody was used at 1:800 dilution and secondary anti mouse HRP conjugate was used at 1:2000 (see Appendix 4). Staining was performed using DAB (Sigma). Photographed using a bright field microscope (Leica) and electronic image capture sytem at 200x magnification. Staining and photography performed by Author.

1.8 The Initiation of the Fibrotic Response

It is suggested that an initial inflammatory response in the liver leads to a healing response. The process of healing results in the release of proliferative and fibrogenic cytokines, as well as initial ECM modifications in the subendothelial space of Dissé. The changes in cytokines available and ECM may therefore affect change in the phenotype of localised HSCs (Bachem *et al.*, 1992). Cytokines, released by many of the cells present in the liver, have been shown to have effects on the HSC. These cytokines include Transforming Growth Factor β (TGFβ), Platelet Derived Growth Factor (PDGF), Tumour Necrosis Factor-α (TNFα), Hepatocyte Growth Factor (HGF), Fibroblast Growth Factor (FGF), Nerve Growth Factor (NGF), Oncostatin M, various interleukins, prostaglandins and thromboxanes (Debleser *et al.*, 1997; Ikura *et al.*, 1997; Knittle *et al.*, 1997; Ikeda *et al.*, 1998; Okuno *et al.*, 1998; Hellerbrand *et al.*, 1999; Knittel *et al.*, 1999a; Dooley *et al.*, 2000, Trim N *et al.*, 2000). It has also been shown that Acetaldehyde and lipid peroxides originating from the hepatocyte may also promote the fibrotic response of HSC. Lipid peroxides may originate from chemical injury by alcohol, iron over load and HCV. The problem is exacerbated in cirrhosis by the depletion of antioxidants (Leo *et al.*, 1993; Houglum *et al.*, 1994; Houglum *et al.*, 1997; Paradis *et al.*, 1997a; Paradis *et al.*, 1997b).

Probably the two most important cytokines, with respect to liver fibrosis and the HSC, are TGFβ and PDGF, which are the most fibrogenic and proliferative respectively. The production of the cytokines TGFβ and PDGF is increased with inflammation in both HSC and non-HSC cells. Upon activation, the HSC up regulates its expression of TGFβ1 and its receptors, increasing the cellular response to this cytokine and initiating endogenous feedback. TGFβ1 acts upon the HSC to increase the production of collagen while also repressing the production of interstitial collagenase. A similar effect is also seen in the HSC with reference to PDGF, which is produced in an autocrine fashion by the activated cells. The proliferation of the HSC is strongly induced by platelet derived growth factor (PDGF). The combination of the response to the constituent change of the basement membrane with the endogenous TGFβ1 and PDGF stimulation is probably

responsible for the self-sustaining nature of the phenotypic change and progression of disease (see Figure 1.8.1) (Pinzani *et al.*, 1994; Wong *et al.*, 1994; Alcolado *et al.*, 1997).

There are a number of cells that are believed to be responsible for the manifestation of the inflammatory response, which leads to the activation of the HSC by the release of cytokines. The main cell believed to be responsible for the largest portion of the cytokine release is the Kupffer cell, the resident tissue macrophages of the liver. Other cells believed to influence the HSC via an exocrine route include the hepatocyte, mast cell, T-cell and Platelet (see Figure 1.8.1) (Brito *et al.*, 1997; Ikura *et al.*, 1997; Ikeda *et al.*, Knittel *et al.*, 1999; Roth *et al.*, 1998).

The activated HSC can potentiate the fibrotic response via an autocrine route, as previously mentioned above. There is increasing evidence to suggest that the HSC can also regulate the effects of the inflammatory cells both by modulating their activities and also by recruiting them to the site. The activated HSC has been shown to express PDGF, colony stimulation factor (CSF) and chemotactic cytokines such as monocyte chemotactic peptide-1 (MCP-1) and cytokine induced neutrophil chemoattractant (CINC). PDGF and MCP-1 have also been suggested to have chemotactic properties towards HSC (Marra *et al.*, 1993; Marra *et al.*, 1997; Sprengner *et al.*, 1997; Maher *et al.*, 1998; Marra *et al.*, 1998a; Marra *et al.*, 1999). The HSC may, in the early stages of activation, reduce the inflammatory response. The partially activated HSC has been shown to produce IL-10 for short periods. This acts upon the Kupffer cells reducing TNFα expression. This observation has been supported *in vivo* in IL-10 knockout mice, which show a greater level of fibrosis (Louis *et al.*, 1998; Thompson *et al.*, 1998a;Thompson *et al.*, 1998b; Wang *et al.*, 1998).

Retinoids stored in the quiescent HSC are lost during the activation of the HSC. In the HSC 9-cis retinoic acid has been shown to have some antifibrotic effects upon the activated cell, including the reduction in expression of Collagens I, III, V and fibronectin (Hellemans *et al.*, 1999). No change in the proliferation of the HSC was observed however. At the same time as the levels of stored retinoids decrease, there is an increased

expression of MMP-2 and metalloproteinase inhibitors. This suggests that the loss of retinoid droplets may represent their release, allowing them to exhibit their pro-fibrotic effects (Arthur *et al.,* 1989; Hellemans *et al.,* 1999; Okuno *et al.,* 1997).

The change in the components of ECM that takes place in fibrosis has been shown to bring about the phenotypic change, or "activation", of the HSC. Collagen types I and III are known to be very potent effectors of the phenotypic change in the HSC. The effect of plating cells out on basement membrane like ECM (Matrigel) is the maintenance of their quiescent phenotype, whereas collagen type 1 promoted activation (see figure 1.8.1). It is believed that this effect is due to the constituents present in Matrigel, including collagen type IV, fibronectin and laminin. Although none of these constituents have been shown to be effective in isolation (Friedman *et al.*, 1989; Kojima *et al.,* 1998; Sato *et al.*, 1998; Hellemans *et al.,* 1999).

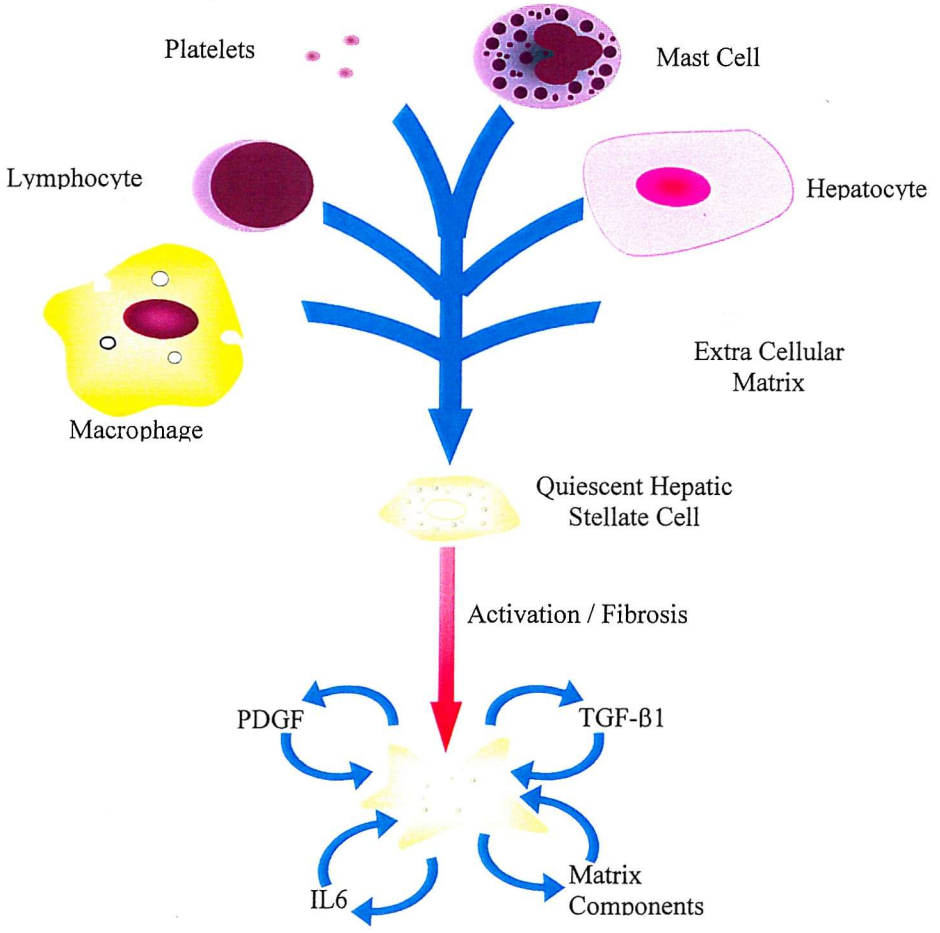

Figure 1.8.1. The factors and cells responsible for the initiation and maintenance of the fibrotic response and the phenotypic change of the HSC.

1.9 The Normal Remodeling of the Extracellular Matrix

In normal liver, as in other tissues, there is a continued remodeling of the ECM, representing balance between ECM deposition and degradation. In general, fibrosis represents a change either in the degradation and/or deposition of ECM, resulting in a shift in equilibrium towards ECM accumulation (Arthur *et al.*, 1990; Werb *et al.*, 1998) (see Figure 1.9.1). The accumulation of collagen in fibrosis could be a consequence of a number of mechanisms. The mechanisms of fibrosis include an increase in the expression of ECM protein, a decrease in the expression or activation of ECM proteases (see Section 1.11 and 1.12) and/or an increase in the inhibition of the proteases present (see Section 1.13) (reviewed in Arthur *et al.*, 1992a).

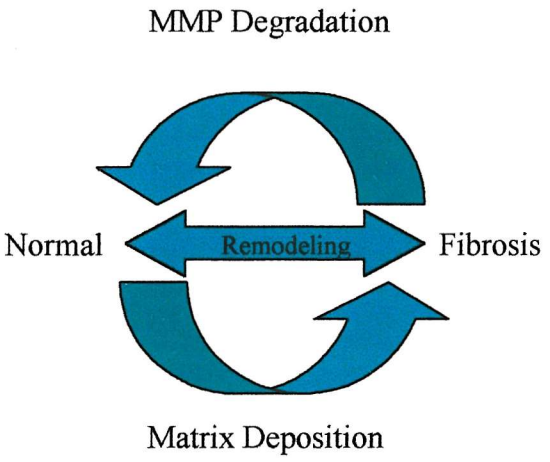

Figure 1.9.1 The balance or interaction between ECM deposition and degradation.

The alteration of ECM expression, and therefore deposition, may also be subdivided and further regulated at any one of a number of levels, leading to the final formation of the ECM. This also applies to proteases and their inhibitory proteins.

The first level at which protein expression can be regulate is gene transcription, leading to an altered rate of messenger Ribonucleic Acid (mRNA) synthesis (reviewed in Verrijzer *et al.*, 1996). The gene transcription may itself be affected by the position of a cell in its cycle or the availability of the gene's promoter region to transcription factors. This availability of a promoter's transcription factor sites is dependent on the state of

DNA compression (reviewed in Paranajape *et al.*, 1994). The regulation of transcription may also occur via altered expression or activation of transcription factors acting upon conserved binding sequences within the gene promoter. Through variation between gene promoter sequences and altered transcription factor expression, it is possible to differentially regulate the expression of a number of genes. Modulation of expression can also be achieved by altering the rate of translation and protein modification, leading to a shortening of the message or protein half-life (reviewed in Surdej *et al.*, 1994). Protein modification is also important in expression, as it may regulate the activity of a protein, identify it for proteolysis by the proteosome or prevent its shuttling across the plasma membrane (Nagase *et al.*, 1983). The general regulation of a protein's translation and expression will be discussed later in greater detail (see Section 1.16).

1.10 The Matrix Metalloproteinases and Extracellular Matrix Degrading Enzymes

The degradation of ECM in the liver is performed by a series of ECM degrading enzymes (see Figure 1.10.1). The degradation of the liver ECM is primarily mediated through a group of enzymes called the matrix metalloproteinases (MMPs) (Arthur, 1990). There are also serine and cysteine proteinases present within the liver during the course of disease, although they are not shown to have a significant role in liver fibrosis. However, the hereditary disorder α1 antitrypsin deficiency is associated with liver fibrosis, but this occurs due to a toxic accumulation of the mutant protein as a polymer within the hepatocytes, rather than as a result of alterations in ECM metabolism (Dabbagh *et al.*, 2001).

The metalloproteinases are a series of zinc dependent proteinases, which also require calcium for activity and are functionally active at a neutral pH (Matrisian, 1992). The MMPs contain a number of highly conserved sites, including the active site provided by the Zn^{2+} ion. The Zn^{2+} ion is bound to a domain formed by the conserved HELGH amino acid sequence, where it is bound by three histidine residues (Matrisian, 1992). The metalloproteinases are produced in a proenzymes form, having a pro-peptide portion that must be cleaved in order that the enzyme can be activated. The pro-peptide region of the enzyme is at the N-terminus of the protein and contains the conserved residue sequence

PRCGVPDV (Van Wart *et al.*, 1990; Springman *et al.*, 1990). The cysteine residue in the conserved N-terminal sequence is responsible for the inactivity of the proenzyme. It binds to the Zn^{2+} ion blocking the active site (Springman *et al.*, 1990).

There are at present in excess of 20 identified MMPs (Marchenko *et al.*, 2001). These have been divided crudely into 4 categories based on substrate specificity. The four categories of MMP are the collagenases, gelatinases, stromelysins, and the membrane-type metalloproteinase (see Figure 1.10.1) (Arthur, 1990; Arthur, 1992a; Cawston, 1998). The collagenases are responsible for the degradation of the interstitial and fibrillary collagens. The collagenases cleave the helix of collagens I, II and III, allowing the further degradation of the previously impervious collagen by other MMPs and proteases (Goldberg *et al.*, 1986; Nagase *et al.*, 1981; Nagase *et al.*, 1983). The activity of these enzymes are of particular significance in liver fibrosis as there is an accumulation of their substrates, collagen types I and III (Arthur, 1990; Friedman, 1993; Li D *et al.*, 1999).

The gelatinases are primarily concerned with the degradation of gelatin and basement membrane type collagen IV. The degradation of collagen type IV is a pathological observation in liver fibrosis (Arthur *et al.*, 1991). The gelatinases also have a role to play in the degradation of fibrillary collagen, once degradation has been initiated by interstitial collagenase (Hahn *et al.*, 1980; Arenson *et al.*, 1988; Arthur *et al.*, 1991; Arthur *et al.*, 1992c).

The stromelysins are broad activity metalloproteinase enzymes, able to degrade a wide variety of ECM proteins. Stromelysins also have an important role in the activation of pro-MMPs, including pro-collagenase and pro-gelatinase B (Murphy *et al.*, 1991; Okada *et al.*, 1992).

The final MMP group is the membrane type MMP's (MT-MMP). These have broad aspecificity, being able to degrade a variety of ECM proteins (d'Ortho *et al.*, 1997). The MT-MMP's are localised to the surface of the plasma membrane. The localisation to the cell surface makes them only proximally active (Okada *et al.*, 1995). This local activity

is important for their roles in angiogenesis, invasion and metastasis (Itoh *et al.*, 2001). The MT-MMP's are also involved in the regulation of metalloproteinase activity, being responsible for the removal of the pro-peptide portion of pro-gelatinase A (Ward *et al.*, 1991). Significantly, with respect to pro-enzyme activation, the MT-MMPs have a conserved 10-12 aa sequence between the pro-peptide and the N-terminal domain. The conserved sequence is recognised by the furin family of serine proteinases and is as such cleaved within the Golgi apparatus. The MT-MMP's are therefore expressed on the cell surface in a constitutively active form (Pei *et al.*, 1995).

Degradation and ECM turnover within the liver is under the control of the MMP's interstitial collagenase (MMP-1), gelatinase-A (MMP-2), gelatinase-B (MMP-9) and stromelysin-1 (MMP-3) (Arthur, 1992a). The data would seem to suggest that in early stages of disease there is an initial rise in the activity of MMP-1. This activity decreases with the onset of fibrosis (Okazaki *et al.*, 1974; Perez-Tamayo *et al.*, 1987). MMP-1 activity has also been shown to increase in recovery models (Rojkind *et al.*, 1978; Iredale *et al.*, 1998). The activities of MMP-2, 3 and 9 have been shown to increase during the development of fibrosis, in both *in vivo* and *in vitro* studies (Arthur *et al.*, 1989; Arthur *et al.*, 1993; Iredale *et al.*, 1993). The role of gelatinases A and B and stromelysin 1 in fibrosis is significant. They are active against the components of the normal-basement-like membrane (Rescan et al., 1993). MMP-2 and 3 degrade collagen type IV and laminin/proteoglycans respectively (an observation also seen in fibrosis) (Arthur *et al.*, 1989; Arthur *et al* 1991; Arthur *et al.*, 1992c; Iredale *et al* 1993).

A list of the MMP's important in fibrosis and the prospective substrates can be seen below in Figures 1.10.1.

MMP Number	Name	Substrate
MMP-1	Interstitial Collagenase	Collagens I, II, III, VII, VIII, X; gelatins, aggrecans, tenascin
MMP-2	Gelatinase-A	Gelatin, collagens I, IV, V, VII, X, XI; 72 kDa gelatinase; type IV collagenase;
MMP-9	Gelatinase-B	Gelatin; collagen I, IV, V, VII, X, XI; 92 kDa gelatinase, vitronectin; elastin; aggrecan; type V collagenase.
MMP-3	Stromelysin-1	Aggrecan; link protein; fibronectin; laminin; elastin; transin; gelatins; proteoglycans; collagen type I, III, IV, V, VIII, IX, XI; activates pro-collagenase; procollagen peptides; vitronectin; tenascin; decorin

Figure 1.10.1 MMP enzymes important in liver fibrosis and a list of their specific substrates.

1.11 The Regulation of Matrix Metalloproteinase Activity

The activity of the MMPs can be regulated at four stages, which are the levels of transcription, the expression of proenzyme, its activation and by specific inhibition.

The regulation of metalloproteinase transcription and expression is regulated in a similar way to that already described for ECM molecules (see Section 1.9). The transcription factors however, differ from gene to gene allowing differential protein expression. The expression of MMPs may also be regulated, as previously discussed, by altered transcription, mRNA / protein stability, during translation or transportation from the cell (Arthur, 1990; Arthur, 1992a; Arthur *et al.*, 1992c; Murphy, 1991). The general mechanisms of transcription and expression regulation will be discussed later in greater detail (see Section 1.16).

1.12 The Activation of the Matrix Metalloproteinases

The alteration of MMP activity may also be dependent on enzymatic activation, as most proteinases are transported out of the cell in an inactive form. Many MMPs leave the cell as a pro-enzyme or zymogen, requiring the enzymatic cleavage of the pro-peptide part of the enzyme to become active (Van Wart *et al.*, 1990; Springman *et al.*, 1990). A reduction in the expression or activity of the proteases associated with this cleavage will reduce the conversion of pro to active metalloproteinase (Arthur, 1990; Arthur, 1992b). Typically, MMP activation can be catalysed by other proteinases, such as urokinase-plasminogen activator (uPA) or tissue-plasminogen activator (tPA). Both uPA and tPA activate pro-MMPs by initiating the proteolytic cascade and converting plasminogen to plasmin (Murphy *et al.*, 1992a). Plasmin can partially activate both pro-stromelysin and pro-collagenase. The partially active pro-stromelysin will cleave the pro-portion of the partially active pro-collagenase, thereby activating the MMP (Murphy *et al.*, 1991; Murphy *et al.*, 1992a). Stromelysin can also activate pro-gelatinase B (Okada *et al.*, 1992). MT-MMP is responsible for the activation of gelatinase A (Atkinson *et al.*, 1995). Other mechanisms of MMP activation include, cleavage by tryptase, elastase and reactive oxygen intermediates (Gruber *et al.*, 1989; Nagase *et al.*, 1990; Okada *et al.*, 1992).

1.13 The Inhibition of Matrix Degradation

There are a series of inhibitors of MMPs. These include promiscuous inhibitors, such as α_2-Macroglobulin, and the more specific inhibitors, such as the family of Tissue Inhibitor of Metalloproteinases, of which four have been identified (TIMPs 1-4, see Figure 1.14.1) (Cawston, 1998). Also included in the list of inhibitors of MMP activity is plasminogen activator inhibitor-1 (PAI-1) (Murphy *et al.*, 1992a).

α_2-Macroglobulin is a 725kD glycoprotein with a broad range of protease inhibitory activity, which is expressed in the liver (Werb *et al.*, 1974; Enghild *et al.*, 1989; Murphy, 1991). α_2-Macroglobulin will generally inhibit active proteinases and may also inhibit pro-enzyme activation. The inhibitor α_2-macroglobulin is significant as it is known to be expressed by both hepatocytes and HSC (Andus *et al.*, 1983; Andus *et al.*, 1987).

PAI-1 acts as an inhibitor of metalloproteinases as it blocks the activity of Plasminogen activator, preventing the conversion of plasminogen to plasmin. This inhibition of plasminogen conversion prevents the subsequent activation of pro-stromelysin and pro-collagenase (Murphy *et al.*, 1991; Murphy *et al.*, 1992a). Significantly PAI-1 has been shown to be expressed by cells that synthesize MMPs (He *et al.*, 1989).

1.14 The Role of the Tissue Inhibitors of Metalloproteinase in the Regulation of Protease Activity

The role of the TIMPs is crucial in the regulation of ECM metabolism. Unlike α_2-Macroglobulin, the TIMPs act only as inhibitors of MMPs and not other proteinases, binding irreversibly and specifically, in a 1:1 ratio (Gromis-Ruth *et al.*, 1997). The role of the TIMPs 1 and 2 is also significant in liver disease as they directly inhibit the activation of the pro-enzyme forms of MMP-9 and MMP-2 respectively (Cawston, 1998). Mutagenesis of TIMP has identified that the N-terminus of the protein is responsible for the inhibition of enzyme activity while the C-terminus blocks pro-enzyme conversion (Howard *et al.*, 1991a; Howard *et al.*, 1991b; Ward *et al.*, 1991; Fridman *et al.*, 1992). As the TIMPs' bring about irreversible inhibition of two of the main control steps in ECM degradation, it is therefore obvious that TIMP expression regulation is crucial for maintaining normal ECM metabolism. It is for this reason that TIMP-1 has been implicated in many pathologies, associated with alterations in the remodeling of the ECM. These pathologies include arthrosclerosis, tumour metastasis, restenosis following angioplasty and arthritis (Batchlelor *et al.*, 1998; Lukashev *et al.*, 1998; Werb *et al.*, 1998; Newby *et al.*, 1999; Sternlicht *et al.*, 1999).

TIMP 1 and 2 have been identified in fibrotic liver and are considered to be crucial to its pathology (Iredale *et al.*, 1995b; Benyon *et al.*, 1996; Iredale *et al.*, 1996; Herbst *et al.*, 1997; Yoshiji *et al.*, 2000). The role of TIMP is discussed later in greater detail (see Section 1.15).

	TIMP-1	TIMP-2	TIMP-3	TIMP-4
MMP Inhibition	All	All	All	All?
Protein Size (kDa)	28	22	22	23
Glycosylation	Yes	No	Yes	No
Localization	Diffusible	Diffusible	ECM bound	?
Expression	Inducible	Constitutive	Inducible	Unknown
Binding To Pro-MMP	MMP-9	MMP-2	?	?
Major Tissue Sites	Bone, Ovary	Lung, Ovary, Brain, Testis, Heart, Placenta	Kidney, Brain, Lung, Heart, Ovary	Kidney, Placenta, Colon, Testis, Brain, Heart, Ovary, Skeletal Muscle

Figure 1.14.1. The Tissue Inhibitors of Metalloproteinases (TIMPs), their different activities and characteristics.

1.15 The Role of the Tissue Inhibitor of Metalloprotein-1 in Liver Fibrosis

Liver fibrosis, as previously mentioned, is characterised by an accumulation of collagen (see Section 1.6). The literature suggests that the reason for the change from normal ECM remodeling to a situation of fibrosis in liver disease is the reduction in ECM degradation, rather than an increase in deposition (Iredale *et al.*, 1992).

Recent work has suggested that the reduction in hepatic ECM degradation appears to be due to an increase in inhibition of MMP activity (Iredale *et al.*, 1992; Iredale *et al.*, 1998; Yoshiji *et al.*, 2000). There is a growing consensus of opinion that the reduction in degradation is brought about via inhibition of MMP activity by TIMP-1, rather than by a reduction in MMP expression or activation. The crucial role of TIMP-1 in liver fibrosis has been identified in a number of ways. The increase in hepatic TIMP-1 expression in liver disease has been shown both *in vitro* and *in vivo*, at the mRNA and protein level. Patients with chronic active liver disease show increased levels of TIMP-1 in their serum (Murawaki *et al.*, 1997). An increase in TIMP-1 mRNA and protein is also detectable in samples obtained from human fibrosis biopsies (Iredale *et al.*, 1995b; Benyon *et al.*, 1996; Iredale *et al.*, 1996).

The important role of TIMP-1 in fibrosis has also been indicated by data collected from rat CCl_4 studies, in which fibrosis was accompanied by an increase in the production of hepatic TIMP-1 by activated HSC (Iredale *et al.*, 1995a). Elevated TIMP-1 has also been associated with the occurrence of human liver disease and its production in the HSC (Benyon *et al.*, 1996). By removing TIMP-1 or unmasking the collagenase activity, it was possible to demonstrate a 20-fold increase in the MMP activity (Iredale *et al.*, 1992). More recently, a rat CCl_4 fibrosis recovery model has also supported these results. Liver fibrosis was induced in rats by administering CCl_4 for four weeks before allowing a period of recovery. The livers of the rats, following recovery, showed an increase in interstitial collagenase activity and a reduction in the expression of TIMP-1. However in this recovery model hepatic ECM returned to normal with no increase in interstitial collagenase expression, indicating that the increase in MMP activity was probably due solely to the reduction in TIMP-1 expression (Iredale *et al.*, 1998). This also supported the crucial role of TIMP-1 as a potentiator of liver disease.

A recent transgenic study showed a seven-fold increase in the severity of liver fibrosis in mice that over express TIMP-1 in a liver specific manner. The liver specific and highly active albumin promoter drove high level expression of the TIMP-1 gene in the mice of the transgenic study. The treatment of the mice with CCl_4 resulted in a significant

increase in fibrosis. The untreated mice however maintained normal liver architecture. These results showed that TIMP-1 is a positive fibrosis potentiator but not an initiator (Yoshiji *et al.*, 2000).

The role of the TIMPs in pathologies resulting from alterations in ECM restructuring is not uncommon. TIMPs are implicated in a number of pathologies, including fibrosis of other tissues, rheumatoid arthritis, restenosis following balloon angioplasty and arthrosclerosis and tumour invasion / metastatic spread (Batchelor *et al.*, 1998; Airola et al., 1999; Newby *et al.*, 1999; Soloway *et al.*, 1999). The regulation of TIMP-1 expression occurs in most tissues at the transcriptional level, apart from its expression by U937 in which there is some alteration in the stability of the mRNA (Iredale *et al.*, 1996; Clark *et al.*, 1997; Doyle *et al.*, 1997; Bahr *et al.*, 1999). The increased expression of TIMP-1 is believed to cause reduction in MMP activity both by the inhibition of MMPs and also by the inhibition of pro-enzyme cleavage. The reduction of MMP activity would maintain the rate of ECM deposition but reduce the rate of degradation resulting in a net accumulation (see Figure 1.15.1).

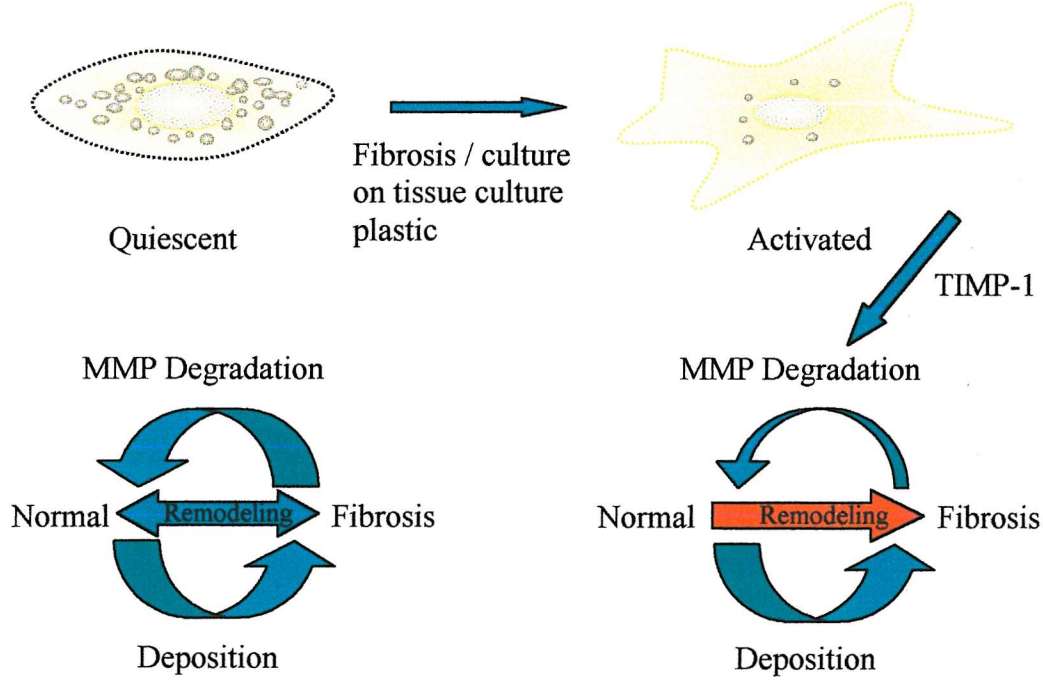

Figure 1.15.1 The role of the HSC and TIMP-1 in the ECM remodelling resulting in the development of fibrosis.

In short, the activated HSC is accepted as the cell central to the development of fibrosis in the liver. The role of the HSC is fundamental, being responsible for the majority of the collagen production, as well as many of the other ECM components found overexpressed in fibrosis (Li *et al.*, 1999). The activated HSC has also been shown to be responsible for the reduction in interstitial collagenase activity both *in vivo* and *in vitro,* in CCl_4 and bile duct ligation models in rat and human (Arthur *et al.*, 1992c; Iredale *et al.*, 1992; Iredale *et al.*, 1993; Benyon *et al.*, 1996). The liver injury models have also shown that TIMP-1 is crucial in the development of liver disease. The expression of TIMP-1 has been localised to the HSC by immuno staining tissue and RNA studies both *in vivo* and *in vitro* (Iredale *et al.*, 1995b). The experimental observations of collagen, TIMP-1, MMP, HSC activation and involvement have been supported by the study of human liver disease biopsies (Iredale *et al.*, 1995b).

The role of the TIMPs in liver fibrosis however cannot be just considered to be functioning as inhibitors of MMP. In the literature TIMPs have been shown to affect the cell growth and proliferation and also regulate apoptosis (Hayakawa *et al.*, 1992; Hayakawa *et al.*, 1994; Alexander *et al.*, 1996). The effect of TIMPs on proliferation and apoptosis is not as well established as those of metalloproteinase inhibition. The different TIMPs diverge in their effects on growth, proliferation and apoptosis. The effects of individual TIMPs also differ between cell types. TIMP-1 has been suggested to act as a survival factor, protecting a number of cell types against apoptosis mediators, such as hydrogen peroxide and X-rays (Li *et al.*, 1999). The cell types in which the protective effects of TIMP-1 have been observed include B cells, mammary epithelia (mouse and human), rabbit corneal epithelium and scleroderma fibroblasts (Alexander *et al.*, 1996; Guedez *et al.*, 1998; Saika *et al.*, 1998; Li *et al.*, 1999; Gaudin *et al.*, 2000). The importance of apoptosis in the resolution of liver fibrosis may be implicated *in vivo* by CCl_4 rat injury studies. The fibrosis recovery model showed an associated increase in HSC apoptosis concurrent with a reduction in TIMP-1 expression, these may or may not be linked (Iredale *et al.*, 1998). Conversely, TIMP 3 and 4 are suggested to be pro-apoptotic in a number of different cell types. The role of TIMP-3 as a pro-apoptotic factor is very well established and has also been demonstrated to be independent of its

ECM remolding function (Bian *et al.*, 1996; Ahonen *et al.*, 1998; Baker *et al.*, 1998, Saika *et al.*, 1998, Baker *et al.*, 1999; Bond *et al.*, 2000). TIMP-2 has been associated with both pro and anti apoptotic effects, being associated with apoptosis and proliferation (Saika *et al.*, 1998; Valente *et al.*, 1998; Barasch *et al.*, 1999; Lim MS *et al.*, 1999).

As previously mentioned, TIMP-2 has been suggested to positively regulate growth proliferation (Hayakawa *et al.*, 1994). There is also even more literature to suggest this of TIMP-1 (Hayakawa *et al.*, 1992; Kikuchi *et al.*, 1997; Saika *et al.*, 1998; Gaudin *et al.*, 2000). Although the effects of the TIMPs on apoptosis, growth and proliferation are not in doubt, the methods by which these take place are. There is confusion in the literature as to the role of the TIMPs, are they growth/survival factors, cytokines (with MAP and tyrosine kinase involvement) (Bian *et al.*, 1996; Saika *et al.*, 1998; LI *et al.*, 1999; Bond *et al.*, 2000), or do they merely exert their effects by stabilising the basement ECM (Hayakawa *et al.*, 1994; Fata *et al.*, 1999)?

It has been suggested above that TIMP-1 can function to effect cell development, growth proliferation and apoptosis, and it is therefore simplistic to consider that its only function in liver fibrosis is to reduce ECM degradation. A diagrammatic representation of the possible roles of TIMP-1 in liver fibrosis is shown below (see Figure 1.15.2)

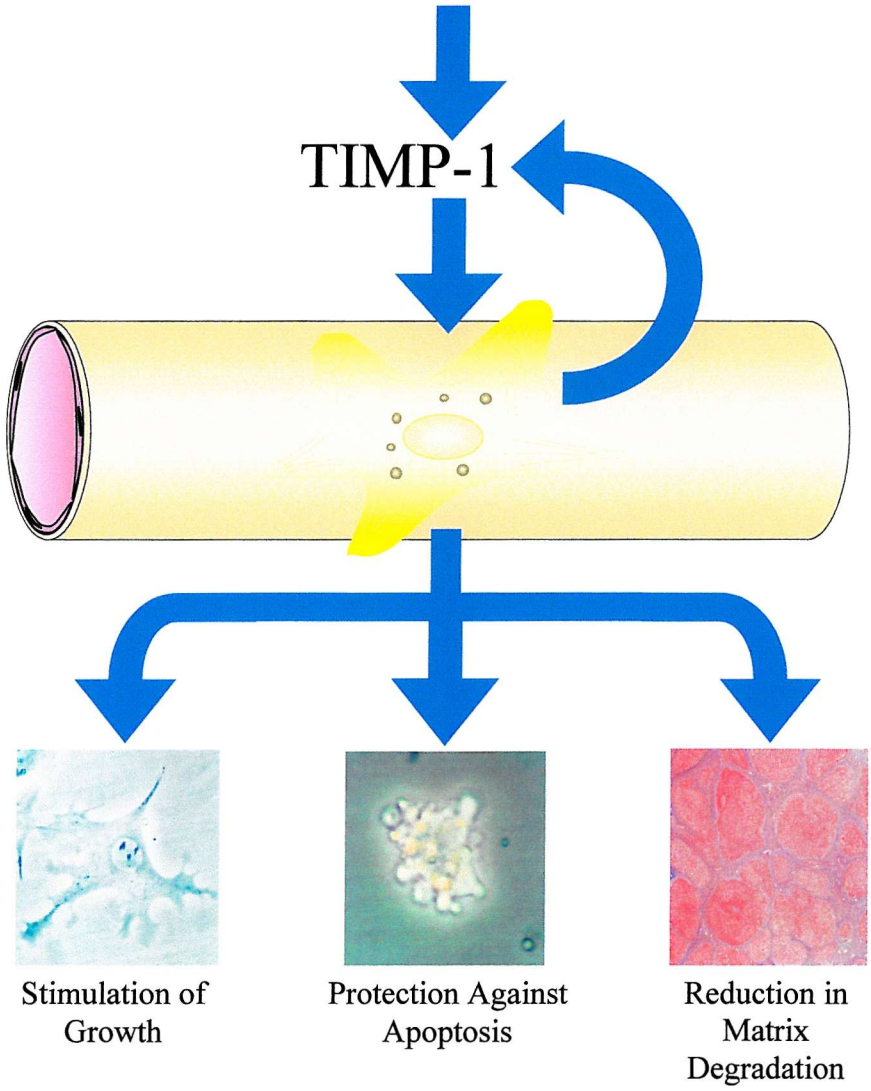

Figure 1.15.2 The suggested effects that TIMP-1 may contribute to the pathogenesis of liver fibrosis, both accepted and postulated by the subject literature.

1.16 The Regulation of Gene Transcription, Translation, Expression and Activity

The final expression of a protein is regulated at a number of levels. The first stage of control is the DNA structural regulation, in which the level of DNA compression effects transcription (Wolffe, 1994). Further stages at which gene regulation can occur include, at the levels of transcription, translation, modification and transport both intracellularly and extracellularly. Regulation can also occur when proteins require extracellular modification or other forms of intervention to acquire their active function, as previously described in Section 1.12 for the MMPs, which are converted from inactive zymogen

through cleavage to an active enzyme. An inhibitor may also block the activity of a protein. Examples of the role of activation and inhibition have already been mentioned with reference to MMPs (see Sections 1.11, 1.12 and 1.13) and as such will not be further discussed.

1.17 The Structural Regulation of Transcription

The structure or state of compression of the genome provides the first level of transcriptional regulation. The DNA in the nucleus is at all times compressed to some extent. The compression of the genome has many roles; it is necessary for the process of mitosis (the condensation of the chromosomes) and also for efficient storage. The role of DNA structure is also important in the regulation of transcription.

The diploid genome is approximately $4x10^9$ base pairs occupying a large volume in an un-compressed form. In order to maximize space, the genome is packaged at a number of levels. The genome is initially coiled around histone proteins forming nucleosomes (Wolffe, 1994). Nucleosomes provide a 6-fold reduction in packing ratio. The packaging of the genome into a nucleosome requires two of each histone subunits: H2a, H2b, H3 and H4 (see Figure 1.17.1 A). Protein H1 is necessary for the further compression of the nucleosomes into the 30nm (nanometer) fibers (Turner *et al.*, 1995). This gives an overall compression of 40 times (see Figure 1.17.1 B). The 30nm fibers are organised as a coil of nucleosomes in a helix, with 6 subunits per rotation. Packaging the DNA makes it inaccessible to the transcriptional apparatus, inhibiting transcription and expression (Jackson *et al.*, 1997). The inhibition of gene expression by the genomic structure is taken to the extreme in heterochromatin, in which the genome is further packaged to a ratio of 10,000 (Jackson *et al.*, 1997).

Heterochromatin is visible in the nucleus, by electron microscope as a dense area around its periphery. This dense chromatin is transcriptionally inert and represents regions of redundant or non-transcribed genes. The heterochromatin provides suppression of cell specific or developmental genes that may act as oncogenes promoting malignancy if expressed out of context (Hancock, 1992; Zuckerkandl, 1997). The euchromatin

provides an area for both genes that are constitutively expressed and ones for which transcription is regulated by other factors. The presence of a gene in euchromatin does not necessarily mean that it will be transcribed, but its presence in the heterochromatin means that it will not (Hancock, 1992; Zuckerkandl, 1997; Wallrath, 1998).

In euchromatin the structural regulation comes from the restriction of the transcriptional apparatus by the nucleosomes. Each nucleosome contains an octamer of histone protein subunits each globular in structure with a flexible N-terminal tail (Svaren *et al.,* 1996; Wu *et al.,* 2000). Modifications to these tails commonly include acetylation and methylation of the free (ε) amino acid (Wu *et al.,* 2000, Rice *et al.*, 2001). Histone acetylation has been linked with transcription factor site accessibility through histone loosening. The activation of gene transcription appears to be particularly associated with the acetylation of the lysine residues on the H3 and H4 subunits (Grunstein, 1997; Wu *et al.,* 2000, Rice *et al.*, 2001). Histone acetylation is under the control of the histone acetyltransferases (HATs) and histone deacetylases (HDAC). The HATs include: HAT1, GCN5, p300/CBP, P/CAF and SRC-1 (Glass *et al.*, 1997; Puri *et al.*, 1997).

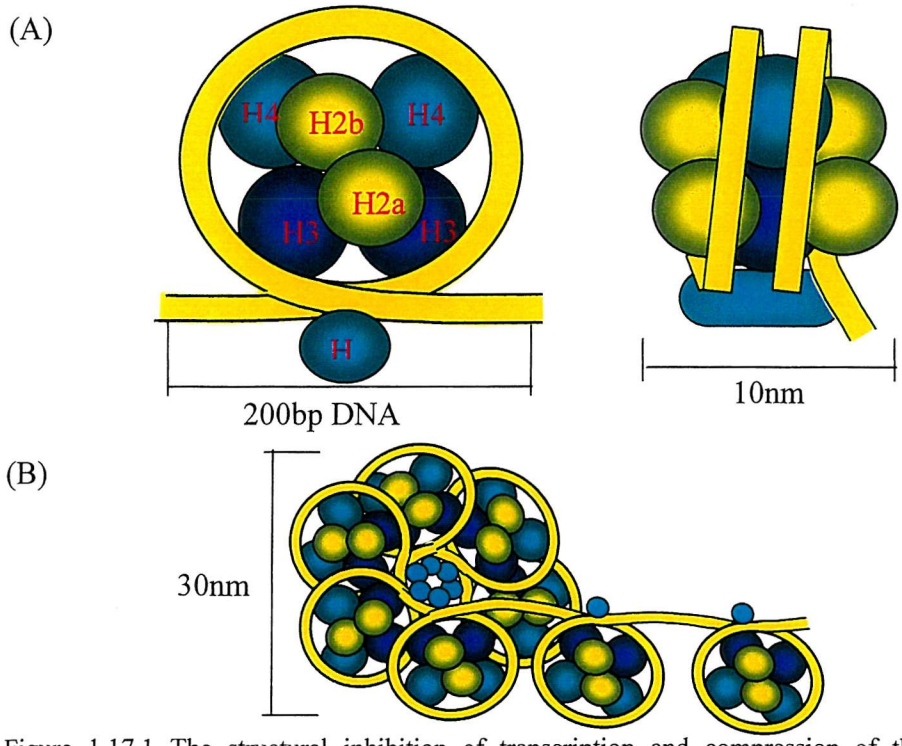

Figure 1.17.1 The structural inhibition of transcription and compression of the genome. A) Single nucleosome B) String of nucleosome "string of beads" C) Euchromatin further compression.

1.18 The Role of Transcription Factors in Transcriptional Regulation

The regulation of transcription occurs through the interaction of trans-activating factors with specific conserved binding sites in the gene. The conserved sequences in the gene that regulate transcription are primarily found in a region called the promoter (see Figure 1.18.1). The promoter is usually an un-transcribed region, 5' of the transcription start site, which contains a number of transcription factor binding sites. These transcription factor-binding sites regulate transcription by either positively or negatively affecting the recruitment of RNA polymerase II to the transcription start site. This recruitment is believed to occur through the binding of the halo enzyme and bending of the promoter so that RNA polymerase II and the TBP associated factors are brought into close proximity with the transcription start site (Kim *et al.*, 1996a; Kim *et al.*, 1996b).

The presence of a specific factor-binding site does not necessarily indicate a role in promoter regulation. The transcription factor binding sites are both position and orientation dependent; they must be an appropriate distance from each other and the transcription start site. The inappropriate positioning of binding sites may result in negative effects on promoter activity (Rajaram *et al.*, 1997). The function of the binding site is also dependent on the required factors being already expressed. In many cases, any one of a family of factors maybe able to bind a particular site, each one having different effects on expression (Chiu *et al.*, 1988; Ryseck *et al.*, 1991). A transcription factor of the same family will often possess different characteristics, such as different trans-activation potential or altered affinity for the site, leading to competition and shortened or prolonged promoter activity (Ryseck *et al.*, 1991).

The activity of the promoter can also be influenced by the effects of enhancers or silencers. These are sequence specific transcription factor binding sites, which are able to operate in a position and orientation independent manner. Enhancers and silencers can be found anywhere in the gene, upstream, downstream or even in the introns (Ogbourne *et al.*, 1998).

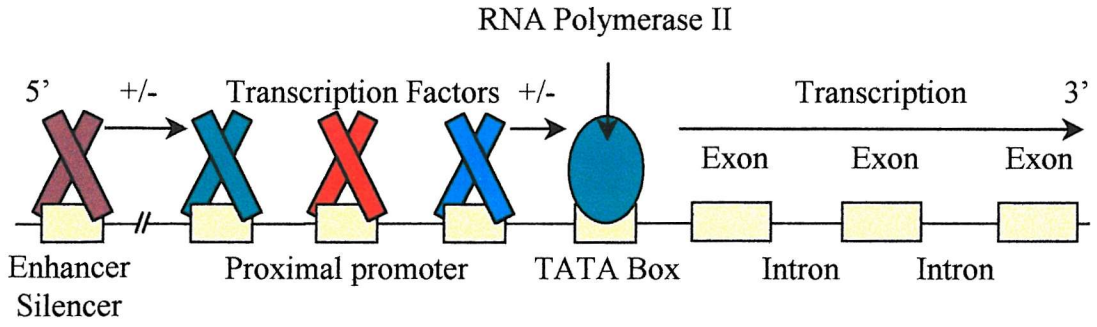

Figure 1.18.1 The general structure of a gene promoter

The general transcriptional apparatus consists of a very large multimeric complex that forms at the TATA box and extends to the transcription start site or cap site (see Figure 1.18.2 A-C). The components of the transcriptional machinery have different functions that culminate in the recruitment and activation of the RNA polymerase II holoenzyme and the subsequent transcription of RNA. The first factor to bind to the DNA is TFIID, which is itself a multimeric protein formed from the TATA binding protein (TBP) and 12 general TBP associated factors (TAFs). The TFIID complex binds to the TATA box, a sequence approximately 25-30 base pairs upstream of the transcription start site, classically defined as $TATA^{A}/_{T}A^{A}/_{T}$ (Patikoglou *et al.*, 1999). The subunit is unusual in that it binds in the minor groove of the DNA, causing considerable bending (Burley *et al.*, 1996; Nikolov *et al.*, 1997). While the bending of the DNA is not necessary for assembly, it brings upstream regions into closer proximity, allowing binding of TFIIA through direct contact with upstream binding sequences and TBP (Buratowski *et al.*, 1989; Geiger *et al.*, 1996; Tan *et al.*, 1996; Nikolov *et al.*, 1997). The binding of TFIIA to the developing complex prevents the binding of an inhibitor complex NC2 (Imbalzano *et al.*, 1994). The binding of the TFIIA and TFIIB subunits has been shown to occur concurrently, both stabilise TBP binding (Buratowski *et al.*, 1989; Imbalzano *et al.*, 1994). The primary roles of the TFIIB subunit are however the recruitment of RNA polymerase II and selection of the start site (Leuther *et al.*, 1996).

Next to bind the developing complex is the RNA polymerase II Holoenzyme and the TFIIF subunit entity. TFIIF acts to target the promoter, through an interaction with TFIIB, destabilizing non-specific binding of the RNA polymerase. The TFIIF subunit

also acts as an elongation factor (Conaway *et al.*, 1993; Zawel *et al.*, 1993; Zawel *et al.*, 1995a; Leuther *et al.*, 1996). The penultimate factor to bind the complex is the TFIIE subunit, which has been suggested to possess DNA melting functions (Holstege *et al.*, 1995). The final factor to bind is the TFIIH subunit, which has helicase activity and also acts to phosphorylate the RNA polymerase II carboxy-terminal domain (CTD) kinase (Drapkin R *et al.*, 1994; Ohkuma *et al.*, 1995). It is believed that, following DNA melting by TFIIH with ATP hydrolysis in the presence of ribonucleoside triphosphates, CTD phosphorylation leads to initiation and a subsequent transition to elongation (Conaway *et al.*, 1993; Zawel *et al.*, 1993). The phosphorylation of the CTD releases the RNA polymerase II from the transcription factors necessary for assembly, activation and initiation. Elongation results in the loss and recycling of TFIIB, TFIIE and TFIIH. The factors TFIID, TBP and TFIIA remain in contact with the TATA box, allowing re-initiation (Van Dyke *et al.*, 1988; Zawel *et al.*, 1995b). At or following termination, the CTD is de-phosphorylated, allowing its recycling to the pre-initiation complex (Chambers *et al.*, 1995).

Promoters lacking consensus TATA boxes have been shown to be activated by alternative mechanisms. Promoters lacking TATA boxes are classically shown to function through GC-rich regions and SP-1 binding domains (Yoshida Y *et al.*, 1996; Korner K *et al.*, 1997; Huber R *et al.*, 1998; Yang M *et al.*, 1998).

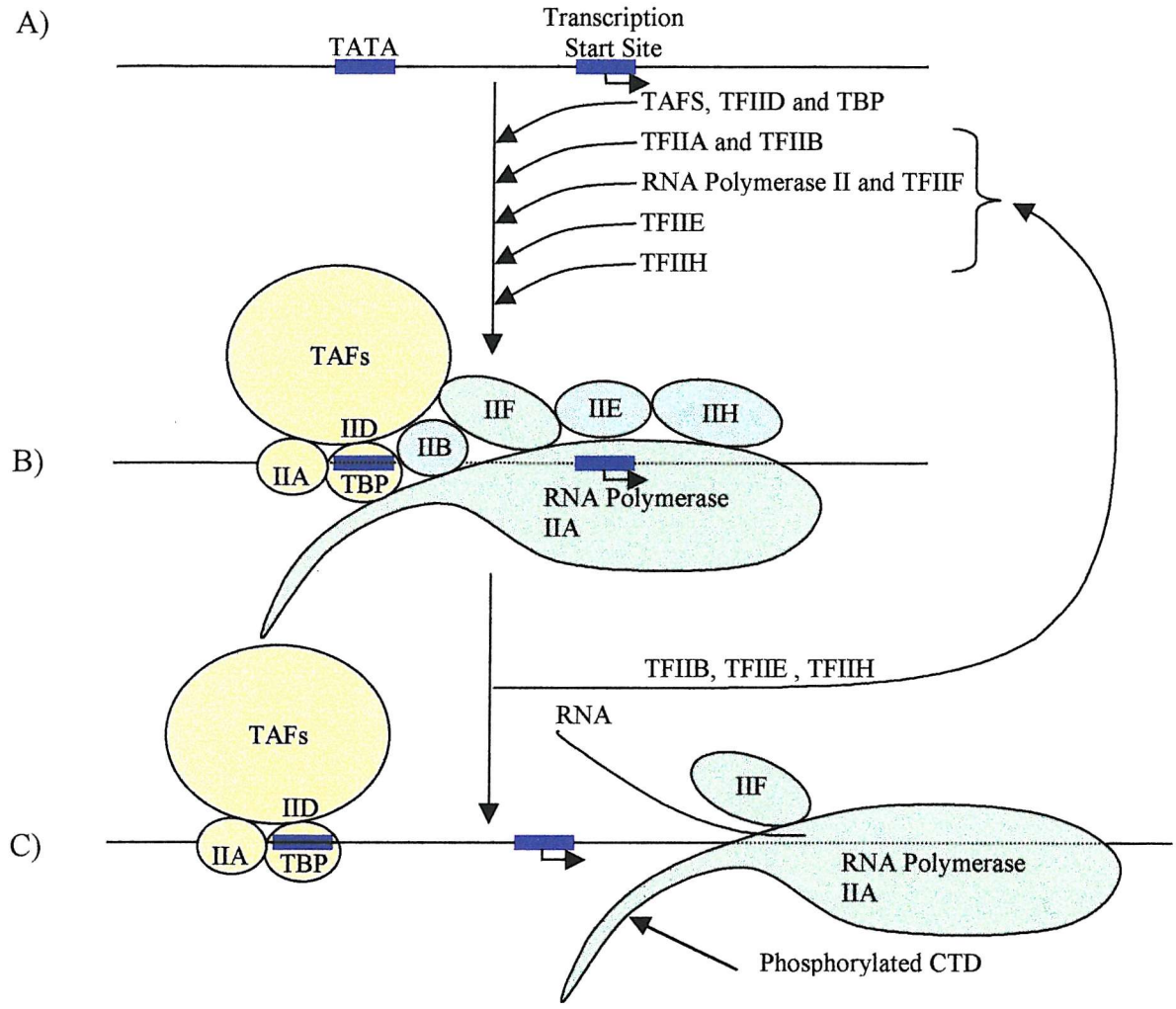

Figure 1.18.2. The order of transcription factor association and disassociation necessary for the function of the RNA transcriptional apparatus. The figures identify the A) bare promoter, B) initiation and C) elongation complexes.

Once transcribed the RNA is capped and spliced before being translated into protein by the ribosomes. Regulation may occur due the splicing and capping, as the absence of these events will prevent transport from the nucleus. Regulation at the level of mRNA occurs through its transportation and the message half-life (Drummond *et al.*, 1985). There is a common association between polyadenylation and mRNA half-life. Virtually all mRNA is polyadenylated at the 3' end by the addition of approximately 200 adenine subunits. The adenine bases are added to the free hydroxyl group at the 3' end of the transcribed mRNA by the enzyme poly (A) polymerase. The actual role of deadenylation

is unknown. For example, in the metallothionein, RNA shortening of the poly (A) tail has been observed, with no RNAs apparent with less than 30-40 residues (Shatkin *et al.*, 2000). This indicates that there is a progressive shortening of the poly (A) tail with time and that 30-40 adenine residues are necessary to prevent rapid degradation (Mercer *et al.*, 1985). In yeast, the GAL1 promoter was exchanged with promoters of a number of genes whose RNA transcript was either very stable or unstable. The results of the transient transfections were that both RNAs underwent deadenylation but it was faster in the unstable gene (Decker *et al.*, 1993). A lot of work has been performed on sequences that destabilise RNA transcripts. Much of this work has been performed on c-Fos, which undergoes rapid degradation. The c-Fos transcript contains a 3' un-translated region (3' UTR), which has been identified to destabilise otherwise stable mRNAs. The addition of the 3' UTR of c-Fos to the stable β-globin mRNA results in a reduction in the transcripts stability. The 3' UTR of c-Fos has been shown by mutation to be dependent on recognised elements called AU-rich elements (ARE) (Shyu A-B *et al.*, 1989; Shyu A-B *et al.*, 1991). The sequence of the ARE is AUUUA repeat, which functions, in a cumulative fashion, to decrease mRNA stability. The c-Fos gene has also been shown to contain a site proximal to the ARE that acts as an enhancer of its mRNA destabilising activity (You *et al.*, 1992).

1.19 The Tissue Inhibitor of Metalloproteinase 1 Promoter

As TIMP-1 has been shown too be crucial in fibrosis and it has been demonstrated that it is regulated at the level of transcription, it is necessary to investigate the role of the promoter in expression.

As with the expression of other proteins, the regulation of TIMP-1 can be controlled at a number of levels. The investigation of TIMP-1 expression in this work concentrates on the transcriptional regulation, resulting from the activity of the promoter region of the gene. The reason for concentrating on the expression of TIMP-1 at the transcriptional level, as previously mentioned, arises from the literature available and previous work in the department. Significant increases in mRNA accumulation and resulting protein production have been seen both *in vitro* and *in vivo* (Iredale *et al.*, 1995b; Benyon *et al* 1996; Iredale *et al.*, 1996). In the literature, TIMP-1 expression has also been shown to be regulated at the transcriptional level in all but one example, U937 cells, where there was shown to be some regulation through mRNA stability (Doyle *et al.*, 1997).

However, the most important reason for the study of the transcriptional regulation in TIMP-1 expression comes from transfection studies of quiescent and activated HSC. Transfection of a TIMP-1 reporter into activated HSCs showed a significant increase in activity, relative to the control, whereas the repeat experiment in quiescent cells showed only basal levels of activity (Bahr *et al.*, 1999). Current research is investigating functional sequences within the active promoter region and is identifying the crucial transcription factors and sites regulating its transcription.

Previous work has identified the minimal active promoter of the human TIMP-1 gene from –102 to +60 base pairs (bp) with reference to the transcription start site (see Figure 1.19.1). The minimal promoter was identified using truncation analysis, in which sequential individual digestions were made both 5' and 3' of the human TIMP-1 promoter. The truncation mutants were ligated into a chloramphenicol acetyl transferase (CAT) reporter construct. The reporter was transfected into a number of different cell types and the promoter activity measured by assay (see Section 2.6). The activity of the

different constructs was then calculated. The minimal promoter for the HSC was very similar to other cell types tested. It showed activity above basal empty vector activity for vectors containing promoter fragments of not less than –102 to +60bp in size. The results of the truncation analysis suggested that the minimal promoter was 162bp in length, with crucial Activator Protein-1 (AP-1) and Leader Binding Protein-1 (LBP-1) sites located 5' and 3' respectively (Bahr *et al.*, 1997; Clark *et al.*, 1997; Bahr *et al.*, 1999). The truncation analysis left a 110 base pair region unmapped for regulatory transcription factor binding sites. A sequence recognition search identified a number of known transcription-factor binding sites present within the minimal promoter. The identification of sites, following computer analysis, does not however prove that they are functionally active in this system. Also, large areas of the promoter were left seemingly free from regulatory regions. Sequence analysis of the TIMP-1 minimal promoter identified putative PEA-3, STAT and SP-1 sites and an AP-2 just outside the 3' end. The AP-1, STAT-1 and PEA3 sites make up a region called the serum response element (SRE) or Tetradecanoyl Phorbol Acetate (TPA) response element (TRE), shown to be responsive to viruses, interleukin-6, phorbol ester and oncostatin M (Gewert *et al.*, 1987; Campbell *et al.*, 1991; Edwards *et al.*, 1992; Bugno *et al.*, 1995; Logan *et al.*, 1996). The search also identified the aforementioned AP-1 and LBP-1 sites (see Figure 1.19.1). The AP-1 site in the TIMP-1 promoter is not a classical AP-1 consensus site (TGA$^{G}/_{C}$TCA) but it is similar (TGAGTAA) (Edwards *et al.*, 1992; Logan *et al.*, 1996).

The activity of the TIMP-1 promoter, classically, is dependent upon the AP-1 c-Jun/c-Fos heterodimer acting in conjunction with the Pea-3 site. The binding of c-Jun and c-Fos to the adjacent AP-1 site is suggested to bind c-Ets and tether it to the PEA3 site. The addition of the c-Ets to the c-Jun/c-Fos complex is suggested too positively regulate the activity of the TIMP-1 promoter (Edwards *et al.*, 1992; Logan *et al.*, 1996).

In the HSC however, the activity of the TIMP-1 promoter is not believed to be due to the interaction of c-Jun/c-Fos with the AP-1 site 5' of the minimal promoter. The previous data, using the tissue culture model of fibrosis, has shown that there is no expression of TIMP-1 when c-Jun and c-Fos are expressed, and vice versa. In the HSC, the classical c-

Jun/c-Fos is replaced by interactions of Jun D, Fra 2 and Fos B, the expression of which precedes that of TIMP-1 (see Figure 1.19.2) (Bahr *et al.*, 1999).

Freshly isolated HSC show increasing expression of c-Jun and c-Fos, peaking at 24 hours of culture. Also present at this time are Fra-1 and Jun-B. The expression of c-Jun, c-Fos and Jun B are not detectable after 48hr. The expression of Fra-1 and Jun B decreases with further activation of the HSC. After five days of culture on plastic the HSCs begin to adopt the "activated" phenotype, expressing Jun D, Fra-2 and Fos B. Jun D is expressed at low levels from freshly isolated cells throughout activation, increasing in expression after five days of culture (see Figure 1.19.2). Jun D also appears, by observation, to undergo changes in relative molecular weight, seen as changes in position on SDS polyacrylamide gel. The reason for the different apparent molecular weight is not as yet understood (Bahr *et al.*, 1999).

Experimental data also show that the HSC mutation of the AP-1 site results in virtually basal promoter activity (70% decrease) but a similar mutation of the PEA3 site has a small decrease in activity (30% decrease). The HSCs show a strong down regulation in the expression of Ets-1/2 with activation, which also contradicts the classical regulation of TIMP-1 (Logan *et al.*, 1997; Bahr *et al.*, 1999; Knittel *et al.*, 1999b). There may be other members of the Ets family binding, although the small change in promoter activity with the mutation of the site suggests that this is not crucial

Another recently identified transcription factor binding site is the previously un-described Upstream TIMP Element-1 (UTE-1), which appears to be crucial for the function of the TIMP-1 minimal promoter in both human and rat HSCs. The interacting protein was shown to be specific and of approximately 30kDa in size. The UTE-1 site was identified as an element of 11 nucleotides in size (TGTGGTTTCCG) by DNase footprinting (see Figure 1.19.1). Using electrophoretic mobility shift assay and the transfection of mutant reporter constructs it was possible to establish that this was specific binding, crucial for TIMP-1 activity. The crucial core nucleotides required for protein binding were

identified as G^{-60} and G^{-59} (TGTGGTTTCCG), although flanking regions also had a role (Trim *et al.*, 2000).

Recent work has suggested, in addition to the classical AP-1 binding proteins, two single stranded proteins bind in a transcriptional active fashion to the non-consensus AP-1 site in the 5' region of the TIMP-1 minimal promoter. These individual single stranded binding factors have also been shown to interact with the consensus AP-1 5' of the minimal promoter in TIMP-1. The presence or role of these single stranded proteins is unknown in the HSC (Phillips *et al.*, 1999).

Another group has also recently identified two negative regulator regions that lie upstream of the minimal promoter and in intron 1, at –1718/-1458 and +648/+748 respectively. The mediator of the upstream repression is unknown but intron 1 repression is believed to be due to an Ets like factor, SP1 and or SP3, although SP3 seems to be most crucial (Dean *et al.*, 2000).

The TIMP-1 promoter has a high level of conservation across at least three species; within the 22 base pairs that encompass the SRE there is only a single mismatch between human, mouse and rat. This high level of cross species homology continues for about the first 40 base pairs, containing only four mismatches, which include a 2 base pair mismatch in the recently defined binding domain for UTE-1 (Trim *et al.*, 2000). These areas of cross species conservation indicate how important the AP-1, PEA3 and UTE-1 domains are for TIMP-1 regulation (see Figure 1.19.1).

There are a number of reasons why this research has been performed using a human promoter construct while working in rat cells. Firstly, there is a high degree of sequence homology between human, mouse and rat (see Figure 1.19.1). The human construct is also not only very active in rat HSC, but contains a slightly larger elongated sequence when compared to those of mouse and rat between the UTE-1 and SP-1 sites. The use of a human promoter construct is also justifiable due to the high levels of conservation in the areas in which the research is being performed, such as the SRE and SP-1 regions.

Transcription factors in the three species are also highly conserved in both their DNA binding and transactivation characteristics. The human promoter is also the best option as the primary concern is the human pathology and ultimately any discoveries would have to be verified in humans.

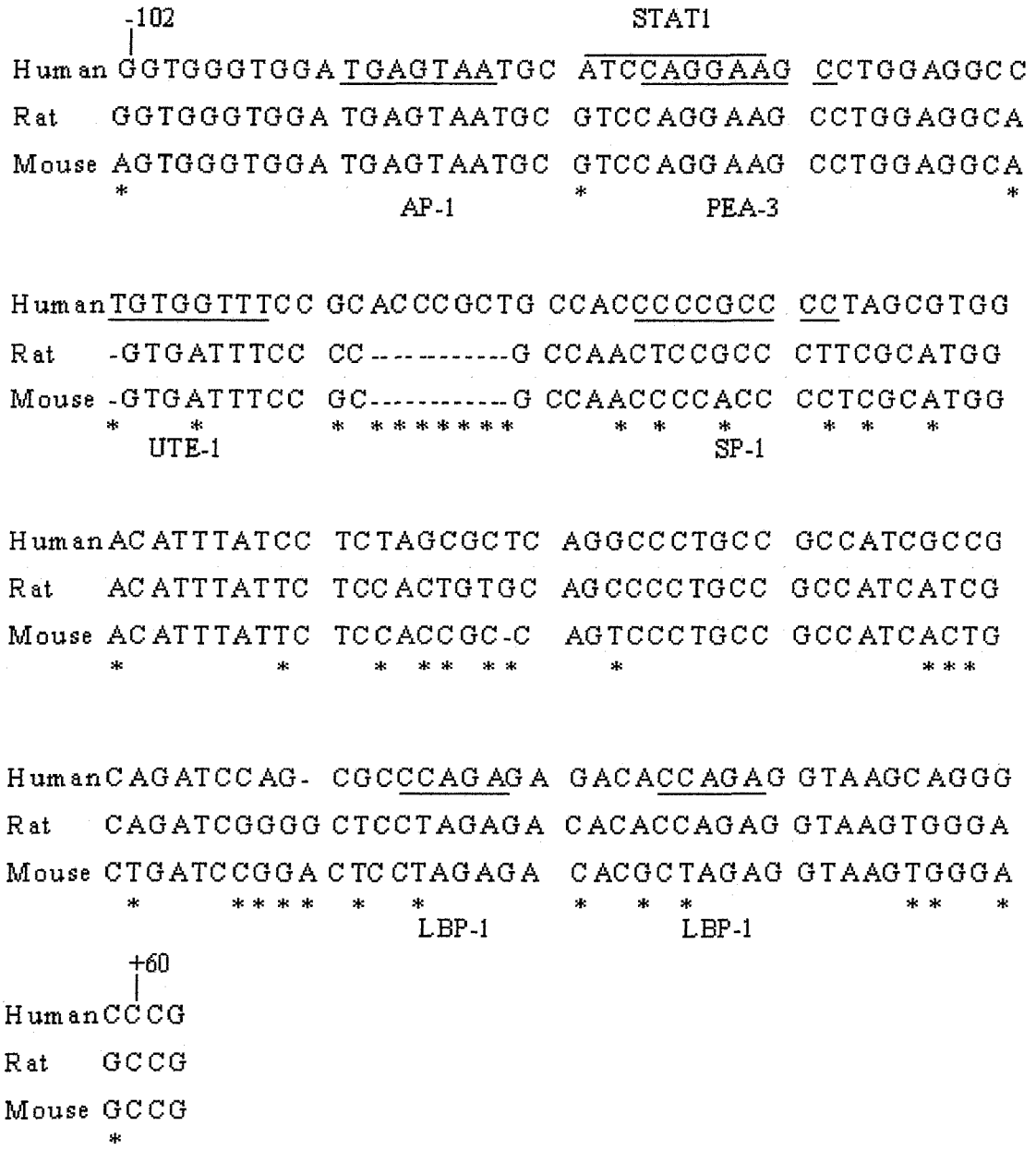

* Base mismatch with human minimal promoter.

Figure 1.19.1 Sequence comparison of the defined TIMP-1 minimal promoter region in rat HSC between species

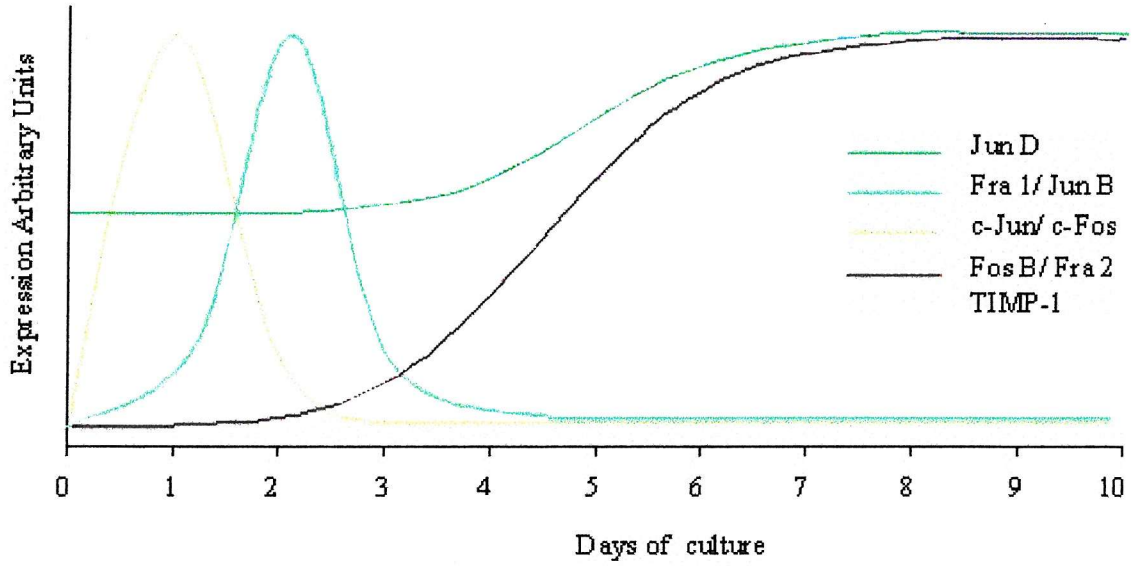

Figure 1.19.2 Diagrammatic representation of the qualitative changes seen in the expression of the JUN, FOS and TIMP-1 proteins with HSC activation on tissue culture plastic (Iredale *et al.*, 1995b; Bahr *et al.*, 1999).

1.20 The Activator Protein-1 Transactivation Domain and its Binding Factors

The Activator Protein-1 (AP-1) binding site or transactivation domain is represented by the palindromic consensus sequence $TGA^{G}/_{C}TCA$. The AP-1 site is often referred to as the Phorbol Acetate (TPA) response element (TRE). The AP-1 binding proteins are divided into two main families, the JUN and FOS families, as well as the more broad helix-loop-helix/leucine zipper superfamily. The members of the FOS and JUN families share a common hydrophobic leucine zipper domain mediating their dimerization, and a basic DNA binding region (Busch *et al.*, 1990).

The mammalian JUN family of DNA binding proteins (early response genes) is made up from three members; c-Jun, Jun B and Jun D (Ryder *at al.*, 1988; Ryseck *et al.*, 1988; Quantin *et al.*, 1988). The oncogene originally identified was *v-jun.* It was isolated from the avian sarcoma virus 17 (ASV 17), a spontaneous chicken sarcoma. The name originates from the Japanese 17 (ju-nana) (Bohmann *et al.*, 1987; Maki *et al.*, 1987). The JUN family proteins are unusual in that they all occur with a single exon free from introns (Hattori *et al.*, 1988; Hartl *et al.*, 1991).

The mammalian FOS family of proteins contains 4 members; c-Fos and Fos B as well closely related Fra 1 and Fra 2 (FOS related antigens). The oncogene *v-fos* was identified in the FBJ (Finkel, Biskis and Jinkins) and FBR (Finkel, Biskis and Reilly) murine osteosarcoma viruses (Nishizawa *et al.*, 1987). Also included in the FOS family is ΔFosB or FosB2, which is a splice mutant of the parent FosB. It is able to form dimers with JUN members but is unable to trans-activate the AP-1 DNA binding site. ΔFosB would appear to be able to initiate DNA replication by a non AP-1 site mediated pathway (Nakabeppu et al., 1991; Yen *et al.*, 1991; Nakabeppu et al., 1993).

The Activating Transcription Factors (ATFs) are a group of factors including ATF2, ATF3/LRF1 and B-ATF. The ATF family, are also leucine zipper family members and are able to dimerize with JUN family proteins and themselves (Ziff., 1990). The ATF dimers are only able to only weakly interact with the consensus AP-1 sites or the transactivation domain (Hai T *et al.*, 1991). The ATF dimer instead interacts with the so-called Cyclic Adenosine Monophosphate (cAMP) response element (CRE) (TGACGTCA). The ATFs are also closely related to CRE Binding Protein (CREB) and CRE Modulating Protein (CREM) that also interact through the CRE (Chatton *et al.*, 1994).

Binding to the AP-1 cis-acting element, or consensus site, is, as previously mentioned, by the formation of a dimer. The classical dimers may be in the form of a JUN homodimer or a JUN/FOS heterodimer. FOS homodimers are too unstable to bind AP-1 sites (Chiu *et al.*, 1988; Ryseck *et al.*, 1991). As a result of the various dimer stabilities there are 18 stable dimeric combinations of JUN and FOS. Dimers of c-Jun bind 10 times stronger to DNA than homodimers of either Jun D or Jun B. The formation of a heterodimer with FOS family proteins increases the affinity of the AP-1 dimer complex to the regulatory site, as well as increasing dimer stability (Smeal *et al.*, 1989; Allegretto *et al.*, 1990). By increasing the affinity of a complex interaction with its relevant site, there is an increase in the half-life of the DNA protein interaction. The FOS proteins enhance JUN affinity to DNA in the form of a heterodimer Fos B> Fra 1> c-Fos. Single base pair substitution in

the flanking regions of the AP-1 binding domain can also confer a ten-fold increase in binding affinity (Ryseck *et al.*, 1991).

Crucially, the regulation performed by the AP-1 site is complex, dependent on the expression, abundance and phosphorylation of the binding factors (Karin *et al.*, 1995). The context of the AP-1 site is also very important, as presence does not indicate function. As with other transcription factors, this is dependent on its position and the proximity of other binding domains etc. Abundance is affected by gene expression and the JUN proteins are also positively regulated. The relative abundance of both c-Jun and c-Fos proteins can be affected by changes in their stability or half-life (Treier *et al.*, 1994; Tsurumi *et al.*, 1995). The altered availability of each of the family members leads to changes in the heterodimeric combinations of AP-1 complexes, resulting in variation of gene expression. Subtle changes in AP-1 regulated genes can be achieved by variation of heterodimeric combinations. The regulation of expression due to the various dimer combinations is suggested to result from the modification of DNA bending, which can enhance or suppress gene transcription (Kerppola *et al.*, 1996).

Activation of JUN and FOS family proteins is through phosphorylation performed by the JUN-N-terminal kinases (JNK), FOS regulating kinase (FRK) and Extracellular signal related kinases (ERK) respectively (Karin, 1995; Whitmarsh et al., 1996). The activating mitogens of the various kinases are listed in the table below (Figure 1.20.1). Phosphorylation by JNK of c-Jun occurs at serine residues 63 and 73, resulting in increased DNA binding and increased stability of the protein (Smeal *et al.*, 1994; Fuchs *et al.*, 1996). JNK binds to all three JUN family members. JNK2 exhibits the highest affinity for c-Jun, although many isoforms have affects on JUN and other transcription factors (Kallunki *et al.*, 1994). JNK binds strongly to the N terminal domain at the putative docking site of c-Jun, formed between amino acids 30 and 60 (Kallunki *et al.*, 1996). This is independent of the phosphorylation of serine 73. Although both c-Jun and Jun B possess a docking site for JNK, c-Jun also possesses specificity conferring residues such as the proline phosphoacceptor site at position P+1 (Kallunki *et al.*, 1996). Jun B can therefore bind JNK but no phosphorylation takes place.

Jun D possesses the same specificity conferring residues as c-Jun but no docking domain. Jun D however undergoes a less efficient phosphorylation by the formation of a dimer with either c-Jun or Jun B and binding JNK (Dérijard *et al.*, 1995; Kallunki *et al.*, 1996). It has been suggested that the phosphorylation of Jun D can also be performed via an intermediate protein called JAB, which forms a complex simultaneously with JNK and Jun D (Claret *et al.*, 1996). More recently opinion has changed, suggesting that while JAB1 is involved in Jun D phosphorylation it functions as part of a larger multimeric complex called COP9 signalosome (Chamovitz *et al.*, 2001). Phosphorylation of c-Jun by JNK has been shown to regulate the stability or half-life of the protein by inhibiting or marking it for ubiquitination. The inhibition of ubiquitination is mediated by JNK through the phosphorylation of Ser^{73}. The phosphorylation of c-Jun in the δ-Domain by JNK2 targets it for degradation (Fuchs *et al.*, 1996; Fuchs *et al.*, 1997). A similar process has more recently been identified in Jun B and ATF2. Jun B phosphorylation has been shown to take place at threonines 102 and 104 via JNK MAP kinase (Li B *et al.*, 1999). Another way that Jun B is suggested to undergo phosphorylation is at mitosis associated with $p34^{cdc2}$-cyclin B Kinase at site positions 23, 150, 186, which correspond to Ser, Thr and Ser respectively (Bakiri *et al.*, 2000). The sequences in these regions is highly conserved in Jun B but not the other JUN proteins (Bakiri *et al.*, 2000). The seemingly contradictory roles for JNK with respect to both protecting and targeting JUN for degradation represent a fine tunable method of gene regulation, which is still not fully understood.

FOS regulating kinase (FRK) phosphorylates c-Fos at Thr-232, which is the homolog of Ser-73 of c-Jun. The amino acid Thr-232 occurs in the C-terminal domain, conserved between c-Jun and c-Fos (Sutherland *et al.*, 1992; Deng *et al.*, 1994). Extracellular signal related kinases (ERK) does not lead to direct activation of c-Fos through its phosphorylation but instead leads to increased c-Fos expression through its phosphorylation of TCF/Elk-1. The complex TCF/Elk-1 is a dimer of ternary complex factor (TCF) and Elk-1 (a member of the Ets family) (Deng *et al.*, 1994; Price *et al.*, 1996b). The phosphorylated dimer TCF/Elk-1 up-regulates c-Fos expression by binding to the c-FOS SRE (Price *et al.*, 1996a).

Kinase	Increased Activity	No Increase in Activity
JNK	UV, TNFα (large increase) and serum or growth factors (small increase).	
ERK	Serum, growth factors and PMA (large increase).	UV and TNFα.
FRK	Serum and growth factors (large increase).	PMA, UV and TNFα.

Figure 1.20.1 The AP-1 kinases and their activating mitogens (Suzuki *et al.*, 1991; Gille *et al.*, 1992; Kyriakis *et al.*, 1994; Minden *et al.*, 1994; Deng *et al.*, 1994; Cobb *et al.*, 1995; Lallemand *et al.*, 1997).

Jun and Fos factors can interact with the nuclear Factor κB (NFκB) p65 subunit through the Rel domain homology with RELA, binding to both AP-1 and NFκB (Stein *et al.*, 1993). Jun can also trans-activate the human MYB promoter by an AP-1-like sequence. The MYB transcription factor appears to be involved in the regulation of the cell cycle, inhibiting differentiation. The mechanism for this is unknown (Nicolaides *et al.*, 1992). Curiously there are also some suggestions of a role of c-Jun and c-Fos in apoptosis. This would appear to contradict the proliferative role. However, this role seems to be dependent on the *de novo* production of protein (Kovary *et al.*, 1991; Coletta *et al.*, 1992; Smeyne *et al.*, 1993; Treier *et al.*, 1994; Johnson *et al.*, 1996; Roffler *et al.*, 1996).

The AP-1 site is present in many gene promoters indicating how crucial it maybe in gene regulation (see Figure 1.23.1). The frequency of its occurrence and the diversity of dimer combinations AP-1 can form show that it has a complex role in the differential expression of many genes simultaneously.

1.21 The Transcription Factor SP-1 Binding Domain and its Factors

The transcription factor SP-1 (Specificity Protein-1) is a member of a family of four closely related factors. The family contains the factors SP-1, SP-2, SP-3 and SP-4. The SP-1 transcription factor is also a member of a bigger super family of zinc finger Krüppel like factors including BTEB, BTEB2 and Zf9. The Krüppel-like factors bind to sites

rich in GC nucleotides (Turner *et al.*, 1999). These sites occur in the gene promoters of both viral and eukaryotic origin (Sun *et al.*, 1989; Lania *et al.*, 1997; Ratziu *et al.*, 1998). The SP-1 consensus site is classically described as $^{T}/_{G}{}^{A}/_{G}GGCG^{T}/_{G}{}^{A}/_{G}{}^{A}/_{G}{}^{T}/_{C}$. The TIMP-1 minimal promoter SP-1 site is however divergent in only one base pair reading as GGGGCGGGGA (Clark *et al.*, 1997)

The SP-1 transcription factor was first identified in the Simian papovavirus number 40 (SV40). The early promoter of the SV40 virus contains three 21 base pair repeats, each repeat contains two SP-1 binding sites (Lania *et al.*, 1997). Using SV40 as a model SP-1 has been shown to act in either a context dependant or enhancer like manner. The enhancer functions appear to work via the interaction of SP-1 monomers both proximally and distally within the same promoter, through folding of the promoter to form homo-multimeric complexes (Courey *et al.*, 1991; Sun *et al.*, 1994).

SP-1 has been implicated in the transcriptional regulation of many of the proteins associated with fibrosis and the metabolism of ECM including collagen α_1 (I), α_2 (I), collagen II, collagen α_1 (IV), collagen α_1 (V), collagen α_1 (VI), biglycan, gelatinase A, gelatinase B and TIMPs 1-3 (Nehls *et al.*, 1991; Laurivcella-Lefebvre *et al.*, 1993; Schmidt *et al.*, 1993; Willimann *et al.*, 1994; Lee *et al.*, 1995b; Savagner *et al.*, 1995; Tamaki *et al.*, 1995; Wick *et al.*, 1995; Hammani *et al.*, 1996; HE *et al.*, 1996; Ungefroren *et al.*, 1996; Clark *et al.*, 1997). The HSC has been shown to express SP-1 by other groups. It has also been suggested that SP-1 is involved in the expression of collagen α_1 (1) in the HSC (Rippe *et al.*, 1995; Armendaris-Borunda *et al.*, 1994)

Recent studies of the GC-box binding factors led to the discovery of the new Krüppel-like transcription factor Zf9. Zf9 was first identified in the activated HSC, where it has been suggested to interact with GC rich areas in the promoter of TGFβ (Ratziu *et al.*, 1998; Kim *et al.*, 1998).

1.22 Leader Binding Protein-1 Binding Domain and its Factors

Leader Binding Protein-1 is a transcription factor first identified as having an active function in the transcription of the simian SV40 (major late promoter) through a 21bp repeat. The factor LBP-1 was initially known as a 63kDa protein, later called SV40 transcription factor (LSF) (Kim *et al.*, 1987; Huang *et al.*, 1990). Binding sites for LBP-1 have been identified in Human Immunodeficiency Virus (HIV) and the TIMP-1 gene (Wu *et al.*, 1988;Yoon *et al.*, 1994, Clark *et al.*, 1997). The sequence identified for LSF in the SV40 promoter was described as CCGCCC, which was also shown to bind SP-1.

The sequence initially identified for the consensus LBP-1 factor-binding site was CTCTCTGG, which appears twice in the HIV leader sequence or promoter (+5/+12 and +37/+44). The binding protein for these sites in HIV was called UBP-1 (Wu *et al.*, 1988). More recent work further characterised LBP-1 binding, determining the consensus binding domain to be $^{A}/_{T}$CTGG, of which three are present in the HIV LTR (-3/+2, +8/+12 and +40/+44) (Yoon *et al.*, 1994). The first two sites were shown to be functionally active, occurring on and/or close to the transcription start site. The binding of LBP-1 to these sites was unusual in that both were required for any binding or promoter activity. A mutation in either half site would result in no binding to that site or the other (Malim *et al.*, 1989; Yoon *et al.*, 1994). It was also shown that mutation and/or insertion of a linker into the flanking region separating the two sites had no effect on their function (Yoon *et al.*, 1994).

The TIMP-1 promoter has been shown, in the literature by other groups, to contain both the longer LSF/LBP-1 binding domain and the two shorter LBP-1 binding domains. These sites have been suggested to also possess transcriptional activity, marking the 3' boundary of the TIMP-1 minimal promoter (see Figure 1.22.1) (Clark *et al.*, 1997).

-12 Sense HIV LTR +22
TTTTGCCTGTACTGGGTCTCTCTGGTTAGACCAGA

+22Antisense HIV LTR +12
TCTGG TCTAA CCAGAGAGAC CCAGT ACAGGCAAAA

+22 Sense TIMP-1 Promoter +57
GATCCAGCGC CCAGAGAGACA CCAGA GGTAAGCAGG

Figure 1.22.1 A comparison of the LBP-1 binding domains found in the HIV LTR and the TIMP-1 minimal promoter. The bases underlined indicate the longer LBP-1/UBP-1 binding domains (Wu *et al.*, 1988). The bases highlighted in red indicate the shorter defined LBP-1 binding sites (Yoon *et al.*, 1994).

Another binding factor that is often mentioned with regard to LBP-1 is Ying Yang-1 (YY1). The reason for the association between YY1 and LBP-1 is that both sites are found in close proximity in the HIV LTR (Margolis *et al.*, 1994). The exact positioning of the YY1 binding site in the LTR is not indicated, but this may have due to the incredible diversity of suggestions for YY1 binding sites. YY1 is a 68 kDa member of the Krüppel family of zinc finger proteins (Shi *et al.*, 1991). The binding sites for YY1 are varied, although all have GC rich elements (see Figure 1.22.2).

Binding Sequence	Origin	Reference
N/A	HIV LTR –16 to +27	Margolis *et al.*, 1994
CGACATTTT, CTCCATTTT	Adeno Associated Virus P5 –60 and +1 respectively	Shi *et al.*, 1991
CGCCATTTT, $C^{G}/_{T}{}^{A}/_{C}$CATTTT	Moloney Murine Leukemia Virus	Flanagan *et al.*, 1992
CCTCCATC	Immunoglobulin κ	Park *et al.*, 1991
GCGGCCATC	Ribosomal proteins rpL30 rpL32	Hariharan *et al.*, 1991

Figure 1.22.2 Five binding sites for the transcription factor YY1, their promoter origin and reference.

1.23 Transcription Factor Regulation in the Hepatic Stellate Cell

A lot of research has been performed into transcription factors expression and activity in the HSC, in terms of the regulation of the activated or fibrotic phenotype (Mann *et al.*, In Press). Work has focused primarily on the molecular biological changes associated with the process of HSC activation and the regulation of some of the genes believed to be associated with the pathological process. It is for this reason that much of the work has focused on the genes of ECM production (pro-collagens etc), degradation (MMPs etc.), inhibitors of degrading enzymes (TIMPs, α_1-anti trypsin etc.), cytokines (IL-6 and TGFβ_1 etc.), apoptosis and structural proteins such as αSMA and desmin. This work has implicated a wide range of transcription factors, including nuclear factor κB (NFκB), activator protein-1 (AP-1), SP-1, BTEB, KLF-6 (formally ZF-9), cMyb, MyoD, Ets, AP-2 and PPARγ. In order to indicate the crucial role for these factors in fibrosis, the figure below shows diagrammatic representations of the promoters of some of the genes believed to be crucial in liver fibrosis (Figure 1.23.1).

The transcription factor binding site for activator protein-1 (AP-1) is present in many of the genes associated with liver fibrosis (Figure 1.23.1). However, in the literature AP-1 has been linked so far to the regulation of TIMP-1, IL-6 and Stromelysin in the HSC (Buttice *et al.*, 1991; Bahr *et al.*, 1999 and Smart *et al.*, 2001). There is definitely a larger role for AP-1 in the HSC, as yet undiscovered. One of the major roles for AP-1 is in the regulation of growth and the cell cycle and, in many cases, apoptosis. The regulation of the JUN proteins are linked to the expression of cyclin D1 and in Jun $D^{-/-}$ knockout animals, fibroblasts underwent premature senescence mediated via p53 (Kovary *et al.*, 1991; Coletta *et al.*, 1992; Smeyne *et al.*, 1993; Faris *et al.*, 1998; Wisdom *et al.*, 1999; Bakiri *et al.*, 2000; Weitzman *et al.*, 2000). The activation of the HSC, as previously mentioned, is associated with an increase in the binding activity of AP-1 factors shown by electrophoric mobility shift assay (EMSA). The changes in the relative expression of the binding proteins have been identified, indicating that there is an accumulation of Jun D, Fra 2 and Fos B in the activated HSC (see Section 1.19 and Figure 1.19.2).

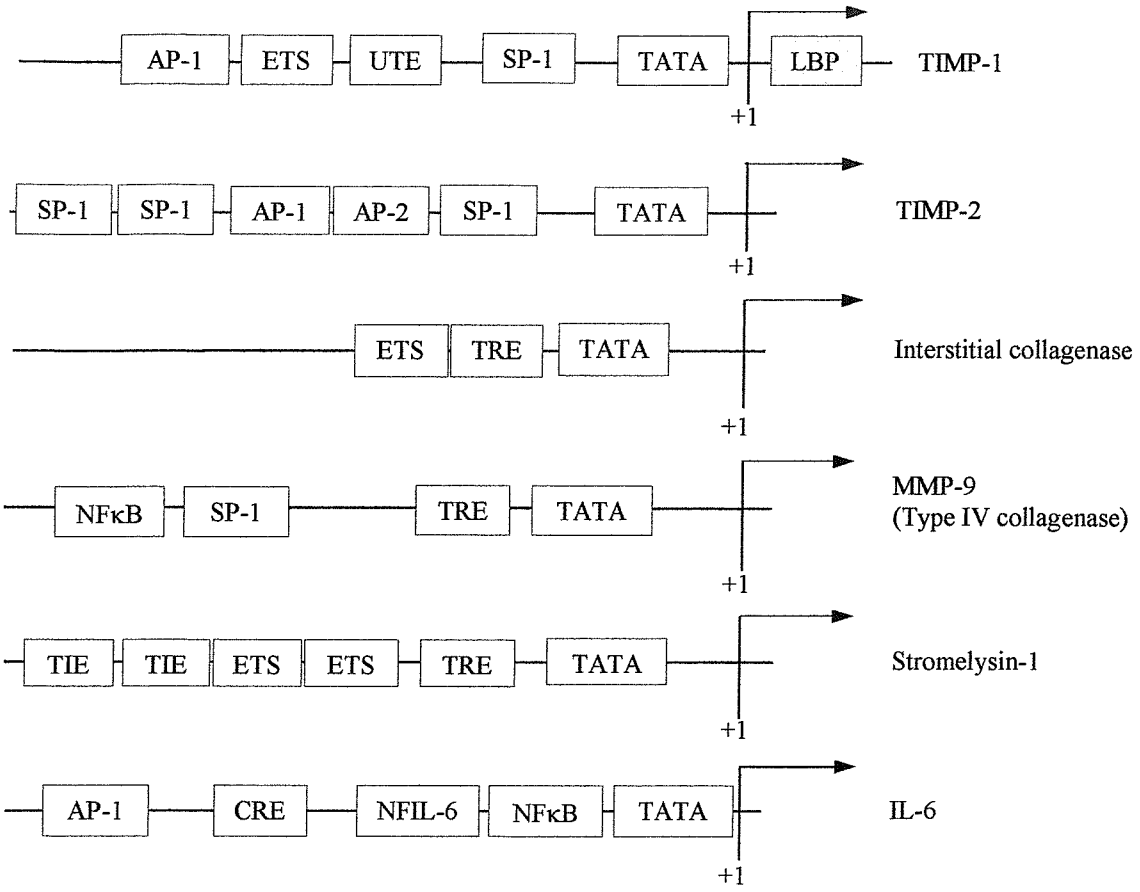

Figure 1.23.1. Diagrammatic representations of the promoter sequences of various gene promoters believed to be crucial to the pathology of liver fibrosis. TRE and TIE are 12-O Tetra decanoylphorbol-13-acetate (TPA) response and TGFβ inhibitory elements respectively (Angel *et al.*, 1987; Gutman *et al.*, 1990; Kerr *et al.*, 1990; Wasylyk *et al.*, 1991; Edwards *et al.*, 1992; Sato *et al.*, 1993; Hammani *et al.*, 1996; Clark *et al.*, 1997; Eikelberg *et al.*, 1999; Trim *et al.*, 2000).

Crucially, not only has the activity of AP-1 been shown to increase in the HSC as a result of *in vitro* culture on plastic, but also JNK and ERK have been shown to be up regulated in response to IL-1α, TNFα and fibronectin (Poulos *et al.*, 1997). Also importantly, JNK activity has been shown to be increased by acetaldehyde and 4-hydroxy-2,3-nonenal (HNE), a lipid peroxide metabolite, both of which could be important mediators in alcoholic liver disease. HNE could also be important in the mediation of liver disease resulting from iron overload, such as hemochromatosis (Parola *et al.*, 1998; Chen *et al.*, 2000; Anania *et al.*, 2001).

The factor NFκB, like AP-1, has binding sites in many genes and again, as with AP-1, many are shown to have functional roles in fibrosis. Genes in the HSC that have been suggested to be regulated by NFκB include IL-6, intracellular adhesion molecule-1 (ICAM-1), macrophage inflammatory protein-1 (MIP-1) and also α1(I) collagen, which has been shown to be negatively regulated (Hellerbrand *et al.*, 1996; Hellerbrand *et al.*, 1998; Rippe *et al.*, 1999; Elsharkawy *et al.*, 1999; Smart *et al.*, 2001).

The activation of the HSC is associated with an initial induction of the classical p50:p65 NFκB heterodimer followed by the persistent induction of both the p50:p65 and p65:p65 dimers. The expression of NFκB has also been shown to protect the HSC against TNFα induced apoptosis (Lang *et al.*, 2000). Additionally expression of NFκB has been shown to be blocked by an inhibitor called gliotoxin resulting in apoptosis (Elsharkawy *et al.*, 1999). Gliotoxin was also recently used in an *in vivo* study resulting in a reduction of observable fibrosis. The reduction in fibrosis was observed as a reduction in thickness of fibrotic septa and numbers of activated HSC when compared with carrier controls. These results identified the HSC as both a fibrotic potentiator and theoretic target (Wright *et al.*, 2001).

The factors SP-1 and BTEB, members of the SP-1 superfamily, have been identified in the HSC, regulating a number of potentiators of fibrosis. The functions of SP-1 and BTEB are over-lapped by the transcription factor ZF9 (formally KFL6). All three are Krüppel-like, possessing three zinc finger domains. These factors all also bind GC rich regions (Lania *et al.*, 1997; Ratziu *et al.*, 1998). ZF9 and SP-1 have been shown to be up regulated in the activated HSC. The factor SP-1 has been shown to be important in the regulation of α1(I) collagen, while the role of ZF9 appears to be associated with the expression of TGFβ1 and TGFβ I and II receptors (Kim *et al.*, 1998). ZF9 has also been associated with the transcriptional activation of the urokinase promoter in the vascular endothelium, which may well translate to the HSC (Kojima *et al.*, 2000). Urokinase plasminogen activator (uPA) is important as it not only activates MMPs (as previously mention, see Section 1.12) but it also activates latent TGFβI (Rippe *et al.*, 1995). A role has also been identified for the SP factor BTEB. This has been suggested both to bind

GC rich sites in α1(I) collagen promoter and also activate JNK, mediating an increase in AP-1 activity. The increase in BTEB has been shown to be induced by both UV and, more importantly as previously mention, by acetaldehyde (Chen *et al.*, 2000).

Oxidative stress in liver fibrosis has identified functions for a number of other transcription factors including c-Myb, CCAAT enhancer binding protein (C/EBP) and AP-1 (Lee *et al.*, 1995a; Garcia-Trevijano *et al.*, 1999). The addition of either TGFβ or H_2O_2 to HSC cells resulted in the increased expression of α1(I) collagen. The increase in expression was shown to be mediated by the binding of C/EBPβ was located to a cis-acting element between –370 and –344 in the collagen promoter (Garcia-Trevijano *et al.*, 1999).

Further work has shown that TNFα leads to an alteration in the C/EBP binding to the α1(I) collagen promoter at a similar site as described for TGFβ response, –378 to –345. The resulting change in complex binding leads to a down regulation in promoter activity. The complex binding upon TNFα stimulation contains p35C/EBPβ, p20C/EBPβ and C/EBPδ. It is believed that the proteins p20C/EBPβ and C/EBPδ are responsible for the negative promoter activity (Iraburu *et al.*, 2000). The expression of c-Myb was also shown to be induced by free radicals, collagen 1 ECM or CCl_4 liver injury. The transcription factor was shown to interact with an E-box-like site within the αSMA promoter (Lee *et al.*, 1995a; Buck *et al.*, 2000).

The E box binding proteins are a series of factors that bind as dimers to a sequence defined loosely as CANNTG. The E-box binding factors are members of the basic-helix-loop-helix (bHLH) family (Blackwell *et al.*, 1990). The bHLH proteins promote fibrosis in the HSC, causing an increase in production of the mannose 6-phosphate/ insulin-like growth factor II receptor (M6P/IGFIIR). The up regulation in M6P/IGFIIR has been shown to occur as a result of CCl_4 induced liver injury and subsequent down regulation of a novel binding repressor of 75kDa called p75 (Weiner *et al.*, 1998; Weiner *et al.*, 2000).

Another E-box binding bHLH transcription factor that may yet be of importance in fibrosis is MyoD, a tissue specific factor. The expression of MyoD in fibroblasts leads them to terminally differentiate into skeletal muscle cells (Yun *et al.*, 1996). A recent study has identified the expression of MyoD in the activated HSC (Vincent *et al.*, 2001). The discovery of MyoD is important because it may account for the adoption of the myofibroblastic phenotype, the expression of αSMA and possibly the contraction of the HSC, believed to contribute to portal hypertension (Nouchi *et al.*, 1991; Bosch *et al.*, 2000).

The transcription factors and the genes they regulate, described above, may all have a role to play in the greater fibrotic picture. For the purposes of this research it is possible to concentrate on only a few.

1.24 Elucidating the transcriptional regulation of the Tissue Inhibitor of Metalloproteinases-1 Gene in the Hepatic Stellate Cell.

TIMP-1 plays a fundamental role in the development of liver fibrosis by inhibiting the normal degradation of collagen (see Section 1.15). It has been previously shown that the expression of TIMP-1 is up regulated with the progression of liver fibrosis, both at the level of protein and message. The data suggest that the level of transcription of TIMP-1 expression is crucial to the progression of liver fibrosis.

Previous work by other members of the group has implicated, by truncation reporter analysis, both the AP-1 site and the LBP-1 site as important in the regulation of TIMP-1 in HSC (see Section 1.19). This role is supported in other cell types. The SP-1 site has been shown by other groups to be important in the regulation of other genes in the HSC, whose expression is also up-regulated with activation and fibrosis. It is possible that this site may also be identified as crucial for TIMP-1 regulation as there is such a site present in the minimal promoter between the AP-1 and LBP-1 sites.

Induction of high level TIMP-1 gene expression in activated HSC and fibrotic liver is due to changes in the expression and/or activity of transcription factors that regulate TIMP-1 gene transcription.

The aims of the work shown in this thesis were to:

- Investigate the specific effects of transcription factors on TIMP-1 expression in the HSC.
- Use mutational analysis to establish whether the transcription factor binding sites for AP-1, SP-1 and LBP-1 have a functional role in the regulation of TIMP-1 and/or phenotypic change in the HSC.
- Establish a mechanism by which the transcription factor-binding site exerts its influence over gene regulation in the HSC by identifying the binding factors present and the interactions with the site.
- Support the results observed *in vitro* wherever possible using an *in vivo* animal liver injury model.

Chapter 2.

Materials and Methods

2.1 Preparation of Plasmid DNA for Transfection

All plasmid stocks were produced by the propagation of transformed competent DH5α *Escherichia coli (E-coli)* bug stocks (long term frozen bacterial stock of clone). The DH5α is a modified laboratory strain containing mutations of the genetic markers ϕ80d*lac* ZΔM15, *rec A*1, *end A*1, *gyr* A96, *thi*-1, *hsd* R17 (r_k^-,m_k^+), *sup* E44, *rel A*1, *deo* R and Δ(*lac* ZYA-*arg F*)U169. The mutations of the DH5α genome allow the uptake of large plasmids, reduce endonuclease activity, prevent plasmid incorporation into genome, reduce β galactosidase activity, suppress UAG mutation and also allow RNA synthesis without protein synthesis.

2.1.1 Production of Competent DH5α *E-coli*

Un-transformed DH5α was streaked onto a Luria Broth (LB) plate and a LB ampicillin plate (see Section 2.18). As a negative control these were incubated overnight at 37°C. A LB standing culture of 10 ml was inoculated with a single colony and incubated overnight at 37°C. The overnight inoculant was used to inoculate a LB culture in an orbital shaker at 220rpm and 37°C. An aliquot of un-inoculated LB was taken and used as a blank for the measurement of optical density (OD) at 550nm (path length 1cm). The culture was incubated until the OD equalled 0.4 to 0.5. Upon reaching the specified OD the culture was incubated on ice for 15 minutes. The culture was centrifuged at 2000g and 4°C for 10 minutes. The pellet was re-suspended in ice cold RF1 (see Section 2.19) at 1/3 original volume. The suspension was incubated again on ice for 15 minutes before centrifuging (as before). The pellet was re-suspended at 1/12.5 original volume in ice cold RF2 (see Section 2.19). DH5α can be used immediately for transformation or stored at –70°C. The aliquots do not have to be snap frozen.

2.1.2 Transformation of DH5α

Between 10 and 100ng of DNA, in a volume of not more than 10μl, was added to 100μl of competent DH5α bacteria and incubated on ice for 30 minutes with occasional agitation. The DH5α were then heat shocked at 42°C for 2 minutes before being incubated on ice again for 5 minutes. The competent cells were allowed to warm to room

temperature before an equal volume of LB was added to the reaction. The inoculant was spread on a LB ampicilin plate and incubated at 37°C overnight.

2.1.3 Bacterial Propagation

Inoculants from frozen bug stocks were streaked onto LB Ampicillin petri dish plates before incubation overnight at 37°C in order to obtain single colonies. A single colony, or clone, from the plate was used to inoculate a sterile conical flask containing 100ml of LB or 30ml of Terrific Broth containing ampicillin (see Section 2.18). The inoculated broth was incubated overnight in an orbital shaker at 220rpm and 37°C. *E-coli* inoculants were centrifuged at 2400 rpm for 10 minutes at 4°C to pellet.

2.1.4 Production of Bacterial Stocks

Useful clones of bacteria transformed or otherwise were stored frozen. One clone from a streak plate was used to inoculate 10ml of LB with Ampicillin and incubated overnight at 37°C. The inoculant was then used to form a bacterial stock by the addition of 0.5ml of sterile 30% v/v glycerol to 0.5ml of the culture. The 15% (v/v) glycerol bacterial stock was mixed before freezing at –80°C.

2.1.5 Large Scale Plasmid Purification

Three different methods have been used for the large-scale purification of plasmid DNA from *E-coli* cultures throughout this research. Initially Sodium-columns (NACS, GIBCO BRL) were used before switching to the Polyethylene Glycol (PEG) extraction method. The initial methods of DNA purification were eventually replaced by the Maxi QIAfilter plasmid kit (Qiagen). The Maxi filter kit was used as it provided increased yields (>500μg), reduced protocol time, RNA and genomic DNA contamination.

2.1.6 Alkaline Lysis

The pelleted bacteria were re-suspended in 800μl of ice cold Solution 1 (see Section 2.20). Lysis was performed by the addition of 2.5ml of Solution 2, (see Section 2.20) while it was incubated on ice for 5 minutes. The reaction was neutralised by the addition of 1.9ml of Solution 3 (see Section 2.20) and incubated for a further 10 minutes on ice.

Centrifugation was performed at 10,000g for 5 minutes. The supernatant was precipitated at –20°C for 1 hour with 2 volumes of 100% ethanol. The subsequent pellet was re-dissolved with 30µl of Tris-HCL EDTA buffer pH 8.0 (TE) (see Section 2.17). The genomic DNA was selectively precipitated on ice for 20 minutes with 150µl of 7.5M Ammonium acetate. The genomic DNA was pelleted by centrifugation at 10,000g for 5 minutes and the supernatant was removed. The extracted nucleic acid in the supernatant was precipitated for 2 hours at –20°C by the addition of 2 volumes of 100% ethanol. The precipitate was pelleted at 10,000g for 10 minutes.

2.1.7 Sodium Column Plasmid DNA Extraction

The nucleic acid pellet obtained from the alkaline lysis (see Section 2.1.6) was dissolved in 500µl of TE + 50mM NaCl and 10µg of RNase A before incubating at 37°C for 15 minutes. Following incubation 500µl of TE + 350mM NaCl was added to the DNA solution to equilibrate it. The NACS column (GIBCO BRL) was initially hydrated with 2ml of TE + 2M NaCl. The column was then equilibrated with 10ml of TE + 0.2M NaCl, before passing through the buffered DNA solution twice. The plasmid was eluted with 1.2ml of TE + 0.7M NaCl. The eluted DNA was precipitated by the addition of 2 volumes of ice-cold 100% ethanol. The precipitating ethanol was incubated at –20°C for 2 hours before centrifuging at 10,000g for 10 minutes. The supernatant was removed and 300µl of 70% ethanol was added before pelleting again at 10,000g for 5 minutes. The supernatant was removed and the pellet air-dried before re-suspending in 200µl of distilled water.

2.1.8 Polyethylene Glycol Plasmid DNA Extraction

The pellet obtained from alkaline lysis (see Section 2.1.6) was re-suspended in 500µl TE with 10µg of RNase A. The re-suspended pellet was incubated at 37°C for 30 minutes. The re-suspension was extracted twice with 400µl of phenol/chloroform and once with 400µl of chloroform/isoamyl alcohol (see Section 2.10.4). The precipitation of the plasmid DNA was performed with an equal volume of isopropanol and then centrifuged at 10,000g for 10 minutes. The pellet was washed with 500µl of 70% ethanol and

allowed to air dry. The pellet was re-suspended with 32µl of H_2O, 8µl of 4M NaCl and 40µl of 13% Poly-Ethylene Glycol (PEG) 8000 before being incubated on ice for 1 hour. The sample was centrifuged at 10,000g for 15 minutes before being washed in 70% ethanol and re-suspended in 200µl of distilled water.

2.1.9 Maxi Filter Plasmid kit DNA Extraction (Qiagen)

The DH5α bug stocks were propagated by the addition of one colony to a 5 hour shaken culture in 10ml of LB and ampicillin as previously specified (see Section 2.1.3). The 10ml culture was used to inoculate an overnight shaken 100ml LB culture with ampicillin (see Section 2.1.3). The overnight culture was used as per manufacturer instructions.

The transformed bacteria were pelleted at 10,000g and 4°C for 10 minutes before performing alkaline lysis as with the previous methods using the supplied buffers. The pellet was re-suspended in 10ml of buffer P1 before alkaline lysis was performed by the addition of 10ml of buffer P2. Following the addition of P2, the bacteria suspension was mixed and the reaction was allowed to continue for 5 minutes. After the 5 minute incubation the lysis reaction was neutralised by the addition of 10ml of the neutralisation buffer P3 (see Section 2.20). The alkaline lysis using the Qiagen kit differs from previous methods in that the re-suspension buffer P1 contains the RNase A digestion set. Following the addition of the buffer P3 the lysate is placed into the supplied filter cartridge and allowed to settle for 10 minutes. During the settling period, the DNA extraction column was equilibrated with 10ml of QBT buffer. The bacterial lysate was added to the equilibrated column, and the precipitate was removed by forcing the solution through the filter cartridge with the supplied plunger. The bacterial lysate was allowed to pass through the Qiagen-tip by gravity flow before washing the column with 60ml of QC buffer. The plasmid DNA was finally eluted from the column in 15ml of QF buffer. The plasmid DNA was precipitate by the addition of 0.7 volumes or 10.5ml of Propan-2-ol. The DNA alcohol solution was cooled to 4°C before pipetting into separate 1.5ml microfuge tubes and centrifuging at 4°C, 10,000g for 30 minutes. The supernatant was removed and 300µl of 70% Ethanol added to each tube. The tubes were centrifuged again

at 10,000g for 5 minutes. The supernatant was removed and the pellets were allowed to air dry before re-suspending them in a total volume of 200µl of distilled water.

2.1.10 Small Scale Production of Plasmid DNA for Manipulation and Sequencing

Plasmid DNA produced for general manipulation was produced by propagation, (see Section 2.1.3) with a reduced overnight LB culture volume of 5-10ml. Plasmid DNA was initially extracted by Wizard Mini Prep (Promega) before changing to QIAprep Spin Miniprep (Qiagen). The plasmid extraction kits were used as protocol; with the exception that DNA was eluted into water in both cases rather than the supplied elution buffers that contain EDTA. The EDTA containing buffers although maximising yield and stabilising DNA, inhibit subsequent enzyme manipulation.

2.1.11 QIAprep Spin Miniprep Plasmid DNA Extraction (Qiagen)

From the 5-10ml of bacterial culture propagated, 1ml was removed into two separate tubes and bug stocks were made (see Section 2.1.4). The bug stocks were used for a permanent record and the second tube was sent for sequencing. 1.5ml of bug culture was pelleted at 10,000g for 5 minutes. The supernatant was removed and the pellet re-suspended in 250µl of the buffer P1. The bacterial suspension was lysed with the addition 250µl of supplied buffer P2. The lysing reaction was mixed by inversion before being incubated at room temperature for 5 minutes. The lysis reaction was neutralised following incubation by the addition of 250µl of the buffer P3, which was again mixed by inversion. The precipitate was removed by centrifugation at 10,000g for 10 minutes. The cleared solution was added to a purification column and centrifuged at 10,000g for 1 minute. The flow through was discarded and 750µl of the supplied PE buffer was added to the column before being centrifuged at 10,000g for 1 minute. The flow through was discarded before repeating the centrifugation. The column was removed to a new tube and 50µl of distilled water was added to the membrane. Before elutriation, a minute incubation was performed to maximise recovery the column was then centrifuged at 10,000g.

2.1.12 Quantitation of DNA Concentration

Plasmid DNA was quantitated using a spectrophotometer (Ultrospec 2100pro UV/Visible). Water from the same batch as that used to dissolve the DNA following plasmid extraction was used as a blank. The sample of the DNA for measurement was diluted at 1:25-250 with the same water and measurements with the spectrophotometer were taken at 260 and 280nm. The concentration of the sample was determined by the following:

$$\frac{\text{Absorbance (260nm)} \times 50 \times \text{dilution factor}}{1000} = \text{Concentration } \mu g/\mu l$$

The purity of the DNA was assessed by the 260/280 ratio and by agarose check gel in combination with restriction digests.

$$\frac{\text{Absorbance (260nm)}}{\text{Absorbance (280nm)}} = > 1.8 \text{ Considered to be of acceptable purity}$$

2.2 Sequencing DNA Constructs

At the beginning of my work I sequenced my own polymerase chain reaction (PCR) mutants and constructs. During the course of my studies the price of automated sequencing dropped sufficiently for commercial sequencing to become viable. Commercial sequencing is now cheaper, faster and offers guaranteed >500bp in under a week from a bug stock or 500ng of DNA. The commercial company primarily used for sequencing was Qiagen Sequencing Service, Germany.

2.2.1 Production of Single Stranded Plasmid DNA for Sequencing

5µg of Plasmid DNA were re-suspended in 50µl of DNA denaturing buffer (see Section 2.22). The reaction was heated at 37°C for 30 minutes before precipitation with 3M sodium acetate (1/10 volume) and 2 volumes 100% ethanol. The single stranded DNA was precipitated at –70°C and pelleted at 10,000g for 10 minutes, before washing with

50µl of 70% ethanol. The pellet was air dried before re-suspension in 7µl of distilled water.

2.2.2 Sequencing of Plasmid DNA

Plasmid DNA was sequenced using the T7 Sequenase Version II kit (Amersham). The kit was used as per protocol, with the preparation of single stranded DNA as stated above. Sequencing reactions were electrophoresed on a preheated 9% poly-acrylamide (Acrylamide: Bis ratio 19:1) denaturing gel, 6.5M Urea and 1x Tris-Base Boric Acid EDTA (TBE) pH 8.2 electrode buffer (see Section 2.17). The electrophoresis gel was heated by pre-running the gel at 40mA for 30 minutes before loading the samples. Electrophoresis was performed on the sequence reaction samples at 30mA for varying lengths of time, determined by the distance of the sequence of interest from the primer. Following electrophoresis, the gel was fixed for 20 minutes in 1 litre of 10% Glacial Acetic Acid, 10% methanol made up to volume with distilled H_2O. The sequencing gel was mounted on blotting paper and dried at 80°c, under vacuum. Imaging of the sequencing gel was performed by either exposure to Blue Autoradiography X-ray film (GRI) over night at –70°C or by exposure to a Phosphor Screen GP (Kodak) and subsequent scanning.

2.3 Eukaryotic Cell Work

2.3.1 Hepatic Stellate Cell Preparation

HSC were prepared from Sprague-Dawley rats (>350g), which were anaesthetised by intraperitoneal injection of 1ml/Kg of pentobarbitone (Sagital 60mg/ml, Gibco BRL). A catheter was inserted into the portal vein and the liver was perfused with 1ml of isotonic heparin (500U/ml) in Hank's buffered saline solution (HBSS) ($-Ca^{2+}$) (see Section 2.23). The liver was subsequently perfused at 10ml/minute with 100ml of HBSS ($+Ca^{2+}$) (see Section 2.23), 100ml of Pronase (2mg/ml) (Boehringer Mannheim) and 200ml of Collagenase (175µg/ml) (Boehringer Mannheim). All perfusions were performed at 37°C and enzyme dilutions were made in HBSS ($+Ca^{2+}$). The diluted enzymes were filter sterilised prior to use. The digested liver was disrupted to break the capsule before filtering through Nybolt nylon gauze. The cells were re-suspended and washed twice,

with 180ml of HBSS ($+Ca^{2+}$) and 20ml of DNAse (0.2mg/ml) (Boehringer Mannheim), and then pelleted by centrifugation (400g for 7 minutes). Primary purification of HSC was performed by density gradient, separating the more buoyant HSCs from the more abundant parenchymal cells. The cells were made up to a volume of 44.4ml with HBSS ($+Ca^{2+}$). This was added to 14ml of Optiprep (Nycomed / Life Technologies) and 15.6ml of HBSS with Ca^{2+}. This gradient was mixed gently before separation into two sterile centrifuge tubes. A 2ml layer HBSS ($+Ca^{2+}$) was placed upon each. Centrifugation was performed (1400g for 20 minutes) at room temperature and the lowest acceleration and brake settings were used. The buoyant cell layer was removed into separate tubes and a four-fold dilution was made in HBSS ($+Ca^{2+}$) before being centrifuged at 400g for 7 minutes. The pellets were combined in a 20ml volume of HBSS ($+Ca^{2+}$). The cells were then further density-purified by centrifugal elutriation (Beckman JE-21 centrifuge fitted with a JE6-B rotor; Beckman instruments, Geneva, Switzerland) at 1500 rpm and a flow rate of 18ml per minute. Elutriation is the separation of material or cells by density using a system of centrifuge counter flow, in which cells and suspension buffer (HBSS ($-Ca^{2+}$)) are pumped into a reservoir against the force induced by centrifugation. The densest matter remains at the entrance while the more buoyant material is eluted off at the centre of the centrifuge and collected (Knook *et al.*, 1976). Cell purity was assessed as better than 95% by vitamin A autofluorescence using an inverted epifluorescence microscope (328nm) and also by immuno histochemical staining for desmin.

2.3.2 Cell Culture

All cells were incubated in a 5% CO_2 atmosphere at 37°C. HSC, NIH3T3 (mouse fibroblast cell line) and Cos-1 cells (an SV40 transformed monkey kidney cell line) were cultured in Dulbecco Modified Eagles Medium (DMEM) plus serum and antibiotics (see Section 2.23).

2.3.3 Microscopy

The microscope used for tissue culture work and photography was a Leica DMIRB inverted microscope with phase contrast. Magnification available for phase contrast work was limited to 100, 160, 200 and 320x. Photography of cultured cells used Wild

MPS46 Photoautomat image processor and a Wild Leitz MPS52 camera (x0.32) attached to the Leica DMIRB microscope. Kodak EPY64T slide film was used for the cell culture photography. An inverted Carl Zeiss microscope was also used at a later date in combination with an AxioCam MR CCD camera and AxioVision 3.0 image capture software.

2.4 Electrophoretic Mobility Shift Assay (EMSA) Overview

2.4.1 Production of γ^{32}P Labeled Electrophoretic Mobility Shift Assay Probe

The oligonucleotides used were both synthesized commercially and obtained via collaboration. The oligonucleotides obtained were present in single strand form. The strand to be labeled was diluted to a concentration of 2.5pmol. 1µl of the strand to be radioactively tagged was placed in a 20µl labeling reaction. The labeling reaction also contained 2µl of 10x T4 polynucleotide kinase buffer (USB, One Phor All Buffer, Amersham), 5µl of [γ^{32}p] dATP (3000µCi/mmol at 10mCi/ml), 1µl of T4 polynucleotide kinase (10U/µl, Amersham) (added last to the reaction) and 11µl of distilled H_2O. The reaction was performed at 37°C for 30 minutes before being terminated with 30µl of TE buffer. The reaction was phenol/chloroform extracted once. The labeled oligonucleotide was precipitated by the addition of 5µl of 1µg/µl Polydeoxyinosinic-Deoxycytidylic acid (dI:dC), 5µl of 3M Sodium Acetate and 2 to 3 volumes of 100% Ethanol. The oligonucleotide was precipitated at –70°C for 30 minutes before centrifugation at 10,000g for 15 minutes. The pellet was washed twice with 70% ethanol before air drying and re-suspending in 17µl of H_2O for single stranded probes and 10µl for double stranded probes. When annealing oligonucleotides for a double stranded probe, 1µl of the re-suspended probe was removed. This was run separately on the gel to demonstrate annealing. The annealing of double stranded probes was performed by the addition of 1µl of 3 molar excess of probe. The reaction was then heated in a hot block to 95°C for 2 minutes and allowed to cool overnight. A hot block was used as it cooled very slowly to maximize annealing.

2.4.2 Production of Crude Nuclear and Cytoplasmic Extracts for Electrophoretic Mobility Shift Assay

Crude extracts were prepared using a modified protocol originally described in Dignam *et al*, 1983. All incubations and reagents were chilled on ice to reduce protease and phosphatase activity. The cells were washed twice in Phosphate Buffered Saline (PBS) (see Section 2.23) and removed from the culture plate mechanically before being pelleted at 5000g for 15 seconds. The cells were re-suspended in a volume of Dignam buffer A (Dig A, see Section 2.24) equal to the volume of the pellet, lysing the plasma membrane. The lysate was then centrifuged at 10,000g for 15 seconds to form a crude nuclei pellet. The supernatant was removed and a half volume of Dignam Buffer C (Dig C, see Section 2.24) was added. This formed the cytoplasmic extract. Nuclear extract was formed by the addition of a volume of Dig C, equal to the nuclei pellet volume, to the pellet. The pellet was incubated with Dig C for 10 minutes with intermittent vortexing. The debris was pelleted at 10,000g for 1 minute and the supernatant formed the crude nuclear extract. A small sample of the extract was removed for protein assay and the rest was aliquoted and frozen.

2.4.3 Determining the Concentration of Protein in Cellular Extracts

Protein concentrations of all crude cytoplasmic, nuclear and whole cell extracts were determined by the use of the DC colorimetric assay (BioRad). The reaction contained 1-5µl of extract made to a volume of 20µl with distilled H_2O, 100µl of Reagent A and 800µl of Reagent B. The reaction was incubated at room temperature for 20 minutes and the absorbance measured at 750nm. The blank for the reaction was made as above using an identical buffer to that of the extract. The protein concentration was ascertained by modification, with a constant obtained from regression of a standard curve between 0 and 20µg bovine serum albumin (BSA). The standard curve was repeated for each batch of DC colorimetric assay kit (BioRad).

2.4.4 Electrophoretic Mobility Shift Assay Protocol

Incubations for the EMSA were all carried out on ice. Each 18µl reaction contained 1µl of 1µg/µl poly dI:dC and 4µl of nuclear extract, adjusted for equal loading, between 5-

10μg of protein. The reaction was made up to volume with distilled water. Reaction volume and ionic concentration were kept constant by maintaining reaction volume. Competition with an unlabeled probe (to assess protein interaction specificity) and NaCl titrations were performed by dissolving them in distilled water and adding, in the place of the water, a reaction component. The reaction was incubated for 10 minutes before the addition of 2μl of the probe previously diluted 1:10 with distilled water to a concentration of 2.5nmol. The reaction was incubated for a further 10 minutes. Following incubation with the probe, 4μl of gel loading dye (see Section 2.17) was added to the reaction mix. The reaction was loaded onto a native 5% poly acrylamide (Acrylamide-Bis 37:1, Promega) electrophoresis gel and run in 0.5 x TBE electrophoresis buffer (see Section 2.17). Electrophoresis was performed at 15mA using a water-cooled gel electrophoresis tank (EMSA, Cambridge Electrophoresis Ltd.) until the free probe reached the bottom of the gel. The gel was mounted onto blotting paper and dried at 80°C under vacuum. Imaging was performed by exposure to Blue Autoradiography X-ray film (GRI) at –70°C.

2.4.5 Supershift Electrophoretic Mobility Shift Assay

The supershift protocol differs from that of the EMSA (2.4.4). In a supershift reaction volume was made up to 16μl instead of the 18μl used for the EMSA. Following the addition of the double stranded probe and subsequent incubation, 2μl of supershift antibody was added. The supershift antibodies were obtained in a purified form, with a low salt concentration and a high titre (1μg/μl) (see Appendix 4). Following the addition of the antibody, the samples were incubated overnight at 4°C before being loaded as normal. Non specific antibodies were added to parallel reactions as controls. The increased size in the complex formed by the specific binding of the antibody resulted in the reduction of motility on the polyacrylamide gel when compared with controls.

2.5 Eukaryotic Transient Transfection

Eukaryotic cells were transfected by a number of different methods. HSC transfection was initially performed by calcium phosphate method (Chen *et al.*, 1988). The calcium phosphate method was replaced by the Effectine (Qiagen), a non-liposomal system

(Fraley *et al.*, 1980). The Effectine method seemed to disrupt the cellular morphology less upon transfection and upon evaluation had considerably higher transfection efficiency. The improved efficiency required the transfection of fewer cells and the use of less DNA to obtain results of sufficient activity for assay.

Transfection efficiency was originally exclusively controlled by Hirt's assay (Hirt, 1967). This has changed in some of the later studies to co-transfection of 100ng of a high activity Renilla expression vector (Stables *et al.*, 1999).

2.5.1 Calcium Phosphate Transfection

The cells to be transfected had previously been plated out on 90mm tissue culture plates. In a laminar flow hood, 10μg of sterile DNA to be transfected (1μg/μl) was added to 240μl of 1M $CaCl_2$ before mixing. The DNA $CaCl_2$ mixture was then added drop wise to an equal volume of 2x Hepes Buffer Saline (HBS) and incubated at room temperature for 5 minutes. This precipitate suspension was added drop wise to a cell culture plate uniformly and the plate was returned to the incubator.

2.5.2 Effectine Transfection (Qiagen)

The cells by this protocol were transfected upon 45mm tissue culture plates when about 60-70% confluent. HSC were typically transfected with 1μg of reporter construct DNA per plate. The Effectine reagent was used as per protocol. In the case of a co-transfection, 3μg of the expression vector were also added and the transfection reagents modified as per manufacturers instructions. The Effectine system works by condensing the DNA and coating it in non-liposomal lipid to form micelles. The DNA for transfection was typically used at a stock concentration of either 1 or 0.5μg/μl. The plasmid DNA to be transfected was added to a sterile 1.5ml microfuge tube. Typically, for a 45mm tissue culture plate this would be 1μg of reporter vector and 100ng of Renilla transfection control plasmid. The supplied enhancer buffer was then added to the tube with the ratio of 3.2μl per μl of plasmid containing solution. The volume of the transfection reaction was made up to 100μl by the addition of the EC buffer. The reaction was vortexed and centrifuged briefly before being left for 2 minutes at room

temperature to incubate. 10µl of Effectine was added and the reaction was vortexed for 15 seconds, before incubating for 10 minutes at room temperature. During the final incubation the cell media was replaced with half the original volume, typically 1ml for 45mm tissue culture plates. Following the 10-minute incubation an equal volume of media was added to the transfection reaction and this was added to the plate of cells.

2.6 Chloramphenicol Acetyl Transferase Assay Overview

The Chloramphenicol Acetyl Transferase (CAT) assay provided a method for establishing the activity of a promoter in a cell type of interest (Laimins *et al.*, 1982). A reporter construct was transfected into the cells, which contained the CAT gene. The promoter of interest regulates transcription and therefore the expression of CAT within the cell. The transcription and subsequent expression of CAT therefore directly reflects the activity of the endogenous protein promoter of interest. The quantity of CAT present was measured by assay and therefore promoter activity was indirectly determined.

2.6.1 Production of Crude Cytoplasmic Extract for Assay

The cells were transfected 48 hours prior to harvest with the reporter construct. The cells were washed with PBS twice before pelleting at 5,000g for 15 seconds. The supernatant was removed and the cells re-suspended in 0.25M Tris-HCl pH7.8. Following suspension in Tris-HCl buffer pH7.8, the cells were snap frozen in liquid nitrogen, defrosted in a 37°C water bath and vortex disrupted three times. The lysates were centrifuged at 10,000g for 1 minute and the supernatant was removed, forming a crude cytoplasmic extract. The protein concentration was determined as previously described.

2.6.2 Chloramphenicol Acetyl Transferase Assay Protocol

Protein concentrations of samples for comparison were modified to 10-25µg of protein in a 50µl volume of 0.25M Tris-HCl pH 7.8. To each 50µl reaction 91µl of a master mix was added. The master mix represented 70µl of 1M Tris-HCl pH 7.8, 20µl of Acetyl Coenzyme A 3.25µg/µl and 1µl of 400µCi/ml [^{14}C] 35-50mCi/mmol Chloramphenicol (Amersham), for each reaction. The reaction was incubated at 37°C for 2 hours before the addition of 400µl of Ethyl Acetate and vortexing of the samples. The duration and

temperature of the incubation have been optimised to maximise Chloramphenicol conversion by previous researchers in the laboratory. The chloramphenicol was preferentially dissolved in the Ethyl Acetate and the samples were centrifuged at 10,000g for 2 minutes. The Ethyl Acetate was removed to a separate tube and dried in a vacuum concentrator (Speed Vac Plus SC10A, Savant). Each sample was re-suspended in 10µl of Ethyl Acetate before being loaded on to a 10x20cm aluminium 60 layer silica gel (F254) Thin Layer Chromatography (TLC) plate (DC, Alufolien). Chromatography was performed on the plate in an equilibrated tank containing 95% Chloroform and 5% Methanol, separating the acetylated product from the substrate chloramphenicol. Imaging was performed by plate exposure to Blue Autoradiography X-ray film (GRI) and quantitation was determined by phosphor image analysis using a Storm scanner and an Imagequant software data analysis package (Molecular Dynamics). The Phosphor screen GP (Kodak) was placed onto the TLC plate overnight and scanned the following day. For each of the products an equal area was analysed. The activity of each sample was calculated as a percentage of the total chloramphenicol that had undergone acetylation. This value would directly relate to the activity of the promoter (see Figure 2.6.2.1).

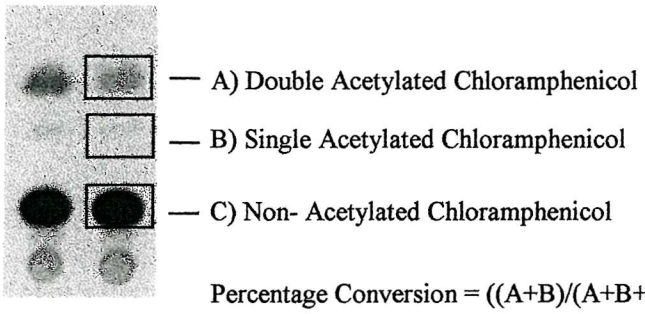

Figure 2.6.2.1 The calculation of percentage chloramphenicol conversion for an individual CAT assay sample.

2.7 Hirt's Assay

The Hirt's Assay is a method for standardising the effect of transfection efficiency. The cell pellets collected following the production of the cytoplasmic extract are assayed for their content of CAT reporter plasmid. The reporter plasmid is mounted onto nitrocellulose before being hybridized with a [^{32}P] labelled CAT probe. The quantity of hybridizing probe is proportional to the relative transfection efficiencies.

2.7.1 Production of Radioactively Labeled Chloramphenicol Acetyl Transferase Gene Probe by Polymerised Chain Reaction

The hybridization probe for Hirt's assay is produced by PCR (seen below).

Sense CAT Primer 100ng/μl	2μl
Anti-sense CAT Primer 100ng/μl	2μl
PBLCAT3 Template 100ng/μl	1μl
10x Taq Buffer	5μl
dNTP 10mM	1μl
dATP [γ^{32}P] (3000μCi/mmol) 1mM	1μl
Taq polymerase	1μl
H_2O	up to 50μl

30 cycles (94°C 1 minute, 55°C 1 minute, 72°C 1 minute)
Using a Perkin and Elmer Cetus DNA Thermal Cycler

The reaction conditions had been previously optimised by researchers in the laboratory. The probe precipitate before being re-suspended in 10μl of TE Buffer. The probe was run on a 1% ethidium bromide agarose gel alongside a λ DNA control in a titration before being excised and extracted. The probe was made up to a concentration of 25ng/μl.

2.7.2 Hirt's Assay Protocol

The cell pellet left over from the CAT assay was re-suspended in Hirt's solution (see Section 2.21) and 10μg of proteinase K was added before incubation at 37°C for 3 hours. The supernatant was recovered and phenol chloroform extracted. The sample was then ethanol precipitated and re-suspended before being normalized for DNA. The normalized cellular DNA was denatured by incubation at 100°C for 10 minutes with 10μl of 10N NaOH and 5μl of 0.5M EDTA in a total volume of 250μl.

The dot blot apparatus wells were then cleaned with 500µl of H_2O and the single stranded cellular DNA was added to the H^+ bond membrane. The DNA was then fixed to the membrane with 500µl of 0.4M NaOH. The NaOH was neutralised by the addition of 500µl of SSC (see Section 2.21). The membrane was pre-hybridised by immersion in 10ml of pre-hybridisation fluid (see Section 2.21) and placed in a hybridization oven at 65°C for 1 hour with 100ng of herring sperm DNA. The membrane was washed twice with SSC 10ml.

The membrane was hybridised with 4µl of the [α^{32}P]-dATP (25ng/µl) probe , added to 10ml of SSC and incubated overnight at 65°C. The membrane was washed twice in 2 x SSC for 15 minutes at 65°C. The membrane was dried before being quantitation determined by a Phosphor Screen GP (Kodak) and storm analysis. In order to control the CAT assay for transfection efficiency the equation shown below was used.

Controlled CAT Activity = CAT Conversion x (Hirt's Activity/Extract Concentration)

CAT Conversion = Percentage of Chloramphenicol Acetylated determined by CAT Assay
Extract Concentration = Cytoplasmic Protein Concentration used in CAT Assay
Hirt's Activity = Amount of hybridised CAT probe activity in as determined by Hirt's assay.

2.7.3 The Renilla luciferase Assay for Transfection Efficiency

The use of Renilla luciferase assay as a means of controlling for transfection efficiency replaced the Hirt's assay. The Renilla assay was used to control all the transfection studies. The cells were co-transfected with a Renilla luciferase expression plasmid as well as the reporter plasmid. The Renilla plasmid was used at a lower concentration than the reporter plasmids typically 100ng of Renilla to the usual 1µg of PBLCAT3 reporter, in a 45mm dish.

The washed transfected cells upon harvest were re-suspended in 1ml of PBS and 100µl of the suspension was removed to another tube. The tube containing the bulk of the suspension was used as previously described for CAT and the 100µl for Renilla assay.

The cells were centrifuged at 5000g for 15 seconds before removing the supernatant. The cell pellet was re-suspended in 50µl of 1x passive lysis buffer (Promega).

To measure the activity of the Renilla a tube containing 100µl of Renilla substrate re-suspended to a concentration of 1x in Renilla solvent and Stop-n-Glow buffer (Promega) was placed in a Luminometer. To the Renilla substrate was added 20µl of the cell pellet in passive lysis buffer. This was mixed 5 times by pipette and the luminosity was measured 3 times and an average taken ($R_{average}$). When the Renilla assay was used to control CAT assays the same equation was used as shown for the Hirt's assay. When using the dual luciferase assay the average Renilla figures for all the samples were compared and the lowest value identified (R_{min}). The equation shown below was then used to correct for transfection efficiency.

Corrected Luciferase Activity = Sample Luciferase Activity x (R_{min} / $R_{average}$)

2.8 Sodium Dodecyl Sulphate Polyacrylamide Gel Electrophoresis

Sodium Dodecyl Sulphate (SDS) Polyacrylamide Gel Electrophoresis (PAGE) was used to separate whole cell protein extracts by size, prior to Western blotting onto nitrocellulose membranes. These membranes were used for immuno-localisation with antibodies raised against specific proteins, for the purposes of identification and quantitation of protein species.

2.8.1 Preparation of Whole Cell Protein Extracts

Cells or liver tissue (see Section 2.13.3) were re-suspended or mechanically disrupted in PBS. Following the production of a homogenous cell suspension, 2µl were taken for protein assay and the rest of the sample was incubated on ice. The protein concentration was ascertained by colorimetric assay, as previously mentioned (see Section 2.4.3). Following the determination of protein concentration the samples were diluted in SDS sample buffer. The dilutions were made according to the lowest common denominator that provides at least a 2 fold excess of SDS sample buffer. Following suspension in SDS

sample buffer all the samples were immediately boiled for 10 minutes before use or freezing in aliquots for storage.

2.8.2 Pouring and Running Sodium Dodecyl Sulphate Polyacrylamide Gel

Electrophoresis was performed on samples on a two-phase SDS polyacrylamide gel run using the BioRad system. The bottom resolving gel (see Section 2.25) was poured to a level of not less than 1 cm below the level of the comb, before layering 100µl of Propan-2-ol on the surface of the setting gel. Once set, the Propan-2-ol was washed off with water and the gel surface blotted dry before the addition of the 4% stacking gel (see Section 2.25) layer with a comb to form the wells. Once set, the comb was removed and the wells washed with dH_2O. The gel or gels were mounted into the electrophoresis apparatus with running buffer. The protein size markers (Broad range, New England Biolabs) and samples were added. Electrophoresis was performed at 200 volts using the Mini Protean II Apparatus (BioRad).

2.8.3 Protein Transfer to Nitrocellulose

The gels were removed from the electrophoresis apparatus and the stacking gel layer was removed. The gels were allowed to equilibrate in transfer buffer (see Section 2.25) for 15 minutes. Transfer was performed using a wet blotting method (Mini Protean II, BioRad) Proteins were transferred to nitro-cellulose (NC Blotting membrane Protran, Schleicher & Schuell, Adinghurst) by horizontal electrophoresis in transfer buffer at 100 volts and 4°C for 1 hour.

2.8.4 Immuno-localisation of Proteins on Nitrocellulose Membranes

Following transfer, the nitro-cellulose membranes were washed for 20 minutes in 1 x Tris Buffered Saline (TBS) (see Section 2.25), 0.3% v/v Monolaurate Polyoxyethylenesorbitan (Tween 20) and blocked to prevent further protein binding. The membranes were placed in Membrane Blocking Buffer (see Section 2.25) overnight at 4°C. The membranes were washed for 1 hour in 1 x TBS-T, 0.05% v/v Tween 20 with frequent changes of buffer. The non-conjugated protein specific antibodies (Santa Cruz, unless otherwise specified, see Appendix 4) were applied to the membranes at

concentrations between 100ng and 1μg /ml, diluted in 1 x TBS-T, 0.05% v/v Tween 20, 0.3% w/v milk protein and 0.3% w/v BSA. The membrane was incubated in antibody for one hour at room temperature on an orbital shaker. Following incubation the diluted antibody was poured off and frozen for reuse (maximum of three times). The membrane was then washed for at least one hour with repeated changes of TBS-T. A species-IgG-specific Horseradish peroxidase (HRP) conjugate antibody, specific to the species in which the initial antibody was raised, was then added to the membrane. The conjugated antibodies (Sigma Aldrich, see Appendix 4) were diluted 1:2-3000 in TBS-T, 0.3% w/v milk protein. The membrane was incubated in conjugate for one hour. Following incubation, the antibody was discarded and the membrane was washed for at least one hour with repeated changes of TBS-T. As all the species-specific antibodies used were HRP conjugates, visualisation was performed using ECL Western Blotting Reagent (Amersham, RPN2106). ECL is a peroxidase catalysed reaction resulting in co-localised emission of light. Following application of ECL, the membrane was visualised by bracketed exposure to X-ray film.

2.9 Polymerase Chain Reaction

2.9.1 Single Step Mutational Polymerase Chain Reaction

Polymerised chain reaction (PCR) was used for the purpose of subcloning inserts from vectors and the generation of mutant promoter reporter constructs. All PCR reactions were performed using a thermocycler (Perkin and Elmer, Centur) and the Vent polymerase (New England Biolabs). Vent polymerase possesses a 5' exonuclease and proofreading activity, not present in many TAQ thermostable polymerases. All reactions were 50μl in volume, containing 200ng of each primer, 100ng of template DNA, 200-400μM dNTPs, 2-8mM $MgSO_4$, 1x Vent reaction buffer and 5 units of Vent polymerase. Samples were loaded with 50μl of mineral oil on the surface. Thermocycler programs varied with primers and template. Products of the reactions were purified from the template by agarose gel electrophoresis using a 1-2% agarose gel. DNA fragments were visualised by Ethidium Bromide 0.1μg/ml (added to the gel and the running buffer) on an UV light box (312nm). For a diagrammatic representation of the basic principal of PCR and single step mutational PCR, see Appendix 8i and 8ii respectively.

2.9.2 Two Step Methods of Mutation by PCR within a Large Construct

It was and still is impractical to generate mutations within large constructs due to the cost and poor production accuracy for long oligonucleotides. For these reasons it was deemed necessary to use an alternative method for mutation by PCR. To create mutation within a large construct a two-step PCR method was used.

Two primary PCR reactions were run simultaneously, each containing a short mutated sense or antisense central primer and its appropriate terminal primer, along with the TIMP-1 minimal promoter template (-111WT). The products of the first reactions were purified by electrophoresis on a 1.5% agarose gel and extracted using a QIAquick gel extraction kit (Qiagen). The fragments produced were then combined in a second reaction without any template (see Appendix 8iii).

2.10 DNA Manipulation

2.10.1 Restriction Enzyme Digests

AP-1 and SP-1 mutant TIMP-1 minimal promoter reporter constructs were produced by mutation PCR (see Chapters 3 and 5). The AP-1 and SP-1 TIMP-1 constructs were produced with 5' *Hind* III and 3' *Pst* I restriction sites. The restriction sites were used to clone the constructs into the compatible sites of the vector pBLCAT3 (see Appendix 2I). The restriction enzymes were used in a double digest with the enzymes *Pst* I and *Hind* III, Multi-Core buffer and acetylated BSA (Promega UK.). Digests were performed in a 40µl reaction volume with 2µl of each enzyme (10u/µl) and 2µg of DNA. The reaction was performed at 37°C for 2 hours with less than 10% enzyme by reaction volume.

2.10.2 DNA Ligation Reactions

Inserts produced by PCR or by enzyme digestion were ligated into vectors by the use of T4 DNA Ligase (Promega). Restriction enzyme digestions were used to produce compatible blunt or sticky ends. The ligation reaction consisted typically of 20pmol and 5 pmol of compatible predigested insert and vector respectively. The reactions were performed in a 20µl volume containing 2µl of the supplied 10x-ligase buffer and 2µl of

T4 DNA Ligase (1-3u/µl). The ligase buffer was aliquoted and stored at –20°C on first use. Ligation reactions were incubated at a temperature of 16°C overnight.

2.10.3 Purification of PCR Products and Restriction Digest Reactions

PCR and restriction digest fragments were size purified by electrophoresis on horizontal agarose gel at between 1-2% with 1xTAE pH 7.2 electrophoresis buffer. The samples were run alongside a DNA size marker ladder, either 1Kb or 100bp (Promega). DNA fragments were stained by Ethidium Bromide 0.1µg/ml (added to the gel and the running buffer) and visualised on an UV light box. The appropriate band was excised with a scalpel upon visualisation and the band was extracted by one of two methods.

The band was freeze thawed three times in liquid nitrogen and 37°C water bath, before being suspended in a small volume of extraction buffer. The tube containing the band was then shaken over night in an orbital incubator at 37°C. The DNA was precipitated with 1/10 volume of 3M Sodium Acetate pH 5.2 and 2 volumes of 100% Ethanol at –70°c for 30 minutes before centrifuging at 10,000g for 10 minutes and washing in 70% Ethanol.

The band could alternatively be excised as before, being purified by the QIAquick gel extraction (Qiagen). The excised band was weighed and 3 volumes or 300µl of the supplied QG buffer were added for every 100mg of gel. The gel and buffer were heated at 50°C with occasional mixing, until all the gel had been dissolved into solution. If the size of the purified fragment was <500bp or >4Kb then 1 volume of Propan-2-ol was added to the mixture. The gel solution was added to the QIAquick spin column and centrifuged at 10,000g for 1 minute. This was repeated if the gel solution exceeded the maximum 750µl of the column. The flow through was poured off and 750µl of PE buffer was added to the column and this was centrifuged at 10,000g for 1 minute. The flow through was again poured off and the centrifugation repeated. The column was removed to a new tube before adding 50µl of distilled water to the membrane. The column was incubated for 1 minute before elution by centrifugation at 10,000g for 1 minute.

2.10.4 Phenol/Chloroform Extraction

Phenol/chloroform extraction was used to remove protein contaminates from DNA in solution. An equal volume of Phenol/Chloroform/Isoamyl alcohol (50:49:1) was added to the sample. The sample was then vortexed for 5 seconds before centrifuging at 10,000g for 2 minutes. The aqueous top layer was removed into a second tube. The Phenol/Chloroform step was repeated more than once if the protein contamination was high. An equal volume of Chloroform/Isoamyl alcohol (48:2) was then added to the sample. The sample was vortexed and centrifuged as before. The top aqueous layer was removed to another tube and this solution contained purified DNA.

2.11 Production of Genomic DNA for Mouse Genotyping

Mouse tail tips were obtained from the weaned 4-week-old mice. The tails were first anaesthetized by the topical application of Lignocaine containing ointment. Following anaesthesia, 4mm of tail was removed with a scalpel and bleeding prevented by direct pressure. The animals were individually identified by ear punching. The tissue sample was divided in two and one half place in the –80°C freezer and the other was placed in 300µl of tissue lysis buffer (see Section 2.26) and incubated at 50°C over night with occasional agitation. Following incubation the digested tail was extracted with 300µl Phenol/Chloroform (see Section 2.17) and the vortex step was replace by manual flicking of the tube. Following the extraction, the DNA was precipitated with 2 volumes of 100% ethanol at –20°C for 1 hour. The DNA was pelleted at 10,000g for 10 minutes before removing ethanol, air drying and re-suspending in 50µl of sterile distilled water.

2.11.1 Genotyping Jun D Gene knockout Mice

The Jun D gene knockout mice were screened by genomic PCR using the oligonucleotide sequences (see Appendix 1) supplied by Dr J. Weitzman (Unité d' Histopathologie, Pasteur Institute, Paris, France) who also supplied the initial 3 breeding pairs of knockout animals. The Knockout was created by the replacement of the Jun D gene with the cDNA for Lac Z (Thepot *et al.*, 2000). As a result of the Jun D gene knockout, the males had a significantly lower fertility due to poor spermatid differentiation. For this reason the mice were bred as heterozygotes, leading to the production of wild type,

heterozygotes and knockouts in a 1:2:1 ratio and therefore it was necessary to genotype them. The oligonucleotides were used in two PCR reactions.

PCR Reaction	
Primer 1 100ng/μl	2μl
Primer 2 100ng/μl	2μl
Tail Genomic DNA	1μl
10x Taq Buffer	5μl
DNTPs 10mM	1μl
DMSO	5μl
Acetylated BSA	5μl
Taq polymerase	1μl
H_2O	up to 50μl

Primers 1 and 2 were Lac Z A or Jun D1 and Lac Z 2 or Jun D2 respectively (see Appendix 1).

1 x (94°C 2 minutes)
1 x (94°C 2 minute, 57°C 2 minutes, 72°C 2 minutes)
29 x (94°C 1 minute, 57°C 1 minutes, 72°C 2 minutes)

The resulting PCR samples were run on a 1.5% agarose TAE check gel along side a 100bp Ladder markers. The Lac Z and Jun D primers produce bands, which are 822bp and 315bp in size respectively.

2.12 Carbon Tetrachloride Liver Injury Models

Intraperitoneal administration of Carbon Tetrachloride (CCl_4) is used as a standard method of induction of acute liver injury and when used over a period of several weeks induces fibrosis (Paquet *et al.*, 1975; Friedman, 1996). In this work two different versions of this method were used. The two methods used were species specific but in both cases adult male animals were used. In the rat model the animals were injected

intraperitoneally twice weekly with 1µl/g (body weight) of either sterile olive oil or CCl_4 diluted in a 1:1 ratio with an olive oil carrier. The injections were performed typically for up to 6 weeks but may be as short as a single injection, in the case of an acute injury. In mice the CCl_4 was again administered intraperitoneally in a volume of 1µl/g (body weight) but this time the CCl_4 was diluted 1:4 with olive oil. The duration of treatment for mice was extended to 8 weeks.

2.13 Sampling Livers Following Injury Studies

The livers were sampled in three ways following CCl_4 liver injury studies, these were:

1) Perfusion and extraction of HSC.
2) Fixation for sectioning, histochemical and immuno-histochemical staining.
3) Frozen for whole liver, protein, RNA and cryo-sectioning.

2.13.1 Perfusion of CCl_4 Liver Injury Samples.

Perfusion for the extraction of HSC was only performed on rats following liver injury. The method of perfusion of rats upon which CCl_4 injury had been performed did not vary from the method described in 2.3.1. Cell extraction in mice was performed by the removal of liver directly into 10 ml of pronase (30mg) and collagenase (10mg). The mice livers were then chopped finely with scissors and incubated at 37°C for approximately 1 hour with rapid agitation before continuing as with the method described in Section 2.3.1. The quantities used in the Optiprep gradient for mice livers were halved and elutriation was not performed, due to lower cell numbers. The final cells were washed and cultured in a single flask.

2.13.2 Fixation of Samples for Staining

Samples of the livers from both mice and rats were sampled for histological staining. A small lobe of liver was removed and cut into 2-3mm sections before being placed into 10% formalin for 24-48 hours maximum. These pieces of fixed tissue were embedded in wax and sectioned by the hospital pathology department.

2.13.3 Preparation of Whole Liver Homogenates

Whole liver homogenates were performed on snap frozen pieces of the mouse or rat liver. Long-term storage of these samples was at –80°C. Samples of whole liver protein were obtained by removing a small section of approximately 0.5g with a scalpel from the frozen block. The sample of liver was placed into about 2ml of PBS. Using a 5ml syringe, the buffer and liver were drawn up and down at least 10 times through a 19G needle, until the homogenate flowed freely. The needle was then replaced with a 25G needle and the process was repeated. Following homogenization, the sample was diluted 2 fold, again in PBS, and placed on ice while a protein assay was performed upon 2µl of the sample. Following protein assay, a sample of the homogenate was taken and re-suspended at 1µg/µl in SDS sample buffer before boiling for 10 minutes.

2.13.4 Preparation of Whole Liver RNA

Whole liver RNA was prepared directly from frozen liver tissue. Using a sterile scalpel, a small fragment of the tissue was removed into a cryotube containing 1ml of ice-cold RTL buffer (Qiagen), to which 10µl per ml of Mercaptoethanol had already been added. The tube was then placed back on ice and the sample was homogenised by passing it through a 19G needle 10 or more times until the homogenate flowed freely. The process was then repeated using a 25G needle. The homogenate was then centrifuged through a QIAshredder at 10,000g for 1 minute (Qiagen). Next the sample was diluted with an equal volume of 70% Ethanol (made with Rnase-free water and ultra pure absolute Ethanol) before passing through 2 separate RNeasy extraction columns (Qiagen) at 10,000g for 30 seconds. The supernatant was discarded and 700µl of RW1 (Qiagen) was added to each column before centrifuging again at 10,000g for 30 seconds. The tube and supernatant were discarded and recovery tubes replaced. The columns were washed twice with 500µl of RPE buffer (Qiagen) at 10,000g and 30 seconds for the first wash and 2 minutes for the second. The recovery tubes were again discarded and this time replaced with Rnase-free microfuge tubes. Finally the samples were eluted from the columns by the addition of 40µl of RNase-free water directly to the membrane of each column. The columns were then centrifuged at 10,000g for 1 minute and the eluant for each sample

was combined. The RNA concentration was measured at 260nm and the integrity was checked by agarose gel electrophoresis.

2.14 Histology

2.14.1 De-Waxing Rehydrating Sections

The slide was immersed in xylene twice for 3 minutes each. Following de-waxing the sections were rehydrated by immersing once in each of the following for 2 minutes: 100%, 95% and 70% v/v Ethanol. The final stage was two 2-minute washes in distilled water in which the sections were left until staining. The section must not be left to air dry.

2.14.2 Dehydrating and Mounting Sections

Dehydrating is the quick immersion of the section in Ethanol, 30 seconds in 70%, 95% and then 2 washes in 100%. The excess ethanol was removed from the slides and they were cleared in xylene for 1 minute before mounting with DPX and a cover slip.

2.14.3 Hematoxylin and Eosin Staining

The sections were de-waxed and rehydrated before being stained with Harris's Hematoxylin for 5 minutes. The sections were then washed with alkaline tap water for 1 minute. Differentiation was performed for 10 seconds with acid alcohol (1%v/v HCL in 70%v/v Ethanol), before washing again in tap water for 5 minutes. The sections were then stained in 1%w/v Eosin for 5 minutes and washed in tap water for 1 minute. The sections were finally dehydrated, cleared and mounted.

2.14.4 Sirius Red Collagen Staining

The sections were de-waxed and rehydrated before treating with 0.2-0.5% Phosphomolybdic acid for 15 minutes. The cells were then treated with 0.1% Picric Sirius red (0.1% Sirius Red in saturated Picric Acid) for 3 hours. The slides were then briefly immersed in 0.01M HCL for 10 seconds. The sections were dehydrated immediately, cleared and mounted.

2.15 Taqman mRNA Quantitation

2.15.1 Production of Whole Liver cDNA

Following the extraction, purification and concentration measurement of the RNA from the whole liver homogenates, the RNA was digested with RNase-free DNase. Two reactions for each sample were performed. Each reaction consisted of 1μg of RNA in a 10μl reaction with 1μl of DNase Buffer, 1μl of DNase (1u/μl, Promega) and DNase. The reaction was performed at 37°C for 30 minutes. Following the incubation, 1μl of stop buffer was added and the reaction was heated to 65°C. Two master mixes were made up for the reverse transcriptase reactions. The first is shown below, the second reaction master mix was the same except that the MMLV was replaced with RNase-free H_2O.

4μl 5 x MMLV reaction buffer

2μ;l dNTPs (10mM)

2μl random primers (500 μg/ml)

0.1μl MMLV (200u/μl, Promega)

0.5μl Rnasin (40u/μl, Promega)

0.4μl RNase free H_2O

One of the DNase treated samples from each mouse was treated with the inclusive reverse transcriptase reaction mix and the other sample was treated with the MMLV free master mix to control for genomic DNA contamination. The two reactions were heated to 37°C for 1 hour and then to 95°C for 10 minutes before 80μl of RNase-free water were added and the reaction was aliquoted in 10μl volumes (10ng/μl).

2.15.2 Taqman Quantitative PCR

For each sample 3 Taqman reactions were performed for each gene tested. The reactions were set up as below, in a 25μl reaction volume. For each sample, one reaction was also performed in which the cDNA was replaced with a sample from the enzyme-free reverse transcriptase step, to identify genomic DNA contamination. The thermal cycling and quantitation were all performed *in situ* on the Taqman (Perkin Elmer ABI Prism 7700

Sequence Detector. The primers were designed by another researcher in the department (X. Zhou).

10ng cDNA (1μl)
0.3μM Forward Primer
0.3μM Reverse Primer
0.3μM Probe
RNase Free Water
1 x (50^{O}C 2 Minutes, 95^{O}C 10 Minutes)
50 x (95^{O}C 30 Seconds, 60^{O}C 1 Minute)

For each separate set of primers (αSMA, procollagen 1, TIMP-1 or GAPDH) there were three reactions performed for each individual. There was also a further reaction for each set of primers and individual, using the sample that was not RT treated, to test for genomic DNA contamination. Each set of three reactions was averaged and the average value for that individual's GAPDH was deducted. All three of the knockout mice values for that particular gene were averaged and the average of the wild types values for the same gene deducted. The relative level of transcription of a given gene in the knockout mice was then calculated by the following equation:

Relative level of transcription $=(1/(2^{A}))*100$
A= Average Knockout Mouse Value – Average Wild Type Mouse Value

The standard errors were obtained by calculating the difference of each individual mouse from the average wild type mouse value. This figure was then placed in the equation above for each mouse and the value calculated. The standard error was then calculated in the usual way.

2.16 General Reagents

All chemicals were obtained from SIGMA unless otherwise stated

Sterilization

Culture media, other non-heat labile buffers and equipment for both the cultures of prokaryotic and eucaryotic cells, were sterilized by autoclaving for 15 minutes at 121°c. Sterilization of heat labile solutions was performed by filtration 0.22μm (millipore).

Water

The water used for dilution of general reagents, where sterility was not necessary, was obtained from a centrally operated distillation facility with reverse osmosis. Where sterility or high purity was required bottled ultra pure water was used.

2.17 General Buffers

All buffers were made up to volume with distilled water unless otherwise stated.

Chloroform/Isoamyl Alcohol	
Chloroform	96% v/v
Isoamyl alcohol	4% v/v

Gel Extraction Buffer	
Ammonium Acetate (pH 8.0)	0.5M
EDTA	1mM

Gel Loading Buffer 6X	
Tris-HCl	10mM
Ficol 400	10% w/v
EDTA pH 8.0	50mM
Xylene Cyanol	0.2% w/v
Orange G	0.2% w/v
Bromo Phenol Blue	0.2% w/v

pH 7.5 Sterilized by filtration.

Phenol/Chloroform	
Phenol	50% v/v
Chloroform	49% v/v
Isoamyl alcohol	1% v/v

TAE 50x (Tris Acetate EDTA) Electrophoresis Buffer

Tris-Acetate pH 7.2	2M
Ethylenediaminetetraacetic acid (EDTA) (pH 8.0)	0.1M

TBE 5x (Tris Boric Acid EDTA) Electrophoresis Buffer

Tris-Base pH 8.3	0.5M
Boric Acid	0.4M
EDTA (pH 8)	10mM

TE (Tris EDTA)

Tris-HCl pH 8.0	10mM
EDTA (pH8.0)	1mM

2.18 Bacterial Culture

Ampicilliin

Ampicillin was used as a method of bacterial selection. The ampicillin stock was made at a concentration of 50mg/ml in distilled water before filter sterilization. The stock was stored in aliquots at –20°c and added to pre-sterilized culture media, where specified, at 50μg/ml. Aliquot freeze thaw was avoided.

LB (Luria Broth) Medium (1 litre)

Tryptone	1% w/v
Bacto. Yeast	0.5% w/v
Sodium Chloride	1% w/v

pH 7.0 (5M Sodium Hydroxide)
1.5% w/v agar was added before for culture plates (LB Agar). Autoclave

Terrific Medium (Broth)

Tryptone	13.5% w/v
Yeast Extract	2.7% w/v
Glycerol	0.45% v/v

Autoclave in 27ml volumes, add 3ml of phosphate buffer prior to inoculation.

Phosphate buffer

Monopotassium phosphate (KH_2PO_4)	0.17M
Dipotassium Phosphate (K_2HPO_4)	0.72M

Autoclave.

2.19 Production of Competent Dh5α *E-coli*

RF1

Rubidium Chloride	100mM
Manganese Chloride Tetrahydrate ($MnCl_2.4H_2O$)	50mM
Potassium Acetate	30mM
Calcium Chloride Dihydrate ($CaCl_2.2H_2O$)	10mM
Glycerol	15% (w/v)

Adjusted to pH 6.8 with Ethanoic (Acetic) Acid and sterilized by filtration.

RF2

Mops	10mM
Rubidium Chloride	10mM
Calcium Chloride Dihydrate ($CaCl_2.2H_2O$)	75mM
Glycerol	15% (w/v)

pH 5.8 with Sodium Hydroxide and sterilized by filtration.

2.20 Plasmid Purification

Alkaline Lysis

Solution 1 (TGE)

Tris-HCl pH 8.0	25mM
EDTA	10mM
Glucose	50mM

Solution 2 (Lysis Buffer)

Sodium dodecyl sulphate (SDS)	1% (w/v)
Sodium Hydroxide	0.2M

Solution 3 (neutralizing buffer)

Potassium Acetate	3M
Ethanoic (Acetic) Acid	5M

10x Ligase Buffer

Tris-HCl pH 7.8	300mM
Magnesium Chloride	100mM
Dithiothreitol (DTT)	100mM
Adenosine Triphosphate (ATP)	10mM

10x Mult-Core Buffer (Promega)

Tris-Acetate pH7.8	250mM
Pottassium Acetate	1M
Magnesium Acetate	100mM
DTT	10mM

P1 Buffer (Qiagen)

Tris-HCl pH8.0	50mM
EDTA	10mM
RNase A	100μg/ml

P2 Buffer (Qiagen)

Sodium Hydroxide	200mM
SDS	1%

P3 Buffer (Qiagen)

Potassium Acetate pH5.5	3M

QBT Buffer (Qiagen)

Sodium Chloride	750mM
MOPS pH7.0	50mM
Isopropanol	15%
Triton X-100	0.15%

QC Buffer (Qiagen)

Sodium Chloride	1.0M
MOPS pH7	50mM
Isopropanol	15%

QF Buffer (Qiagen)

Sodium Chloride	1.25M
Tris-HCl pH8.5	50mM
Isopropanol	15%

2.21 Hirt's Assay

Hirt's Solution

SDS	10mM
Tris-HCl	10mM
EDTA pH 8.0	10mM

SCC 20x

Sodium Chloride	3M
Sodium Citrate	0.3M

Denhardt's Stock Solution

Albumin	2% w/v
Ficol 400	2% w/v
Polyvinylpyrrolidon	2%w/v

Pre-Hybridization Fluid

20x SSC	3ml
Denhardt's Solution	0.5ml
20% SDS	250µl
Make up to 10ml dH_2O	

2.22 DNA Sequencing

DNA Denaturing Buffer

Sodium Hydroxide	200mM
EDTA pH8	200µM

Acrylamide Gel (Denaturing)

Acrylamide	8% w/v
Urea	7M
TBE.	x1
Ammonium Persulphate (APS)	0.008% w/v
N,N,N',N'-Tetramethylethylenediamine (TEMED)	0.16% v/v

Formamide Loading Buffer

Formamide	95% v/v
EDTA	20mM
Bromophenol Blue	0.05% w/v
Xylene Cyanol FF	0.05% w/v

Gel Fixative

Methanol	10% v/v
Ethanoic (Acetic) Acid	10% v/v

2.23Eukaryotic Cell Culture

Hank's Buffered Saline (- or + Ca^{2+}) (HBSS)

Obtained as a 10x stock (Gibco)

HBSS 10x	100 ml
Sodium bicarbonate (7.5%)	4.6 ml
Hepes (1M)	5ml

Made up to 1 Litre with sterile water.

Dulbecco Modified Eagle Medium (DMEM)

DMEM 10x (Gibco)	500 ml
Glutamine (200mM)	50 ml
Sodium Bicarbonate (7.5%)	250ml

Adjust to pH 7.1 and volume to 5L Filter sterilise

Serum and Antibiotics

Fetal Calf Serum (Gibco)	16%
Penicillin and Streptomycin (Gibco)	500U/ml

Phosphate Buffered Saline
Obtained in tablet form (Sigma, P4417)
Dissolved in distilled H_2O and autoclaved

Phosphate Buffered Saline

Sodium Chloride	137mM
Potassium Chloride	2.7mM
Disodium Phosphate (Na_2HPO_4)	4.3mM
Monopotassium Phosphate (KH_2PO_4)	1.47mM
pH 7.4	

2.24Electrophoretic Mobility Shift Assay

Acrylamide Gel (Non-denaturing)

Acrylamide-Bis 37:1	5% w/v
TBE	0.5x
APS 10% w/v	0.8% v/v
TEMED	0.16% v/v

Nuclear Extraction
Dignam A – Inhibitors (Plasma Membrane Lysis Buffer)

Hepes	10mM
Magnesium Chloride	1.5mM
Potassium Chloride	10mM
DTT	0.5mM
Tergitol (NP40)	0.2% v/v

Dignam C – Inhibitors (Nuclear Membrane Lysis Buffer)

Hepes	20mM
Glycerol	25% v/v
Sodium Chloride	0.42M
Magnesium Chloride	1.5mM
DTT	0.5mM
EDTA	0.2mM

Proteinase and Phosphatase inhibitors
Added to Dignam A and C Extraction Buffers

Sodium Orthovanadate (Na_3VO_4)	1mM
Sodium Floride	1mM
4-(2-Aminoethyl)benzenesulfonyl fluoride (AEBSF)	1mM
Aprotinin	2µg/ml

2.25 Sodium Dodecyl Sulphate Polyacrylamide Gel Electrophoresis and Western Blotting

SDS Sample Buffer

Tris-HCl 0.5M pH 6.8	12.5% v/v
Glycerol	10% v/v
Sodium Lauryl Sulphate (SDS)	2% w/v
Bromo Phenol Blue	0.004% w/v
DTT	10mM

SDS PAGE 5X Electrophoresis Buffer

Tris Base	124mM
Glycine	1M
SDS	173mM

Volume adjusted with distilled water, pH 8.3 don't adjust

SDS PAGE 4% Stacking Gel

Tris-HCL pH 6.8	375mM
SDS	3.5mM
Acrylamide-Bis 37:1	4.0% w/v
APS	0.1% w/v
TEMED	0.1% v/v

SDS PAGE 7.5% Resolving Gel

Tris-HCl pH 8.8	375mM
SDS	3.5mM
Acrylamide-Bis 37:1	7.5% w/v
APS	0.05% w/v
TEMED	0.1% v/v

Transfer Buffer (Western)

Tris-Base	25mM
Glycine	192mM
Methanol (BDH)	20% v/v

Adjust volume with distilled water, pH 8.3 don't adjust

Tris Buffer Saline (TBS) X 20

NaCl	4M
Tris-HCl pH 7.4	0.4mM

Membrane Blocking Buffer

TBS	1x
Tween 20	0.3% v/v
Skimmed Milk protein (Mavel)	3% w/v

TBS-T

TBS	1x
Tween 20	0.15% v/v

Antibody Binding Buffer

TBS	1x
Tween 20	0.15% v/v
Skimmed Milk protein (Mavel)	0.6% w/v
Bovine Serum Albumin (BSA)	0.6% w/v

2.26Genomic PCR

Tissue Lysis Buffer

Tris-HCl pH 8.5	100mM
EDTA	5mM
SDS	0.2%w/v
NaCl	200mM
Proteinase K	0.01%w/v

Chapter 3.

The Role of AP-1 Proteins as Regulators of TIMP-1 and IL-6 Gene Transcription.

3.1 Introduction

As previously mentioned (see Section 1.7) during fibrosis or culture on plastic the HSC becomes "activated", leading to a biochemical and phenotypic change. This culminates in an increase in TIMP-1 promoter activity and the subsequent expression of protein.

Truncation analysis of the human TIMP-1 gene in the HSC implicated the putative Activator Protein-1 (AP-1) and Leader Binding Protein-1 (LBP-1) transcription factor sites as crucial elements of the minimal promoter (see Appendix 6). The AP-1 site between –92 and –86 of TIMP-1 gene marked the 5' end of the minimal promoter. Repetition in other cell types supports these findings, by identifying identical minimal promoters (Clark *et al.*, 1997; Bahr *et al.*, 1997). The 5' TIMP-1 AP-1 binding site contains an alteration from the established consensus sequence, TGAGTAA and TGAGTCA respectively.

A consistent change in the expression of the AP-1 binding proteins had also been observed with the activation and phenotypic change of the HSC. Electrophoretic Mobility Shift Assay (EMSA) performed by another PhD student in the department (now Dr KJ Vincent) had identified an alteration in the binding of proteins to the AP-1 like site. The oligonucleotides used to probe for AP-1 binding in the EMSA were the AP-1-like TIMP-1 binding site (5' TIMP-1 minimal promoter) and an AP-1 consensus double stranded oligonucleotide (collagen I promoter). Super shift analysis and Western blotting, performed by Dr KJ Vincent and Dr MC Wright (also in the department) respectively, implicate Fos B, Fra-2 and Jun D protein interactions with the AP-1 binding sites in the activated HSC (Bahr *et al.*, 1999).

Classically the expression of TIMP-1 is associated with the expression of the c-Jun and c-Fos AP-1 transcription factors, enhanced by the formation of a complex with c-Ets (Edwards *et al.*, 1992; Logan *et al.*, 1996). In the HSC, however, the TIMP-1 promoter would not appear to be classically regulated. Previous data have shown a down regulation of c-Jun, c-Fos and c-Ets with "activation" of HSC, concurrent with an increase in TIMP-1 expression (Bahr *et al.*, 1999; Knittel *et al.*, 1999). The c-Jun / c-Fos

AP-1 proteins are replaced by Jun D, Fra-2 and Fos B (see Figure 1.19.2), concurrent with enhanced TIMP-1 expression. Jun D is expressed at low levels in freshly isolated cells and expression increases with HSC activation (Bahr *et al.*, 1999).

3.2 Mutation of Activator Protein–1 Transcription Factor Site

Previous work on the TIMP-1 promoter in the HSC had circumstantially implicated the AP-1 site as the functional regulator of transcription in the TIMP-1 gene. This work had only identified its presence and the availability of binding factors such as the JUN and FOS proteins (Bahr *et al.*, 1997). To test whether the AP-1 site was in fact crucial, a mutated minimal promoter reporter (5'AP-1 mutant) was constructed by mutational PCR (see Section 2.9.1). The mutant construct was produced using a wild type 3' and a mutated 5' primer (see Appendix 1) corresponding to the 3' and 5' ends of the TIMP-1 minimal promoter. The primers contained restriction sites for *Hind III* and *Pst I* situated 5' and 3' respectively (see Section 2.10.1). The PCR product was ligated into pBLCAT3 (see Section 2.10.2), which is a recognised chloramphenicol acetyl transferase (CAT) reporter vector, containing no promoter sequence (see Appendix 2i).

The effect of an AP-1 mutation in the TIMP-1 minimal promoter was established by the parallel transfection of the mutated and the TIMP-1 wild type-CAT reporter (-111WT). The activity of the two promoters was then compared by CAT assay and the role of AP-1 established.

Transfection of the 5' AP-1 mutant identified a significant decrease of 70% in the activity of the minimal promoter when compared to the wild type (Figure 3.2.1). This indicated that the AP-1 site is indeed crucial for the high level activity of the TIMP-1 minimal promoter in activated HSC (Bahr *et al.*, 1999)

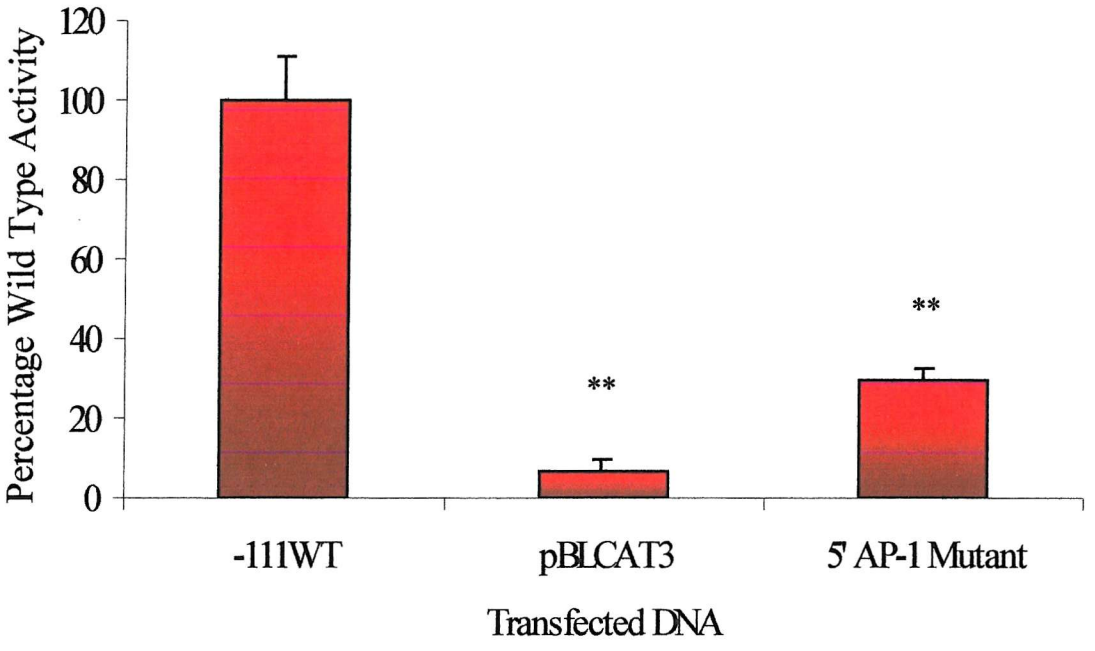

Figure 3.2.1. The effect of a mutation in the AP-1 transcription factor binding site on the activity of the TIMP-1 minimal promoter. 10μg of each of the plasmids was transfected into a 90mm petri dish using calcium phosphate precipitation. Each petri dish was initially plated out with $2.5x10^6$ cells at day 0 and transfections performed at >7 Days culture upon the plate reaching 60-70% confluence. Following transfection the cells were cultured for 48hr before harvesting. The results are plotted as mean and standard error of a representative triplicate transfection, performed on three occasions using cells from different individuals. Transfection efficiency was established by Hirt's assay (see Section 2.7). An indication of the data significance can be obtained from the presence of a * or **. These represent P values of <0.05 and <0.01 respectively, established by Student's T-test of un-equal variance with two tails. For the primary data see Appendix 3.

3.3 Elucidating the Role of JUN and FOS Proteins in Hepatic Stellate Cells

The ability of an AP-1 binding site to effect the transcription of a gene can be regulated by its availability to specific binding proteins and its position with respect to other transcription factor binding sites with which it may interact. The activity of a transcription-factor-binding site may be closely controlled by the relative expression and/or activation of its binding proteins. This may lead to variation in binding dimeric combinations; each may possess differing characteristics. The requirement of the AP-1 site in the minimal promoter of TIMP-1 suggests that its binding proteins are both stoichiometrically available and that it is positioned such that it can influence transcription. As previously mentioned, classically, the expression of TIMP-1 is associated with the expression of c-Jun and c-Fos (Edwards *et al.*, 1992; Logan *et al.*, 1996). In freshly isolated HSC, however, expression of c-Jun and c-Fos are associated with undetectable levels of TIMP-1 expression. The reverse is true of activated HSC, in which TIMP-1 is expressed and c-Jun and c-Fos are absent.

In order that the roles of the various JUN and FOS proteins could be established, a series of AP-1 protein expression vectors were obtained via collaboration with Dr. PR Dobner (Dept. Mol. Genetics and Microbiology, University of Massachusetts) (McCabe *et al.*, 1996). The AP-1 expression vectors each contained the relevant cDNA in the pCMV2 (see Appendix 2ii) expression vector. The pCMV2 cDNA expression vector is driven by the Cytomegalovirus (CMV) promoter. These expression vectors were intended to investigate the roles of the various AP-1 proteins by modulating their expression, and therefore the dimeric combinations following co-transfection with a TIMP-1 minimal promoter reporter construct.

3.4 Verifying JUN and FOS Expression Vector Function

The AP-1 vectors were initially transfected into 45mm tissue culture dishes of activated HSC, which had been cultured for more than 7 days. The HSC were transfected with 1μg of expression vector or empty vector as a control (see Section 2.5.2) and cultured for 24 hours before making whole cell lysates (see Section 2.8.1). The lysates from the HSC transfections with AP-1 protein expression vectors were used for SDS PAGE and

subsequent Western blotting (see Section 2.8.1-5), to establish the validity of the constructs (data not shown). The results from the Western blots of the transfections of HSC did not show a satisfactorily increased expression of the appropriate proteins. The transfections of the expression vectors were repeated in Cos-1 cells also using 45mm dishes with 1μg per dish by the Qiagen Effectine system.

In Cos-1 cells the expression vectors showed a satisfactory up-regulation of AP-1 protein expression (Figure 3.4.1 A-C and 3.4.2 A-C). The results indicate that c-Jun and Jun B are indeed expressed at their expected molecular weights of 39 and 42kDa respectively (Figure 3.4.1 A and B). Cells transfected with Jun D-pCMV2 expressed two main species in the expected size range for Jun D, which is between 40 and 50 kDa (Figure 3.4.1). The variation in the molecular weight of Jun D is believed to occur for two reasons; altered states of Jun D phosphorylation or as a result of the short and long isoforms of Jun D, which are 39 and 44 kDa respectively. The two different forms of Jun D are produced through initiation of translation from the third rather than the first AUG site (Okazaki *et al.*, 1998).

The Western blots for c-Fos and Fra-2 identified the expression of a protein at the correct molecular weight, 62 and 35 kDa respectively (Figure 3.4.2 A and C). The Western blot for Fos B (Figure 3.4.2 C) identified an increased expression of a lower band. The supplementary band, with an affinity for the Fos B antibody, is probably a Fos B protein fragment, resulting from the rapid turnover of protein. No results for Fra 1 are shown as this was never successfully demonstrated by western blot.

The unsatisfactory results of the Western blots, following transfection of the HSC, are probably due to a number of factors, including the low transfection efficiency presently achievable (approximately 10%) and lower expression vector promoter activity. Cos-1 cells are more easily transfected than many primary HSC. Cos-1 cells also possess a higher transcriptional activity of the gene transfected, due in part to the SV40 transformation and also the presence of an SV40 replication site within the plasmid. The

SV40 transformation leads to multiple plasmid copies within each cell, resulting in an increased amount of protein produced.

Although the results of the transfection of the HSC had been unsatisfactory by Western blot, the Cos-1 cell work had shown the constructs to be functional. It was felt that the low level of transfection would not be a problem as so long as the expression vector was in excess, relative to the reporter construct. It was also suggested that the expression vector DNA would follow that of the reporter, in the same way that one may use a constitutively active β-galactosidase plasmid to control for transfection efficiency.

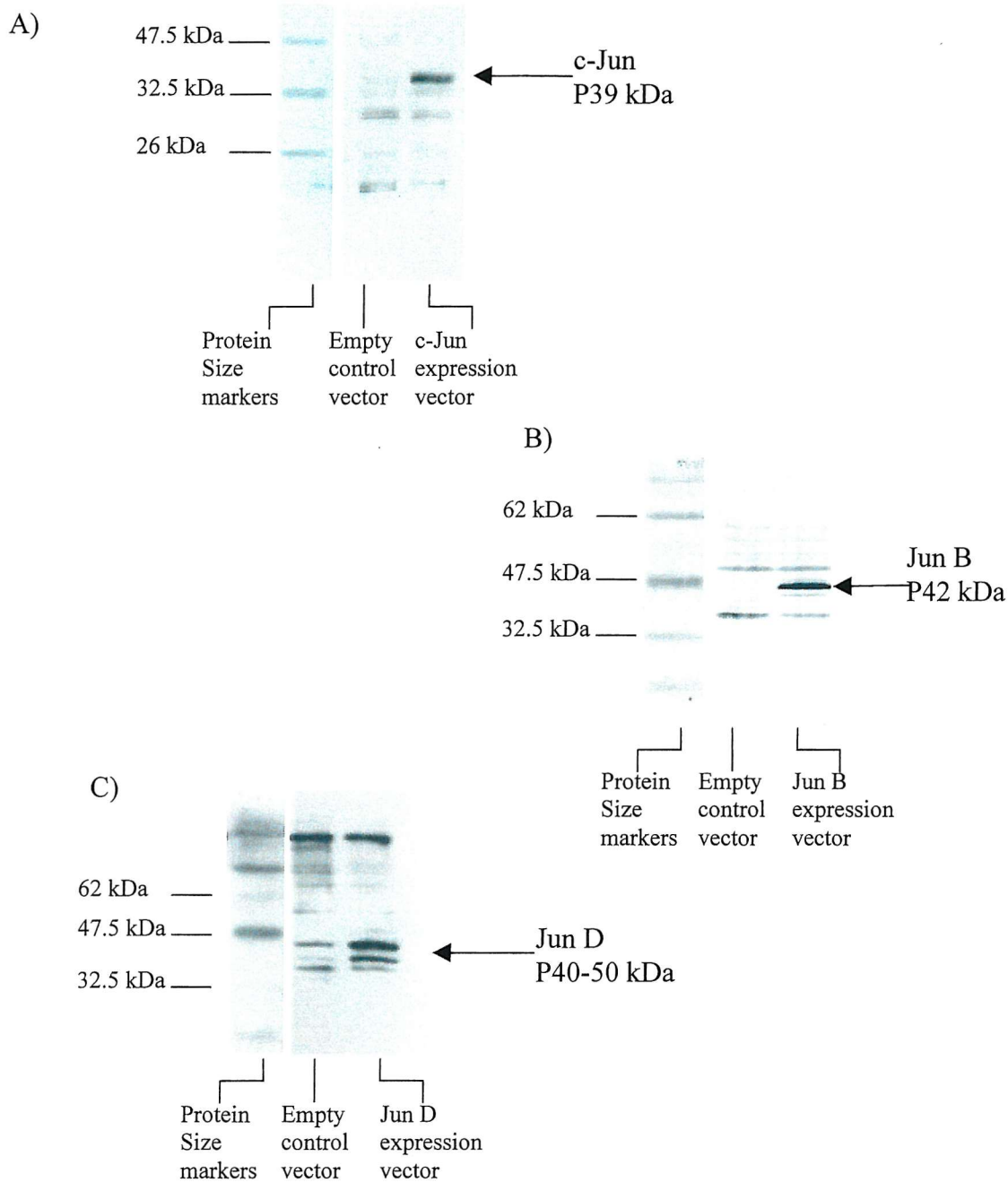

Figure 3.4.1 The Western blots of JUN family AP-1 proteins following transfection into Cos-1 cells of, A) c-Jun-pCMV2 expression vector B) Jun B-pCMV2 expression vector and C) Jun D-pCMV2 expression vector. In each experiment the Cos-1 cells were grown on 45mm tissue culture plates until 60-70% confluent. The Cos-1 cells were transfected with 1μg of JUN-pCMV2 protein expression vector or empty control pCMV2. The primary JUN specific polyclonal antibodies were all raised in rabbit (Santa Cruz) and used at 1μg/ml and the secondary rabbit IgG specific horseradish peroxidase (HRP) conjugate antibody (Sigma) was used at 1:2000 dilution. For all antibodies see Appendix 4.

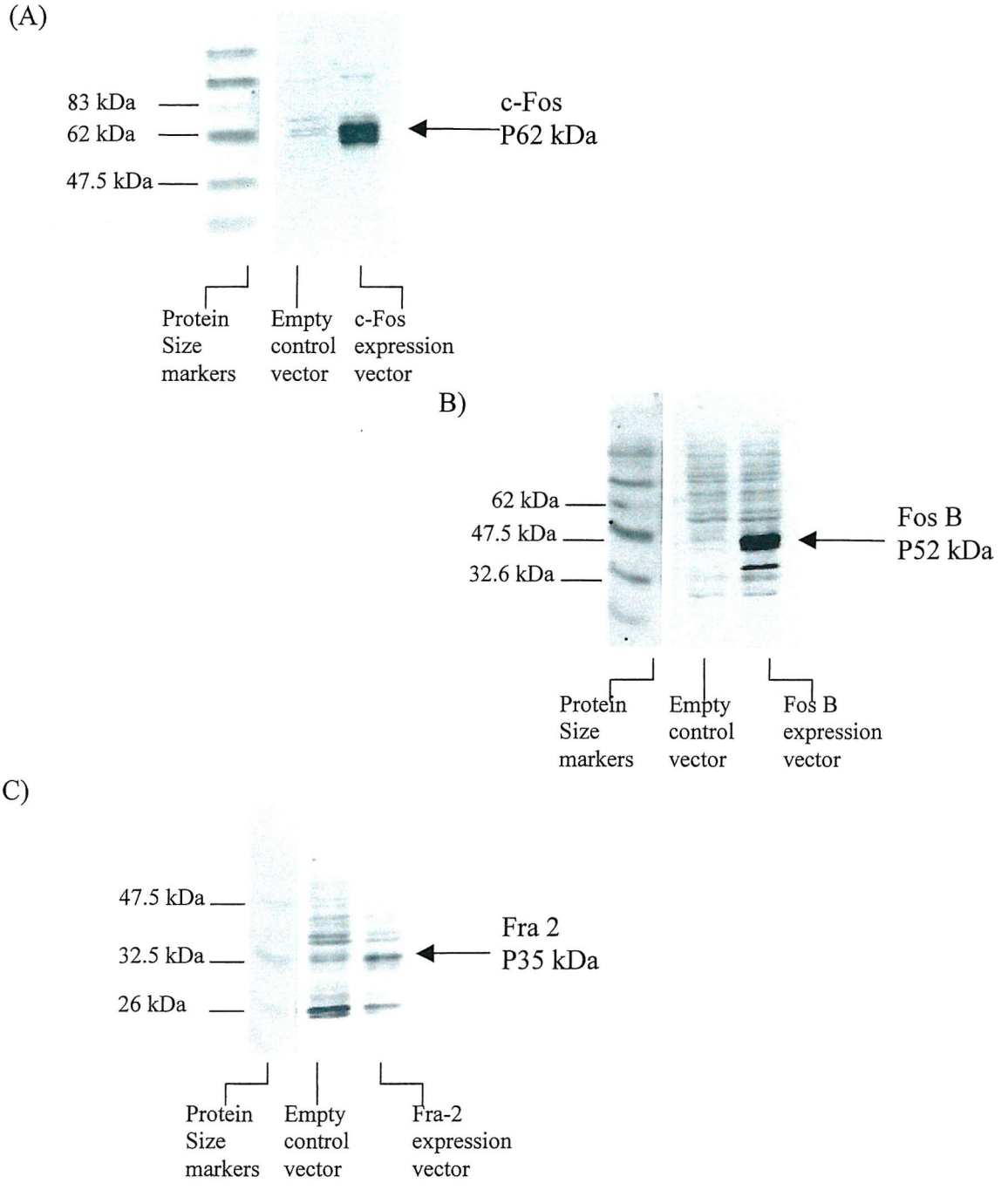

Figure 3.4.2. The Western blots of FOS family AP-1 proteins following transfection into Cos-1 cells of, A) c-Fos-pCMV2 expression vector B) Fos B-pCMV2 expression vector and C) Fra-2-pCMV2 expression vector. In each experiment the cells were grown on 45mm plates until 60-70% confluent. The Cos-1 cells were transfected with 1μg of Fos-pCMV2 protein expression vector or empty control pCMV2. The primary FOS specific polyclonal rabbit antibodies (Santa Cruz) were all used at 1μg/ml and the secondary rabbit IgG specific HRP conjugate antibody (Sigma) was used at 1:2000 dilution. For all antibodies see Appendix 4.

3.5 The Effect of JUN Protein Expression on Tissue Inhibitor of Metalloproteinase-1 Promoter Activity

The AP-1 protein expression vectors were used in a series of co-transfections with the TIMP-1 minimal CAT reporter construct –111WT. 3μg of expression vector and 1μg of reporter construct were transfected into 45mm dishes of HSC, before incubation for 48 hours and performing the CAT assay. The transfections were to establish the roles of each of the JUN and FOS proteins in the expression of TIMP-1.

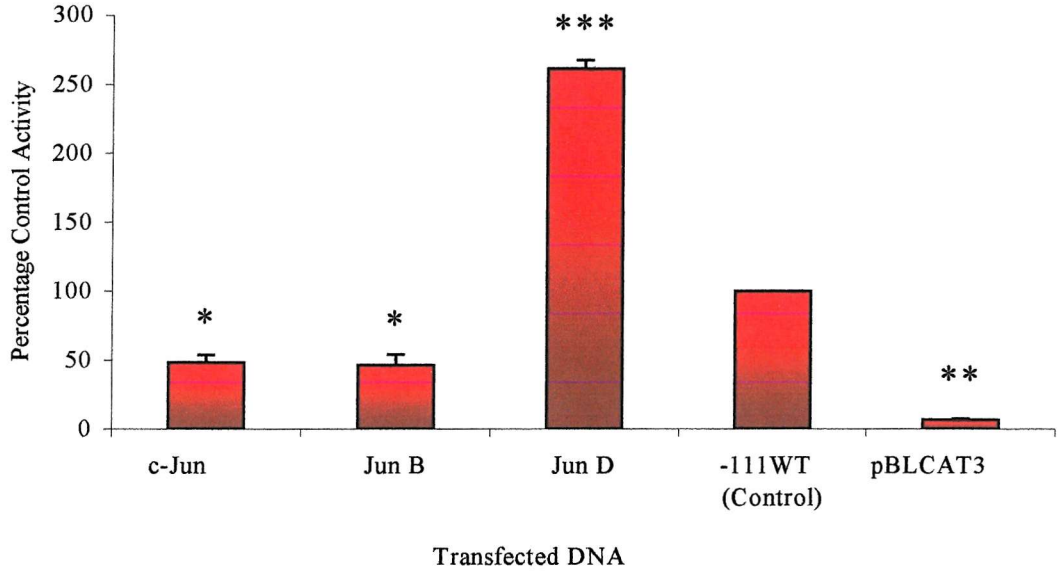

Figure 3.5.1. The effect on TIMP-1 minimal promoter activity of JUN expression vector co-transfection. The results displayed are the mean percentage and the standard error of control activity from three triplicate transfections of cells from different individuals. The primary HSC were plated out at 10^6 cells per 45mm dish. The cells were cultured >7Day to allow them to activate and become 60-70% confluent. The cells were transfected with 3μg of either the JUN-pCMV2 or pCMV2 empty expression vector and 1μg of –111WTreporter construct or pBLCAT3 by the Effectine method (Qiagen). The vectors pBLCAT3 and pCMV2 were used as controls for the reporter and expression vector transfection respectively. Each plate was also co-transfected with 100ng of Renilla-Luc expression plasmid to normalise for differences in transfection efficiency. The activity of the promoter was established and the results modified for transfection efficiency (see Section 2.7.3). The cells were cultured for 48 hours following transfection and cytoplasmic extract was harvested for CAT assay. An indication of the data significance can be obtained from the presence of a *, **, ***. These represent P values of <0.05, 0.01 and 0.005 respectively, as shown by Student's T-test test of un-equal variance with two tails. For Primary data see Appendix 3.

Increased expression of the JUN family proteins resulted in various changes in the activity of the TIMP-1 minimal promoter (Figure 3.5.1). The increased expression of c-Jun and Jun B both resulted in significant reductions in promoter activity of 48.2 and 46.4% of wild type respectively. The increased expression of Jun D consistently resulted in a significant increase in promoter activity of 261%. This suggests that c-Jun and Jun B may function as negative regulators and Jun D as a positive regulator of TIMP-1 expression in the activated HSC.

3.6 The Effect of FOS Protein Expression on Tissue Inhibitor of Metalloproteinase-1 Promoter Activity

In order to investigate the roles of the FOS AP-1 proteins on the activity of the TIMP-1 minimal promoter, the co-transfections of the –111WT TIMP-1 minimal promoter reporter were repeated in activated HSC with FOS-pCMV2 expression vectors.

The results of the co-transfection of FOS-pCMV2 expression vectors into rat HSC (Figure 3.6.1) showed a 33 to 52% reduction in activity, although this could not be shown to be a significant effect on the TIMP-1 minimal promoter for all of the FOS expression vectors. The co-transfection of the Fos B and Fra 2 vectors did however result in the significant reduction of the activity of the TIMP-1 minimal promoter to 45% and 52% of control activity respectively.

The results also indicated a trend decrease in the activity of the promoter for each of the other FOS expression vectors when compared to the controls.

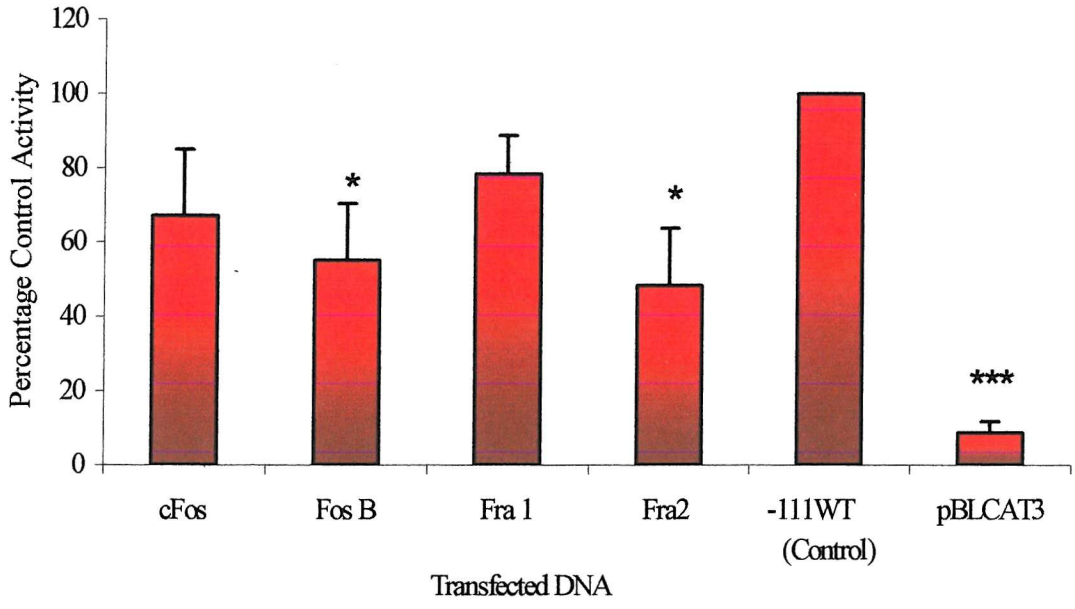

Figure 3.6.1 The effect on the activity of the TIMP-1 minimal promoter of FOS expression vector co-transfection. The results displayed are the mean percentage and the standard error with respect to control activity from seven transfections of separate individuals. The primary HSC were plated out at 10^6 cells per 45mm dish. The cells were cultured for >7Day to allow them to activate and become 60-70% confluent. The cells were transfected with 3μg of either the FOS-pCMV2 or pCMV2 empty expression vector and 1μg of –111WTreporter construct or pBLCAT3 by the Effectine method (Qiagen). The vectors pBLCAT3 and pCMV2 were used as controls for the reporter and expression vector transfection respectively. Each plate was also co-transfected with 100ng of Renilla-Luc expression plasmid to normalise for differences in transfection efficiency. The activity of the promoter was established and the results modified for transfection efficiency (see Section 2.7.3). The cells were cultured for 48 hours following transfection and cytoplasmic extract was harvested for CAT assay. An indication of the data significance can be obtained from the presence of a * or **. These represent P values of <0.05 and 0.01 respectively, as shown by Student's T-test test of un-equal variance with two tails. For primary data see Appendix 3.

3.7 Elucidating the Role of Jun D and the Other JUN Family Members in the Hepatic Stellate Cell

As JUN family members are crucial for AP-1 dimer formation it was deemed necessary to investigate the role of JUN and the dimeric combinations in the transcription of TIMP-1 thoroughly. The work concentrated in particular on the role of Jun D, the only JUN member shown to be present in culture activated HSC, which has also previously been shown to be a positive regulator of TIMP-1 transcription (Figure 3.5.1).

Two modified Jun D expression vectors were obtained through collaboration. The first expression vector, a modified Jun D vector RSV-β-Δ-Jun D was obtained in collaboration with Dr. Lengyel (Department of Obstetrics and Gynecology, Technische Unniversität München, Germany) (Ried *et al.*, 1999). The RSV-β-Δ-Jun D vector produces a dominant-negative Jun D protein, lacking the transactivation domain (amino acids 1-162). The mutant protein dimerizes with endogenous proteins as well as itself. The dominant negative protein acts as a competitive inhibitor, with reduced transcriptional activity but with the same binding kinetics as dimers of the wild type Jun D (see Figure 3.7.1 A). This vector was also used in co-transfection studies with the TIMP–1 (-111WT) reporter in order to access the requirement for endogenous Jun D activity.

The second vector Jun D/Eb1-pDP7, was obtained in collaboration with Dr Castellazzi (Ecole Normale Supérieure de Lyon, France) (Vandel *et al.*, 1995, Reid *et al.*, 1999). The protein expressed by Jun D/Eb1-pDP7 contains a modified Jun D cDNA in which the dimerization domain has been exchanged for that of the Ebstein-Barr virus transcription factor Eb1 (see Appendix 2 iii). The new mutant Jun D protein is thus only able to dimerize with itself and can therefore only form transcriptional active Jun D homodimers (see Figure 3.7.1 B). Jun D/Eb1-pDP7 therefore provides a means to test the ability of Jun D homodimers to trans-activate the TIMP-1 promoter. Also supplied with this vector (at a later date) were similar vectors for the two other JUN proteins c-Jun and Jun B. A control transfection was initially established using the empty vector PcDNA3 (see Appendix 2 iv) having been unable to obtain the empty vector pDP7. Following the arrival of a vector map (Dr Castellazzi) and the plasmid pLMVP via collaboration with

Dr. Lengyel (Ried *et al.*, 1999), the control transfections were repeated with pLMVP as a control. pLMVP shares Rat Sarcoma Virus (RSV) promoter in common with pDP7 where as the vector PcDNA3 uses the Cytomegalovirus (CMV) promoter.

The new expression vectors were used in co-transfections with the TIMP-1 minimal promoter reporter in order to establish the significance of the role played by the JUN proteins, and in particular the role of Jun D.

The co-transfection of the RSV-β-Δ-Jun D resulted in a significant reduction (65%) in TIMP-1 minimal promoter activity (Figure 3.7.2). This result supports a role for Jun D as a crucial regulator of the TIMP-1 promoter in activated HSC.

In order to establish the function of Jun D homodimers, co-transfections were performed using Jun D/Eb1-pDP7 and the TIMP-1 minimal promoter reporter –111WT. The expression of Jun D/Eb1-pDP7 resulted in a 350% increase in TIMP-1 promoter activity (Figure 3.7.3). This result indicated that Jun D homodimers have a strong transactivation potential for the TIMP-1 promoter in the activated HSC.

Following the investigation of the function of Jun D it was decided to investigate the role of the other JUN protein homodimers. Co-transfections were therefore performed using expression vectors cJun/Eb1-pDP7 and Jun B/Eb1-pDP7. The expression of Jun B/Eb1-pDP7 gave rise to a slight but non-significant change in the activity of the TIMP-1-CAT reporter (Figure 3.7.4). By contrast expression of c-Jun/Eb1-pDP7 homodimers resulted in a significant two-fold increase in TIMP-1 promoter activity.

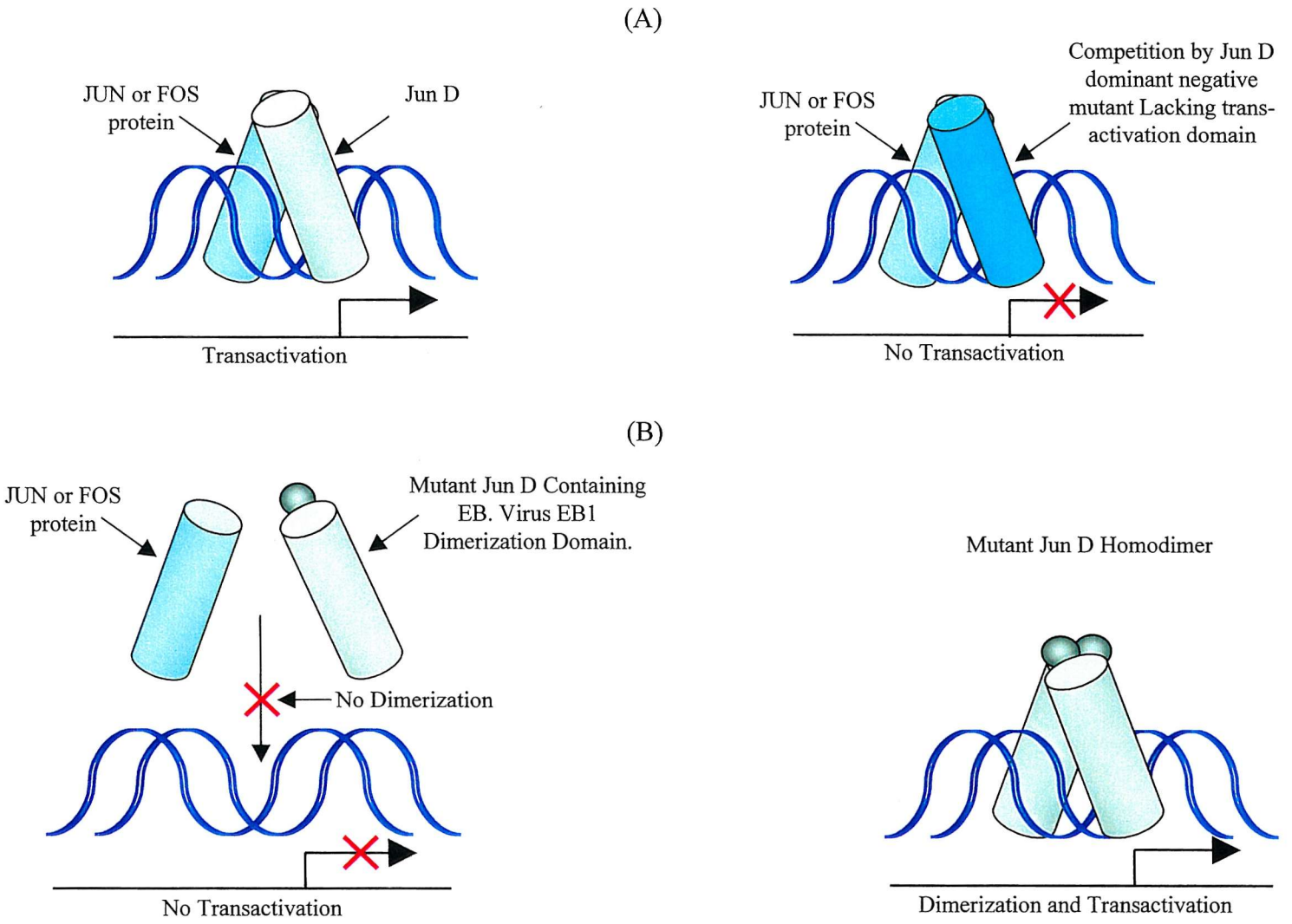

Figure 3.7.1 The functional mechanism of the A) Dominant negative Jun D RSV-β-Δ-Jun D and B) Exclusive Homodimer Forming Vector Jun D/Eb1 pDP7.

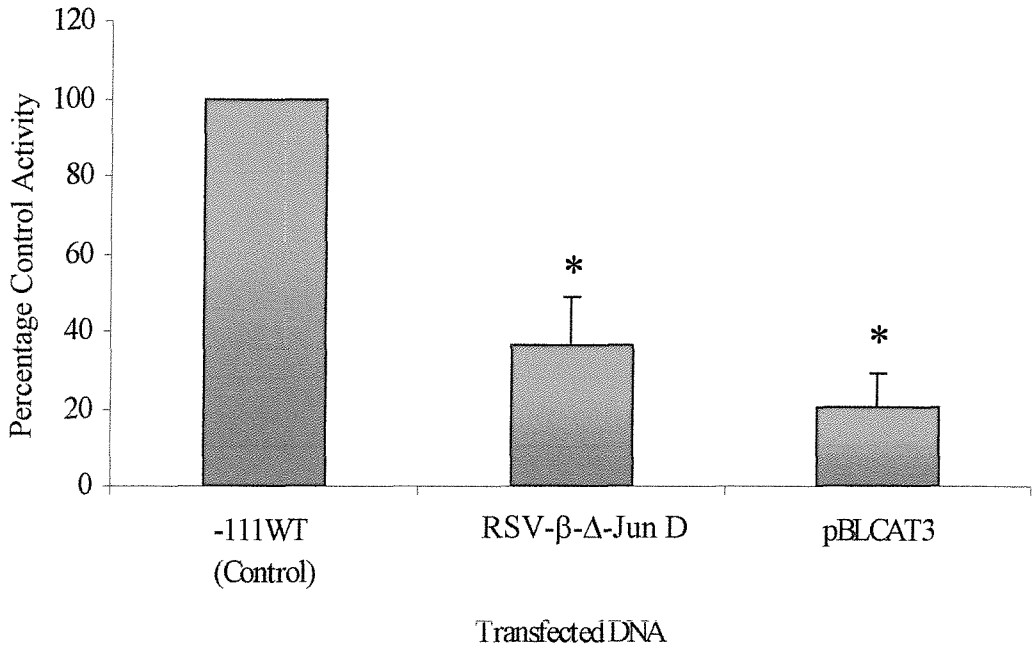

Figure 3.7.2. The effect on TIMP-1 minimal promoter activity of the co-transfection of a Jun D dominant-negative mutant expression vector. The results displayed are the percentage mean and the standard error of control activity from data obtained from three triplicate transfections of cells from separate individuals. Primary HSC were plated out 45mm tissue culture dishes at a density of 10^6 cells per plate. The cells were allowed to activate over >7days and were transfected upon reaching 60-70% confluence. The cells were transfected with 3μg of either RSV-β-Δ-JunD or its parent empty vector pLMVP and 1μg of –111WT TIMP-1 or pBLCAT3 reporter vector. The vectors pBLCAT3 and pLMVP were used as controls for reporter and expression vector transfection respectively. Each plate was also co-transfected with 100ng of Renilla-Luc expression plasmid to normalise for differences in transfection efficiency. The activity of the promoter was established and the results modified for transfection efficiency (see Section 2.7.3). The cells were cultured for 48 hours before cytoplasmic extracts were harvested and CAT assays performed. An indication of the data significance can be obtained from the presence of a *. This represent a P value of <0.05, as shown by Students T-test test of un-equal variance with two tails. For primary data see Appendix 3.

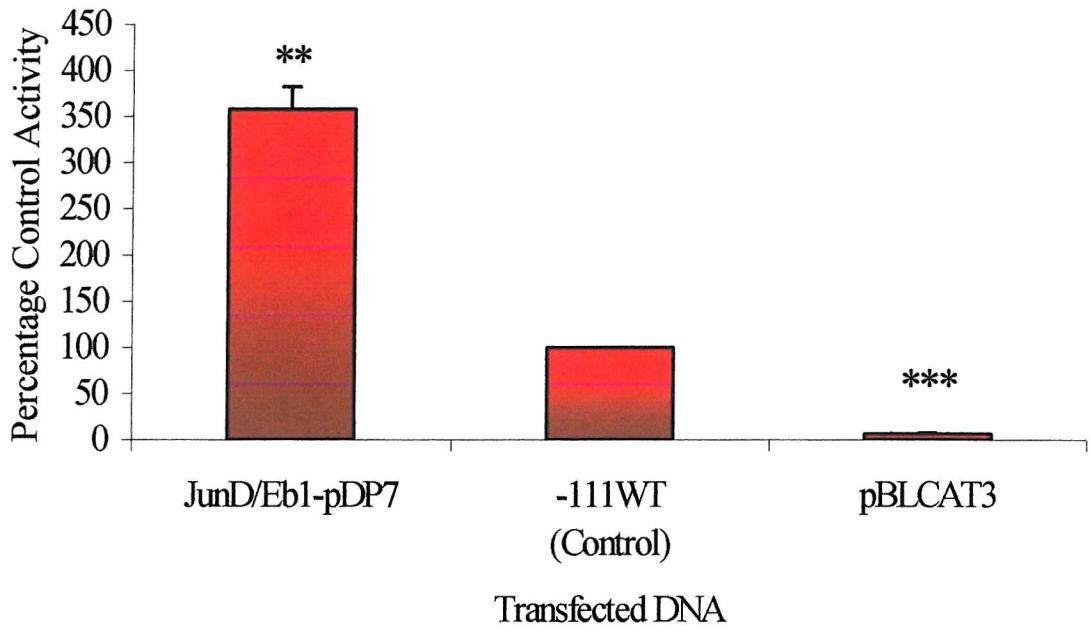

Figure 3.7.3. The effect of co-transfection on TIMP-1 minimal promoter activity of an exclusive Jun D homodimer forming expression vector. The results displayed are the mean percentage and the standard error of control activity from three triplicate transfections of cells from separate individuals. Primary HSC were plated out on 45mm tissue culture dishes at a density of 10^6 cells per plate. The cells were allowed to activate over >7days and were transfected upon reaching 60-70% confluence. The cells were transfected with 3μg of the Jun D/Eb1-pDP7 or pLMVP expression constructs and 1μg of –111WT TIMP-1 or pBLCAT3 reporter vectors. The vectors pBLCAT3 and pLMVP were used as controls of reporter and expression vector transfection respectively. Each plate was also co-transfected with 100ng of Renilla-Luc expression plasmid to normalise for differences in transfection efficiency. The activity of the promoter was established and the results modified for transfection efficiency (see Section 2.7.3). The cells were cultured for 48 hours before cytoplasmic extracts were harvested and CAT assays performed. An indication of the data significance can be obtained from the presence of a *, ** or ***. These represent P values of <0.05, 0.01 and 0.005 respectively, as shown by Students T-test test of un-equal variance with two tails. For primary data see Appendix 3.

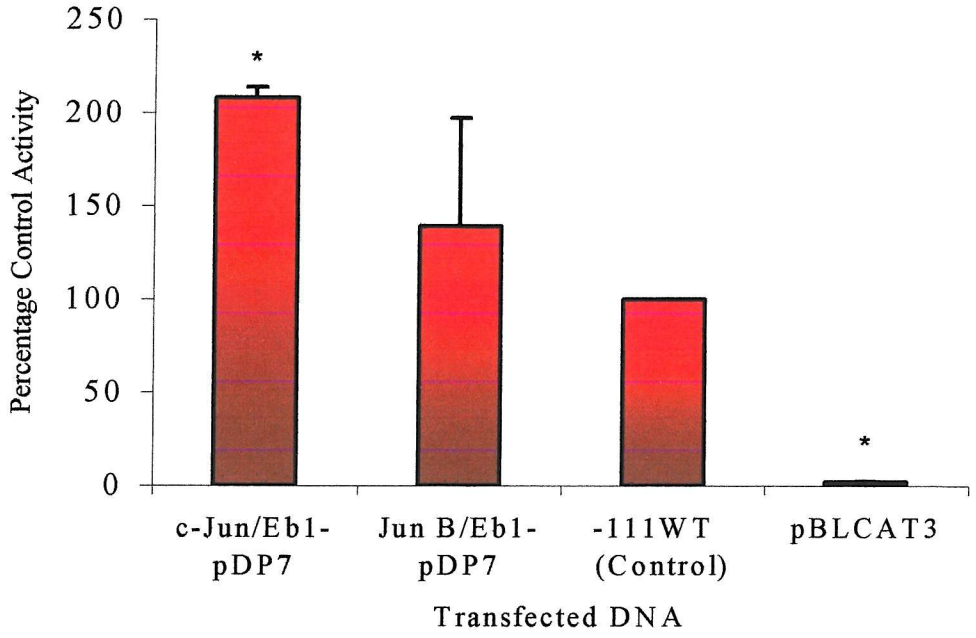

Figure 3.7.4. The effect of co-transfection on TIMP-1 minimal promoter activity of an exclusive c-Jun/Eb1-pDP7 and Jun B/Eb1-pDP7 homodimer forming expression vectors. The results displayed are the mean percentage and the standard error of control activity from a representative triplicate transfection. Primary HSC were plated out 45mm tissue culture dishes at a density of 10^6 cells per plate. The cells were allowed to activate over >7days and were transfected upon reaching 60-70% confluence. The cells were transfected with 3μg of the c-Jun/Eb1-pDP7, Jun B/Eb1-pDP7 or pLMVP expression constructs and 1μg of –111WT TIMP-1 or pBLCAT3 reporter vectors. The vectors pBLCAT3 and pLMVP were used as controls of reporter and expression vector transfection respectively. Each plate was also co-transfected with 100ng of Renilla-Luc expression plasmid to normalise for differences in transfection efficiency. The activity of the promoter was established and the results modified for transfection efficiency (see Section 2.7.3). The cells were cultured for 48 hours before cytoplasmic extracts were harvested and CAT assays performed. An indication of the data significance can be obtained from the presence of a *, which represents a P value of <0.05, as shown by Students T-test test of un-equal variance with two tails. For primary data see Appendix 3.

3.8 The Regulation of Tissue Inhibitor of Metalloproteinase-1 in the Quiescent Hepatic Stellate Cell

Results of previous experiments established the requirement for the AP-1 site in the promoter of TIMP-1. The data also demonstrated a functional role for Jun D homodimers as the mediator of AP-1 dependent TIMP-1 promoter activation. For these reasons co-transfection of the JUN and FOS expression vectors were repeated in quiescent (freshly isolated) HSC in order to establish whether modulation of JUN and FOS expression could directly induce TIMP-1 transcription.

The comparative co-transfections of quiescent HSC with the AP-1 protein expression vectors and TIMP-1 reporter showed no increase in promoter activity. By contrast co-transfection of activated HSC with the JUN and FOS expression vectors resulted in similar changes in promoter activity as previously observed in Figures 3.5.1 and 3.6.1. The results are shown (Figure 3.8.1) as a single transfection, without quantitation. The co-transfections of JUN and FOS vectors were repeated on a number of occasions and the results were found to be reproducible. The data shown in Figure 3.8.1 were collected from quiescent and activated HSC prepared from the same liver and used similar quantities of protein in a parallel CAT assay.

In order to demonstrate that the quiescent HSC can be transfected, the activity of a co-transfected Renilla luciferase vector was examined and compared with the activity of the same vector in activated HSC. The results of the Renilla assay indicated that there is 53% lower transfection efficiency in quiescent HSC when compared to the wild type cells (Figure 3.8.2). The lack of TIMP-1 promoter activity in quiescent HSC therefore reflects a failure of AP-1 proteins to stimulate transcription rather than defects in transfection.

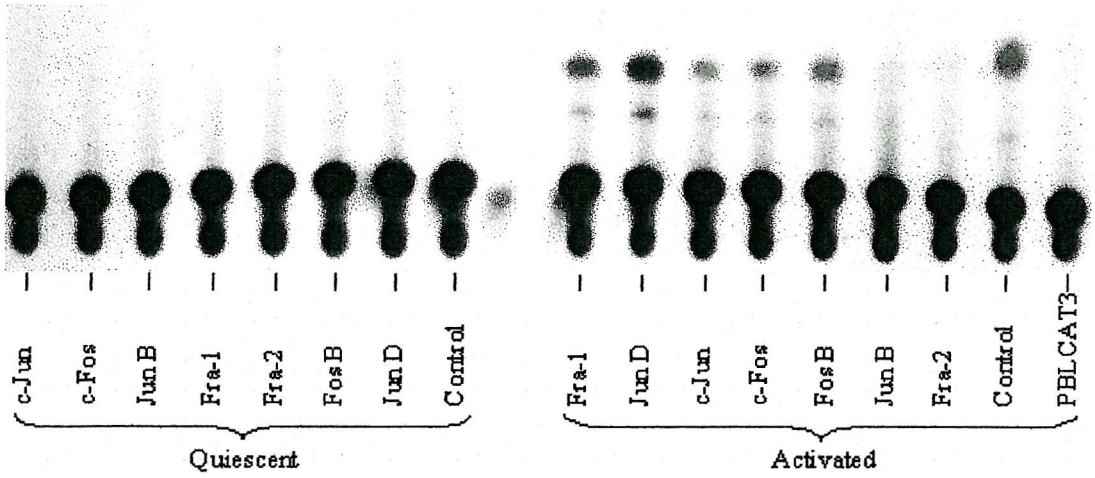

Figure 3.8.1. A representative TLC plate form a CAT assay showing the effects on TIMP-1 minimal promoter activity of the co-transfection of JUN and FOS expression vectors in quiescent and activated HSC. The HSC were seeded at a density of $2.5x10^6$ (Quiescent) or $5x10^5$ (Activated) cells per 45mm plate when first isolated. The cells came from the same rat and were cultured for 24hours or 8days before transfection. The cells were transfected with 3μg of both the JUN-pCMV2, FOS-pCMV2 or pCMV2 empty expression vector and 1μg of –111WTreporter construct or pBLCAT3 by the Effectine method (Qiagen). pCMV2 and pBLCAT3 acted as control for the expression vector and reporter constructs respectively. Each plate was also co-transfected with 100ng of Renilla-Luc expression plasmid to normalise for differences in transfection efficiency. The activity of the promoter was established and the results modified for transfection efficiency (see Section 2.7.3). The cells were harvested after 48hours and 25μg of cytoplasmic protein was used for the CAT assays in both cases.

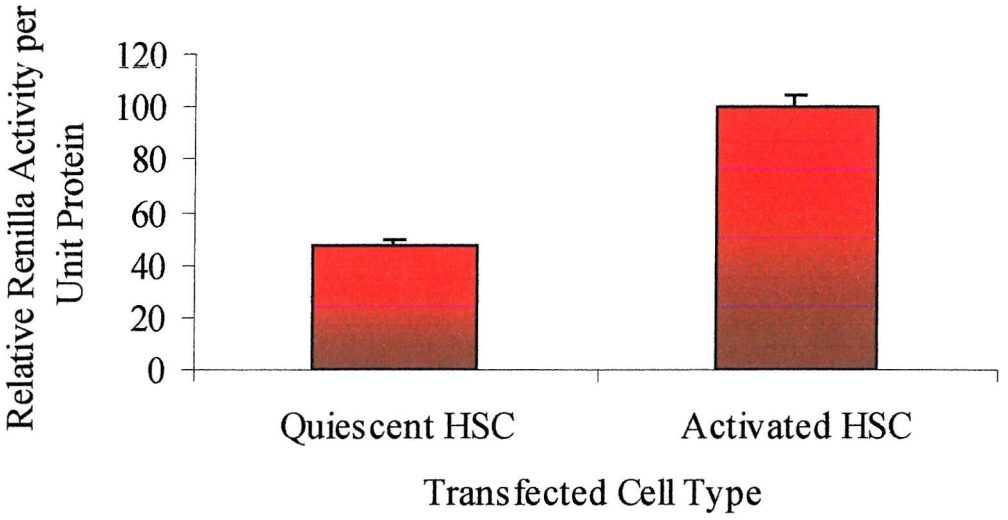

Figure 3.8.2 The relative Renilla activity per unit protein for quiescent and activated HSC seen in Figure 3.8.1. The HSC were seeded at a density of $2.5x10^6$ (Quiescent) or $5x10^5$ (Activated) cells per 45mm plate when first isolated. The cells came from the same rat and were cultured for 24hours or 7days before transfection. The cells were transfected with 100ng of Renilla transfection efficiency vector by the Effectine method (Qiagen). The cells were harvested after 48hours and protein and Renilla assays performed. The values for the Renilla activity was divided the protein sample concentration and results were displayed as the percent mean and standard error with respect to the activated cell transfection.

3.9 The Use of Antisense Oligonucleotides to Elucidate the Roles of the Endogenous AP-1 Proteins

In order to further establish the role of the endogenous HSC AP-1 proteins as regulators of TIMP-1 transcription, antisense sequence specific oligonucleotides were used. The sequence specific oligonucleotide sequences (see Appendix 1) were obtained from the literature (Robertson *et al.*, 1995; Wang *et al.*, 1996a; Crocker *et al.*, 1998). The oligonucleotides were phosphorothioated throughout their sequence, in order to reduce their degradation.

Antisense and sense oligonucleotides were initially added to the culture media at a concentration of 40μg per ml, as described in the literature (Wang *et al.*, 1996a). In preliminary experiments the addition of oligonucleotides to the media had no effect on the activity of the TIMP-1 promoter (data not shown). The addition of such a large

quantity of phosphorothioated oligonucleotides to the media was however very demanding on resources and moreover also appeared to cause changes in cellular morphology. As the changes in morphology were independent of oligonucleotide or strand, the effects seen were believed to be non-specific toxicity.

It was therefore decided to try to introduce smaller quanties of oligonucleotides into the HSC by transfection, using the Effectine reagent. To establish whether transfection of antisense oligonucleotides could effectively reduce the expression of a target protein, an antisense oligonucleotide to Jun D was transfected into HSC as a titration. The same quantity of sense Jun D oligonucleotide was also transfected in parallel as a control.

The HSC transfected with antisense Jun D oligonucleotide (Figure 3.9.1-A) showed an observable reduction in the expression of Jun D when compared to equal quantities of the sense oligonucleotide. Increasing the quantity of transfected sense oligonucleotide to 5μg also showed no decrease in the expression of Jun D. A parallel Western blot was probed for the expression of Fos B. The Fos B Western blot showed no observable reduction with either sense or antisense Jun D oligonucleotides (3.9.1-B).

Densitometric analysis was performed on the Western blots for Jun D and Fos B in order to quantify the change in Jun D expression with the transfection of specific antisense Jun D oligonucleotides. The data from the densimetric analyses for Fos B was used to control the data obtained from the Jun D Western blot. The results indicated that the transfection of specific antisense oligonucleotides produced a reduction in endogenous Jun D protein expression by 50%, when compared with sense controls (Figure 3.9.2). The data also indicate that it may be possible to use this system to test the effects of modulating the expression of endogenous AP-1 proteins on TIMP-1 promoter function.

In the subsequent transfections, 3μg of either sense or antisense oligonucleotides and 1μg of TIMP-1 reporter were used in order to assure that the oligonucleotides would be present in a sufficiently effective quantity in TIMP-1 promoter transfected cells.

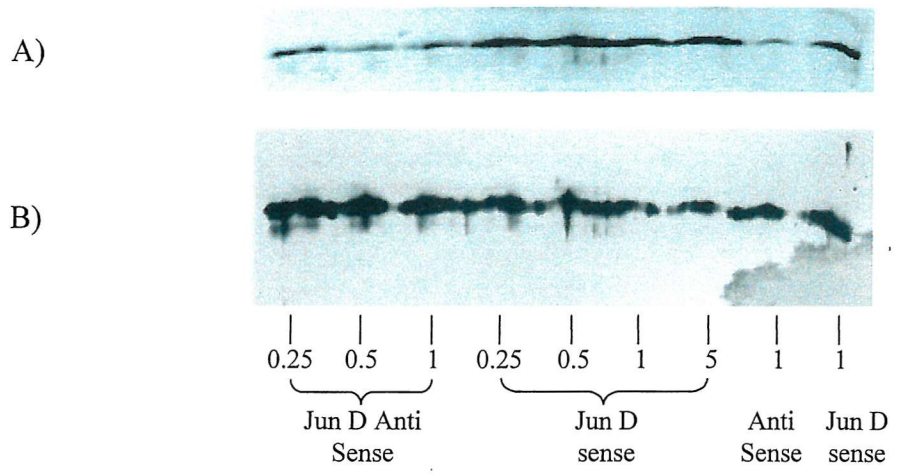

Figure 3.9.1. The effect of Jun D mRNA specific oligonucleotides on the expression of Jun D proteins in the rat HSC. A) Western blot for the AP-1 protein Jun D. B) Western blot for the AP-1 protein Fos B. Representative Western blots showing the effect of a titration (μg) of sense and antisense Jun D oligonucleotides that had been transfected into rat HSC using the Effectine method (Qiagen). The cells were plated out in 45mm culture dishes and transfected upon reaching 60-70% confluence and >7 days culture with 0.25 - 5μg of oligonucleotide. The cells were washed, harvested and whole cell lysates produced after 24 hours of culture. The samples were loaded at 20μg per well on a 9% SDS PAGE gel before electrophoresis and subsequent transfer was performed. Primary Jun D or Fos B specific polyclonal rabbit antibodies were used at 1μg/ml and secondary rabbit IgG specific polyclonal HRP conjugate antibody was used at 1:2000 dilution (see Appendix 4).

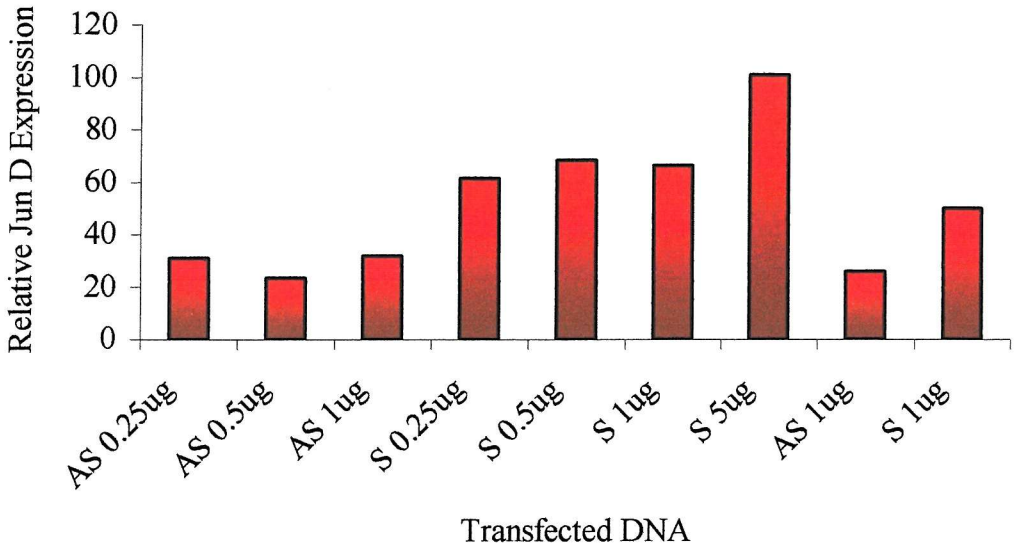

Figure 3.9.2 The change in endogenous Jun D expression relative to that of Fos B upon transfection of specific antisense Jun D oligonucleotides. The data was obtained from the division of the values from the densimetric analysis of the Jun D Western blot (Figure 3.9.1 A) by those obtained from the Fos B Western blot (3.9.1 B). The abbreviations AS and S denote Jun D antisense and sense oligonucleotide transfection respectively. The results are presented as relative protein expression in arbitrary units. The films were analysed using the Storm Image Quant Software package. For both proteins an equal cross sectional area of film for each band was analysed, corresponding to the size of the largest entire band. For each film an area of background of equal size was measured and this figure was deducted from each band measurement.

3.10 The Effect of Antisense AP-1 Oligonucleotides on Tissue Inhibitors of Metalloproteinase-1 Promoter Activity

Antisense oligonucleotides to Jun D, Fos B and Fra-2 were chosen for investigation as each of these proteins were shown to be expressed in the activated HSC. The Jun D sense oligonucleotide was used as a control since it had previously been shown to have no effect on the expression of Jun D, Fos B or cell morphology.

The co-transfection of each of the specific antisense oligonucleotides in the HSC demonstrated a decrease in promoter activity with respect to the sense Jun D control (Figure 3.10.1). The results were shown to be significant with P values of less than 0.005 for both Jun D and Fra 2. Fos B however was greater than the P=0.05 tolerance and as such could not be shown to be significant. The data indicate that Jun D and Fra 2 may form active dimers and may be involved in the transactivation of the TIMP-1 minimal promoter but those of Fos B could not be shown to have an effect. The negative effect of the AS Fra-2 is contradictory to the results of the FOS expression vector transfection (Figure 3.6.1).

It was felt that further work was needed to understand the contradictory data for Figure 3.6.1 and 3.10.1. In order to ascertain whether there was a positive active role for Fra 2 in the form of a heterodimer with Jun D, a series of co-transfections were performed using both the Jun D-pCMV2 and Fra 2-pCMV2 expression vectors. The Jun D and Fra 2 vectors were simultaneously transfected into HSC, along with the TIMP-1 minimal promoter construct. In these triple co-transfections the quantities of DNA were all halved as it was felt that the quantities of DNA and transfecting liposomes involved could be toxic and it would be too costly for transfection reagent. The quantity of reporter construct used was also halved in order to maintain a three to one ratio of each expression vector to the reporter construct. Four μg of DNA had been successfully used in the previous co-transfections and had shown no deleterious effects.

Previous work by other groups had supported the findings of the FOS-pCMV2 transfection experiment (Figure 3.6.1), indicating that c-Jun/Fra 2 and Jun B/Fra 2

heterodimers were inhibitory. There were mixed findings, however, for the Jun D/Fra 2 heterodimer (Suzuki *et al.*, 1991; Sonobe *et al.*, 1995; Rutberg *et al.*, 1997).

The results of the triple transfections of Jun D, Fra 2 and the TIMP-1 reporter indicated that the transfection of Fra 2 on its own or in combination with the Jun D expression vector resulted in a 50% reduction in the activity of the TIMP-1 promoter (Figure 3.10.2). As expected there was an increase in promoter activity with the co-transfection of Jun D and reporter, although this was not as large as previously seen. The triple transfection of both the Jun D-pCMV2 and Fra 2-pCMV2 vectors was a single experiment in triplicate so no statistical analysis has been drawn, however the data would seem to suggest that both of the transfections containing Fra 2-pCMV2 resulted in a significant decrease in activity.

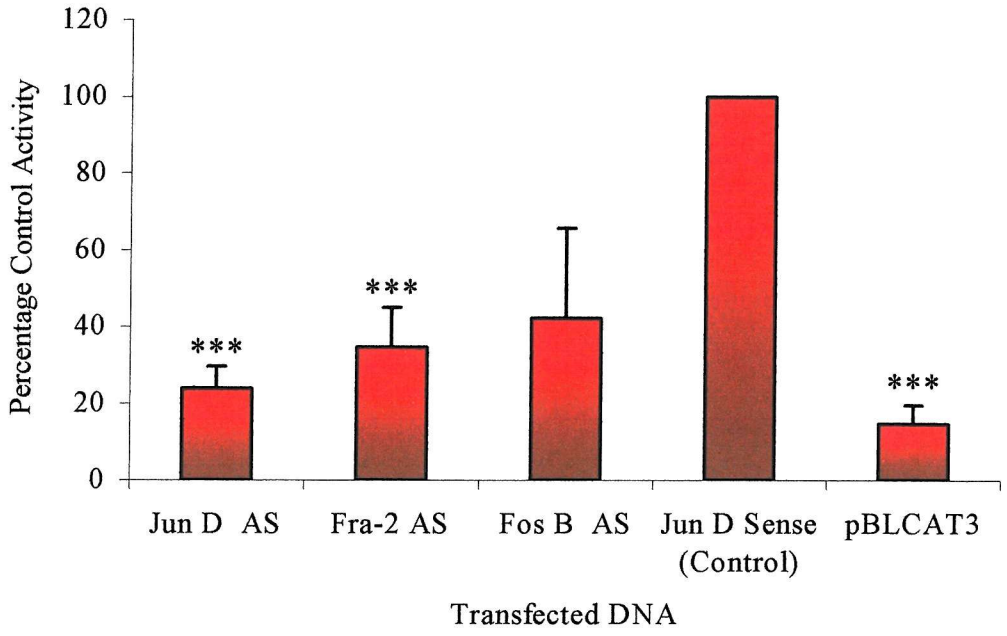

Figure 3.10.1 The effect on TIMP-1 minimal promoter activity of antisense JUN and FOS oligonucleotide transfection. The results displayed are the percentage mean and the standard error with respect to control activity of triplicate transfections of three to five separate individuals. The primary HSC were plated out at a cell density of 10^6 cells per 45mm culture plate. Transfections were performed following >7 days culture and 60-70% confluence. Cells were transfected by the Effectine method (Qiagen) with 3μg of sense or antisense oligonucleotide and 1μg of –111WT or empty pBLCAT3 reporter. pBLCAT3 and Sense oligonucleotides acted as negative controls for the reporter construct and antisense DNA respectively. Each plate was also co-transfected with 100ng of Renilla-Luc expression plasmid to normalise for differences in transfection efficiency. The activity of the promoter was established and the results modified for transfection efficiency (see Section 2.7.3). The cells were cultured for 48 hours following transfection and cytoplasmic extracts harvested for CAT assay. An indication of the data significance can be obtained from the presence of a *, ** or ***. These represent P values of <0.05, <0.01 and <0.005 respectively, as shown by Students T-test test of un-equal variance with two tails. For primary data see Appendix 3.

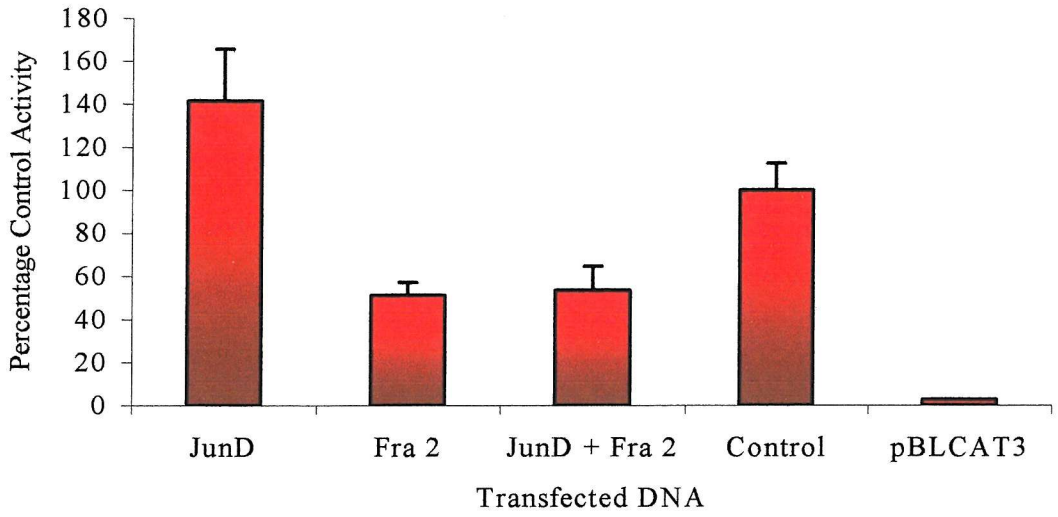

Figure 3.10.2. The effect on TIMP-1 minimal promoter activity of Jun D and Fra 2 simultaneous expression vector co-transfection. The results displayed are the mean percentage and the standard error of control activity from a representative triplicate transfection. The primary HSC were plated out at 10^6 cells per 45mm dish. The cells were cultured for >7Day to allow them to activate and become 60-70% confluent. The cells were transfected with any two of the following 1.5μg of Jun D-pCMV2, 1.5μg Fra 2-pCMV2 and 1.5μg pCMV2 empty expression vector. The cells were also transfected with 0.5μg of –111WTreporter construct or pBLCAT3 by the Effectine method (Qiagen). The vectors pBLCAT3 and pCMV2 were used as controls for the reporter and expression vector transfection respectively. Each plate was also co-transfected with 100ng of Renilla-Luc expression plasmid to normalise for differences in transfection efficiency. The activity of the promoter was established and the results modified for transfection efficiency (see Section 2.7.3). The cells were cultured for 48 hours following transfection and cytoplasmic extract was harvested for CAT assay. For Primary data see Appendix 3

3.11 Investigating the Regulation of Interleukin 6 for the Purpose of Elucidating the Functions in JUN / FOS Heterodimers.

To further investigate the role of JUN and FOS transcription factors in the HSC and liver fibrosis, it was decided to examine the role of AP-1 as a transcriptional regulator of a second gene, IL-6. IL-6 was chosen because its expression is induced during HSC activation and IL-6 promoter studies in other cell types have indicated a role for an AP-1 site that is conserved in the promoter of the human, mouse and rat IL-6 genes (Tiggelman *et al.*, 1995; Eickelberg *et al.*, 1999; Smart *et al.*, 2001).

There is evidence to not only support a role for IL-6 in liver fibrosis but also to implicate the HSC as a major source. Two particularly important papers support the role for IL-6 in liver fibrosis. The first paper suggests that there was an observable reduction of fibrosis in IL-6 knockout mice following CCl_4 induced liver injury (Natsume *et al.*, 1999). The second paper repeated the CCl_4 study and also utilised a hepatectomy model. This study showed, in support of the previous group's work, that there was indeed less fibrosis in the IL-$6^{-/-}$ knockout mice. The second group did however also show that the IL-$6^{-/-}$ knockout mice had a lack of liver regeneration, increased apoptosis and necrosis of hepatocytes, and that there was less healing (Kolalovich *et al.*, 2000). These results suggest that while IL-6 potentiates fibrotic liver disease, it may be necessary for wound healing. There is also further evidence to link IL-6 with potentiation of disease, with a significant correlation with disease pathology (Napoli *et al.*, 1994; Oyanagi *et al.*, 1999). A pathological role of IL-6 has also been implicated in promoting fibrosis, as it has been shown to increase matrix production in fibroblasts and also increase the production of TIMP-1 in the liver and other tissues (Duncan *et al.*, 1991; Roeb *et al.*, 1993; Roeb *et al.*, 1994). IL-6 expression has been shown in human liver myofibroblasts in HCV infection; however, expression was mainly due to inflammatory cells, in particular the Kupffer cell. The expression of IL-6 has been shown to be present in many different cell types in liver fibrosis including, as previously mentioned, the HSC, as well as in endothelial cells and hepatocytes (Tiggelman *et al.*, 1995; Oyanagi *et al.*, 1999; Smart *et al.*, 2001).

The evidence suggesting a role of IL-6 as a potentiator of disease, its expression in the activated HSC and its activity at promoting the expression of fibrotic markers led to the investigation of IL-6.

3.12 Identifying Functional Transcription Factor Site in the Interleukin-6 Minimal Promoter.

The IL-6 minimal promoter (Figure 3.12.1 and also see Appendix 7) contains a number of consensus transcription factor binding sites including AP-1, Nuclear Factor Kappa B (NFκB), Nuclear Factor IL-6 (NFIL-6 or CEBP β) and a cyclic adenosine monophosphate response element (CRE) (Figure 3.12.1). A series of IL-6 mutated minimal promoter constructs were supplied via collaboration with Dr. Oliver Eickelberg (Deparment of Research and Internal Medicine, University Hospital, Basel, Switzerland) (Eickelberg *et al.*, 1999). The constructs had been cloned into the Promega vector pGL3-Basic and this was used as a control for transfection.

Figure 3.12.1 A digramatic representation of the IL-6 minimal promoter.

Constructs containing mutations of the AP-1, NFIL-6 and NFκB site were transfected into activated HSC in order to identify crucial transcription factor binding sites. For the sequence of the depicted region of the IL-6 promoter showing binding site positions see Appendix 7. Transfections of the IL-6 mutant constructs were performed in activated rat HSC as previously performed for the TIMP-1 promoter.

The mutation of the various transcription factor-binding sites in the IL-6 promoter indicated that the NFκB site was crucial for transcription, with a mutation of this motif resulting in a 60% reduction in activity (Figure 3.12.2). The mutation of the NF-IL6 site did not result in a significant reduction in promoter activity but a synergistic effect was seen when combined with the mutation of the NFκB site, with a decrease of 90%.

Unexpectedly the AP-1 site was found to act as a negative regulator of the IL-6 transcription, as mutation of the site resulted in a 2-fold induction in promoter activity. This contradicts previous work in primary human lung fibroblasts that had not only shown the AP-1 site to be crucial, but also that the activity was mediated by Jun D homodimers (Eikelberg *et al.*, 1999).

In the light of these results, co-transfections were performed with the IL-6 wild type reporter and the expression vectors for wild type Jun D (Jun D-pCMV2, see Section 3.3), dominant negative Jun D (RSV-β-Δ-Jun D, see Section 3.7) and the chimeric homodimer forming vector (Jun D/Eb1-pDP7, see Section 3.7).

The expression of wild type Jun D (Jun D pCMV2) enhanced IL-6 promoter activity by 50%, indicating that Jun D is a positive regulator of IL-6 gene transcription. The dominant negative and chimeric homodimer forming Jun D expression vectors were both inhibitory resulting in reduction of 60% and 50% respectively (Figure 3.12.3). The result of the wild type Jun D co-transfection is contradictory to that of the AP-1 site mutation (Figure 3.12.2). Moreover the negative effect of Jun D/Eb1 differs from the positive function for this reagent with the TIMP-1 promoter and indicates Jun D homodimers may be repressors of IL-6 transcription.

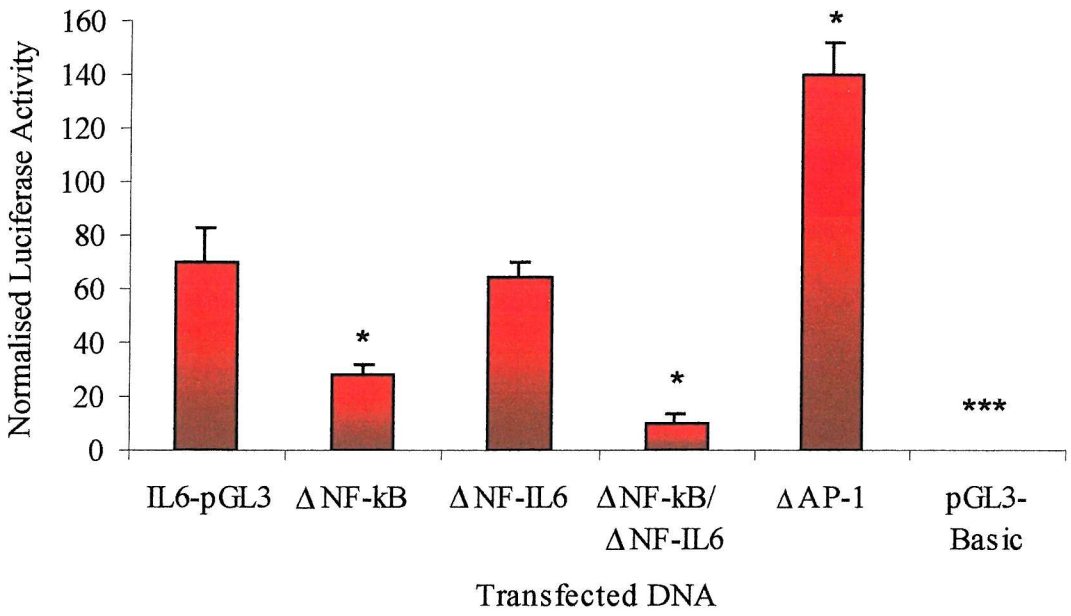

Figure 3.12.2. A comparison of the activities of various transcription-factor binding site mutations on the activity of an IL-6 luciferase minimal promoter reporter construct. The results displayed are the mean percentage and the standard error of wild type activity from a representative triplicate transfection repeated on three separate occasion with cell from different individuals. The primary HSC were plated out at 10^6 cells per 45mm dish. The cells were cultured for >7Day to allow them to activate and become 60-70% confluent. The cells were transfected with 1μg of IL-6–pGL3 or pGL3 Basic empty vector by the Effectine method (Qiagen). Each plate was also co-transfected with 100ng of Renilla-Luc expression plasmid to normalise for differences in transfection efficiency. The cells were cultured for 48 hours following transfection and lysed with 1x passive lysis buffer (Promega). The activity of the promoter was established and the results modified for transfection efficiency using the Dual Luciferase Assay (Promega) (see section 2.7.3). An indication of the data significance can be obtained from the presence of a *, **, ***. These represent P values of <0.05, 0.01 and 0.005 respectively, as shown by Student's T-test of un-equal variance with two tails.

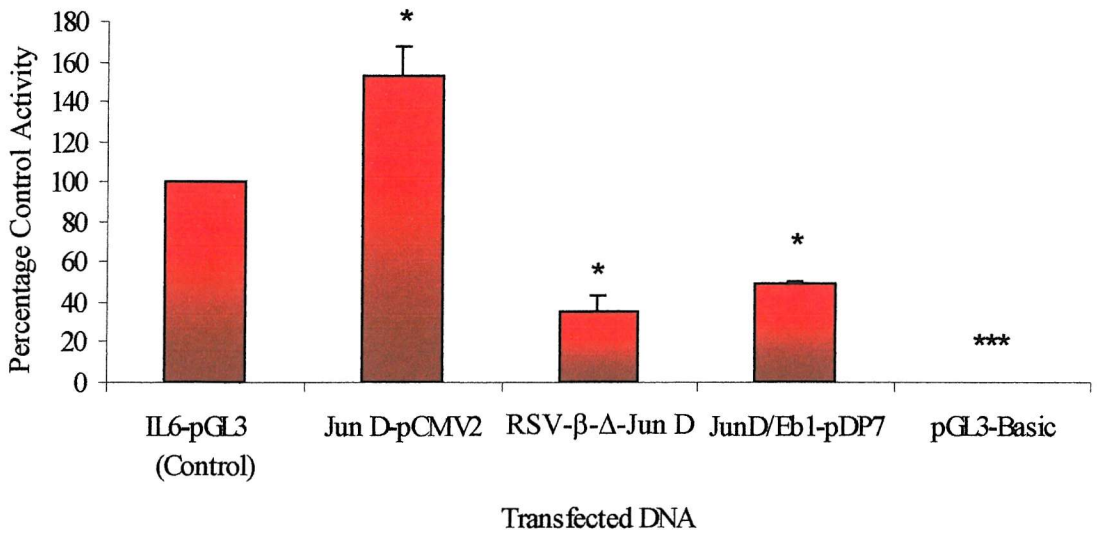

Figure 3.12.3. The effect of wild type Jun D (Jun D-pCMV2), dominant negative Jun D (RSV-β-Δ-Jun D) and Jun D chimeric homodimer forming Jun D/Eb1-pDP7 expression vector co-transfection on IL-6 minimal promoter activity. The results displayed are the mean percentage and the standard error of control activity from a representative triplicate transfection repeated in three individuals. The primary HSC were plated out at 10^6 cells per 45mm dish. The cells were cultured for >7Day to allow them to activate and become 60-70% confluent. The cells were transfected with 3μg of Expression vector and 1μg of IL-6-Luc reporter construct or pGL3-Basic by the Effectine method (Qiagen). The vectors pGL3-Basic and pCMV2 were used as controls for the reporter and expression vector transfection respectively. Each plate was also co-transfected with 100ng of Renilla-Luc expression plasmid to normalise for differences in transfection efficiency The cells were cultured for 48 hours following transfection and lysed with 1x passive lysis buffer (Promega). The activity of the promoter was established and the results modified for transfection efficiency using the Dual Luciferase Assay (Promega) (see Section 2.7.3). An indication of the data significance can be obtained from the presence of a *, **, ***. These represent P values of <0.05, 0.01 and 0.005 respectively, as shown by Student's T-test of un-equal variance with two tails.

3.13 Discussion

Previous work has suggested that a nonclassical mechanism regulates TIMP-1 gene transcription in the activated HSC that involves AP-1 factors distinct from c-Jun and c-Fos (Bahr *et al.*, 1999). In this chapter, a role for Jun D homodimers as the critical AP1 dependant regulators of TIMP-1 transcription has been indicated.

It was firstly important to identify that the AP-1 site was indeed crucial for TIMP-1 promoter activity. The results of the AP-1 site mutation on a CAT reporter indicated a significant reduction in promoter activity (Figure 3.2.1). This indicated that the TIMP-1 promoter was AP-1 dependent.

Co-transfection of HSC with JUN and FOS expression vectors and a TIMP-1 promoter reporter made it possible to identify the roles of the various AP-1 transcription factors. The expression vectors used in these studies were shown to be functional by the confirmation of correct protein production following transfection and subsequent Western blot of Cos-1 cell extracts (Figures 3.4.1, 3.4.2, A-C). Previous work had failed, for many of the vectors, to show visible protein expression when transfecting HSC. The failure of the HSC Westerns was believed to be due to low transfection efficiency (at best 10%). Cos-1 cells were used as they divide rapidly and high transfection efficiency has been suggested to be dependent on a high level of proliferation. The other reason for the use of Cos-1 cells was their SV40 transformation (T antigen) leading to both the replication and subsequent high level of plasmid transcription, resulting in larger quantities of the protein in each cell. The failure of the Western blots in the HSC was believed not to be a problem of the reporter expression vector. The expression vectors would be co-transfected in excess, relative to the TIMP-1 reporter construct, and the two vectors would form a complex that would enter the cell. This method would function in the same way as the complex formed between a reporter and a transfection efficiency control construct.

The effect of over-expression of any of the AP-1 binding proteins was a change in relative concentrations and proteins available, allowing alternative dimeric combinations.

The changes in possible AP-1 dimer complexes in the endogenous HSC and with AP-1 protein over expression are shown diagrammatically in Figure 3.13.2. A table showing an overview of the results of the expression vector transfections and possible relative changes in the endogenous dimeric combinations can be seen in Figure 3.13.3.

The result of Jun D over-expression upon co-transfection in activated HSC was a significant increase in the TIMP-1 minimal promoter activity, while the transfection of c-Jun and Jun B resulted in significant decreases in activity (Figure 3.5.1.). These results are similar to those seen in HSC activation. In quiescent cells or early cultured HSC, c-Jun and Jun B are expressed but TIMP-1 is not. However, in the activated HSC the increase in Jun D expression coincides with that of TIMP-1 (Bahr *et al.*, 1999).

The increase in TIMP-1 promoter activity with the expression of Jun D may suggest a number of possibilities; the first is that Jun D is a limiting factor in this system. The second possible reason is that over-expression of Jun D may lead to a shift in balance, favouring the greater occupancy of the AP-1 site by a Jun D homodimer over that of a Jun D/Fos B or Jun D/Fra 2 heterodimer. Heterodimers of JUN/FOS are more stable than the homodimers of any of the JUN proteins and the FOS heterodimers also possess a 10x higher binding affinity than that of the JUN homodimers (Fos B> Fra 1> c-Fos). As a result of the higher stability and increased DNA binding affinity of the heterodimers it is expected that a JUN/FOS dimer would be more competitive dominating AP-1 interactions (see Figure 3.13.1 A). An increase in Jun D expression would shift the balance of JUN and FOS proteins, favouring the formation of homodimers, increasing their competition for binding (see Figure 3.13.1 B) (Smeal *et al.*, 1989; Allegretto *et al.*, 1990; Ryseck *et al.*, 1991).

The over expression of c-Jun and Jun B also reduced the minimal promoter activity by competition with the transcriptionally active dimers. This competition must have resulted from dimerizing with themselves or the endogenous Jun D, Fra 2 and Fos B in the activated HSC. The homodimers formed by c-Jun have a greater affinity for the AP-1 site than those of Jun D (c-Jun > Jun D> Jun B), so c-Jun homodimers would

predominate over those of Jun D with c-Jun over expression (see Figure 3.13.1 C). The heterodimers of c-Jun with Fos B and Fra 2 would have increased stability over the similar Jun D dimers and would as such displace them. The affinity of JUN/FOS heterodimers is greater than that of the JUN/JUN homodimers, and therefore in a system in which there is endogenous FOS, such as the activated HSC, heterodimer binding is likely to predominate. As the over expression of c-Jun or Jun B lowers transcriptional activity, the dimers that they form must possess lower transcriptional activity in this system, acting as competitive inhibitors (Smeal *et al.*, 1989; Allegretto *et al.*, 1990; Ryseck *et al.*, 1991).

Work in F9 cells by other groups has indicated that heterodimers c-Jun/Fra 2 and Jun B/Fra 2 are negative transcriptional regulators (Suzuki *et al.*, 1991; Sonobe *et al.*, 1995; Rutberg *et al.*, 1997). The research into the effects of Jun D/Fra 2 heterodimers on transcription are however contradictory (Suzuki *et al.*, 1991; Rutberg *et al.*, 1997). The negative regulatory properties of Fra 2 heterodimers support the results seen in Figure 3.5.1 for both c-Jun and Jun B in the HSC, the over expression of which resulted in reduced promoter activity, probably due to the formation of heterodimers with the endogenous Fra 2. The formation of c-Jun/Fra 2 and Jun B/Fra 2 heterodimers is highly favourable, as previously mentioned, because of the higher dimerization and DNA binding affinities of JUN/FOS over JUN/JUN (Ryseck *et al.*, 1991). The inhibitory function of the c-Jun expression vector transfection probably results from the formation of a stable c-Jun/FOS heterodimer, which has a greater stability and AP-1 binding affinity than either the Jun D/FOS heterodimer or the Jun D/Jun D homodimer (see Figure 3.13.1, 3.13.2 and 3.13.3).

An alternative reason for the lack of c-Jun transcriptional activity may be due to the absence of the protein c-Ets, which usually binds to the PEA3 site but has been shown to be down regulated with HSC activation (Bahr *et al.*, 1999; Knittel *et al.*, 1999). The transcription factor c-Ets was shown to act in conjunction with c-Jun and c-Fos to drive TIMP-1 promoter activity in fibroblasts. The very low level of c-Ets expression in the activated HSC makes this an unlikely mechanism of c-Jun activity (Logan *et al.*, 1996).

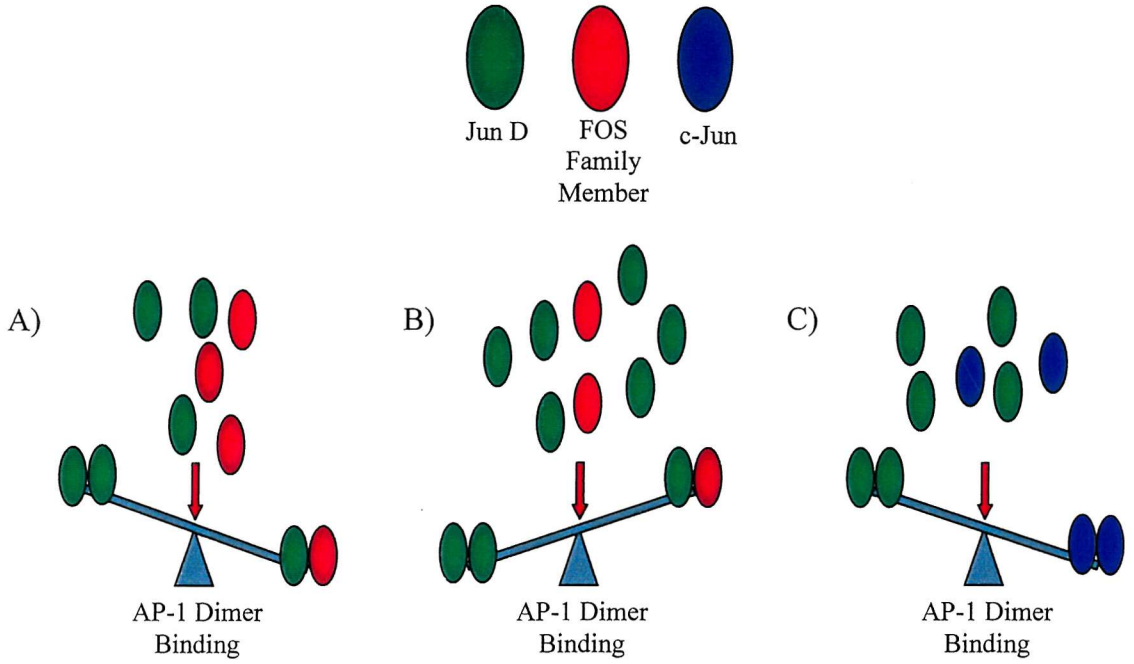

Figure 3.13.1 The effect of binding affinity and dimer stability on the JUN and FOS complexes interacting with the AP-1 binding domain. A) The high affinity of JUN/FOS heterodimers results in competition of JUN homodimers binding. B) Over expression of JUN proteins results in competition shifting the balance of heterodimer to JUN homodimer formation and DNA binding. C) c-Jun Homodimers have a higher binding have increased stability and higher affinity than Jun D, inhibiting Jun D DNA binding.

The co-transfections of the HSC were repeated with FOS expression resulting in the down-regulation of promoter activity for all of the vectors (Figure 3.6.1.). As mentioned with reference to the JUN vectors, the reduction in promoter activity is due to competition resulting from the formation dimers with a lower transcription activity and or a higher binding affinity. As with the JUN expression vectors the over expression of various Proteins effected the various endogenous dimeric combinations (see Figure 3.13.2. and 3.13.3).

The data obtained from the transfections of the HSC indicated that only the FOS vectors Fos B and Fra 2 resulted in significant decreases in the activity of the TIMP-1 minimal promoter. These results suggest that the dimers Jun D/Fra 2 and Jun D/Fos B (the only endogenous possible heterodimeric combinations, see Figure 1.13.2) as previously suggested negatively regulate the activity of the TIMP-1 minimal promoter.

The role of Fra 2 as a negative regulator in the literature has been previously mentioned with respect to c-Jun and Jun B. There is, as already mentioned, some confusion in the literature as to the role of the Fra-2/Jun D heterodimer (Suzuki *et al.*, 1991; Rutberg *et al.*, 1997). The down regulation of promoter activity, with the over expression of Fra 2, suggests that it is in fact inhibitory and competes for binding with the Jun D homodimers in this system. Little is known about the function of Jun D/Fos B heterodimer transcriptional activity. Fos B appears to behave in a similar way to c-Fos; classically it is not suggested to negatively regulate promoter activity. The heterodimers of Fos B however, possess the highest binding affinities of all the dimeric combinations so they would actively compete for AP-1 binding over the Jun D homodimer (Ryseck *et al.*, 1991). It is possible that in the HSC, endogenous negative regulation may occur through the expression of the truncated form of Fos B (Fos B2 or ΔFos B), which could have been competed out by Jun D over expression, as seen in Figure 3.5.1 (Yen *et al.*, 1991). In the literature c-Fos has been shown to be a powerful positive regulator of TIMP-1 transcription, however, as previously mentioned with respect to c-Jun, this required the presence of c-Ets binding to the PEA3 site (Edwards *et al.*, 1992; Logan *et al.*, 1996). The expression of c-Ets has previously been shown to be strongly down regulated in the activated HSC and mutation of the PEA3 site has only been shown to lead to a 30% reduction in promoter activity (Bahr *et al.*, 1999; Knittel *et al.*, 1999).

In order that a firm role for Jun D could be established, a dominant negative Jun D expression vector was obtained via collaboration. The results of the dominant negative RSV-β-Δ-Jun D expression vector co-transfection with the TIMP-1 minimal promoter reporter construct indicated a significant decrease in TIMP-1 promoter activity (Figure 3.7.2). This result adds further weight to the crucial nature of Jun D, indicating that the removal of this single endogenous transcription factor leads to a large reduction in TIMP-1 promoter activity. Jun D does form active dimers and these actively compete for binding of the AP-1 site. Also the fact that the blockade of a single transcription factor leads to a reduction in promoter activity suggests that Jun D may be a possible therapeutic target.

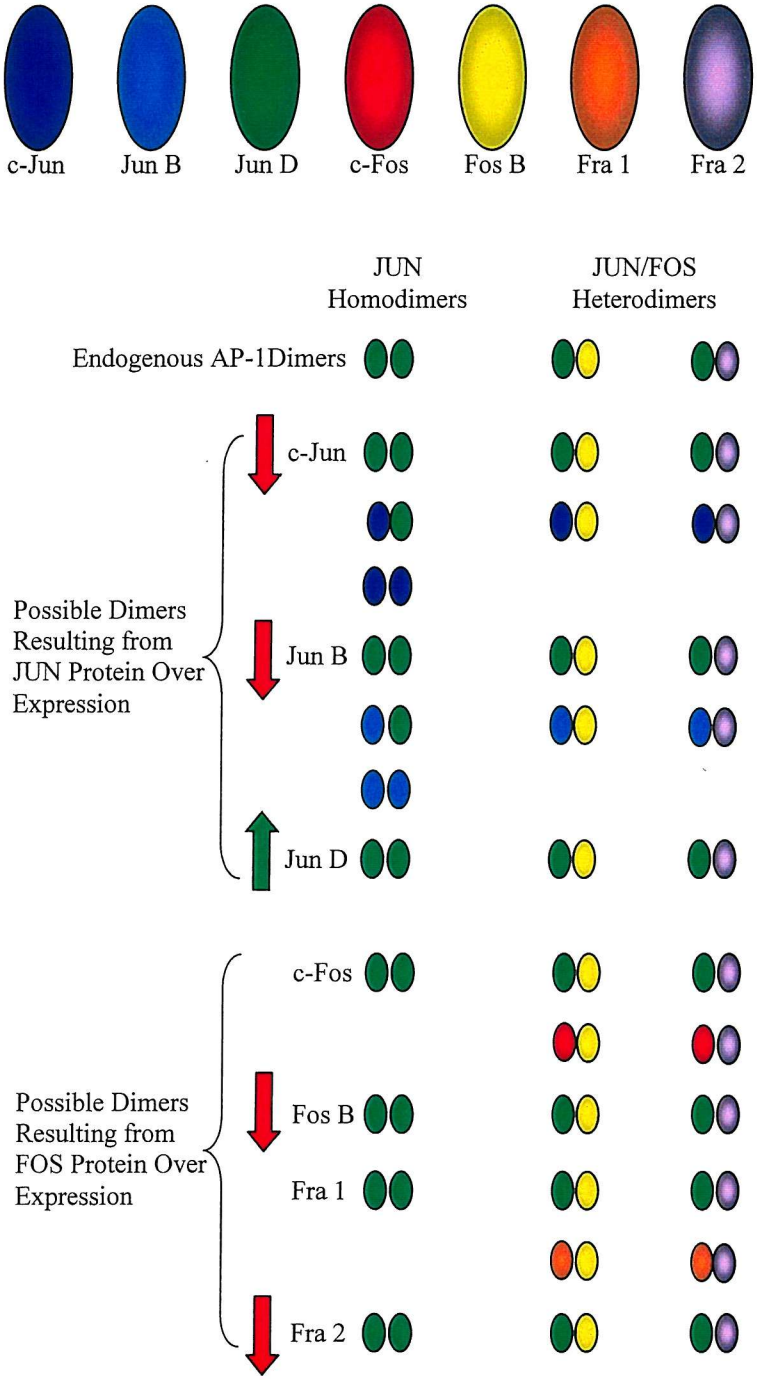

Figure 3.13.2 The possible AP-1 site DNA binding dimers available endogenously in culture activated HSC and as a result of over expression of the various JUN and FOS family members. The coloured arrows green and red correspond to increases and decreases in TIMP-1 minimal promoter activity with the over expression of an individual JUN or FOS protein. Over expression was produced by the transfection of a specific expression vector into culture activated HSC (see Figure 3.5.1 and 3.6.1).

In order to establish whether the Jun D homodimers were, as expected, transcriptionally active in the HSC with respect to the TIMP-1 promoter, a chimeric Jun D homodimer forming expression vector was obtained via. The results of the co-transfection of the homodimer forming Jun D expression vector and the TIMP-1 reporter construct –111WT indicate a significant increase in the activity of the promoter (Figure 3.7.3). This shows that the Jun D homodimer is very active in the transactivation of the TIMP-1 promoter in the HSC.

As part of the same collaboration two more expression vectors were made available at a later date, these also expressed chimeric proteins but this time for Eb1 and the JUN proteins c-Jun and Jun B. The results of these co-transfections indicated a significant increase in promoter activity with c-Jun homodimer forming vector but no change in promoter activity with Jun B homodimer expression. The data, when combined with that of the pCMV2 data (Figure 3.5.1), would seem to suggest that the inhibitory effect of c-Jun and Jun B over expression was due to the formation of heterodimers with either Fra 2 or Fos B, as previously suggested. They are very stable, with a higher affinity for the AP-1 site than c-Jun/c-Jun, Jun D/Jun D, c-Jun/Jun D or even Jun D/Fra 2 dimers (Ryseck *et al.*, 1991; Suzuki *et al.*, 1991; Sonobe *et al.*, 1995; Rutberg *et al.*, 1997). The results also suggest that c-Jun homodimers can trans-activate the TIMP-1 minimal promoter independently of c-Ets, which was previously shown to be required for c-Jun/c-Fos mediated transactivation of TIMP-1 (Edwards *et al.*, 1992; Logan *et al.*, 1996). The Jun B homodimers were found not to affect the activity of the promoter and were therefore either of equal transcription activity to the endogenous AP-1 dimers in the HSC or were unable to compete for the AP-1 site in the TIMP-1 promoter. It has been shown in the literature that the affinity of the Jun D homodimer is greater than that of Jun B. This would explain the lack of a significant effect of Jun B/Eb1-pDP7 transfection (Ryseck *et al.*, 1991). With Jun D homodimers as the most active AP-1 dimer, any dimer to affect promoter activity would either need to have greater binding affinity or be in excess (see Figure 3.13.1A-C). The results for the Jun B homodimer therefore, again, incriminate the heterodimers with Fra 2 or Fos B for the negative regulation seen within the pCMV2 expression vector data (Figures 3.5.1 and 3.6.1).

Over Expressed	Jun D Jun D	Jun D Fra2	Jun D Fos B	Suggested Reason For Change in Promoter Activity
c-Jun	⇓	⇓	⇓	c-Jun has higher affinity than Jun D, dominated by c-Jun / FOS in active dimers.
Jun B				Unknown
Jun D	⇑	⇒	⇒	Fra 2 and Fos B saturated relative increase in Jun D Homodimer levels
c-Fos				Unknown
Fos B	⇓		⇑	Higher affinity than Jun D homodimer reduced Jun D levels
Fra 1				Unknown
Fra 2	⇓	⇑		Increased formation of inhibitory Fra 2 heterodimer
RSV-β-Δ-Jun D	⇓	⇓	⇓	Active Wild type Jun D competed out
Jun D/Eb1-pDP7	⇑	⇒	⇒	Jun D homodimer is a positive regulator
c-Jun/Eb1-pDP7	⇒	⇒	⇒	c-Jun homodimer is a positive regulator and has higher affinity than Jun D
Jun B/Eb1-pDP7	⇒	⇒	⇒	All endogenous dimers have higher affinity

Figure 3.13.3 The results and possible effects on endogenous dimeric combinations following the transfection of the various expression vectors. The three possible endogenous dimeric combinations in the activated HSC (Jun D/Jun D, Jun D/Fra 2 and Jun D/Fos B) are listed. The expected changes in their relative concentration following the various transfections are shown by the symbols ⇑ increases, ⇓ decrease and ⇒ remains the same. The names of the expression vectors are shown in red, green or black, indicating that the TIMP-1 promoter activity decreases, increase or remains the same upon their co-transfection. Any spaces indicate the lack of data.

Following the research into the effects of the various AP-1 factors on TIMP- 1 promoter activity it was felt necessary to establish whether TIMP-1 promoter activity could be induced in quiescent HSC by the transfection of the various JUN and FOS expression vectors (Figure 3.8.1). This transfection was repeated on a number of occasions but in the representative result shown, there were equal amounts of protein used in the parallel CAT assays. The cells for both the activated and quiescent transfections were obtained from the same individual. The results indicated no activity in any of the quiescent

transfected cells. The activated cells follow the expected pattern of expression, with reference to the Figures 3.5.1 and 3.6.1. There are a number of possible reasons for the lack of expression in the quiescent cells; the first is lower transfection efficiency in the quiescent cells due to the lack of cell proliferation. The quiescent HSC have been shown to be transfectable through data obtained from Renilla transfection efficiency plasmid co-transfection, although the level of transfection is approximately 50% lower (Figure 3.8.2). The second possible reason for the lack of TIMP-1 induction is the absence of another crucial factor such as UTE-1, which has been shown to be crucial in activated cells but is absent in quiescent cells (Trim *et al.,* 2000). Only the binding site for UTE-1 is known at present but when the protein is identified, further investigations can be performed in quiescent cells.

Following the investigation of the effects of positive modulation of the various JUN and FOS family proteins, it was felt necessary to investigate the endogenous transcription factors. The sequences for mRNA-specific oligonucleotides to Jun D, Fra 2 and Fos B were obtained from the literature (see Appendix 1) (Robertson *et al.,* 1995; Wang *et al.,* 1996a; Crocker *et al.,* 1998). A titration of both sense and antisense Jun D specific oligonucleotides was performed; the sense oligonucleotide was used as a control. The transfection of antisense Jun D DNA was shown by a Western blot to effectively reduce Jun D protein expression with no reduction in a comparative sense control transfection (Figure 3.9.1.A).

Co-transfections were performed in activated HSC using Jun D, Fos B and Fra 2 antisense oligonucleotides and the TIMP-1 minimal promoter. The Jun D sense oligonucleotide was again used as a control. The results of the co-transfections indicated significant reductions in promoter activity for the Jun D and Fra 2 antisense oligonucleotide transfections (Figure 3.10.1.).

The most significant reduction in promoter activity was with Jun D, which supports the expression vector findings (Figure 3.5.1) and also the dominant negative results (Figure

3.7.3). The result is not unexpected, as Jun D is the only endogenous JUN factor in the activated HSC; it would have to be present in any AP-1 dimer.

The expression vector study of the FOS proteins suggested that over expression resulted in a significant decrease in promoter activity for both Fos B and Fra 2. The results of the antisense study seem to contradict this, suggesting that Fra 2 is crucial for TIMP-1 promoter activity. The reduction observed with Fos B was not shown to be significant, but this may have been due to a lower n number.

The over expression of the FOS proteins has been shown to reduce the activity of the TIMP-1 promoter, probably through the formation of inactive heterodimers (Figure 3.6.1). The inactive heterodimers are more stable and possess a higher affinity for the AP-1 site, making them highly competitive when compared to the active Jun D homodimers. The results of the antisense study would appear to contradict the previous data, indicating that Fra 2 may also have a positive effect on transcription. Under these circumstances it is suggested that Fra 2 and, to a lesser extent, Fos B containing dimers may have a secondary effect on TIMP-1 promoter activity. The secondary role of Fra 2 and Fos B may be through the regulation of another gene required for TIMP-1 promoter activity such as IL-6 (see later) UTE-1 or Jun D itself (Trim *et al.*, 2000). The possibility that Jun D is regulated by Fra 2 and/or by Jun D itself is not a complete surprise. All the JUN protein promoters contain AP-1 binding sites (see Figure 3.13.4), whether they be the 12-O-Tetradecanoylphorbol-13-acetate (TPA)-response element (TRE) of c-Jun and Jun D or the serum response element (SRE) and cyclic AMP response element (CRE) of Jun B (Angel *et al.*, 1988; de Groot *et al.*, 1991; Kitabayashi *et al.*, 1993; Mechta-Grigoriou *et al.*, 2001). The TRE of Jun D is not very responsive to either serum or phorbol ester as the gene is usually constitutively active, suggesting that this is not the root of action (de Groot *et al.*, 1991).

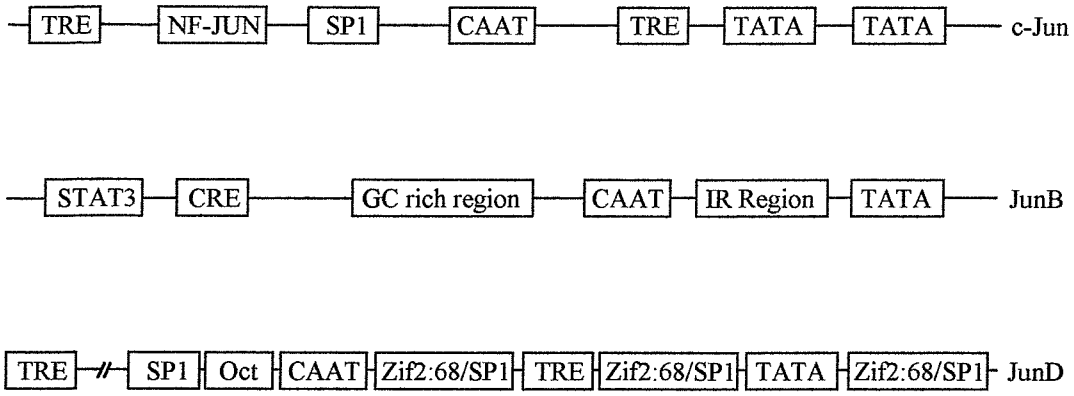

Figure 3.13.4. Diagrammatic representations of the promoter of the JUN AP-1 proteins indicating the identified regulatory regions of the genes (Machta-Grigoriou *et al.*, 2001)

The negative role of Fra 2 heterodimers in TIMP-1 promoter activity is further supported by the co-transfection of Jun D and Fra 2 expression vectors, individually or in combination (Figure 3.10.2). The results indicated an increase in promoter activity for Jun D and a decrease for Fra 2, as expected. The inability of Jun D to reverse the reduction in promoter activity when in co-transfection with Fra-2 supports the role of the Fra 2/Jun D heterodimer as a negative regulator, as suggested in the literature. It is possible that the erroneous results for the Fos B and Fra 2 antisense experiments resulted from non-specific effects of the oligonucleotides. If these experiments were repeated, it would be necessary to consider investigating the specificity of individual oligonucleotides used, as those for Jun D were.

To support the work on the TIMP-1 promoter a comparative study was performed. The comparative study used a series of mutant constructs obtained via collaboration for another classically AP-1 regulated gene. The IL-6 gene has previously been implicated in liver fibrosis and has also been shown to be expressed by the HSC, increasing with activation in a similar way to TIMP-1 (Napoli *et al.*, 1994; Eickelberg *et al.*, 1999; Natsume *et al.*, 1999; Oyanagi *et al.*, 1999; Kolalovich *et al.*, 2000; Smart *et al.*, 2001). The results of the research into the regulation of the TIMP-1 promoter indicated a crucial role for the AP-1 site in transcription. The TIMP-1 *in vitro* work had also identified a

positive regulatory role for Jun D and, in particular, its homodimers in transcription. It was expected that the results for IL-6 would be the same as those seen for TIMP-1 in the HSC, as IL-6 is also an accepted pro-inflammatory / pro-fibrotic cytokine (Duncan *et al.*, 1991; Roeb *et al.*, 1993; Roeb *et al.*, 1994). It was also known that the activated HSC expresses IL-6 and that in lung fibrosis Jun D homodimers were known to positively regulate transcription, which suggested a similar mechanism for its regulation as TIMP-1 (Tiggelman *et al.*, 1995; Eickelberg *et al.*, 1999; Oyanagi *et al.*, 1999).

The transfection of the mutant IL-6 minimal promoter constructs into the HSC indicated that NFκB was crucial (Figure 3.12.2). The mutation of the NF-IL-6 site did show a slight, but not significant, change in the promoter activity. A combined mutation of NFκB and NF-IL-6 also showed a significant reduction in promoter activity, greater than that of NFκB on its own, suggesting that the NF-IL-6 site may have a genuine effect but only through synergy with the NFκB site. Surprisingly the mutation of the AP-1 site resulted in an increase in IL-6 promoter activity suggesting that, in the activated HSC, this site is inhibitory. This result was unexpected both with respect to the TIMP-1 data and the IL-6 literature. Another PhD student working in the department (Jelena Mann, unpublished data) has shown that the IL-6 AP-1 site mutant also shows lower transcriptional activity than the wild type in dendritic cells, supporting the literature.

In an attempt to explain the negative regulatory function for AP-1, a series of co-transfection were performed using Jun D wild type, dominant negative and homodimer forming expression vectors (Figure 3.12.3). These results indicated that the wild type Jun D is a positive regulator. The results, at first glance, seem contradictory to those of the mutational analysis (Figure 3.12.2). However the results of the other co-transfections indicated that the homodimer forming Jun D and dominant negative resulted in a reduction in IL-6 promoter activity.

Taken together, the promoter mutational analysis and co-transfection studies seem to indicate that the AP-1 site may act both as a positive and negative regulator at the same time. There are a number of possible causes for these effects. The increase in activity

with AP-1 site mutation indicates that this site in the activated HSC is functioning as a negative regulator of transcription. This suggests that the binding of AP-1 dimers are inhibitory. It is strongly suggested from previous work in this chapter that AP-1 dimers in the culture activated HSC system are, with regard to TIMP-1, made up from Jun D homodimers with Jun D/FOS heterodimers acting as competitors. As seen with TIMP-1, the co-transfection of Jun D expression vectors increased IL-6 promoter activity, which may be due to changes in dimer composition favouring Jun D containing dimers over other combinations of AP-1 dimers (Figure 3.5.1). The positive role of Jun D is also supported by the dominant negative co-transfection, which showed a reduction in activity as previously mentioned (Figure 3.12.3). The reduction in activity resulting from the transfection of the homodimer Jun D/Eb1-pDP7 expression vector suggests that, unlike TIMP-1 (HSC) and IL-6 (Lung fibroblasts), the positive regulation of IL-6 in the HSC is not by Jun D homodimer binding (Figure 3.12.3). The positive activity of the Jun D protein may be mediated through another site such as the CRE (-300/-293) (Figure 3.12.1, see Appendix 7). To bind to the CRE, Jun D would have to dimerize with one of the ATF family members. This may explain the negative activity of the homodimer forming Jun D expression vector. The binding of the Jun D homodimer to the negative regulatory AP-1 would result in promoter activity reduction. On close examination of the IL-6 promoter it was also obvious that, as well as the sites previously identified, others were also present including a second consensus CRE (-142/-135) and an AP-1 (-38/-32) site with a single base pair mismatch (Eickelberg *et al.*, 1999). The mismatch in the AP-1 site changes it from the consensus TGAGTCA to TGAGTCT in much the same way as 5' TIMP-1 minimal promoter site is changed to TGAGTAA (see Appendix 7). These other sites could be possible positive regulatory regions that respond to JUN/FOS and JUN/ATF heterodimers.

The possible involvement of the second AP-1 site in the activity of the IL-6 promoter may explain the paradoxical effects of Fra-2 and Fos B on TIMP-1 expression, in which both over expression and specific antisense resulted in decreased promoter activity. Previous experimentation has shown that IL-6 enhances TIMP-1 and its production. This research includes CCl_4 liver injury studies on IL-6 knockout mice and treatment studies

in rheumatoid arthritis and acute lung injury patients (Natsume *et al.*, 1999; Maiotti *et al.*, 2000; Seitz *et al.*, 2000; Shinoda *et al.*, 2000 Ward *et al.*, 2000). As previously mentioned, IL-6 and its respective receptor have been shown to be expressed in the HSC and raised levels of IL-6 are seen in liver fibrosis (Tiggelman *et al.*, 1995; Oyanagi *et al.*, 1999; Toda *et al.*, 2000, Smart *et al.*, 2001). For these reasons it is suggested that one way of explaining the divergent results, when looking at the roles of the FOS proteins in TIMP-1 regulation, is the secondary effects of IL-6. The AP-1 site of the TIMP-1 promoter was shown to act as a positive regulator when Jun D homodimers were bound and Fos heterodimers were inhibitory. In contradiction to the results of the over expression of Fra 2 and Fos B, their reduction with antisense oligonucleotides resulted in a reduction in promoter activity, suggesting a positive role. The binding of the Jun D/FOS and, in particular, Fra 2 to the AP-1 sites of the IL-6, may explain the confusion, as an increase in IL-6 production could lead to an enhancement of TIMP-1 expression but the removal of FOS proteins would not lead to a total absence. This suggestion may be supported by the mutation data of the PEA3 site, which results in a 30% reduction in promoter activity in the activated HSC even though c-Ets expression is virtually non-existent. The Pea3 site overlaps the STAT1 site (see Appendix 6) and this mutation would result in removal of the role of IL-6 activity.

Future work would be to look at the recently identified transcription factor UTE-1 that has been shown to be crucial for TIMP-1 minimal promoter activity in the activated HSC (Trim *et al.*, 2000). It is possible that UTE-1 in the HSC may take over the function of the interaction between c-Ets (PEA3) and AP-1 seen in other cell types. The novel role of Jun D in the transcription of TIMP-1 in the HSC may be due to direct interaction between the Jun D homodimers and UTE-1 proteins.

It is also necessary to determine how Jun D is regulating IL-6, by what transcription factor binding site and with what dimer partner. It may also be necessary to look at the various members of the ATF family in order to establish their role. It would also seem necessary to investigate whether IL-6 expression is modulating that of TIMP-1 and if this is through the STAT1 site or via another route.

Chapter 4.

Establishing the Cell Specific Effects of JUN and FOS Expression on the Tissue Inhibitor of Metalloproteinase-1

4.1 Using Fibroblasts as a Classical Model of TIMP-1 Regulation.

The effects of JUN and FOS proteins on TIMP-1 expression in HSC were shown to contrast those seen in literature for other cell types. The transcriptional regulation of TIMP-1 by AP-1 is classically mediated by c-Jun and c-Fos, which is in contrast to the Jun D homodimer regulation suggested in the HSC (see Chapter 3) (Edwards *et al.*, 1992; Logan *et al.,* 1996). It was therefore felt necessary to establish whether the effects seen for JUN over expression on TIMP-1 promoter activity in the HSC are cell specific. For this reason many of the experiments performed in the HSC were repeated in an alternative cell type, the murine NIH3T3 cell. The NIH3T3 is a fibroblast cell line, classically used in the literature. This was therefore used for a comparative study with the myofibroblast-like HSC.

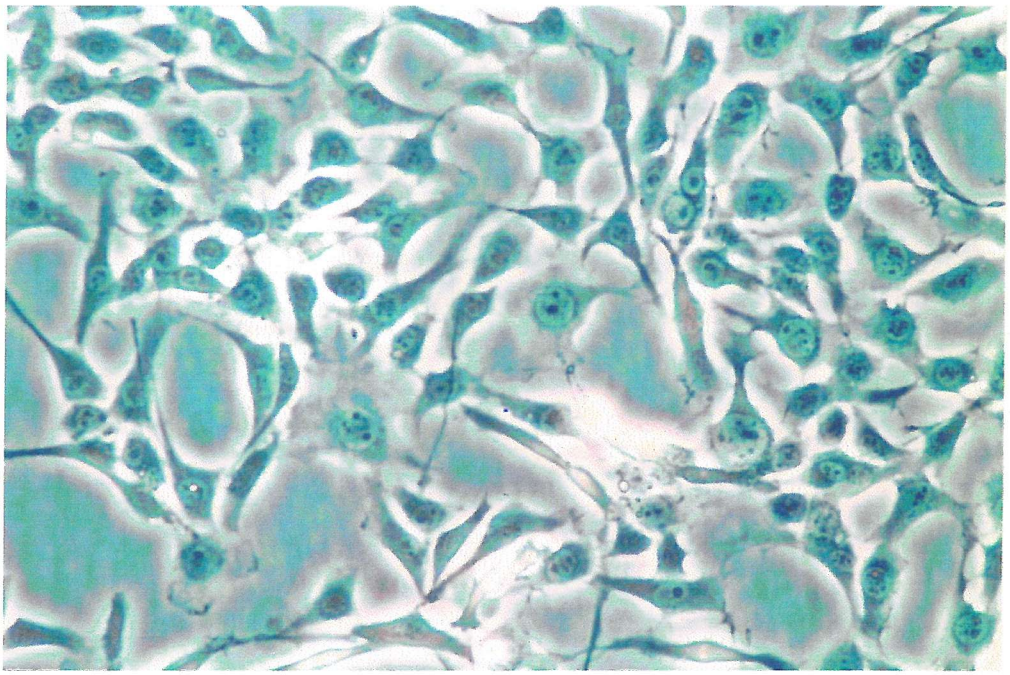

Figure 4.1.1 NIH3T3 fibroblasts cultured on tissue culture plastic. The cells show the classical elongated fibroblast phenotype. Photographed using an inverted phase contrast microscope (Leica) and an automatic exposure system (Leica) at 200x magnification.

In order to establish if effects seen in the HSC were cell specific, co-transfections of the JUN expression vectors were performed in NIH3T3 fibroblasts with the TIMP-1 minimal promoter reporter. The results in the NIH3T3 fibroblasts suggest that the transfection of any of the JUN expression vectors significantly down-regulates the activity of the TIMP-1 minimal promoter (Figure 4.1.2). The reduction in promoter activity was more

significant for the Jun D and Jun B expression vectors. A comparison of TIMP-1 minimal promoter activity upon JUN expression vector transfection of rat HSC and NIH3T3 fibroblasts can be seen in Figure 4.1.3.

With all the Jun proteins showing inhibitory effects, it was felt necessary to look at the effect of the co-transfection of the various expression vectors on the generic activity of AP-1. In order to establish the basic AP-1 activity in NIH3T3 cells, a co-transfection was performed with both AP-1 expression vectors and a luciferase reporter containing five AP-1 sites (5xAP-1-Lux). The results of the co-transfection of the AP-1 luciferase construct with the expression vectors for c-Jun-pCMV2, Jun B-pCMV2, Jun D-pCMV2 and Jun D/Eb1-pDP7 indicated a significant reduction in promoter activity by all of the expression vector transfections, with respect to the controls (Figure 4.1.4). The order of activity for the transfections is from c-Jun-pCMV2, which was the most active, Jun D-pCMV2, Jun B-pCMV2 and then Jun D/Eb1-pDP7, which was the least active (reductions of 57, 81, 78 and 81% respectively).

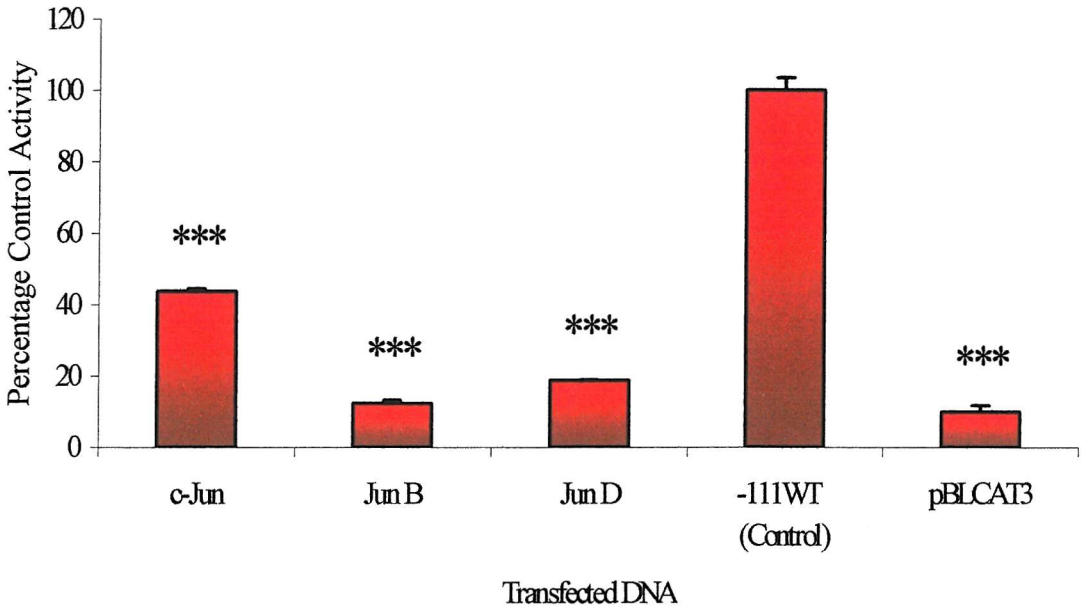

Figure 4.1.2 The effect on TIMP-1 minimal promoter activity of JUN expression vector co-transfection. The results displayed are the mean percentage and the standard error with respect to control activity from a representative triplicate transfection. The NIH3T3 fibroblasts were plated out at low density in 45mm dishes. The cells were cultured to allow them to become 60-70% confluent. The cells were transfected with 3μg of the JUN-pCMV2 or pCMV2 empty expression vectors and 1μg of –111WT reporter construct or pBLCAT3 by the Effectine method (Qiagen). The vectors pBLCAT3 and pCMV2 were used as controls for the reporter and expression vector transfection respectively. Each plate was also co-transfected with 100ng of Renilla-Luc expression plasmid to normalise for differences in transfection efficiency. The activity of the promoter was established and the results modified for transfection efficiency (see Section 2.7.3). The cells were cultured for 48 hours following transfection and cytoplasmic extract was harvested for CAT assay. An indication of the data significance can be obtained from the presence of a *, ** and ***. These represent P values of <0.05, 0.01 and 0.005 respectively, as shown by Student's T-test test of un-equal variance with two tails. For primary data see Appendix 3.

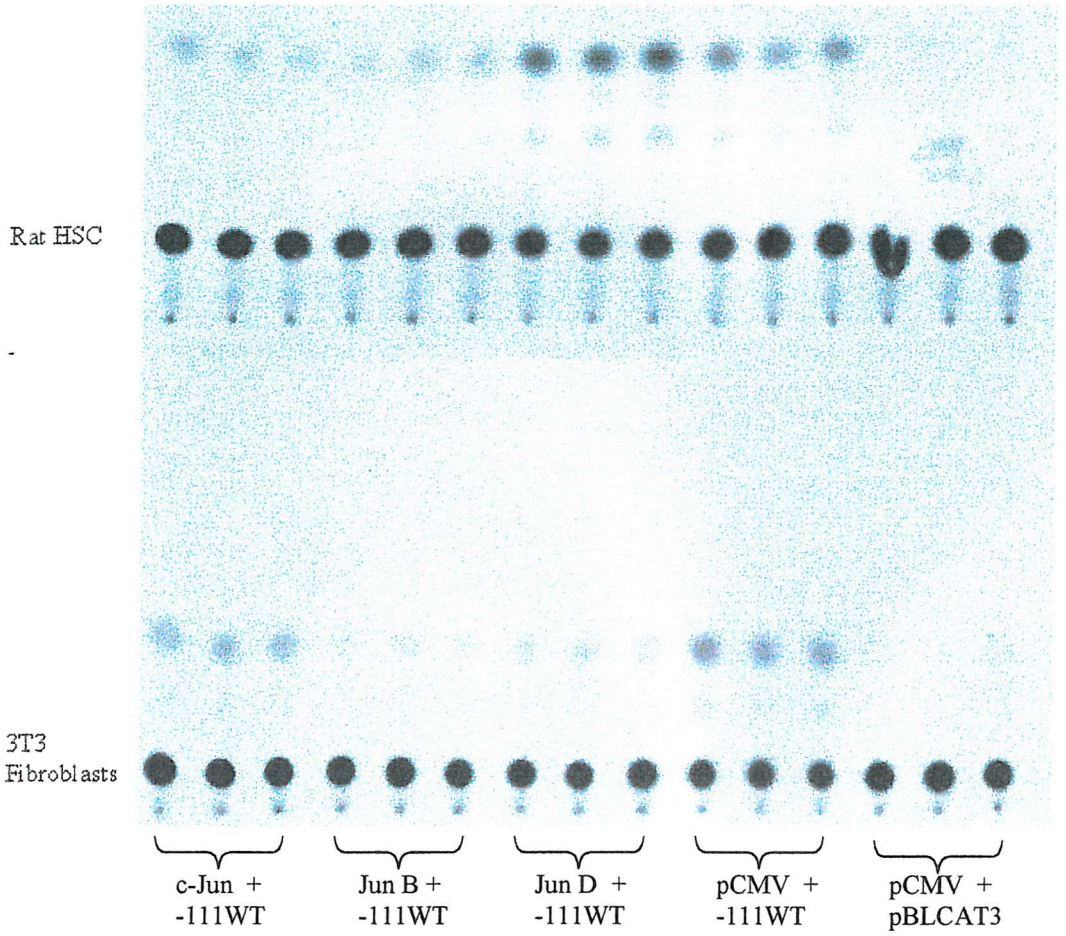

Figure 4.1.3. Primary data obtained from CAT assays of NIH3T3 murine fibroblasts and rat HSC cells. Comparison of JUN AP-1 protein expression vector co-transfection with the TIMP-1 –111WT minimal promoter reporter. The qualitative data shown here is quantitated in Figures 3.5.1 and 4.1.2. The figure is an autoradiograph obtained from the two CAT assay TLC plates.

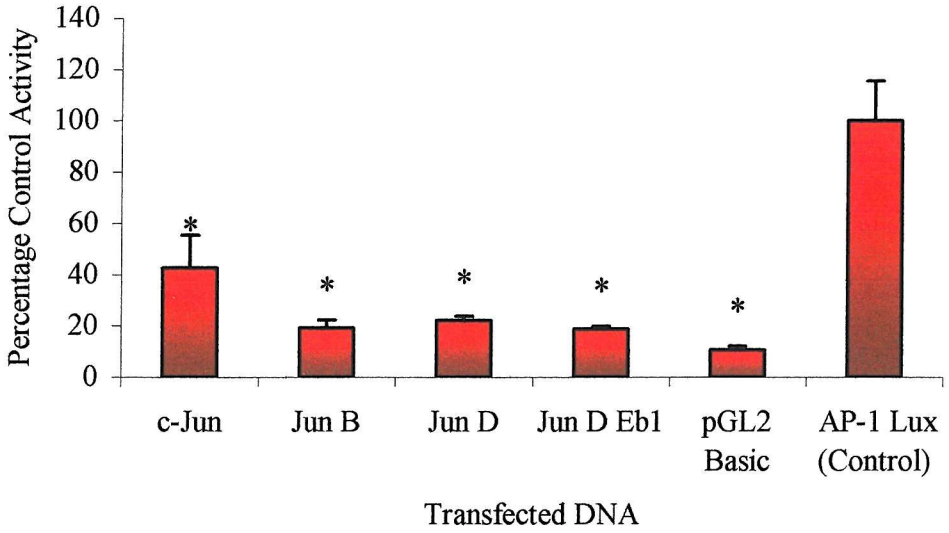

Figure 4.1.4 The effect of JUN expression vectors on the activity of a consensus AP-1 luciferase reporter. The results are the mean and standard error relative to the control activity, from a representative triplicate transfection. The NIH3T3 were plated in a 45mm culture plate and transfections were performed once the culture reached 60-70% confluence. The NIH3T3 cells were co-transfection with 3μg of c-Jun-pCMV2, Jun B-pDP7, Jun D-pDP7, Jun D/Eb1-pDP7 or pCMV2 and 1μg of 5xAP-1-Lux (Luciferase AP-1 reporter construct) or pGL2 Basic The Cells were transfected by the Effectine method (Qiagen). The vectors pGL2 Basic and pCMV2 were used as controls for the reporter and expression vector transfection respectively. Each plate was also co-transfected with 100ng of Renilla-Luc expression plasmid to normalise for differences in transfection efficiency. The cells were cultured for 48 hours following transfection and cytoplasmic extracts harvested for luciferase assay. The activity of the promoter was established and the results modified for transfection efficiency using the Dual Luciferase Assay (Promega) (see section 2.7.3). An indication of the data significance can be obtained from the presence of *, which represents a P value of <0.05. For primary data see Appendix 3.

4.2 The Serum Shocking of NIH3T3 Fibroblasts to Activate Protein Kinases

The results of the co-transfections of the NIH3T3 fibroblasts were unexpected as the literature suggested that the regulation of TIMP-1 in fibroblasts (C3H 10T/2) is classically mediated via c-Jun and c-Fos (Edwards *et al.*, 1992). With respect to the relative JUN and FOS protein expression in the NIH3T3 cell, the literature suggests that un-shocked or normal cycling cells, cultured in serum-containing media, express c-Jun, Jun D and Fra 2. However from 1 hour to 8 hours after serum shock, NIH3T3 fibroblasts induce the expression of c-Fos and Fos B (Lallemand *et al.*, 1997). It was also

demonstrated that both the JUN and FOS family members all underwent an increased level of phosphorylation in the first 12 hours following serum shock. The level of Jun and FOS phosphorylation or protein kinase activity was demonstrated to return to its normal low level after 12 hours of culture (Lallemand *et al.*, 1997). A similar result of serum treatment is also seen in 3T3T mouse mesodermal cells (Wang *et al.*, 1996b). For these reasons, the co-transfection with the TIMP-1 reporter construct and expression vectors was repeated in NIH3T3 cells. This time the cells underwent serum shock following transfection. The serum shocking of the NIH3T3 cells was intended to establish whether the reductions in promoter activity seen in the initial transfections were due to a lack of protein kinase activity and/or the lack of necessary dimeric partners (Lallermand *et al.*, 1997). As previously mentioned, the phosphorylation of the JUN and FOS proteins is performed by the kinases JNK and FRK (see Section 1.20).

The over expression of the JUN proteins in serum shocked cells (Figure 4.2.1) had a completely different outcome from that seen in un-shocked NIH3T3 fibroblasts (Figure 4.1.2). Over expression of Jun B and c-Jun led to significant increases in the activity of the TIMP-1 minimal promoter of 200 and 300% respectively over the control. In contrast to the HSC (Chapter 3), the over-expression of Jun D had no effect on TIMP-1 promoter activity. These results seem to suggest that the activity of the kinase apparatus may account for the inactivity of the JUN-pCMV2 expression vectors seen in un-stimulated cells (Figure 4.1.2, 4.1.3 and 4.1.4). The other possible reason, as previously suggested, may be due to the induction of other immediate early genes, possibly other AP-1 binding proteins, by the serum shock. The result does however agree with the role suggested for c-Jun in TIMP-1 regulation in the literature.

To further identify the role of the JUN proteins, a series of modified expression vectors were used in co-transfections with the TIMP-1 reporter. These were used to determine, in particular, the function of the JUN homodimers. The vectors used were a series of chimeric homodimer forming expression vectors obtained via collaboration with Dr Castellazzi (Ecole Normale Supérieure de Lyon, France) (Vandel *et al.*, 1995). These vectors were used in co-transfections with the TIMP-1 minimal promoter. The vectors

supplied (Jun D/Eb1-pDP7, Jun B/Eb1-pDP7 and c-Jun/Eb1-pDP7) are described earlier in greater depth (see Section 3.7). The result of the co-transfection of homodimer forming expression vectors with the TIMP-1 minimal promoter reporter was an increase in promoter activity for each of the vectors (Figure 4.2.2). The increases in promoter activity for the three vectors c-Jun/Eb1-pDP7, Jun B/Eb1-pDP7 and Jun D/Eb1-pDP7 were 400, 250 and 415% respectively.

Co-transfections of the TIMP-1 reporter and the FOS expression vectors were also performed in the presence of serum shock. The results of the FOS transfections were increases in promoter activity of 100 and 280% for co-transfection of Fra 1 and c-Fos respectively. The transfection of Fos B and Fra 2 resulted in reductions of 80 and 95% with respect to control transfections (Figure 4.2.3).

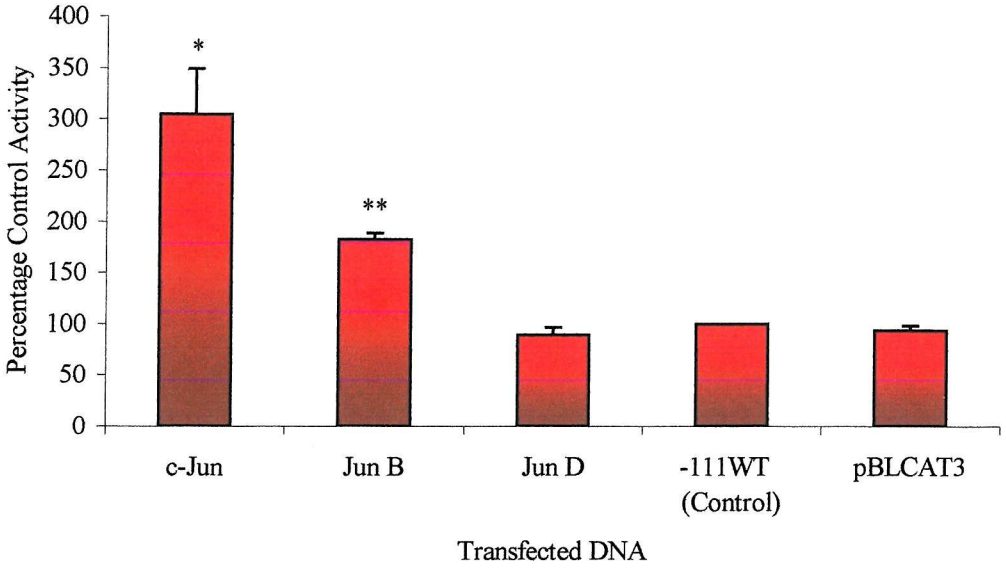

Figure 4.2.1. The effect on TIMP-1 minimal promoter activity of JUN expression vector co-transfection and subsequent serum shock. The results displayed are the mean percentage and the standard error with respect to control activity from a representative triplicate transfection. The NIH3T3 fibroblasts were plated out at low density in 45mm dishes. The cells were cultured to allow them to become 50-60% confluent. The cells were transfected with 3μg of JUN-pCMV2 or pCMV2 empty expression vector and 1μg of –111WTreporter construct or pBLCAT3 by the Effectine method (Qiagen). The vectors pBLCAT3 and pCMV2 were used as controls for the reporter and expression vector transfection respectively. Each plate was also co-transfected with 100ng of Renilla-Luc expression plasmid to normalise for differences in transfection efficiency. The activity of the promoter was established and the results modified for transfection efficiency (see Section 2.7.3). Following transfection the cells were cultured for 24 hours before being washed 3 times with Hanks Buffered Saline (HBSS). The Dulbecco modified eagle medium (DMEM) was replaced with serum free DMEM and the cells were cultured as normal. After a further 24 hours the media was replaced with DMEM + 10% serum. The incubation was continued for 48 hours before harvesting the cytoplasmic extract. An indication of the data significance can be obtained from the presence of a * or **. These represent P values of <0.05 and 0.01 respectively, as shown by Student's T-test test of un-equal variance with two tails. For primary data see Appendix 3.

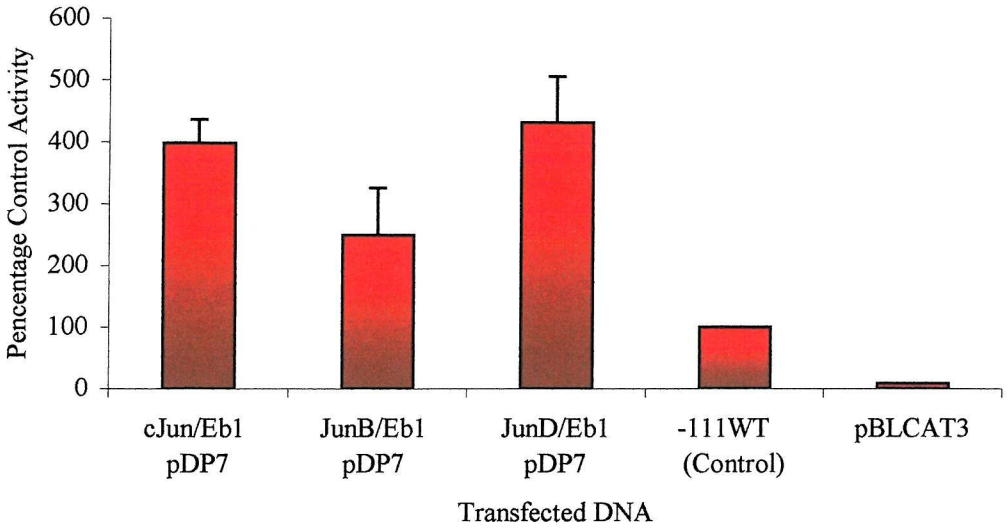

Figure 4.2.2. The effect of JUN homodimers on the activity of the TIMP-1 minimal promoter in serum shocked NIH3T3 cells. The results are the mean and standard error relative to control activity from a triplicate transfection. The NIH3T3 were plated in a 45mm culture plate and transfections were performed once the culture reached 50-60% confluence. The NIH3T3 cells were co-transfected with 3μg of c-Jun D/Eb1-pDP7, Jun B/Eb1-pDP7, Jun D/Eb1-pDP7 or pLMVP and 1μg –111WT TIMP-1 reporter or pBLCAT3 by the effectine method (Qiagen). The vectors pLMVP and pBLCAT3 were used as controls for the expression and reporter vectors respectively. Each plate was also co-transfected with 100ng of Renilla-Luc expression plasmid to normalise for differences in transfection efficiency. Following transfection the cells were cultured for 24 hours before being washed 3 times with HBSS. The media was replaced with serum free DMEM and the cells were cultured as normal. After a further 24 hours the media was replaced with DMEM + 10% serum. The incubation was continued for 48 hours before harvesting the cytoplasmic extract. The activity of the promoter was established and the results modified for transfection efficiency (see Section 2.7.3). For primary data see Appendix 3.

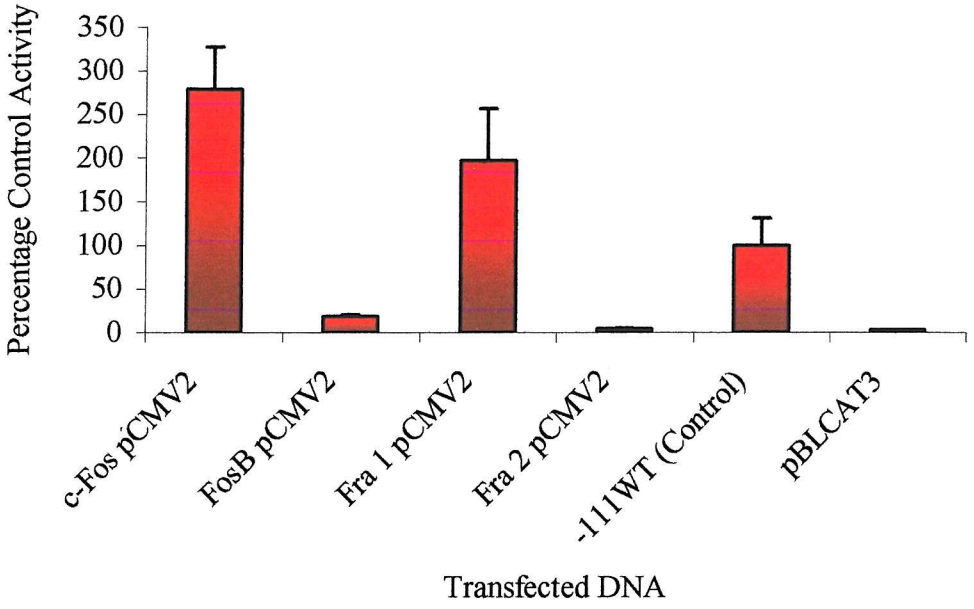

Figure 4.2.3. The effect on TIMP-1 minimal promoter activity of FOS expression vector co-transfection and subsequent serum shock. The results displayed are the mean percentage and the standard error with respect to control activity from a triplicate transfection. The NIH3T3 fibroblasts were plated out at low density in 45mm dishes. The cells were cultured to allow them to become 50-60% confluent. The cells were transfected with 3μg of the FOS-pCMV2 or pCMV2 empty expression vector and 1μg of –111WTreporter construct or pBLCAT3 by the Effectine method (Qiagen). The vectors pBLCAT3 and pCMV2 were used as controls for the reporter and expression vector transfection respectively. Each plate was also co-transfected with 100ng of Renilla-Luc expression plasmid to normalise for differences in transfection efficiency. The activity of the promoter was established and the results modified for transfection efficiency (see Section 2.7.3). Following transfection the cells were cultured for 24 hours before being washed 3 times with HBSS. The media was replaced with serum free DMEM and the cells were cultured as normal. After a further 24 hours the media was replaced with DMEM + 10% serum. The incubation was continued for 48 hours before harvesting the cytoplasmic extract. For primary data see Appendix 3.

4.3 The Role of Jun D and Fra 2 Protein Interactions in NIH3T3 Cells

The results from the *in vitro* study in HSC suggested that heterodimers of Jun D and Fra 2 proteins act as a negative regulator (Chapter 3). The literature also supports this negative regulatory role for Fra 2 in combination with c-Jun and Jun B proteins. There is some confusion in the literature however to the activity of the Jun D/ Fra2 heterodimer (Suzuki *et al.*, 1991; Sonobe *et al.*, 1995; Rutenberg *et al.*, 1997). It has been previously

shown that normal cycling NIH3T3 fibroblasts constitutively express Fra 2 and that there is an increase in the expression of Fra 2 following serum shock (Lallemand *et al.*, 1997). In order to investigate if Fra 2 could act as an inhibitor of TIMP-1 promoter activity in NIH3T3 fibroblasts, the cells were triple transfected as previously performed in the HSC (see Section 3.10.2). The triple transfections consisted of different combinations of Fra-2-pCMV2 and Jun D-pCMV2 with the TIMP-1 minimal promoter reporter.

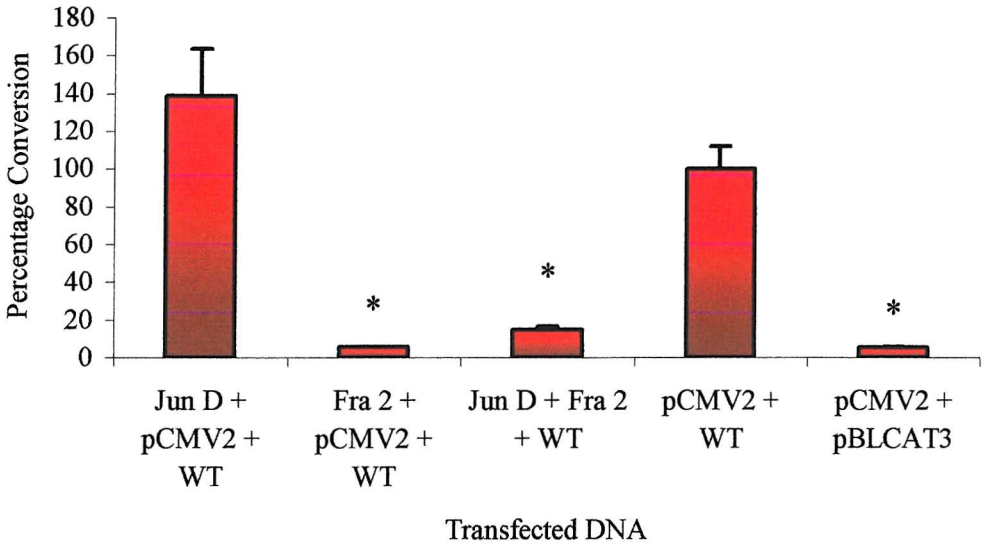

Figure 4.3.1 The effect of various combinations of Jun D and Fra 2 expression on the activity of the TIMP-1 minimal promoter in serum shocked NIH3T3 cells. The results are the mean and standard error with respect to the control activity from a representative triplicate transfection. The NIH3T3 cells were plated in a 45mm culture plate and transfections were performed once the culture reached 50-60% confluence. The NIH3T3 cells were co-transfected with combinations of 1.5μg pCMV2, Jun D-pCMV2 or Fra-2-pCMV2 and 0.5μg –111WT TIMP-1 reporter or pBLCAT3. Transfections were performed using the Effectine method (Qiagen). The vectors pBLCAT3 and pCMV2 were used as controls of reporter and expression vector transfection respectively. Each plate was also co-transfected with 100ng of Renilla-Luc expression plasmid to normalise for differences in transfection efficiency. The activity of the promoter was established and the results modified for transfection efficiency (see Section 2.7.3). Following transfection the cells were cultured for 24 hours before being washed 3 times with HBSS. The media was replaced with serum free DMEM and the cells were cultured as normal. After a further 24 hours the media was replaced with DMEM + 10% serum. The incubation was continued for 48 hours before harvesting the cytoplasmic extract. An indication of the data significance can be obtained from the presence of a * or **. These represent P values of <0.05 and <0.01 respectively. For primary data see Appendix 3.

The results of the co-transfection of NIH3T3 fibroblasts with Fra-2 and Jun D in serum shocked cells resulted in a slight but insignificant increase with Jun D of 38%. The transfection of Fra 2 however, resulted in significant decreases in promoter activity both with and without Jun D expression of 85 and 94% respectively. This is a similar effect as was seen in the HSC.

4.4 The Role of Phosphorylation in AP-1 Protein activity

To examine the role of phosphorylation on the activity of AP-1 for both the HSC and NIH3T3 fibroblast, co-transfections were performed using a dominant negative JNK and the TIMP-1 promoter. The dominant negative JNK vector used was obtained via collaboration with Dr. I. M. Clark (School of Biomedical Science, University of East Anglia, Norwich UK). The JNK mutant (sRSPA-HA-SAPKβp54 KK→RR) contains a JNK mutation at amino acids 55 and 56, these are changed from Lysines to Arginines resulting in inactive phosphorylation domain. The JNK dominant negative expression is under the influence RSV promoter, for this reason the empty vector pLMVP was used as a control (see Appendix 2v).

The results indicate that there is a significant 50% decrease in the activity of the TIMP-1 minimal promoter with the transfection of the dominant negative JNK (Figure 4.4.1). This suggests that JNK is important for the function of TIMP-1 in the NIH3T3 fibroblast.

The co-transfection of the dominant negative JNK was repeated in HSC cells for the purposes of comparison. The result of the transfection of the dominant negative JNK indicated a 51% increase in promoter function with respect to the control, when co-transfected with the TIMP-1 minimal promoter in HSC. This was however not shown to be significant (Figure 4.4.2).

JNK is unable to act directly on Jun D as previously mentioned in the introduction (see Section 1.20). Although Jun D has a JNK phosphorylation domain like c-Jun, it lacks a docking domain for JNK. For this reason Jun D cannot recruit JNK by itself and requires a chaperone protein. The proteins c-Jun and Jun B are important chaperones for Jun D,

recruiting JNK to it for phosphorylation (Dérijard *et al.*, 1995; Kallunki *et al.*, 1996). However in the activated HSC, neither c-Jun or Jun B proteins are present and so cannot be responsible for Jun D phosphorylation (Bahr *et al.*, 1999). An alternative protein capable of chaperoning Jun D is JAB 1 (Claret *et al.*, 1996). It is now also believed that JAB 1 can act as part of the JNK independent COP9 signalosome to phosphorylate the JUN proteins (Chamovitz *et al.*, 2001).

In order to establish whether JAB1 is present in HSC, Western blots were performed using whole cell extracts from human and rat HSC. The result of the JAB1 Western blot showed that JAB1 is in fact present in human and rat HSC and also that JAB1 expression increases with cell activation (Figure 4.4.3). The presence of JAB1 in the activated HSC indicates a possible mechanism for Jun D activation in the HSC. It was felt necessary to establish whether the differences in the role of Jun D in HSC and fibroblasts are due to JAB1, whole cell NIH3T3 extracts were produced. A comparative Western blot for JAB1 was performed in which NIH3T3 whole cell extracts were run alongside those of rat HSC. The Western blot comparing the expression of JAB1 in 8 day activated rat HSC and NIH3T3 cells clearly shows that there is a significantly higher expression of this protein in the fibroblasts than in the HSC cells. A large, strong signal was clearly seen on the autoradiography film for the NIH3T3 cells at an exposure that left the HSC band only just visible (Figure 4.4.4). The longer exposures of the film, which would have identified a JAB1 band in the HSC lane, were over exposed due the comparative high level of JAB1 expression by the NIH3T3 fibroblasts.

Another factor that has been suggested to participate in the classical c-Jun and c-Fos regulation of TIMP-1 transcription is c-Ets-1 (Edwards *et al.*, 1992; Logan *et al.*, 1996). To test whether c-Ets-1 could have a role in the regulation of TIMP-1 via interaction with c-Jun and c-Fos in the NIH3T3 cell line, the cells were cultured both with and without serum shock and whole cell extracts were made. These whole cell extracts were used for Western blotting to determine if c-Ets-1 was present and whether it changed dramatically with serum shock. The results of the Western blot for c-Ets-1 in the NIH3T3 fibroblasts

indicate that it is present in both normal cycling and serum shocked cells at similar concentrations (Figure 4.4.5).

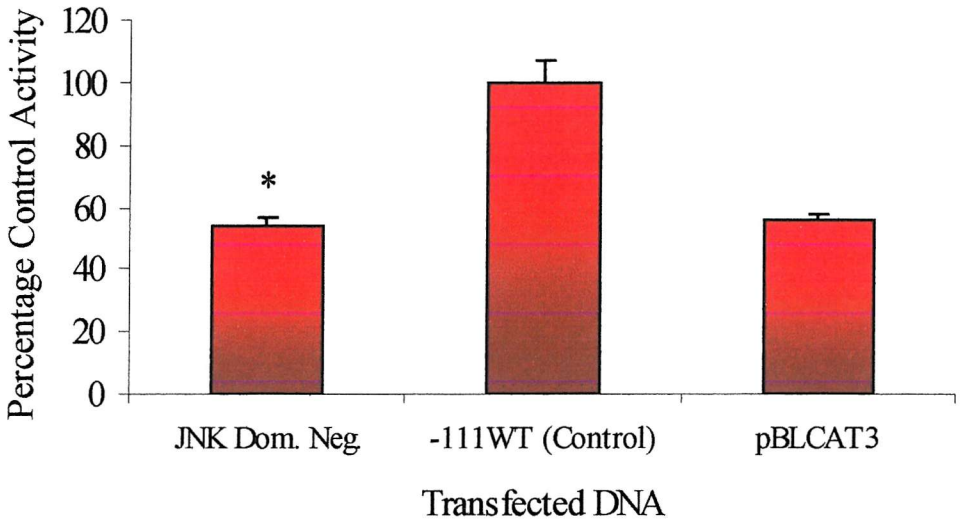

Figure 4.4.1. The effect of a dominant negative JNK on the activity of the TIMP-1 minimal promoter in serum shocked NIH3T3 cells. The results are the mean and standard error relative to the control activity from a representative triplicate transfection. The NIH3T3 fibroblasts were plated in a 45mm culture plate and transfections were performed once the culture reached 60-70% confluence. Cells were transfected by the effectine method (Qiagen) with 3μg of the dominant negative JNK expression vector (sRSPA-HA-SAPKβp54 KK→RR) or pLMVP control and 1μg of –111WT TIMP-1 reporter or pBLCAT3. The vectors pLMVP and pBLCAT3 were used as controls for the expression vector and reporter respectively. Each plate was also co-transfected with 100ng of Renilla-Luc expression plasmid to normalise for differences in transfection efficiency. The activity of the promoter was established and the results modified for transfection efficiency (see Section 2.7.3). Following transfection the cells were cultured for 24 hours before being washed 3 times with HBSS. The media was replaced with serum free DMEM and the cells were cultured as normal. After a further 24 hours the media was replaced with DMEM + 10% serum. The incubation was continued for 48 hours before harvesting the cytoplasmic extract. An indication of the data significance can be obtained from the presence of a *, representing a P value of <0.05, as shown by Student's T-test test of un-equal variance with two tails. For the primary data see Appendix 3.

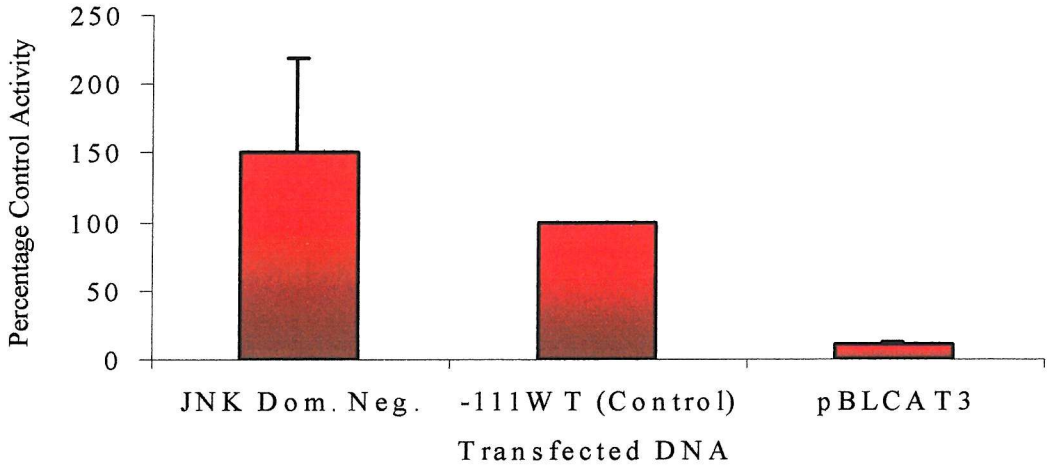

Figure 4.4.2. The effect on TIMP-1 minimal promoter activity of the co-transfection of a dominant-negative JNK expression vector. The results displayed are the percentage mean and the standard error of control activity from a representative triplicate transfection of cells. Primary HSC cells were plated out 45mm tissue culture dishes at a density of 10^6 cells per plate. The cells were allowed to activate over >7days and transfected upon reaching 60-70% confluence. The cells were transfected with 3μg of the dominant negative JNK (sRSPA-HA-SAPKβp54 KK→RR) or pLMVP and 1μg of –111WT TIMP-1 or pBLCAT3 reporter vector. The vectors pBLCAT3 and pLMVP were used as controls for reporter and expression vector transfection respectively. Each plate was also co-transfected with 100ng of Renilla-Luc expression plasmid to normalise for differences in transfection efficiency. The activity of the promoter was established and the results modified for transfection efficiency (see Section 2.7.3). The cells were cultured for 48 hours before cytoplasmic extracts were harvested and CAT assays performed. For primary data see Appendix 3.

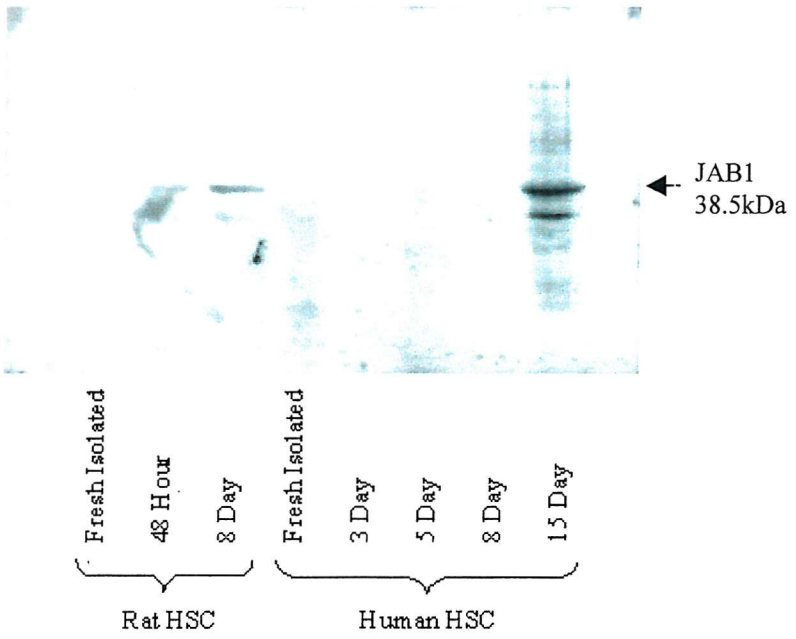

Figure 4.4.3 Western blot for JAB1 in rat and human HSC. The Western blot was performed using 20μg of whole cell extract from a time course of rat or human cells cultured on tissue culture plastic. The primary JAB1 specific goat polyclonal antibody (Santa Cruz) was used at 1μg/ml and the secondary goat IgG specific polyclonal HRP conjugate antibody (Sigma) was used at 1:2000. For anti-bodies see Appendix 4.

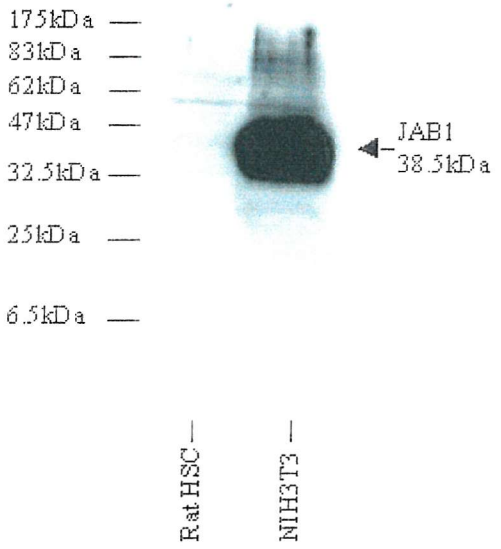

Figure 4.4.4. A comparative Western blot for JAB1 protein expression in rat HSC and NIH3T3 fibroblasts. Western blot was performed using 25μg of whole cell extract from 8 day activated HSC and NIH3T3 fibroblasts culture on tissue culture plastic. The primary JAB1 specific goat polyclonal antibody (Santa Cruz) was used at 1μg/ml and the secondary goat IgG specific polyclonal HRP conjugate antibody (Sigma) was used at 1:2000. For anti-bodies see Appendix 4.

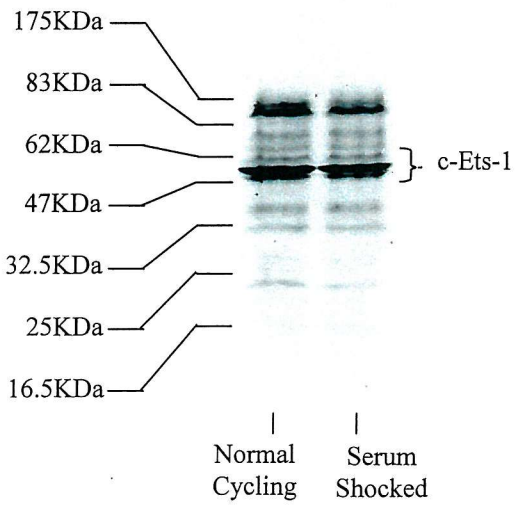

Figure 4.4.5 The expression of c-Ets-1 in normal cycling and serum shock NIH3T3 fibroblasts. NIH3T3 fibroblasts were cultured on 100mm plates for 4 Days before removing the media from both plates and replacing one with serum free DMEM and the other with DMEM + 10% serum. The cells were cultured for 24 hours and then the media was again removed from the serum free plate and replaced with DMEM +10% serum. Both plates were again cultured for 3 hours before being harvested and whole cell extracts made. 30μg of whole cell extract from each sample was run on a 9% SDS PAGE gel. Following transfer, the membrane was immuno localised with a primary c-Ets-1 specific rabbit polyclonal antibody (Santa Cruz) at 1μg/ml and the secondary rabbit IgG specific polyclonal HRP conjugate antibody (Sigma) was used at a dilution of 1:2000. For anti-bodies see Appendix 4.

4.5 Discussion

The results of the *in vitro* study in HSC contradict the literature with respect to other cell types, indicating a positive role for Jun D homodimers. The AP-1 activity associated with TIMP-1 expression has previously been shown to be mediated by c-Jun and c-Fos. It was felt necessary to look at the transcription of TIMP-1 in a fibroblast cell line, as they make up the classical model of regulation (Edwards *et al.*, 1992; Logan *et al.*, 1996). It was also deemed important to determine whether the proteins produced by the expression vectors had the expected function and thereby establish if method of regulation in the HSC is cell specific.

The co-transfection with the JUN expression vectors in murine NIH3T3 fibroblasts resulted in a significant reductions in the activity of the TIMP-1 promoter for all three of the JUN expression vectors (Figure 4.1.2).

While it is possible that there is a general down regulation of TIMP-1 promoter activity with an increased expression of JUN transcription factors, it seems more likely that this is artefactual. This suggestion arises from the literature in which other cell types, including fibroblasts, have shown the AP-1 site to be crucial (Bahr *et al.*, 1999; Clark *et al.*, 1997; Edwards *et al.*, 1992; Logan *et al.*, 1996). The suggestion of a negative role for all of the JUN expression vectors in a system in which AP-1 is believed crucial is contradictory. If the promoter is AP-1 dependent then one of the JUN family must be present, as FOS proteins are known to be unable to form homodimers and are not therefore transcriptionally active (Ryseck *et al.*, 1991). There are two possible reasons for these contradictory results; the lack of phosphorylation of the JUN expression vector products by cellular kinases JNK and FRK, or the formation of inactive dimers. The NIH3T3 cells would have been stimulated during passage, activating JNK, ERK and FRK, and leading to a subsequent activation of the immediate early genes (see Section 1.20). In the NIH3T3 cells, following culture and in the absence of subsequent stimulation, the protein kinases return to a basal state, resulting in low level kinase activity. The comparative low level of phosphorylation in normal cycling NIH3T3 fibroblasts has been demonstrated in the literature (Lallermand *et al.*, 1997). It has also been shown that there is an increase in phosphorylation with serum shock and that this returns to normal following 12 hours of culture (Lallermand *et al.*, 1997). The lack of kinase activity in normal cycling NIH3T3 cells may lead, with transfection of JUN expression vectors, to the increased abundance of unphosphorylated and therefore inactive JUN proteins. The production of the inactive JUN proteins may result in a general quenching of other protein transcription, as a result of competition for transcriptional apparatus.

The second reason for the lack of activity upon transfection and over expression of JUN is that the endogenous JUN and FOS proteins present in un-shocked cells lead to the formation of inactive dimers. Normal cycling NIH3T3 fibroblasts have been shown to express c-Jun, Jun D and Fra 2 (see Figure 4.5.1) (Lallemand *et al.*, 1997). These available endogenous proteins lead to the possible dimer combinations c-Jun/Fra 2, Jun D/Fra 2 and c-Jun/Jun D. The additional dimers Jun B/Fra 2, Jun B/Jun D and Jun B/c-Jun are available with Jun B over expression. As previously mentioned, c-Jun/Fra 2 and

Jun B/Fra 2 heterodimers have been suggested to be inhibitory, and there is also some confusion as to the role of Jun D/Fra 2 (Suzuki *et al.*, 1991; Sonobe *et al.*, 1995; Rutenberg *et al.*, 1997). Also, Fra 2 heterodimers have a higher binding affinity than JUN/JUN dimers (Ryseck *et al.*, 1991). Therefore the transfection of any of the JUN expression vectors is likely to lead to the formation of JUN/Fra 2 dimers due to their increased stability over other dimeric combinations available in normal cycling NIH3T3 fibroblasts. However, this is not likely to be the whole picture as in Chapter 3 it was suggested that the inhibitory dimers could be out competed by Jun D over expression, which is not seen here.

	Normal Cycling Cells	Serum Free	<1 Hour 10% FCS	<24 Hours 10% FCS	>24 Hours 10% FCS
c-JUN	X		X	X	X
Jun B			X	X	
Jun D	X	X		X	X
c-Fos			X	X <16Hrs	
Fos B			X	X <16Hrs	
Fra 1				X	X
Fra 2	X			X	X

Figure 4.5.1 The effects of serum shock on the expression of JUN and FOS protein in NIH3T3 cells (Lallemand *et al.*, 1997). The presence of an X indicates protein expression. At time greater then 24 hours the protein expression is shown to revert to that in normal cycling cells.

In order to investigate a general role or function of AP-1 the co-transfections of the JUN-pCMV2 expression vectors was repeated, this time with a multiple AP-1 sited luciferase reporter construct (5xAP-1-lux) (Figure 4.1.4). The result of the co-transfection of the 5xAP-1-lux vector was the same as seen with the TIMP-1 reporter (Figure 4.1.2). There was a decrease in promoter activity for each of the transfections when compared with the controls. Again, the reductions in activity for the JUN-pCMV2 (c-Jun, Jun B and Jun D) vectors may be due to the formation of inactive dimers with Fra 2 or as a result of the lack of phosphorylation. The results from the homodimer-forming vector Jun D/Eb1-

pDP7 suggest that the inhibitory effect of the endogenous Fra 2 may only be a minor regulating factor being unable to form heterodimers, again implicating phosphorylation.

In order to determine the effects of endogenous AP-1 protein interactions and the role phosphorylation in the transcriptional activity of the TIMP-1, it was necessary to repeat the co-transfections. It was felt necessary to induce protein kinase activity in the co-transfections to establish the formation of functional dimers. Cellular stresses such as serum shock or deprivation, UV radiation and phorbol ester have long been recognised as mitogens, increasing transcription factor phosphorylation through increased activity of JNK, ERK and FRK kinases (see Section 1.20) (Frost *et al.*, 1994; Adler *et al.*, 1995; Sale *et al.*, 1995; Chen A *et al.*, 1999; Le-Niculescu *et al.*, 1999). Also, previous work by another group had identified that the expression of the various AP-1 proteins in the NIH3T3 cells changed with serum shock (see Figure 4.5.1) and that there was also an increase in AP-1 phosphorylation (Lallemand *et al.*, 1997). As the method of serum shock was simple and had already been characterized, the co-transfections of the NIH3T3 cells were repeated with serum shock.

The results of the co-transfections of the TIMP-1 reporter and JUN-pCMV2 expression vectors, in combination with the serum shock, identified increased promoter activity for each of the vectors with respect to the controls (Figure 4.2.1). Significant increases in promoter activity relative to the controls, were measured for Jun B and c-Jun respectively. Jun D over expression resulted in insignificant decrease in activity. These results agree with those seen in other cell types, in which c-Jun is shown to be positively regulating (Edwards *et al.*, 1992; Logan *et al.*, 1996). The lack of a significant increase in the expression of TIMP-1 with the increased expression of Jun D suggests that the positive role for Jun D in HSC may be cell specific. The increase in promoter activity seen in serum shock also supports the role of protein kinase in the regulation of AP-1 activity in the TIMP-1 promoter in NIH3T3 cells.

To further clarify the roles of the various JUN proteins in the activity of the TIMP-1 promoter for NIH3T3 cells, co-transfections were performed using a series of

homodimer-forming JUN expression vectors (Figure 4.2.2). The results for this series of co-transfections showed an increase in promoter activity for all of the JUN vectors. As this experiment has only been performed on a single occasion, all be it in triplicate, no statistics are shown in the figure, but analysis of these results would seem to suggest that c-Jun and Jun D homodimers lead to a significant positive increase in promoter activity. The increase seen with the co-transfection of Jun B may not be significant, although this may well change with repetition. The results of the homodimer forming vector Jun D/Eb1-pDP7 transfection support the role of protein kinase activity in the regulation of TIMP-1. As the chimeric Jun D vector is unable to for a heterodimer, the increased activity following serum shock is most likely due to an increase in phosphorylation (Figure 4.1.4 and 4.2.2). However, the significant increase in promoter activity of the Jun D homodimer and the lack of an increase with wild type Jun D-pCMV2 transfection (Figure 4.2.1) indicates that inhibitory dimers are formed in the NIH3T3 cell. The results of the chimeric vector transfections for the JUN proteins are similar to those seen in the HSC, in which c-Jun is shown to be strongly affected by inhibitory dimer formation (see Chapter 3 and Figure 3.5.2).

Vector Transfected	**Cell Type**	
	NIH3T3	**HSC**
c-Jun-pCMV2	300% increase	48% decrease
c-Jun-pDP7 (Homodimer)	400% increase	200% increase
Jun D-pCMV2	12% decrease	260% increase
Jun D-pDP7 (Homodimer)	410% increase	350% increase

Figure 4.5.2 The effect c-Jun and Jun D over expression in NIH3T3 fibroblasts and HSC (Figures 3.5.1, 3.7.3, 3.7.4, 4.2.1 and 4.2.2).

Following the JUN expression vector experiments, the co-transfections were repeated with FOS vectors, also with serum shock (Figure 4.2.3). As with the HSC (Figure 3.6.1), the results of the FOS co-transfections indicated that Fra 2 and Fos B resulted in decreases in transcriptional activity. Unlike the HSC, the transfections of the vectors c-Fos and Fra 1 resulted in increases in promoter activity. The results were obtained form a

preliminary triplicate transfection so no statistics are shown in the figure, but would seem to suggest that there may be a increase in promoter activity with c-Fos and decreases with Fra 2 and Fos B. The lower level of induction, and larger errors for Fra 1 when compared with c-Fos, suggest that it is not significant, although this may change with repetition. The decrease in activity of the promoter with Fra 2 over expression supports previous work by other investigators, suggesting that Fra 2 heterodimers are inhibitory (Suzuki *et al.*, 1991; Sonobe *et al.*, 1995; Rutenberg *et al.*, 1997). The increase in promoter activity with c-Fos over expression also agrees with the literature, as hoped, on the classical regulation of TIMP-1 and again supports the cell specific nature of TIMP-1 regulation in the HSC (Edwards *et al.*, 1992; Logan *et al.*, 1996). It is important to note that JUN/FOS heterodimers have a higher affinity for formation and AP-1 binding than the JUN/JUN dimers. The affinity of c-Fos heterodimers is however, the lowest of all the FOS heterodimers (Ryseck *et al.*, 1991). It is also important to remember that with serum shock there is an increased expression of both c-Fos and the inhibitory Fra 2 (Lallemand *et al.*, 1997). Therefore serum shock, with the resulting change in endogenous AP-1 protein expression, allows the possible formation of the classical c-Jun/c-Fos heterodimers but at the same time negatively regulates transcription with an increase in Fra 2 expression (Figure 4.5.1). Fos B may also be inhibitory, as it has a higher binding affinity for the AP-1 site than c-Fos (Rysect *et al.*, 1997).

The inhibitory role of Fra 2 in TIMP-1 promoter regulation was tested by the use of triple transfections. Combinations of Jun D-pCMV2 and Fra 2-pCMV2 were transfected with serum shock (Figure 4.3.1). The results of these triple transfections, as expected, supported the result for the HSC, in which the combination of Jun D and Fra 2 were shown to negatively regulate TIMP-1 transcription. These results again agree with the negative function suggested for Fra 2 heterodimers (Suzuki *et al.*, 1991; Sonobe *et al.*, 1995; Rutenberg *et al.*, 1997).

In an attempt to elucidate the role of protein kinase activity in the regulation of AP-1 induced TIMP-1 transcription, it was necessary to examine the role of JNK. To investigate the JNK role in JUN activation and the overall regulation of TIMP-1

transcription, co-transfections were performed in NIH3T3 cells with a dominant negative JNK and the TIMP-1 reporter (Figure 4.4.1). The co-transfections were also repeated in the activated HSC (Figure 4.4.2). The results for the co-transfections of the dominant negative JNK vectors indicate a significant reduction in promoter activity for the NIH3T3 cells and an insignificant increase for HSC. This would appear to suggest that the activity of the AP-1 proteins in the NIH3T3 cells is dependent on JNK but AP-1 function in HSC in independent of JNK. The JNK independent nature of HSC regulation is not a surprise, as the previous work indicated that c-Jun and Jun D are negative and positive regulators respectively (Chapter 3). The significance of this is that JNK cannot, as previously mentioned, phosphorylate Jun D directly due to its lack of a binding domain. JNK must rely on chaperones such as c-Jun or Jun B, which both have this site (see Section 1.20) (Dérijard *et al.*, 1995; Kallunki *et al.*, 1996). In the activated HSC however, there are no other JUN factors present (Bahr *et al.*, 1999). An alternative method of phosphorylation may be by means of JAB1, which was originally suggested to act as a chaperone but is now believed to function as part of the larger COP9 signalosome (Claret *et al.*, 1996; Chamovitz *et al.*, 2001).

Western blots for JAB1 indicated an increase in JAB1 with activation in both rat and human HSC time courses (Figure 4.4.3). It was believed that the presence of JAB1 in the HSC may explain how Jun D is activated. However when a comparative Western blot was performed using extracts made from NIH3T3 fibroblasts and rat HSC, the fibroblasts were shown to have a significantly more JAB1 (Figure 4.4.4). The expression of JAB1 therefore does not explain cell specific differences between NIH3T3 and the HSC.

In the literature, as previously mentioned, the classical regulation of the TIMP-1 promoter is through the interactions of c-Jun with c-Fos and c-Ets-1 with the PEA3 site (Edwards *et al.*, 1992; Logan *et al.*, 1996). Previous work by other investigators has demonstrated that the expression of c-Ets-1 is dramatically reduced with HSC activation (Bahr *et al.*, 1999; Knittel *et al.*, 1999). A Western blot was performed using whole cell extracts made from both normal cycling and 3 hour post serum shock NIH3T3 fibroblasts (Figure 4.4.5). The Western blot identified strong immuno localisation of a band

corresponding to the 52kDa form of c-Ets-1. The level of c-Ets expression was approximately the same in both the serum shocked and normal cycling fibroblasts, suggesting that it is constitutively expressed. It is therefore suggested, as previously mentioned, that the cell specific differences in the AP-1 regulation of TIMP-1 between the HSC and the NIH3T3 fibroblast may be due to low-level c-Ets-1 expression in the HSC. The low level of c-Ets-1 in the HSC is believed to result in the inactivity of the JUN/FOS heterodimers, leaving only the JUN homodimers, and in particular those of Jun D, to be transcriptionally active (Chapter 3). It is possible that the Jun D homodimer, which is shown to be functional in the HSC, interacts with a novel protein UTE-1, but it is not known whether the NIH3T3 cells express this protein (Trim *et al.*, 2000; Smart *et al.*, 2001).

This chapter set out to discover whether the regulation of TIMP-1 in the HSC was cell specific and as such prove that the regulation in the NIH3T3 fibroblasts was classical. It was also hoped that the investigation in the NIH3T3 fibroblasts would explain the unusual regulation in the HSC. A number of methods of TIMP-1 transcriptional regulation in the NIH3T3 cells were highlighted. These included protein kinases activity, formation of inhibitory dimers and the lack of necessary dimeric pairs or other endogenous transcription factors.

Further work is necessary in this study to repeat the preliminary results for the role of the JUN homodimers and FOS proteins. It would also be interesting to establish if there is any UTE-1 binding activity in the NIH3T3 fibroblasts. It is however most important to establish the method of JUN phosphorylation in the HSC as, although JAB1 is expressed and maybe a regulator, it is at a considerably lower level than in the NIH3T3 fibroblast. Further investigation is also needed to look at phosphorylation in the NIH3T3 cells, incorporating alternative methods of kinase induction, as serum shock is non specific inducing JNK, ERK, FRK as wells as immediate early genes, in particular c-Fos. The use of UV also induces JNK without but without FRK or ERK, which may also prevent the induction of c-Fos expression (see Section 1.20 and Figure 1.20.1). It would also be a good idea to also use other mitogens to investigate phosphorylation of the HSC.

Chapter 5.

The role of Jun D *In Vivo* and in Fibrosis

5.1 Is Jun D Expressed *In Vivo* by the Fibrotic Stellate Cell

Previous work in Chapter 3 has demonstrated Jun D's function *in vitro* as a positive regulator with regard to the transactivation of the TIMP-1 minimal promoter. The activity of Jun D has also been shown to be mediated via the activity of homodimers. No investigation has been performed to determine if the pattern of Jun D expression is repeated in liver injury and fibrosis *in vivo*. It is also unknown whether Jun D regulates endogenous TIMP-1 expression in a similar way to its regulation of the TIMP-1 minimal reporter construct *in vitro*.

An investigation was performed to establish whether Jun D is regulated in a similar fashion *in vivo,* following liver injury, to that seen *in vitro*, with activation on tissue culture plastic. Western Blotting was performed using nuclear extracts from the purified HSC of CCl_4 injured male rats 48 hours post intra peritoneal injection. The rats were injected with either CCl_4 diluted 1:1 with olive oil as a carrier or with the carrier on its own, as a control (see Section 2.13). Male rats were used for the *in vivo* studies, as is the tradition in liver fibrosis research, primarily because more males develop fibrosis than females, but also because males are often surplus to requirements for breeding etc. The gender difference in the development of fibrosis has been under investigation in humans for many years, but cause is hard to identify due to differences in body mass and social and environmental factors. There is scientific evidence to suggest oestrogen is a protective agent (Shimizu I *et al.*, 1999; Thurman, 2000) but on the other hand, females stomachs contain no alcohol dehydrogenase so they may be at greater risk from alcoholic fibrosis (Baraona *et al.*, 2001).

The results of the Western blot for Jun D compared rats that underwent CCl_4 injury to rats that underwent a sham injury with the carrier only. The experiment clearly showed an increase in the production of a 44 kDa Jun D band (Figure 5.1.1). When comparing the CCl_4 injured animals to the controls a reduction in a 39 kDa band was observed together with an increase in the 44 kDa form of Jun D. This result supported the findings of the *in vitro* work (Chapter 3) suggesting a probable role for Jun D *in vivo* and in fibrosis. As a

result of the work on Jun D and AP-1 *in vitro* (see Chapter 3) and *in vivo* (Figure 5.1.1), it was decided to progress into a Jun D Knockout liver injury model.

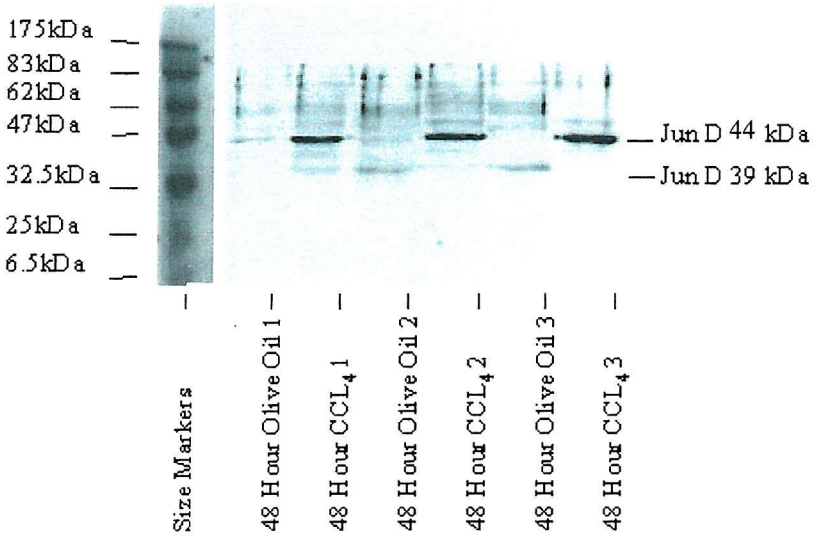

Figure 5.1.1. The effect of Carbon Tetrachloride (CCl_4) induced liver injury on Jun D expression in freshly isolated rat HSC. Primary rat hepatic stellate cells from six individuals were harvested as previously described (see Section 2.3.1). The cell extractions were performed 48 hours after a single intra peritoneal injection of 0.2ml/100g (body mass) of CCl_4 with 1:1 of olive oil as a carrier; olive oil was used as a control in sham animals. Following cell harvest nuclear extracts were made from the cells of each individual. The protein concentration of the nuclear extracts was determined and the samples were boiled in SDS PAGE loading buffer. 20μg of each sample was run in each lane on a 4% stacking and 9% resolving gel. The Jun D specific rabbit polyclonal antibody (Santa cruz, See Appendix 4) was used at 1μg/ml and the secondary rabbit IgG specific polyclonal HRP conjugate antibody (Sigma, See Appendix 4) was used at 1:2000 dilution.

5.2 In Vivo Carbon Tetrachloride Liver Injury in Jun D Knockout Mice

A study was necessary to determine whether Jun D has a functional role in fibrosis, not only *in vitro* but also *in vivo,* and to address whether or not Jun D may act as a possible therapeutic drug target of the future. Via collaboration Dr. J Weitzman and Professor M Yaniv, three breeding pairs of Jun $D^{-/-}$ knockout mice were obtained. The Jun $D^{-/-}$ knockout mice were first described by Thepot *et al.,* 2000, in which they were shown to possess a phenotype that leads to defective spermatogenesis. There was no effect on litter sizes and only small effects on the growth of the mice. It has been shown more recently

that the Jun $D^{-/-}$ knockout mice fibroblasts may also undergo premature senescence or apoptosis. The premature senescence results from an increased accumulation of p53 and $p19^{Arf}$. The production of cyclin D1 in cells is dependent on regulation by AP-1 binding proteins and as such the absence of any binding would lead to a reduction in cyclin D1 and result in cellular arrest (Bakiri *et al.*, 2000; Weitzman *et al.*, 2000). To establish whether Jun D expression would effect HSC TIMP-1 expression and fibrosis, the knockout mice were to be used in CCl_4 liver injury study with the wild types used as controls (see Section 2.13). Before starting a large-scale study it was felt necessary to perform a preliminary study of just 6 animals, 3 wild type and 3 knockouts. These individual wild type and knockout mice have been designated MW1-3 and MK1-3 respectively. This study was to establish the level of fibrosis in the wild type, in order to establish whether an eight-week study would be long enough. It was also necessary to perform the small study to access the level of suffering and to see if there was any obvious phenotype for the purposes of ethical approval.

As a result of the poor spermatogenesis by the male Jun $D^{-/-}$ knockout, it was not possible to breed the mice from homozygotes, so breeding was performed using heterozygotes. As a result of the heterozygote breeding and the lack of an observable gross phenotype, genotyping was performed by PCR (see Sections 2.11, 2.12 and Appendix 8i). In the knockout animals, the Jun D gene was replaced by that of β-Galactosidase (Lac Z). Two sets of primers were used in the genomic PCR of the mice, corresponding to Jun D and Lac Z, making it possible to identify all three phenotypes (see Appendix 1). The PCR reactions with their corresponding primers gave fragments of 315 and 822 for Jun D and Lac Z respectively (see Figure 5.2.1). The method first used contained all four primers for the two genes in one reaction. This single reaction method was supplied, along with the primer sequences, by our collaborators. The single reaction method would result in one or two PCR fragments for each animal, depending on the phenotype (see Figure 5.2.2).

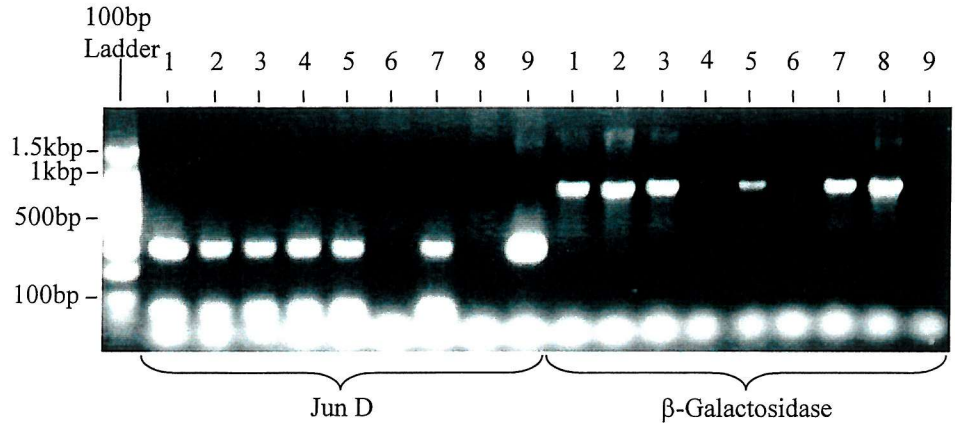

Figure 5.2.1. A sample gel showing the Jun D and β galactosidase genotyping reactions for nine individual mice producing 315 and 822bp fragments respectively.

The two genotyping PCR reactions shown above (Figure 5.2.1) indicate that individuals 1-3, 5 and 7 are all heterozygote animals, as products of 315 and 822bp are present corresponding to Jun D and Lac Z respectively. Animals 4 and 9 were wild types, showing only a band for Jun D, whereas animal 8 was shown to be a Jun $D^{-/-}$ from the presence of a band corresponding Lac Z only. Individual 6 showed no bands for either LacZ or Jun D. The PCR for this animal, as with all the others, would be repeated, however the quantity of DNA would be increased in the subsequent PCR. The result for animal 6 does, however, conveniently show that there is no background contamination of the PCR reactions producing false positives.

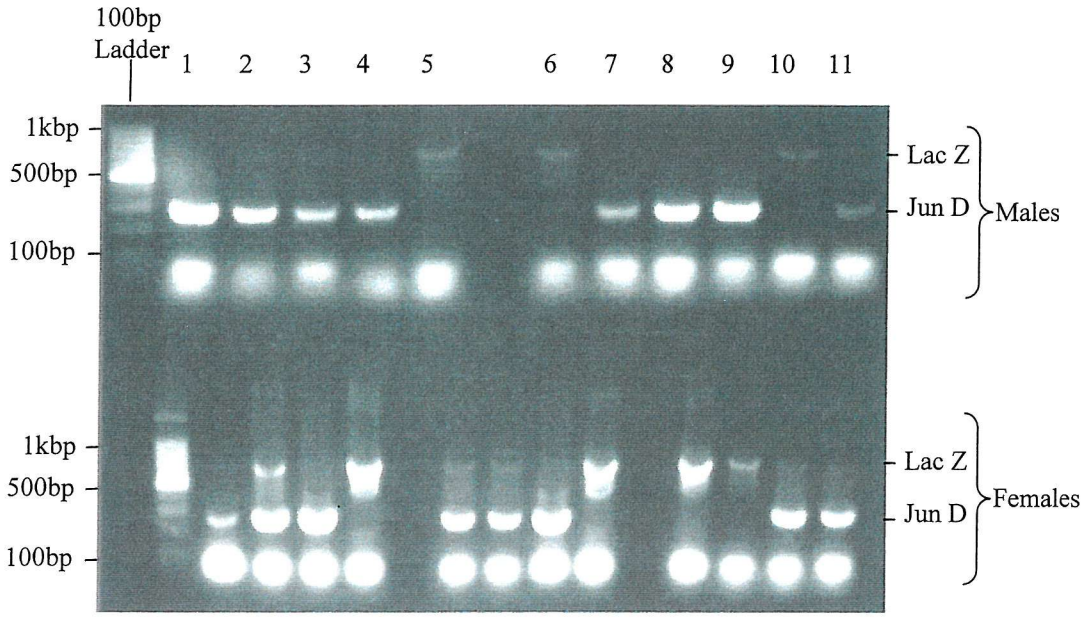

Figure 5.2.2. The PCR reactions from the initial 23 animals born from the 3 breeding pairs obtained via collaboration.

The results from the first PCR performed, using the combined PCR method for Jun D and Lac Z, identified 3 male knockouts, animals 5, 6 and 10 for the preliminary study (Figure 5.2.2). This combined reaction also identified a problem with the protocol supplied via collaboration. The Lac Z PCR produced very little product in comparison with the Jun D PCR and in heterozygotes the more active Jun D PCR inhibited the Lac Z reaction.

For this reason it was decided to separate the primers and perform two separate reactions for each sample (Figure 5.2.1). The ambiguous PCR reaction samples were retested using the Lac Z primers only.

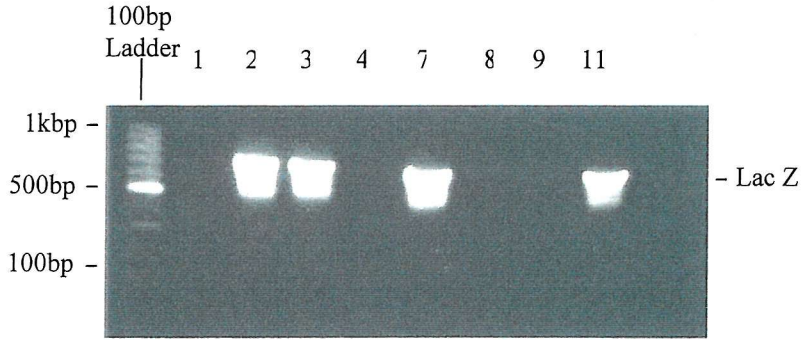

Figure 5.2.3. The Lac Z PCR reaction repeated for the ambiguous individuals (male mice 1-4, 7-9 and 11) from the results seen in Figure 5.2.2.

The results of the separate reaction for Lac Z (Figure 5.2.3) indicated that the presence of the Jun D primers was inhibiting the Lac Z reaction even in the absence of any Jun D activity. The effect of this inhibition can be seen as a greatly increased amount of Lac Z product in the single reaction when compared to the combined one (Figure 5.2.2). The gel shows the presence of an 822bp fragment for mice 2, 3, 7 and 11. The results from the two PCR reactions (Figure 5.2.2 and 5.2.3) were combined to give the results in the table below (Figure 5.2.4).

Mouse	Genotype	Mouse	Genotype
1	Wild Type	7	Heterozygote
2	Heterozygote	8	Wild Type
3	Heterozygote	9	Wild Type
4	Wild Type	10	Knockout
5	Knockout	11	Heterozygote
6	Knockout		

Figure 5.2.4. The genotypes of the male mice resulting from the PCR reactions shown in Figure 5.2.2 and 5.2.3.

5.3 The Effects of CCl_4 Induced Liver Injury on the Histology of Jun D Knockout Mice

The three wild type (MW1-3) and 3 knockout (MK1-3) mice were injected twice weekly for 8 weeks according to the protocol (see Section 2.13). Following the trial the animals were culled and the livers removed. Some of the liver from each animal was fixed and mounted in wax for histology (see Section 2.13.2) and the rest was snap frozen in liquid nitrogen for RNA and protein studies. The wax blocks were sectioned and sections from each animal were stained with Sirius red, which identifies fibrillary collagens such as types I and III. As previously mentioned, the increased accumulation of collagens I and III is characteristic of liver fibrosis (Friedman, 1996).

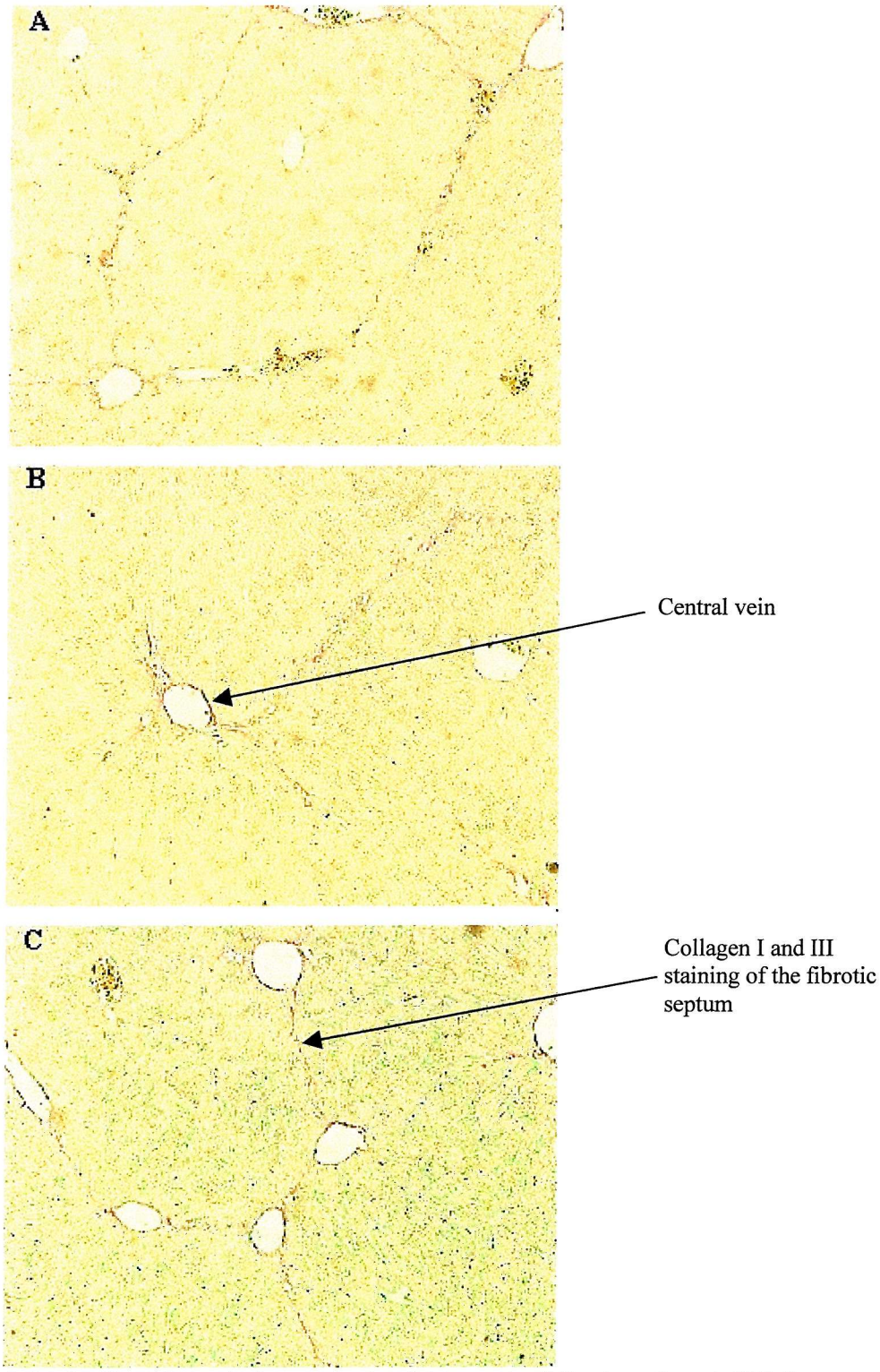

Figure 5.3.1. Sirius red staining for collagen in three separate wild type mice following a 8 week CCl_4 liver injury study. Figures A, B and C correspond to sections from the livers of individual mice MW1, MW2 and MW3 respectively.

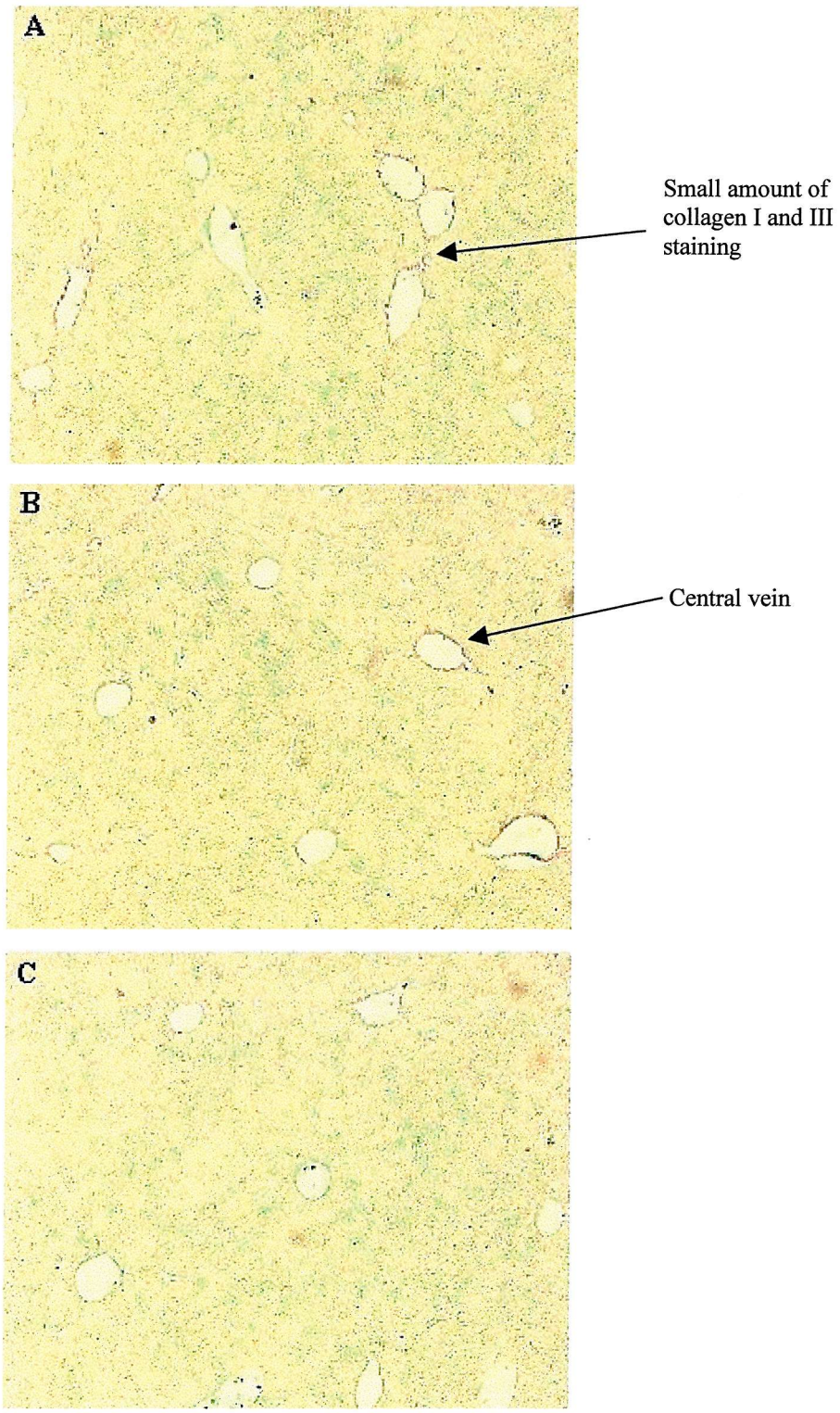

Figure 5.3.2. Sirius red staining for collagen in three separate Jun $D^{-/-}$ knockout mice following a 8 week CCl_4 liver injury study. Figures A, B and C correspond to sections from the livers of individual mice MK1, MK2 and MK3 respectively.

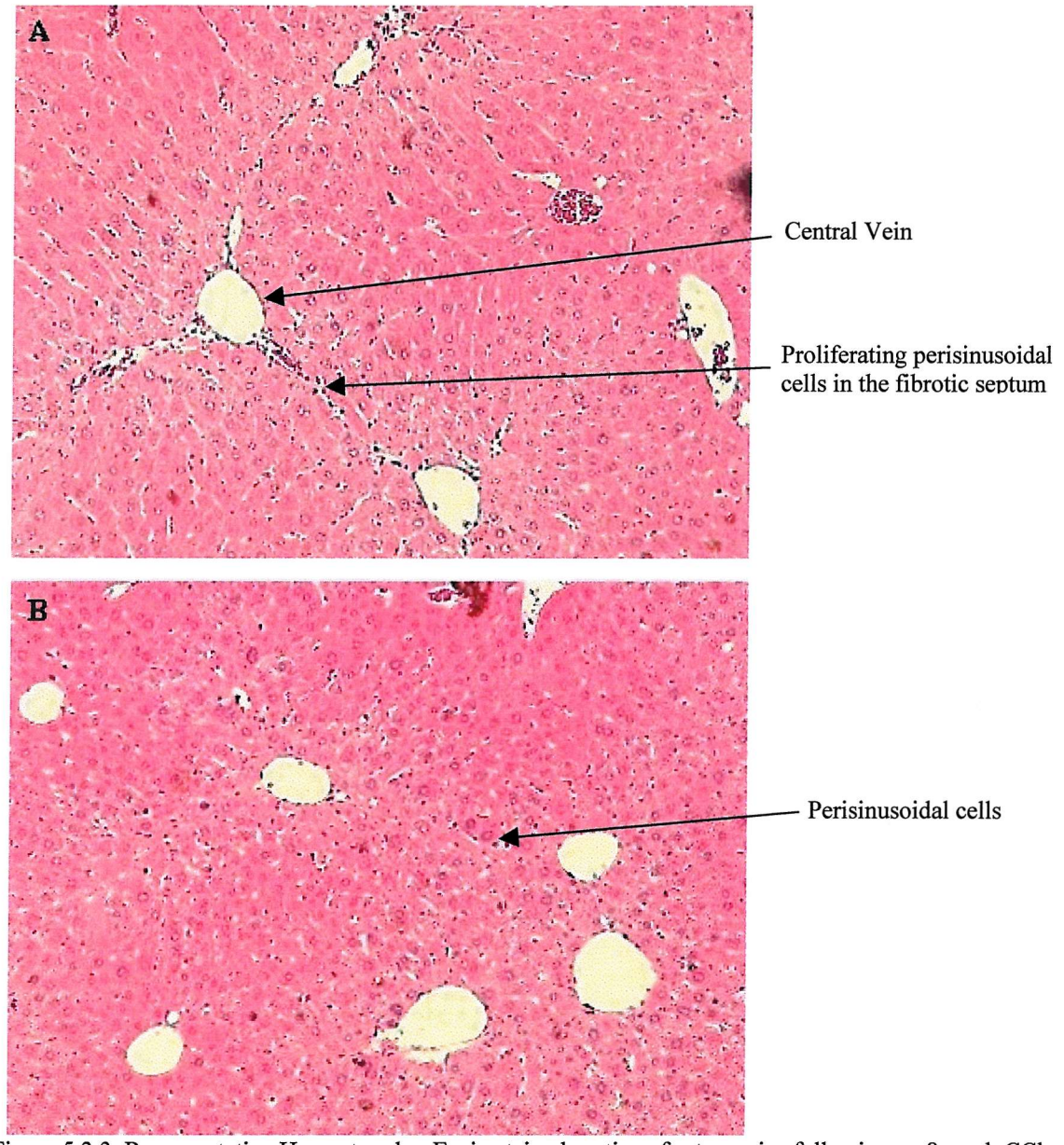

Figure 5.3.3. Representative Haematoxylon Eosin stained sections for two mice following an 8 week CCl_4 Liver injury study. (A) Wild type MW1 and (B) Jun $D^{-/-}$ knockout mouse MK1.

The results of the Sirius red of the wild type (Figure 5.3.1 A-C) and Jun $D^{-/-}$ knockout mouse sections (Figure 5.3.2 A-C) indicate that there is significantly less collagen staining in the Jun $D^{-/-}$ knockout animals. The collagen staining in the wild type mice originates in the central vein, radiating, forming fibrotic septa. In some fields the collagen can been seen to link together a number of veins (Figures 5.3.1 A and C). This is a common feature seen in cirrhosis, in which the hepatocytes form regenerative islands

or nodules. All the fixing, mounting, Sirius red and Haematoxylon Eosin staining was performed in parallel for both the wild types and knockouts.

The results of the hematoxylin and eosin are shown as representative sections. The proliferation of the HSC along the fibrotic septa can be easily observed in the wild type sections (Figure 5.3.3 A). This observation is absent in the Jun $D^{-/-}$ knockout animals (Figure 5.3.3 B).

5.4 The Effect of CCl_4 Induced Liver Injury on the Expression of α Smooth Muscle Actin in Jun D Knockouts

The cytoskeleton protein α smooth muscle actin is, as previously mentioned, an accepted marker of the phenotypic change of the HSC to a myofibroblast-like cell (see Section 1.7). It is this change that is also seen both *in vitro* and *in vivo* (Nouchi *et al.*, 1991; Rockey *et al.*, 1992). As a crucial marker of HSC activation it was important to look at its expression in the Jun D knockout CCl_4 liver injury model. Whole liver protein extracts (see Section 2.13.3) were made, run on SDS gel and transferred onto nitrocellulose before Western blotting the membranes for αSMA.

The Western blot for α-SMA indicates lower levels of expression in the Jun $D^{-/-}$ knockout animals (MK1-3) than the wild types (MW1-3); the 43kDa αSMA band is indicated (Figure 5.4.1). The top unmarked band corresponds to non-specific binding with protein of the whole liver homogenate.

The Western blot was repeated for β-actin to establish whether the samples were equally loaded for the purposes of quantitation. A band of 42kDa corresponding to β-Actin was identified; the band intensity was approximately equal for each sample, indicating that they were evenly loaded (Figure 5.4.2). To quantify the result of the Western blots for αSMA and β-actin, densimetric analysis was performed on the two membranes. The top unmarked band corresponds to mouse immuno globulin in the whole liver homogenate. The results of the β-Actin controlled αSMA densimetric analysis indicate that there is a

50% reduction in the expression of αSMA in Jun $D^{-/-}$ knockout mice compared with the wild type control animals following 8 weeks CCl_4 induced liver injury (Figure 5.4.3).

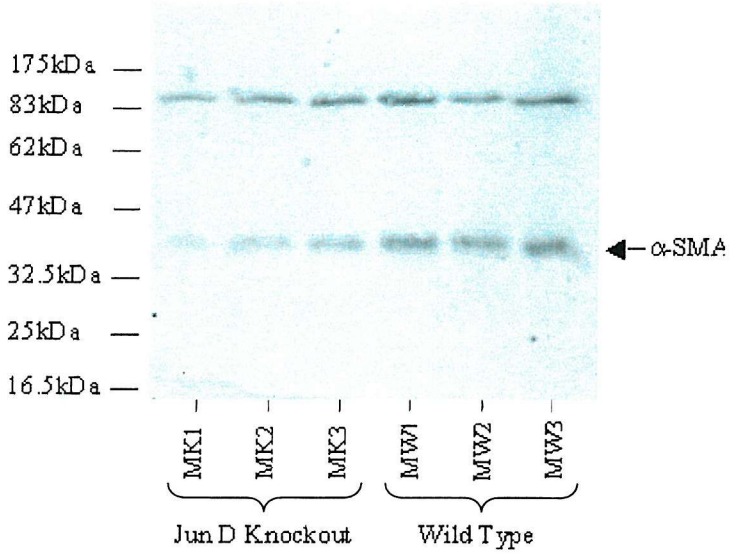

Figure 5.4.1 Western blot for αSMA using samples of whole liver from each of the study animal livers. 28μg of protein was added from each subjects liver homogenate and run on a 12% SDS poly-acrylamide gel. The primary antibody used was a αSMA specific mouse monoclonal IgG (Sigma, see Appendix 4) and used at 1:1000 and the secondary was a mouse IgG specific polyclonal HRP conjugate antibody (Sigma, see Appendix 4) was used at 1:2000 dilution.

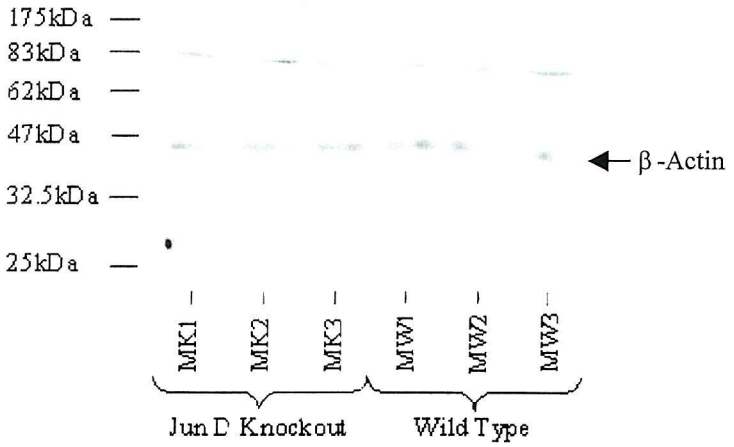

Figure 5.4.2 Western blot for β-Actin using samples of whole liver homogenate from each of the study animal livers. 28μg of protein was added from each subject liver homogenate and run on a 12% SDS acrylamide gel. The primary β-actin specific mouse monoclonal antibody was used (Sigma, see Appendix 4) at a dilution of 1:1000 and the secondary mouse IgG specific HRP conjugate antibody (Sigma, see Appendix 4) was used at a dilution of 1:2000.

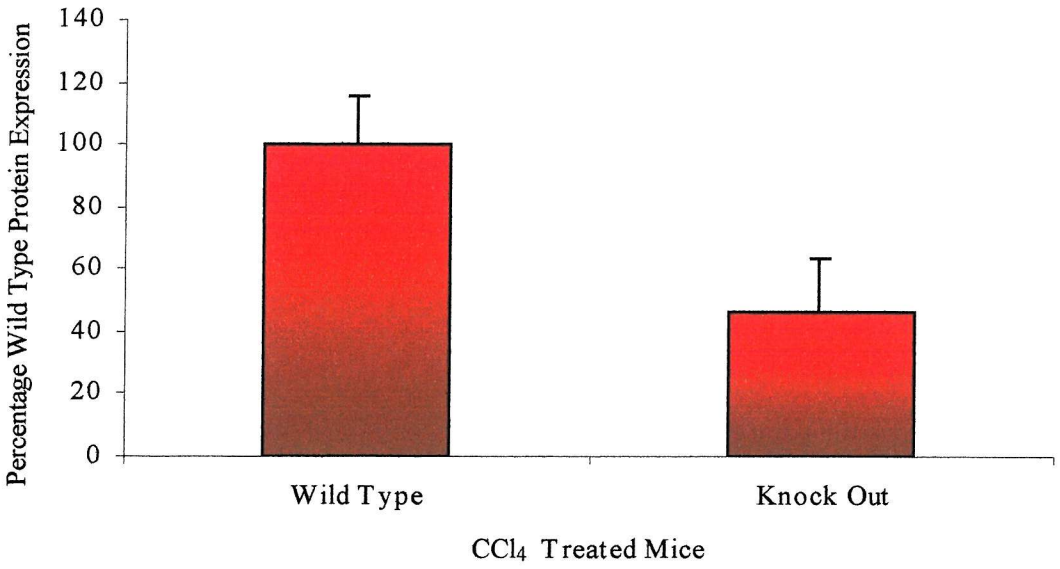

Figure 5.4.3 Densimetric analysis of the data obtained from the Western blot for α-Smooth muscle actin (Figure 5.4.1) using β-Actin (Figure 5.4.2) as a control. The results are displayed mean and standard error for the β-actin corrected expression of αSMA in wild type and Jun D knockout mice following 8 weeks CCl_4 injury. The films were analysed using the Storm Image Quant Software package. For both the αSMA and β-actin an equal cross sectional area of film for each band was analysed, corresponding to the size of the largest entire band. For each film an area of background of equal size was measured and this figure deducted from each band measurement. To correct the samples for β-actin the figure for αSMA for each animal was divided by the figure for the same individual's β-actin.

5.5 The Effects of CCl_4 Induced Liver Injury on the Expression of Fibrosis Markers mRNA

It was felt necessary to establish a molecular biological mechanism for the lower levels of fibrillary collagens seen in the livers of Jun D knockout mice following CCl_4 induced liver injury. Sirius red staining of the Jun $D^{-/-}$ knockout mice livers showed lower levels of fibrosis following liver injury. However it was unknown whether this was due to a specific reduction in the production of collagen or TIMP-1, or by some other mechanism (see Figure 5.3.1 and 5.3.2). The previous work *in vitro* (see Chapter 3) had suggested that Jun $D^{-/-}$ knockout mice would have less fibrosis due the crucial role played by Jun D in the regulation of TIMP-1 and Jun D had also been implicated *in vivo* in a CCl_4 rat model (see Figure 5.1.1). In order to establish the molecular biological mechanism of the

reduced fibrosis in the Jun $D^{-/-}$ knockouts, whole liver RNA samples were extracted from the frozen livers of the preliminary animal study (see Section 2.13.4). Following a single reverse transcriptase step, quantitative Taqman PCR was performed on the samples for αSMA, TIMP-1, procollagen I and Glyceraldehyde-3-phosphate dehydrogenase (GAPDH) (see Section 2.15).

The results of the Taqman quantitative PCR indicate that there were very similar levels of mRNA and subsequent cDNA in each of the samples (Figure 5.5.1). The values for the expression of GAPDH mRNA were used to correct the relative expressions of the markers of liver fibrosis.

The results of the Taqman quantitative PCR reactions indicate that there are reductions of 78 and 83% in the levels of mRNA for TIMP-1 and procollagen I in the Jun $D^{-/-}$ knockout mice relative to the wild type controls following 8 weeks CCl_4 treatment (Figure 5.5.2). The results suggest that there is an increase in the expression of αSMA in the Jun $D^{-/-}$ knockout animals, although this is not significant with such a large error.

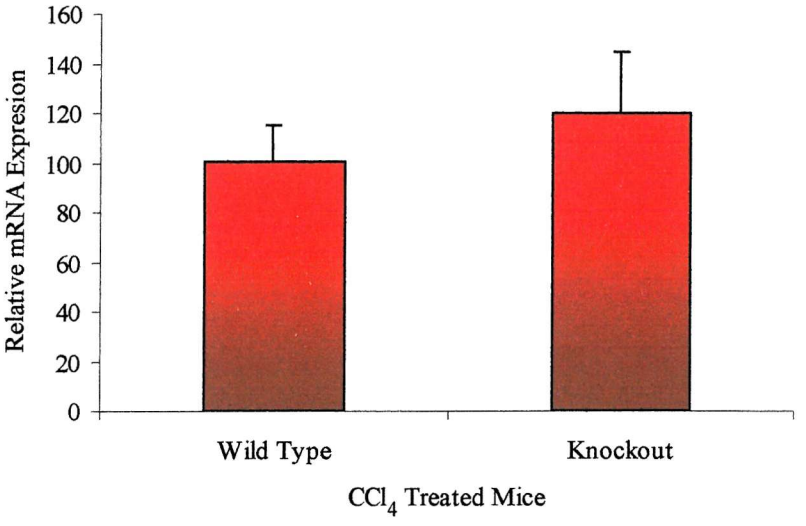

Figure 5.5.1 The relative expressions of GAPDH mRNA in wild type and Jun $D^{-/-}$ knockout mice following 8 weeks CCl_4 induced liver injury. The results are the mean and standard errors from three mice in each group. The Taqman quantitative PCR was repeated in triplicate for each mouse. The figures plotted on the graph represent the mean of the average triplicate values for each group. For the calculation of the values see 2.15.2.

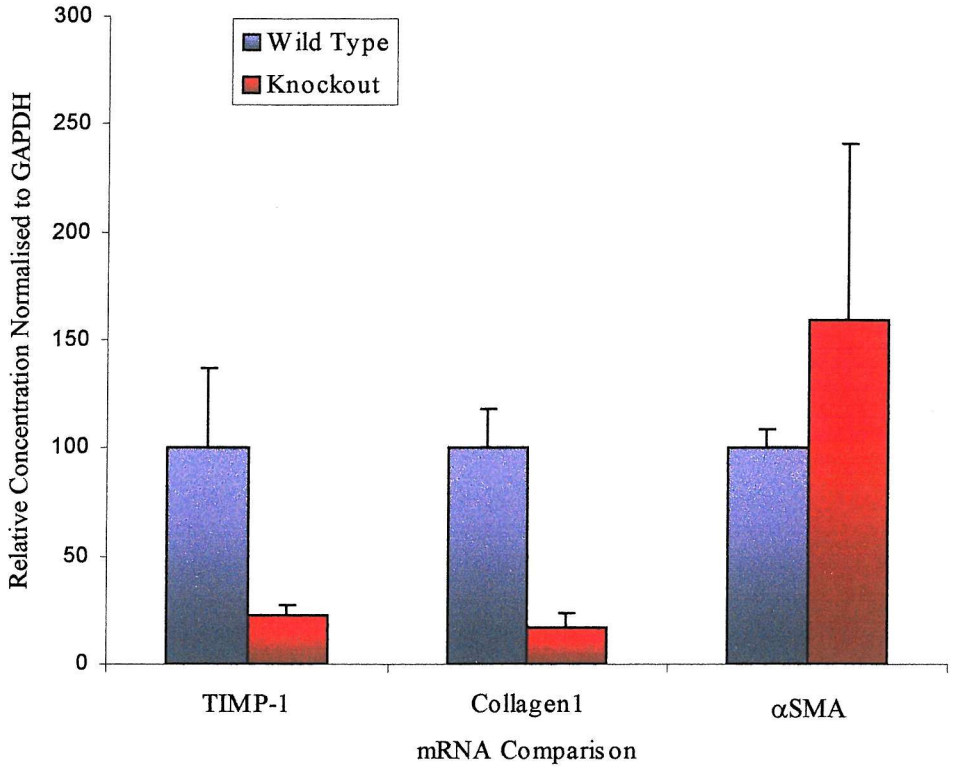

Figure 5.5.2 The relative mRNA concentrations of three of the markers of liver fibrosis corrected by GAPDH in wild type and Jun D knockout mice following 8 weeks CCl_4 induced liver injury. The results are presented as the mean and standard error for each group relative to the wild type mRNA concentration following GAPDH correction. The figures plotted on the graph represent the mean of the average triplicate values (GAPDH corrected) for each group. The plotted value is calculated as a percentage of the wild type value. The standards error is calculated with an value of n=3.

5.6 Discussion

Chapter 3 focused on the role of the AP-1 site in the transcriptional regulation of TIMP-1 in the hepatic stellate cell. The results of the AP-1 investigation indicated that the site was indeed crucial and also that the activity was due to the binding of Jun D homodimers. This primary work was, however, all performed *in vitro,* leaving many questions unanswered. Is Jun D also crucial to the regulation of TIMP-1 expression *in vivo*? Would the removal of Jun D in stellate cells lead to a reduction in TIMP-1 expression or would there be compensation by one of the other JUN proteins? Would there be compensation *in vivo* as a result of the loss of TIMP-1 via the increased expression of one

of the other TIMPs? All of these questions together are necessary to establish whether Jun D could be used as a therapeutic drug or gene therapy target.

A Western blot performed using HSC nuclear extracts made from CCl_4 injured rats indicated that there was an increase in the expression of Jun D with CCl_4 treatment when compared to the untreated olive oil controls (Figure 5.1.1). This result supports the role for Jun D identified *in vitro* (Chapter 3). The Western blot identified two bands for Jun D, which are suspected to correspond to the 39kDa and 44kDa Jun D isoforms. With CCl_4 treatment there appeared to be a switch from low-level expression of the 39kDa Jun D to high level expression of the 44kDa Jun D. We had previously suggested that there was an increase in expression of Jun D with culture activation of HSC and that there was Jun D present at all points throughout activation (Bahr *et al.*, 1999). The results of the CCl_4 injury Western blot indicate that in uninjured cells, the Jun D expression is in the form of a 39kDa protein, but this may in fact be an inhibitory isoform of Jun D. The 39kDa form results from translation beginning from the third, rather than the first AUG. This shorter version of Jun D lacks the N-terminal transactivation domain of the full-length 44kDa version but is still able to form AP-1 dimers (Okazaki *et al.*, 1998). This suggests that the increase in Jun D expression with HSC activation may also be coupled with a change in Jun D protein activity through the expression of an alternative isoform. This change in form and level of expression are obviously not the only reasons for the increase in TIMP-1 expression, as transfection of the Jun D expression vector into freshly isolated cells led to no increases in TIMP-1 promoter activity (Figure 3.8.1).

In order to elucidate the role of Jun D *in vivo,* three breeding pairs of heterozygote Jun D knockouts were obtained via collaboration. The results of the Sirius red staining of the mouse liver sections following CCl_4 injury indicated that there were obvious differences between the wild type (Figure 5.3.1 A-C) and Jun $D^{-/-}$ knockout (Figure 5.3.2 A-C) animals. In the wild type mice, there are obvious veins of red collagen staining radiating from the central veins. In some areas the radiating bands of fibrosis were shown to link the veins together, forming islands of hepatocytes or regenerative nodules which are a common feature in cirrhosis. This is particularly apparent in mouse MW1 (Figure 5.3.1

C). This indicates that the wild type mice have indeed developed fibrosis as a result of the CCl_4 injection. The level of fibrosis is only moderate and as a result, in a later study, treatment will be extended from 8 to 12 weeks. In the Jun $D^{-/-}$ knockout animals, little fibrosis was observed. There was, however, a little collagen staining visible around the central veins, as expected (Figure 5.3.2 A-C). The results of the Sirius red staining indicate that this background of mice do undergo fibrosis and that there is no observable fibrosis in the Jun $D^{-/-}$ knockout animals.

The results of the hematoxylin and eosin staining identified fibrotic bands, which contained numerous elongated nuclei in the wild type liver sections (Figure 5.3.3.A and B). The smaller sinusoid width is most likely due to the smaller quantity of collagen present, observed in the Sirius red staining, while the origin of the elongated nuclei requires further investigation. Early fibrosis is classically associated with deposition of collagen, primarily in the space of Dissé, making the sinusoid appear larger (Minto *et al.*, 1983; Bissell *et al.*, 1987; Mak *et al.*, 1988).

Western blotting identified a decrease in αSMA staining for whole liver samples when comparing Jun $D^{-/-}$ knockout mice to the wild types (Figure 5.4.1). There was, however, some αSMA present in the Jun D knockout lanes. It is not known whether this is of activated HSC origin or from vascular tissue. To check the loading of the whole liver samples, a Western blot was performed for β-actin using an identical membrane as used for αSMA (Figure 5.4.2). The results of the β-actin blotting indicated that the lanes were equally loaded (Figure 5.4.3).

The results of the densitometric analysis for β-Actin and αSMA indicated that there are significantly lower levels of αSMA in the Jun $D^{-/-}$ knockout mice than the wild types. The reduced level of αSMA in the livers of the knockouts may be explained by a generally lower level of transcription by the cells, the presence of less αSMA containing HSC or changes in αSMA of the blood vessels. In order to establish whether there is fewer HSC it would be necessary to perform further immunohistochemical staining for αSMA, desmin and GFAP. The altered expression of αSMA could also occur as a result

of changes in HSC activation, this again would require further staining to establish. The regulation of αSMA at this stage is unknown but there is a suggestion that the promoter region of this gene is negatively regulated in fibroblasts by c-Jun and c-Fos. However, this was in Ras transformed cells (Bushel *et al.*, 1995).

It was felt necessary to identify the underlying mechanism that led to the reduction in the level of αSMA observed by Western blotting and the reduction in collagen deposition, as seen by Sirius red staining in the Jun $D^{-/-}$ knockout mice.

The results of the Taqman study indicated that there was a significant decrease in the levels of mRNA present for TIMP-1 and procollagen I (Figure 5.5.2). The relative quantities of GAPDH cDNA were shown to be very similar, validating the Taqman reactions (Figure 5.5.1). The reduction in the level of transcript for TIMP-1 in the Jun D knockout mice agrees with the data already obtained *in vitro* (Chapter 3), and also suggests that Jun D was crucial for TIMP-1 transcription in the activated HSC *in vivo*. The reduction in the level of procollagen I mRNA was not completely unexpected as the collagen promoter had previously been shown to be regulated by AP-1 (Armendariz-Borunda *et al.*, 1994). It was important to assess the level of collagen transcription, as the overall mechanism of deposition is dependent on the relative expressions of the matrix protein, the degrading enzymes and the inhibitors. The reduction in expression of either TIMP-1 or collagen I would account for the reduction in the level of deposition of fibrillary collagen seen by histology (Figure 5.3.1 A-C and 5.3.2 A-C), but in future studies it will also be necessary to establish the relative expression of the metalloproteinases.

The results of the Taqman assay for αSMA showed no significant change between the wild type and Jun $D^{-/-}$ knockout mice due to a large error (Figure 5.5.2). This result is in contrast to the result seen in the αSMA Western blot (Figure 5.4.1 and 5.4.3). This may represent an error in sampling with such a small volume of tissue taken for making RNA, compared with that used for SDS page sample preparation. The problem with sampling is of particular significance for αSMA as the HSC makes up only a tiny fraction of its

production in the liver. The reverse however is true for TIMP-1 and collagen I production (Arthur *et al.*, 1992c; Iredale *et al.*, 1992; Iredale *et al.*, 1993; Iredale *et al.*, 1995b; Benyon *et al.*, 1996).

Further investigation is necessary to establish if there is a difference in the number of HSC, rather than a reduction in transcription, that is responsible for the low levels of αSMA in the knockout animals by Western blot. As the HSC are also the main producers of TIMP-1 and collagen in liver fibrosis it is possible these are also affected by reduced cell numbers. It is also necessary to re-investigate the mRNA transcription for αSMA using an increased number of animals and possibly larger sampling to improve the Taqman data. Investigations into the expression of the various AP-1 proteins by the knockout HSC and the relative proliferation are at present continuing. It will also be necessary to repeat the CCl_4 injury study upon more animals with untreated and or olive oil control animals. The olive oil controls will be particularly useful in determining basal levels of expression. This is necessary to establish whether the removal of Jun D prevents or reduces the pathology.

Further studies are also necessary to determine the relative expressions of the various MMPs and in particular MMP-1. These experiments are crucial to establish that the change in collagen deposition is due solely to the change in relative expression of Collagen 1 and TIMP-1. It will also be important *in vitro* to establish if there is a difference in the proliferation and apoptosis of wild type and knockout animals. It would be useful to see if the phenotype could be reversed initially *in vitro* and then *in vivo* with the replacement of Jun D expression by a viral system. Finally by the addition of TIMP-1 to the media of cultured Jun $D^{-/-}$ knockout HSC it may be possible to establish if TIMP-1 has anti apoptotic and growth factor properties.

Chapter 6.

The role of SP-1 and LBP-1 Binding Sites in the Control of TIMP-1 Promoter Function in HSC.

6.1 Introduction

As previously mentioned, truncation of the TIMP-1 promoter had identified the minimal regulatory region or minimal promoter, which incorporated AP-1 and LBP-1 transcription factor binding sites at the 5' and 3' ends respectively. The truncation analysis was combined with the results obtained by computer sequence search, indicating the presence of a number of known transcription factor binding sites. The results of the sequence analysis identified AP-1, PEA3, STAT1, SP-1 and LBP-1 (see Figure 6.1.1) (Bahr *et al.*, 1997; Clark *et al.*, 1997). Sequence analysis, however, is only able to indicate the presence of a site and as such is unable to identify whether it is functionally active in a particular gene or cell type. Sequence analysis is also unable to identify novel transcription factor binding sites. For a complete sequence of the TIMP-1 minimal promoter see Appendix 6. This also contains the position and sequence of the UTE-1 binding site.

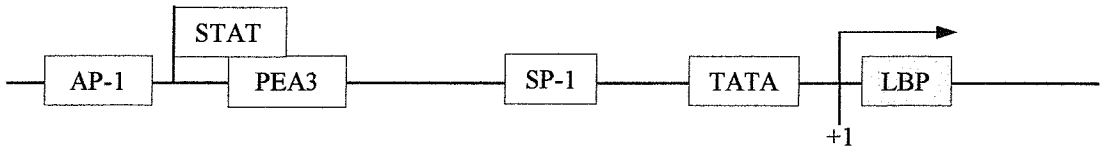

Figure 6.1.1 A diagrammatic representation of the TIMP-1 minimal promotor, as suggested by sequence analysis. The UTE-1 site is not indicated as it was identified at a later date by Dnase1 footprinting (Trim *et al.*, 2000).

6.2 Production of SP-1 TIMP-1 Mutant Reporter Construct

The role of the SP-1 transcription factor in the HSC cell has been the cause of some controversy. The controversy revolves around whether SP-1 is or is not present in the activated HSC and therefore whether it can enhance gene expression. Previous work published by other groups, concerning regulation of the procollagen α 1 gene in the HSC, has suggested that there is an increase in the expression of SP-1 with HSC activation (Rippe *et al.*, 1995; Miao *et al.*, 1999; Rippe *et al.*, 1999).

The TIMP-1 minimal promoter does contain a GC-Box or SP-1 binding site (TIMP-1, CCCCCGCCCC), however this does differ slightly from the consensus sequence

($^{T}/_{G}{}^{A}/_{G}$GGCG$^{T}/_{G}{}^{A}/_{G}{}^{A}/_{G}{}^{T}/_{C}$) (see Section 1.21). The role of the SP-1 site in the TIMP-1 minimal promoter is at present unknown but it is possible that it could bind SP-1 or another GC-Box binding factor. Results in primary HSC by two other researchers in the group had previously demonstrated that SP-1 is expressed in freshly isolated HSC. The expression of SP-1 declines rapidly with culture and may represent an artefact of isolation. This theory is supported by their discovery that trypsin passaging of HSC resulted in the prolonged expression of a SP-1 binding complex by EMSA and SP-1 protein, suggested by Western blot (unpublished data).

In order to establish whether the SP-1 site is crucial for TIMP-1 transcription, a mutation of this transcription factor binding site in the minimal promoter was performed by two-step mutational PCR (see Section 2.9.2). The site was altered to produce 5' and 3' mutations (Figure 6.2.1). The oligonucleotides used for the mutation of the SP-1 site are given in Appendix 1. The mutant minimal promoter constructs were ligated into the pBLCAT3 CAT reporter (see Appendix 2i) plasmid via the *Pst* I and *Hind* III restriction sites.

SP-1 GCCACCCCCGCCCCTAGCGT	Wild Type
GCCATTGATGCCCCTAGCGT	5' SP-1 Mutant
GCCACCCCCGTAGATAGCGT	3' SP-1 Mutant

Figure 6.2.1 The mutations placed in the putative SP-1 site of the TIMP-1 minimal promoter by two step mutational PCR.

6.3 The Effect of SP-1 Mutation on TIMP-1 Promoter Activity

The SP-1 3' and 5' mutants were transfected into activated HSC to establish whether the SP-1 site of the TIMP-1 minimal promoter was functionally active.

Transfection studies using the mutated promoter constructs alongside the wild type promoter identified a significant difference in the activity of the 3' SP-1 mutant promoter from that of the wild type or 5' mutant (Figure 6.3.1). The results show a significant 70% reduction in the activity of the 3' SP-1 mutant. These results suggest that the 3' region of

the SP-1 binding site is crucial for the activity of the TIMP-1 promoter in the activated HSC. The transfection of the SP-1 mutant constructs was repeated in NIH3T3 fibroblasts in order to establish whether the difference in function of the SP-1 binding site in the HSC is cell specific.

The results of the transfection of the TIMP-1 SP-1 mutants in NIH3T3 fibroblasts was a reduction of 80 and 40% in the activity of the promoter for the 3' and 5' mutant constructs respectively (Figure 6.3.2). The mutation of the 3' end of the SP-1 site resulted in a significant reduction in promoter activity, again suggesting it is important for the SP-1 site activity. Mutation of the 5' SP-1 site also resulted in a reduction in promoter activity, which was treading towards significance. The data suggest that, as with the HSC, the 3' end of the TIMP-1 SP-1 site is crucial for high-level transcription. In the NIH3T3 cell however it seems that the 5' end of the SP-1 site may play a bigger role than in the HSC, although this was not shown to be significant.

In order to investigate the activity and respective inactivity of the wild type TIMP-1 and TIMP-1 3'/ 5'SP-1 mutant reporters, the vectors were co-transfected into NIH3T3 fibroblasts both with and without a SP-1 PAC expression vector that produced recombinant SP-1 in transfected cells. The empty PAC vector was used as a control.

The results of the co-transfections of the wild type TIMP-1 reporter with the SP-1 PAC or PAC expression vector indicated that there was a 400% increase in the activity of the TIMP-1 promoter with SP-1 over expression (Figure 6.3.3). The results of the transfection of the 3' and 5' TIMP-1 SP-1 mutants in the absence of SP-1 over expression agree with those seen in Figure 6.3.2. The SP-1 mutants indicate that in NIH3T3 fibroblasts both 3' and 5' ends of the SP-1 site are necessary for high-level transcription. There was no response to the activity of the PAC SP-1 expression vector in the 3' and 5' SP-1 mutants when compared with the controls.

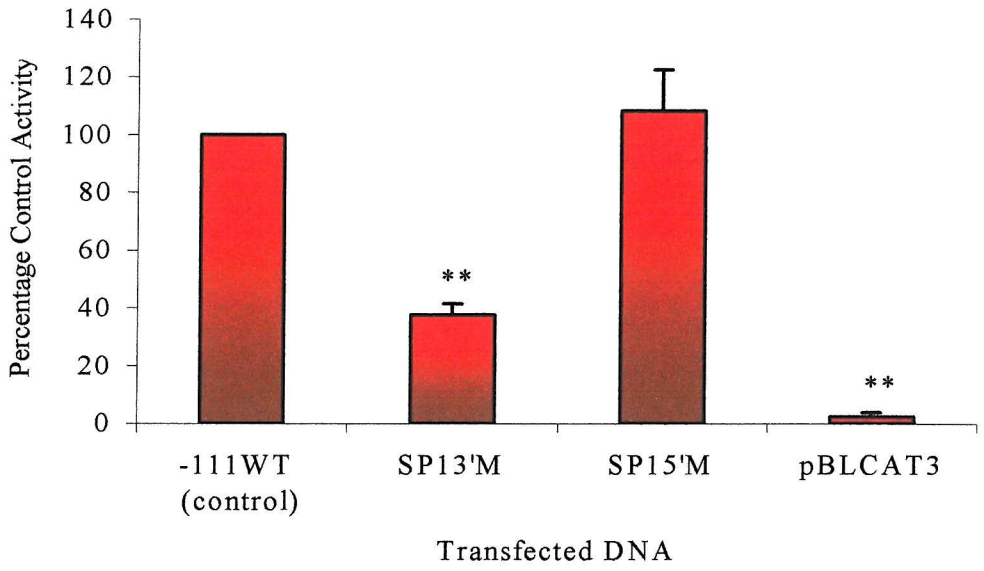

Figure 6.3.1 The effect of SP-1 site mutation on TIMP-1 promoter activity in HSC. Results are mean and standard error with respect to wild type control activity from 3 separate triplicate transfections of cells from separate individuals. The primary rat HSC cells were plated out at a density of $1x10^6$ cells per 45mm culture plate. The cells were cultured for >7 days to become activated before transfection at 60-70% confluence with 1μg of either the 3' SP-1 mutant, 5' SP-1 mutant, –111WT TIMP-1 or pBLCAT3 reporter constructs. The vector pBLCAT3 was used as a control for reporter activity. Each plate was also co-transfected with 100ng of Renilla-Luc expression plasmid to normalise for differences in transfection efficiency. The cells were cultured for 48 hours before the cells were harvested. The activity of the promoter was established and the results modified for transfection efficiency (see Section 2.7.3). An indication of the data significance can be obtained from the presence of a * or **. These represent P values of <0.05 and <0.01 respectively. For primary data see Appendix 3.

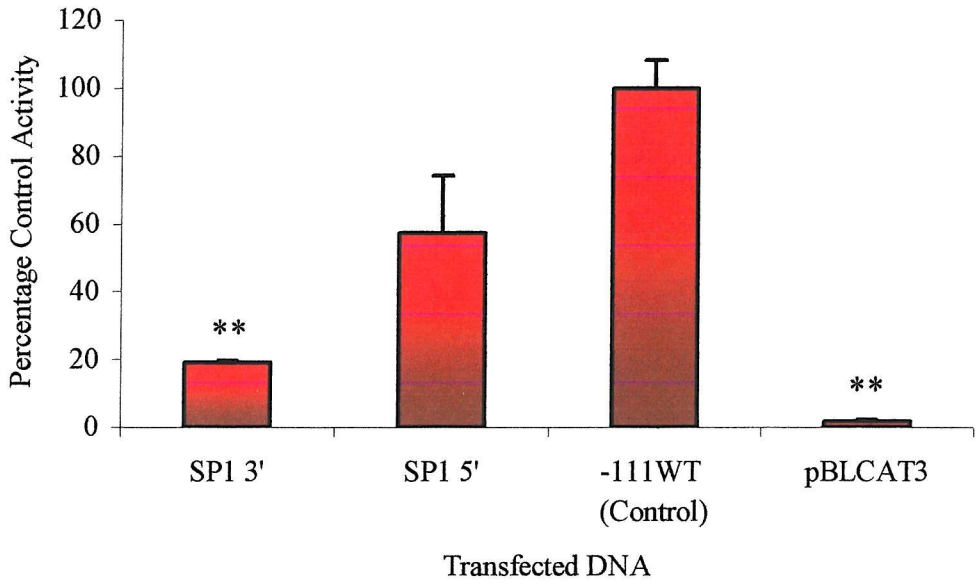

Figure 6.3.2. The effect of SP-1 site mutation on TIMP-1 promoter activity in fibroblasts. The NIH3T3 cells were plated out at low density in 45mm culture plates. The results are the mean and standard error with respect to the wild type control activity for three triplicate transfections performed on separate occasions. The cells were cultured until 60-70% confluence before transfection with 1μg of 3' SP-1 mutant, 5' SP-1 mutant, –111WT TIMP-1 or pBLCAT3 reporter constructs. The vector pBLCAT3 was used as a control for reporter activity. Each plate was also co-transfected with 100ng of Renilla-Luc expression plasmid to normalise for differences in transfection efficiency. The cells were cultured for 48hours following transfection before harvesting extracts for assay. The activity of the promoter was established and the results modified for transfection efficiency (see Section 2.7.3). An indication of the data significance can be obtained from the presence of a * or **. These represent P values of <0.05 and <0.01 respectively. For primary data see the Appendix 3.

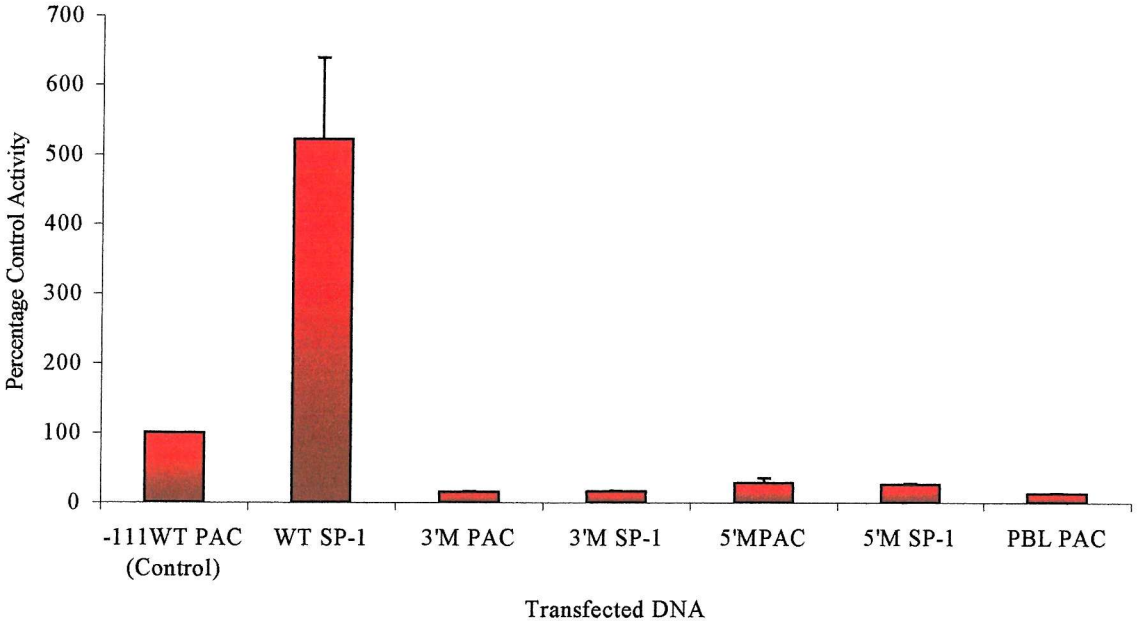

Figure 6.3.3 The effect of SP-1 expression vector co-transfection on the activity of the TIMP-1 wild type, 5' and 3' SP-1 mutant minimal promoter reporter constructs, in NIH3T3 cells. The results are the mean and standard error with respect to the wild type control from a triplicate transfection. The NIH3T3 cells were plated out at low density in 45mm culture plates. The cells were cultured until 60-70% confluence before transfection with 3μg of SP-1 PAC or PAC expression vector and 1μg of 3' SP-1 mutant, 5' SP-1 mutant, -111WT or pBLCAT3 reporter construct. The PAC and pBLCAT3 were used to control for the expression vector and reporter construct respectively. The cells were also transfected with 100ng of Renilla-Luc expression plasmid to normalise for differences in transfection efficiency. The cells were cultured for 48hours following transfection before harvesting extracts for assay. The activity of the promoter was established and the results modified for transfection efficiency (see Section 2.7.3). For primary data see the Appendix 3.

6.4 Identifying the Complexes that Interact with the Putative SP-1 Site

In order to identify the complexes interacting with the SP-1 site in the HSC and NIH3T3 cell a series of EMSA were performed.

A comparison between two sets of extracts from separate rats indicates the presence of four binding complexes, low mobility complex 1 & 2 (LMC-1&2) and high mobility complex 1 & 2 (HMC-1&2) (Figure 6.4.1). In both cases, as expected, there is strong complex binding to the TIMP-1 SP-1/GC-Box probe with extracts from freshly isolated

cells. The addition of the probe to 7day nuclear extracts indicates that there is only weak complex binding in both sets of samples. The strong complex formation shown in freshly isolated cells can however, be seen to return after 10 or more days of activation. An approximately equal level of probe binding was observed when comparing complex binding in freshly isolated and 10-day cells from individual B. These results may explain the confusion over the expression of SP-1 binding proteins in the HSC. It appears that expression of SP-1 and DNA binding activity are initially lost upon culture and are then recovered after 10 days of culture activation.

The results of the competition EMSA indicated that three of the SP-1 binding complexes (LMC-1, 2 and HMC-1) were completely competed by a 50 fold excess of unlabelled TIMP-1 SP-1 double stranded oligonucleotide in both the HSC and NIH3T3 cells (Figure 6.4.2). There were only slight deviations in the intensity of protein binding complexes following the addition of 3' and 5' TIMP-1 SP-1 mutants, the TIMP-1 AP-1, or AP-2 and AP-1 consensus oligonucleotides, indicating that the binding of the three complexes are specific in both NIH3T3 and HSC cells. The fourth complex, HMC-2, seen previously in Figure 6.4.1, is just visible in Figure 6.4.2, just above the free probe in the NIH3T3 EMSA. It is believed to be non-specific, as it shows no competition with the 50 fold excess of unlabelled probe.

In order to determine the protein interactions occurring with HSC and NIH3T3 nuclear proteins and the TIMP-1 SP-1 DNA probe, a further series of EMSA were performed with the specific antibodies. Antibodies specific to SP-1, SP-2, SP-3, SP-4 and ZF-9 were added to the EMSA reactions, as they are all known to bind GC-Boxes. The factor ZF9 was also included as it is known to be strongly up regulated in the activated HSC (Ratziu *et al.*, 1998). The antibodies AP-2α, AP-2β and Ap-2χ were used to act as antibody controls.

The results of the supershift EMSA for HSC nuclear extracts identified specific blocking of the binding interactions with the SP-1 probe as a consequence of some antibody additions (Figure 6.4.3). The specificity of the complex binding blockade is indicated by

the lack of effect by the control antibodies, AP-2α, AP-2β and AP-2χ. The results of the antibody additions are tabulated below (Figure 6.4.5). The results also supported those seen in the competition EMSA (Figure 6.4.2). The binding to the SP-1 site (complexes LMC-1, 2 and HMC-3) was again completely competed by the addition of 50 fold excess of unlabelled TIMP-1 SP-1 oligonucleotide.

As with the supershift in the HSC, the repeat EMSA for NIH3T3 nuclear extracts also identified specific blockade of the binding complexes by some of the antibodies used (Figure 6.4.4). The results of the antibody blockades are tabulated below (Figure 6.4.6). The EMSA again identified complete competition of all DNA binding complexes with the addition of a 50 fold excess of the unlabelled TIMP-1 SP-1 double stranded oligonucleotide.

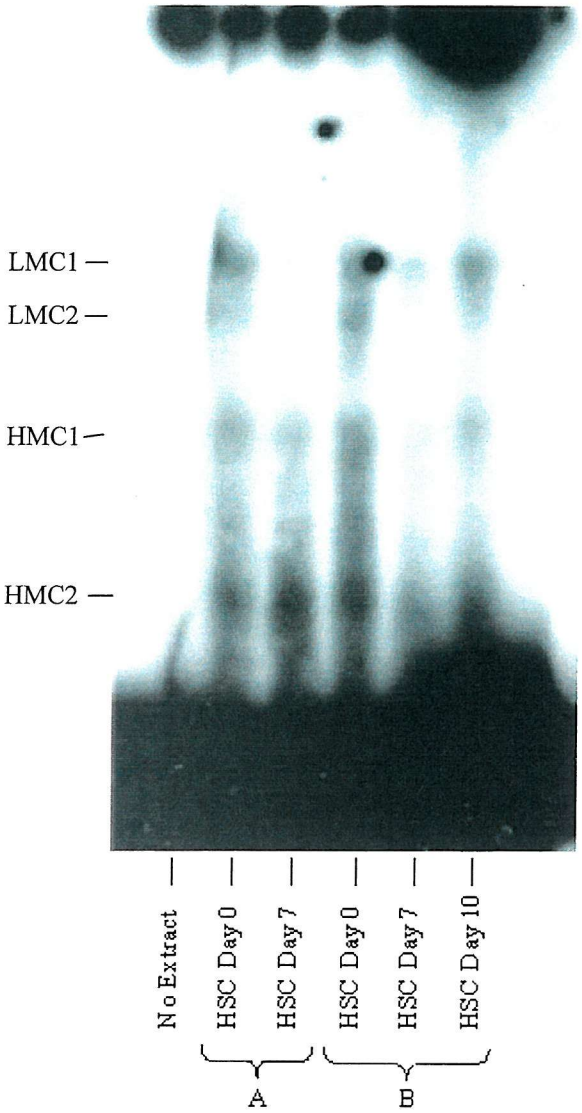

Figure 6.4.1 A representative EMSA showing a comparison of the interactions of two sets of rat HSC nuclear extracts with a TIMP-1 SP-1 probe. 10μg of primary HSC nuclear extracts from Day 0 and Day 7 (Individual A) and Day 0, Day 7 and Day 10 (Individual B) were used. 0.2ng of $\gamma^{32}P$ labelled TIMP-1 SP-1 oligonucleotide probe was added to each sample (see Appendix 1). The samples were run on a 5% non-denaturing polyacrylamide gel and run at 15mA for approximately 2 hours.

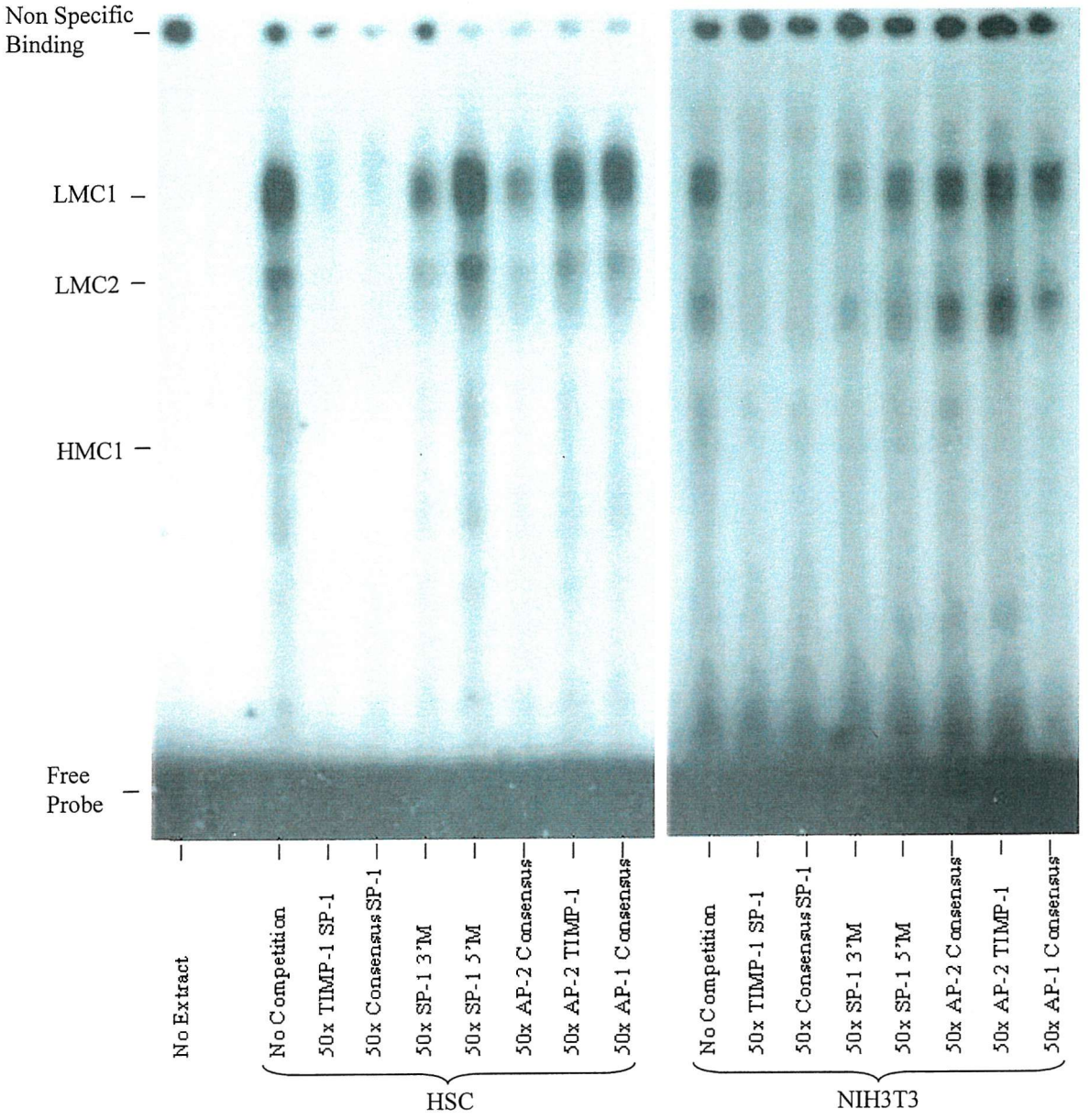

Figure 6.4.2 Competition assay for DNA binding using rat activated HSC and NIH3T3 nuclear extracts with a TIMP-1 SP-1 probe, analysed by EMSA. 5µg of nuclear extracts from either 14 day rat HSC or NIH3T3 fibroblasts were loaded into each well with 0.2ng of $\gamma^{32}P$ labelled TIMP-1 SP-1 oligonucleotide Probe (see Appendix 1). Competition unlabelled oligonucleotides (see Appendix 1) were added at a volume of 2µl in the place of reaction water. The samples were run on a 5% non-denaturing polyacrylamide gel and run at 15mA for approximately 2 hours.

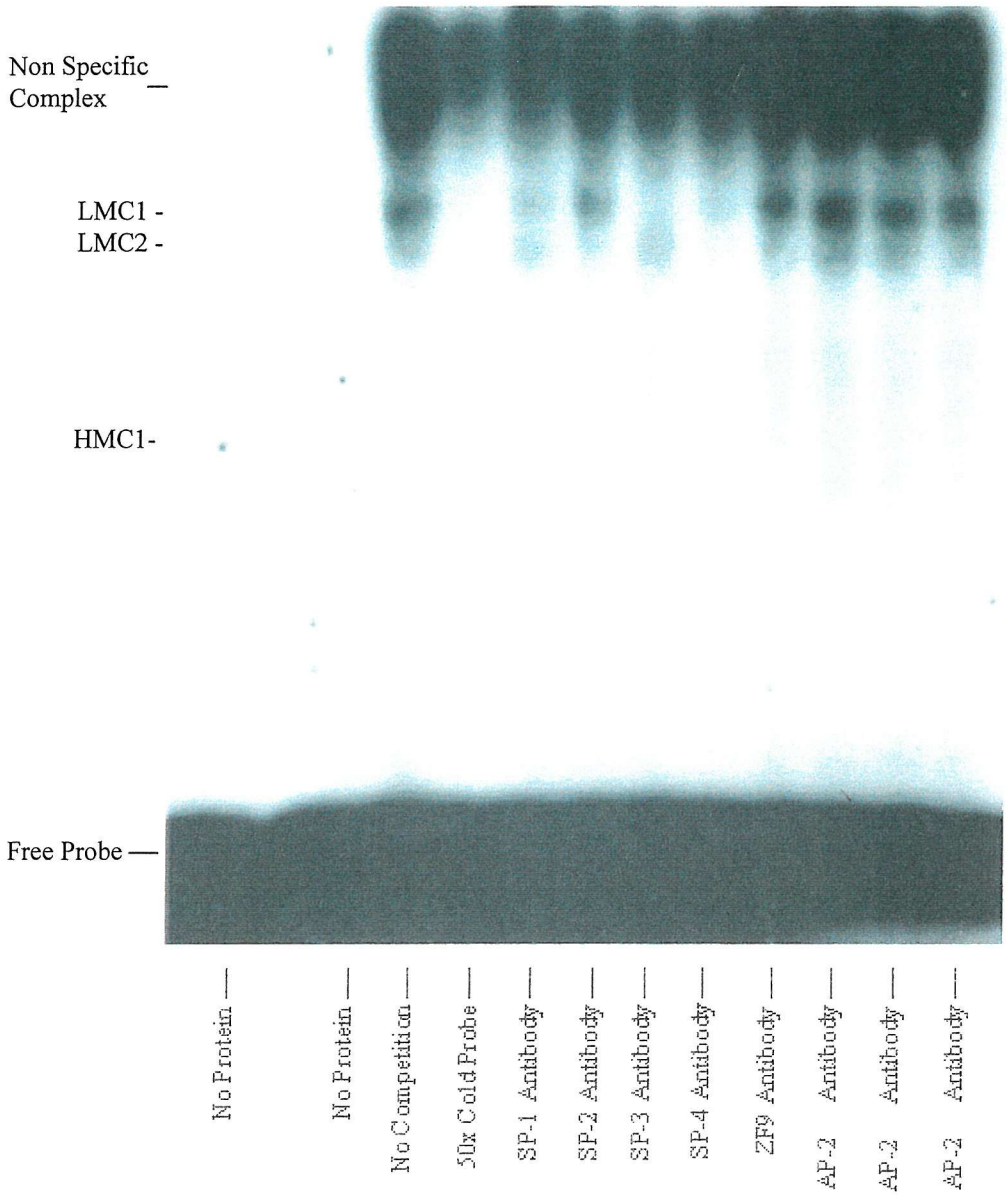

Figure 6.4.3 The supershift of SP-1 binding protein interactions for rat activated HSC nuclear extracts with a TIMP-1 SP-1 probe, analysed by EMSA. 5μg of nuclear extracts from 14 day rat HSC were loaded into each well with 0.2ng of $\gamma^{32}P$ labelled TIMP-1 SP-1 oligonucleotide Probe (see Appendix 1). Competition unlabelled oligonucleotides (see Appendix 1) and super shifts performed by the addition of antibodies (see Appendix 4) were added at a volume of 2μl in the place of reaction water. The antibody stocks for supershift were at a concentration of 1μg/μl. The samples were run on a 5% non-denaturing polyacrylamide gel and run at 15mA for approximately 2 hours.

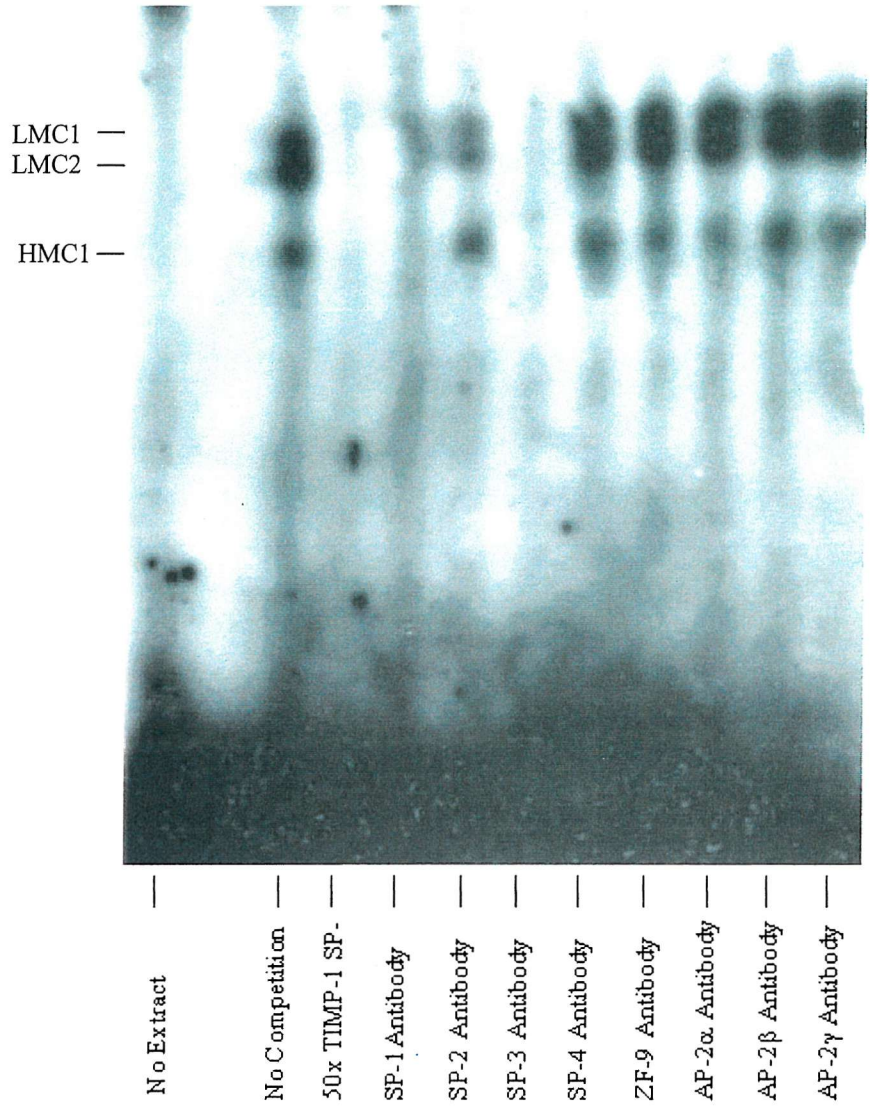

Figure 6.4.4 The supershift of DNA binding protein in NIH3T3 nuclear extracts interacting with a TIMP-1 SP-1 probe, analysed by EMSA. 5μg of nuclear extracts from normal cycling NIH3T3 fibroblasts were used in each reaction with 0.2ng of $\gamma^{32}P$ labelled TIMP-1 SP-1 oligonucleotide probe (see Appendix 1). Competition unlabelled oligonucleotides (see Appendix 1) and supershift antibodies (see Appendix 4) were added at a volume of 2μl in the place of reaction water. The antibodies stocks for supershift were at a concentration of 1μg/μl. The samples were run on a 5% non-denaturing polyacrylamide gel and run at 15mA for approximately 2 hours.

Antibody	DNA Binding Complex		
	LMC1	LMC2	HMC1
SP-1	⇓	⇓	⇒
SP-2	⇒	⇒	⇒
SP-3	X	⇒	⇒
SP-4	X	X	X
ZF9	⇒	⇒	⇒
AP-2 α	⇒	⇒	⇒
AP-2 β	⇒	⇒	⇒
AP-2 χ	⇒	⇒	⇒

Figure 6.4.5 A diagrammatic representation of the results of the supershift EMSA using extracts from HSC cells (Figure 6.4.3). The symbols ⇒, ⇓ and X indicate whether the DNA binding complex remained the same, was reduced or was completely absent with each specific antibody.

Antibody	DNA Binding Complex		
	LMC1	LMC2	HMC1
SP-1	⇓	⇓	X
SP-2	⇓ (small)	⇓ (small)	⇒
SP-3	X	X	X
SP-4	⇒	⇒	⇒
ZF9	⇒	⇒	⇒
AP-2 α	⇒	⇒	⇒
AP-2 β	⇒	⇒	⇒
AP-2 χ	⇒	⇒	⇒

Figure 6.4.6 A diagrammatic representation of the results of the supershift EMSA using extracts from NIH3T3 cells (Figure 6.4.4). The symbols ⇒, ⇓ and X indicate whether the DNA binding complex remained the same, was reduced or was completely absent with each antibody addition.

In order to identify which of the SP-1 family of proteins were present Western blots were performed using whole cell extracts for primary HSC and NIH3T3 cells.

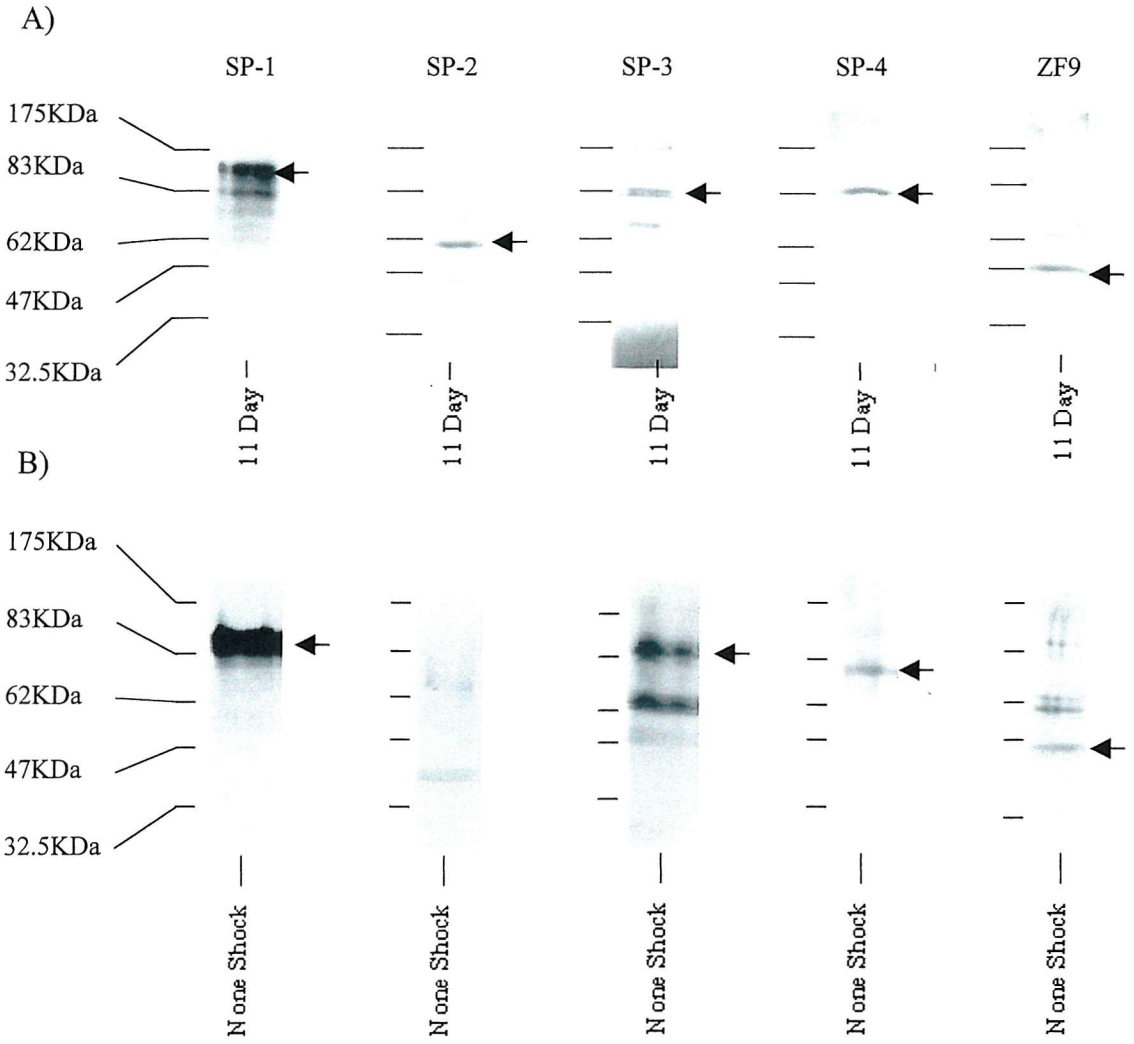

Figure 6.4.7 The Krüppel-like GC-Box binding factors in: A) 11 day Rat activated HSC whole cell extract. B) NIH3T3 Fibroblast whole cell extract. Western blots were performed with 30μg of whole cell extract. The samples were loaded on a 9% denaturing polyacrylamide gel with a 4% stacking gel. Each sample was run alongside Coomassie prestained markers (New England Biolabs). The antibodies the individual Krüppel like factor specific rabbit antibodies (See Appendix 4) were added at 1μg/μl. The secondary rabbit IgG specific polyclonal HRP conjugate antibodies were added at a dilution of 1:2000. The expected molecular weight for SP-1 is 95-106kDa, SP-2 62kDa, SP-3 120kDa, SP-4 96kDa and ZF-9 47kDa (see Appendix 5). The exposures for NIH3T3 blots were (SP-1, 10 seconds), (SP-3, 20 seconds) (SP-2. 4 and ZF-9, 40 seconds). The exposures for the HSC blots were (SP-1 15 seconds) (SP-2, 3, 4, ZF-9, 60 seconds).

The result of the Western blots for the Krüppel like GC-Box binding factors indicate the expression of almost all of the proteins examined in both HSC and NIH3T3 cells. The relative expression of each protein in the HSC and NIH3T3 is however impossible to quantify. It would appear that in the NIH3T3 cell, the dominant GC-Box binding factors are SP-1 and SP-3, with comparatively little of the others and only a very faint band where SP-2 is expected to migrate in the gel. In the HSC however it would appear that SP-1 predominates but by a smaller amount than seen in the NIH3T3. The other proteins are all expressed at with similar intensities for SP-2, 3, 4 and ZF-9, shown by Western blot.

6.5 The Functional role of Leader Binding Protein 1 (LBP-1) in the TIMP-1 Promoter

As previously mentioned the 3' terminus of the minimal promoter is marked by the presence of two LBP-1 half sites (see Appendix 6). These LBP-1 sites have been suggested to be crucial by truncation mutagenesis (see Section 1.22) (Bahr *et al.*, 1997).

A series of LBP-1 TIMP-1 minimal promoter mutant reporter constructs were obtained by collaboration from I.M. Clark (School of Biomedical Science, University of East Anglia, Norwich UK). The constructs contained various mutations of either or both of the LBP-1 sites. The constructs as with previous mutational work, had all been placed in the pBLCAT3 reporter vector (see Appendix 2i) and therefore, as before, the wild type control –111WT was used. The constructs (Tm SMA 2-8) are listed below (Figure 6.5.1).

GATCCAGCGCCCAGAGAGACACCAGAGGTAAGCAGGG	Human Timp-1 LBP-1 Consensus
GATCCAGCGCCACTAGAGACACACTAGGTAAGCAGGG	Tm SMA 2
GATCCAGCGCCCAGAGAGACACCAGATTCAAGCAGGG	Tm SMA 4
GATCCAGCGCAACTAGAGACACCAGAGGTAAGCAGGG	Tm SMA 5
GATCCAGCGCCCAGAGAGACAAACTAGGTAAGCAGGG	Tm SMA 6
GATCCAGCGCAACTAGAGACAAACTAGGTAAGCAGGG	Tm SMA 7
GATCCAGCGCCCAGAGAGAAAACACCAGAGGTAAGCAGGG	Tm SMA 8

Consensus LBP-1 binding sites.
Base match with human Timp-1 sequence
Base mutation from Timp-1 or HIV sequence

Figure 6.5.1. A diagrammatic representation of the TIMP-1 minimal promoter LBP-1 mutant reporter constructs.

The LBP-1 mutant reporter constructs were transfected into activated rat HSC to elucidate the role of the two half sites marking the 3' end of the TIMP-1 minimal promoter.

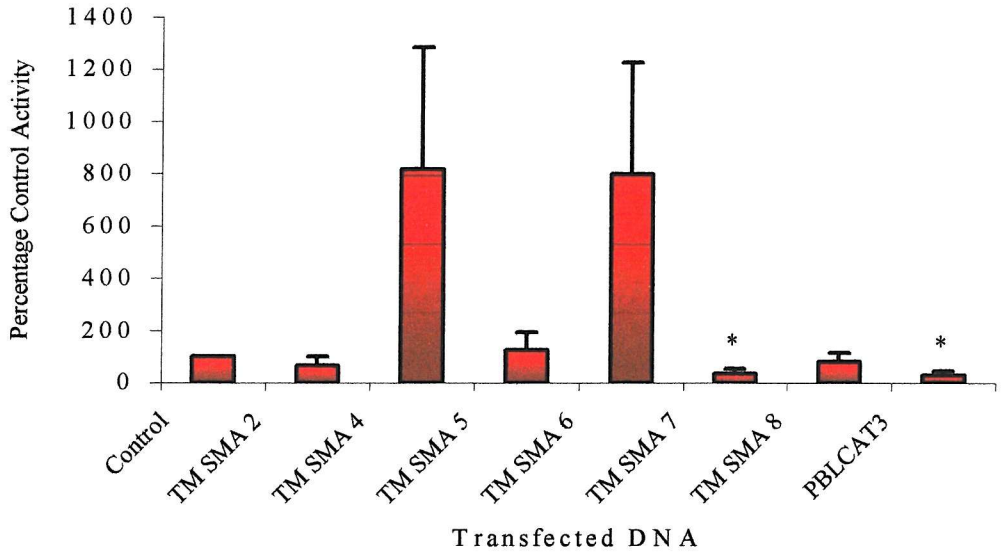

Figure 6.5.2. The effect of LBP-1 transcription factor binding site mutations on the activity of the TIMP-1 minimal promoter. The results represent the mean and standard error of four individual transfections performed on separate occasions with cells from different individuals. Primary rat HSC cells were plated at a density of $1x10^6$ cells per 45mm culture dish. These HSC cells were allowed to activate for >7days and transfected at between 60-70% confluence. The cells were transfected with 1μg of LBP-1 mutant or with -111WT or pBLCAT3 plasmid as positive and negative controls. Cells were cultured for 48 hours after transfection before a CAT assay was performed. Transfection efficiency was controlled by Hirt's assay.

The results of the LBP-1 mutant reporter analysis showed reductions in the activity of the promoter for constructs Tm SMA 2, Tm SMA 7 and Tm SMA 8 of 35, 66 and 20% respectively. Increases in promoter activity were demonstrated for Tm SMA 4 and Tm SMA 5 and Tm SMA 6 of 717, 25 and 700% respectively (Figure 6.5.2). Due to the relative size of the errors, only the promoter activity reduction that occurred as a result of Tm SMA 7 could be shown to be significant. Tm SMA 7 had complete mutations of both LBP-1 sites.

6.6 Protein Binding to the LBP-1 Site in the TIMP-1 Promoter

Oligonucleotides for Electro-Mobility Shift Assay (EMSA) were supplied by I.M. Clark, which contained variations and mutations of the LBP-1 site. The complete list of LBP-1 oligonucleotides and the others used in the EMSA are listed in Appendix 1, or shown diagrammatically below (Figure 6.6.1)

Human Timp-1 LBP-1
GATCCAGCGCCCAGAGAGACACCAGAGGTAAGCAGGG

Timp-1 LBP-1 first half site mutant.
GATCCAGCGCCACTAGCGCCACCAGAGGTAAGCAGGG

Timp-1 LBP-1 both half sites mutant.
GATCCAGCGCCACTAGCGCCACACTAGGTAAGCAGGG

Timp-1 LBP-1 splice site mutant.
GATCCAGCGCCCAGAGAGACACCAGATTCAAGCAGGG

Timp-1 LBP-1 first site only.
GATCCAGCGCCCAGAGAGACA

Timp-1 LBP-1 second site only.
CACCAGAGGTAAGCAGGG

LBP-1 binding site from HIV-1.
CATGACCCAGAGAGACCAATC

LBP-1 binding site mutant from HIV-1.
CATGACCCAGAGATCAAAATC

Consensus LBP-1 binding sites.
Base match with human Timp-1 sequence
Base mismatch with human Timp-1 sequence
Base mutation from Timp-1 or HIV sequence

Figure 6.6.1 Comparison of the oligonucleotides used in the LBP-1 EMSA analysis.

The EMSA analysis identified 4 complexes, low mobility complex-1 and 2 (LMC-1 & 2) and two high mobility complexes 1 and 2 (HMC-1 & 2) (Figure 6.6.2.). Only HMC-1

and 2 were present in the HSC time course extracts, although they were not shown to be specific. The complexes HMC-1 & 2 were not competed by either the LBP-1 or NFκB 100x cold unlabelled probes or by an alternative unlabelled double stranded oligonucleotide. The complex LMC-1 was only just visible in the cell line extracts MT11 (a Jurkat cell line), Hela and RAW cells (a macrophage cell line).

Using crude nuclear extracts from MT11 Jurkat and RAW cells as a source of concentrated LBP-1 binding protein, a series of competition assays were performed on the LMC-1 & 2 (Figure 6.6.3). The EMSA also repeated the MT11 crude nuclear extract binding in the presence of a NaCl titration in an attempt to increase the LMC-1 & 2 binding affinity. The reason for the titration was a difference in the standard protocols used for EMSA in our group and that of Ian Clark, who had supplied the reporter constructs and mutant TIMP-1 LBP-1 oligonucleotides. It was realised that the two protocols used different NaCl concentrations in the reaction buffer. This was 84mM for our group and 184mM as used by Ian Clark's group (Bahr *et al.*, 1999; Clark *et al.*, 1997).

The results identified that LMC-2 in the MT11 crude extract may be specific as it was competed by unlabelled probe (Figure 6.6.3). LMC-1 was too faint to observe whether it was competed by the unlabelled probe. There was also no visible competition of HMC-1 & 2 in either the MT11 or the RAW cell extracts corresponding to their lack of specificity. The titration of the NaCl resulted in a dramatic increase in the binding of LMC-1 at a concentration of 144mM. There was also shown to be a slight increase in LMC-2 binding. The value of 144mM falls between the 84mM previously used by our group and the 184mM concentration used by that of Ian Clark. All subsequent EMSA were performed at a concentration of 144mM.

Using the new concentration of 144mM NaCl and MT11 extract, a competition assay was performed with double stranded competition oligonucleotides representing normal TIMP-1 and HIV LBP-1 sites, as well as mutations (Figure 6.6.1.), to map the binding sequence (Figure 6.6.4). The competition analysis using MT11 crude nuclear extract identified that

LMC-1 binding was not competing with any of the constructs and is therefore not specific. The competition assay showed that binding of LMC-2 could be titrated by both LBP-1 and AP-1 consensus. The complex could also be competed by a double stranded oligonucleotide containing the first LBP-1 site on its own, but not by a similar one containing the second site. The binding was also competed by the HIV consensus and splice site mutant, both 100x double-stranded unlabelled oligonucleotides. The double stranded oligonucleotides for the first half site and the HIV consensus and double site mutants did not compete. Therefore, of the LBP-1 site oligonucleotides, only the first half site from TIMP-1 and the HIV consensus would compete, although the same consensus site also appears in the second half sites.

In order to address the results of the competition assay (Figure 6.6.4) in which the LMC-2 seemed to have mixed specificity, a second competition assay was performed with other known transcription factor binding sites. The EMSA was performed on a HSC time course and passaged HSC extracts. Passaged HSC extracts had previously been used to strongly form the complex LMC-2 and were therefore used for the competition assay. The EMSA indicated no visible formation of the LMC-2 in the time course of HSC, although it is present in passaged HSC extracts (Figure 6.6.6). The freshly isolated extract was shown to contain high levels of the non-specific HMC-1 and 2 complexes. The competition assay using the passaged HSC extract indicates that binding of LMC-2 is titratable by cold LBP-1 Full-length probe, AP-1 consensus but not by NFκB or SP-1. The competition results also indicate that the complex formation can be inhibited by a single stranded unlabelled sense oligonucleotide in a titratable fashion.

As a result of the competition of LMC-2 by titration of the sense strand of the probe, a competition EMSA was performed in which a sense single strand LBP-1 full-length probe was used (Figure 6.6.6). The EMSA was repeated on both freshly isolated and activated HSC extract. The results of the competition assay indicated that there was strong binding of one complex (LMC-2) to the single stranded probe but there was no binding of LMC-1, HMC-1 or HMC-2 observed. The binding of LMC-1 was present in both freshly isolated and activated HSC crude nuclear extracts, although there is a lower

binding activity in the freshly isolated cell extract. In both cases, the formation of LMC-2 could be competed by sense, anti sense and double stranded TIMP-1 LBP-1 first site oligonucleotide but not by similar oligonucleotides corresponding to the second LBP-1 half site.

To further elucidate the binding of LMC-2 a final competition assay was performed using freshly isolated 10day culture activated HSC nuclear extract (Figure 6.6.7). The competition assay identified that the LMC-2 was not strand specific in LBP-1, AP-1 (TIMP-1 non-consensus) or AP-1 consensus, although, as previously shown, there was some sequence specificity.

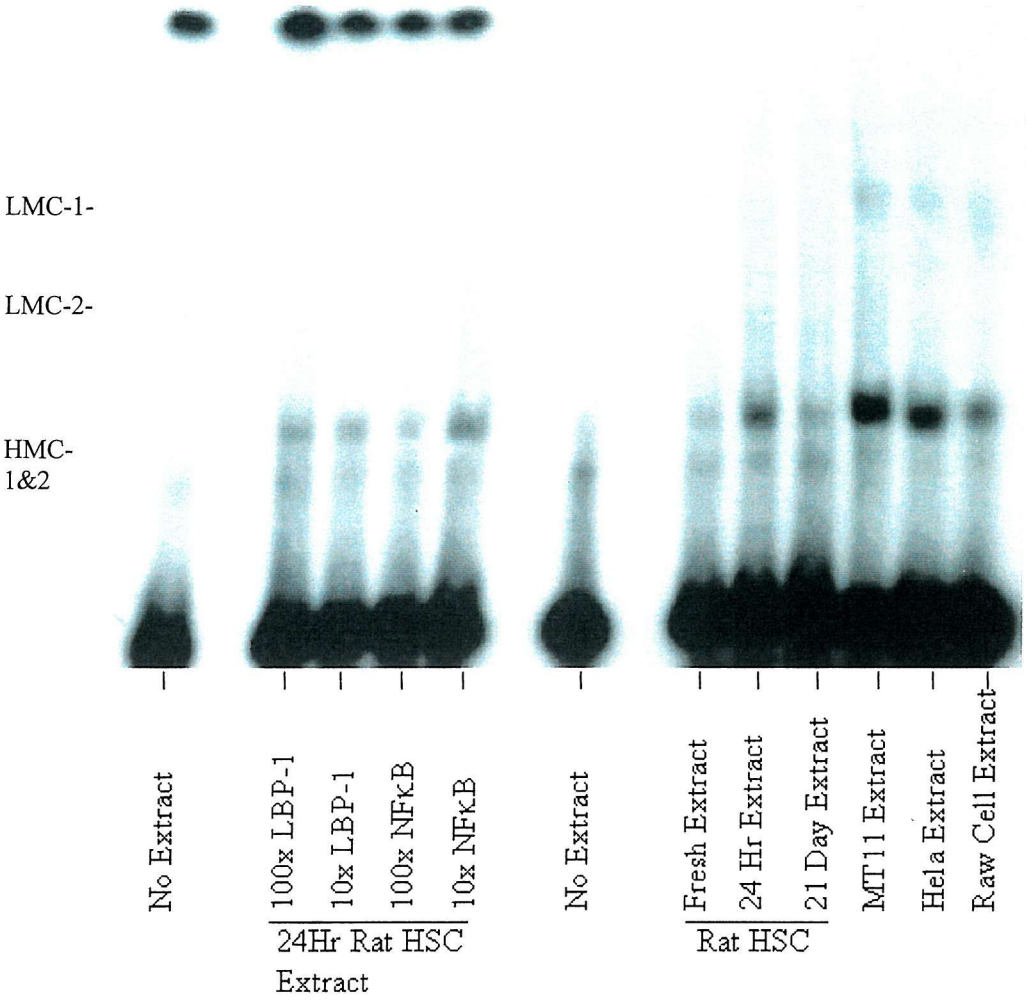

Figure 6.6.2. An EMSA analysis of protein interactions using a time course for rat HSC and other cell line extracts. 10μg of specified crude nuclear extract was added to each well with 0.2ng of LBP-1 full length TIMP-1 wild type double stranded LBP-1 $\gamma^{32}P$ labelled oligonucleotide. Competition was performed by the addition of double stranded unlabelled oligonucleotides to the reaction prior to the addition of the probe in solution, in the place of an equal volume of reaction water. The samples were run on a 5% polyacrylamide TBE non-denaturing gel run at 15mA for approximately 2 hours.

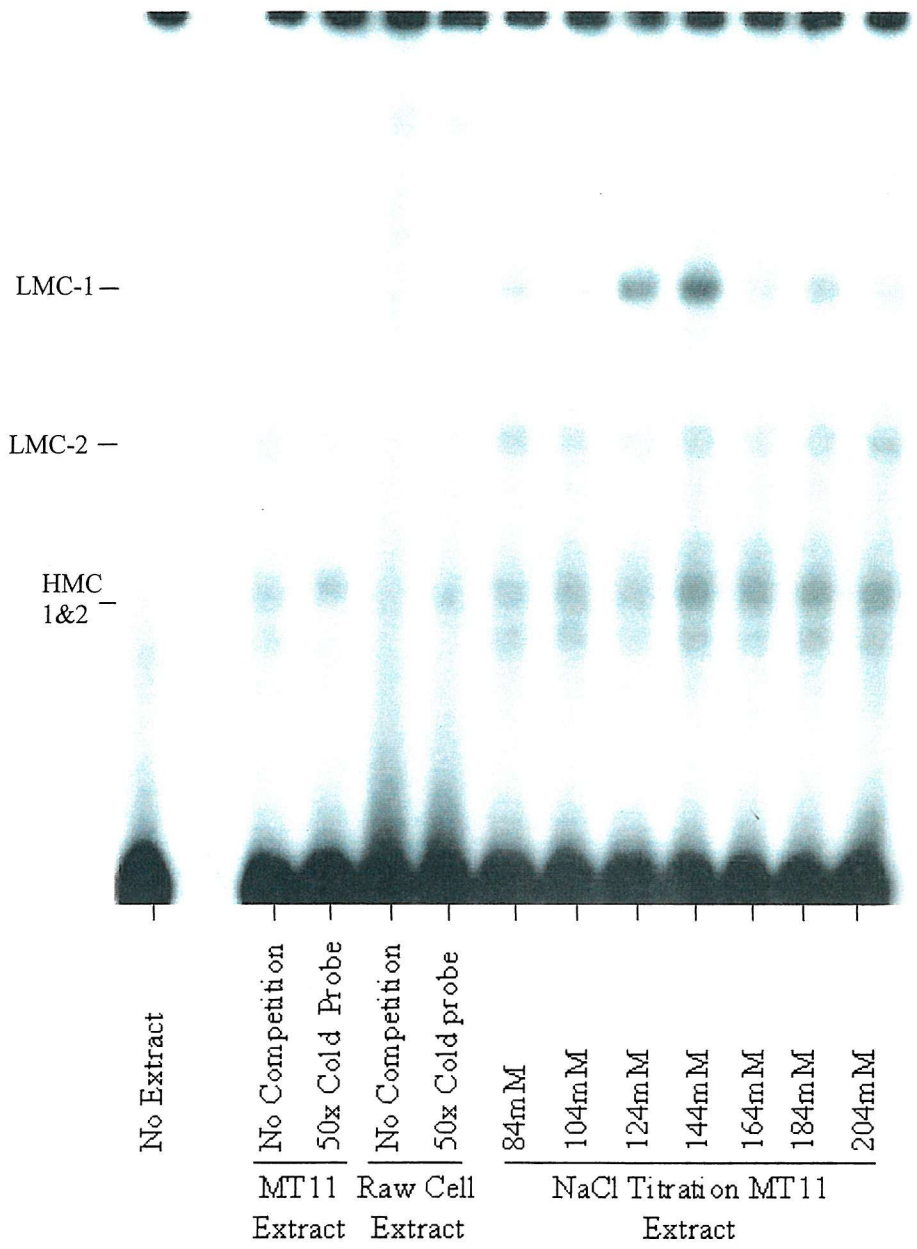

Figure 6.6.3 Comparison of protein interactions with the TIMP-1 LBP-1 double stranded full-length probe by EMSA for different cells types and the effect of salt titration on binding specificity. 10μg of Jurkat crude nuclear extract was added to each well with 0.2ng of wild type LBP-1 probe. Competition and NaCl titrations were performed by the addition of dilute unlabelled double stranded oligonucleotide (cold probe) or NaCl to the final reaction in the place of reaction water, in order that the concentration of the other ions remained constant. The concentration of 84mM is the established concentration of NaCl used in the group, representing the unmodified reaction concentration.

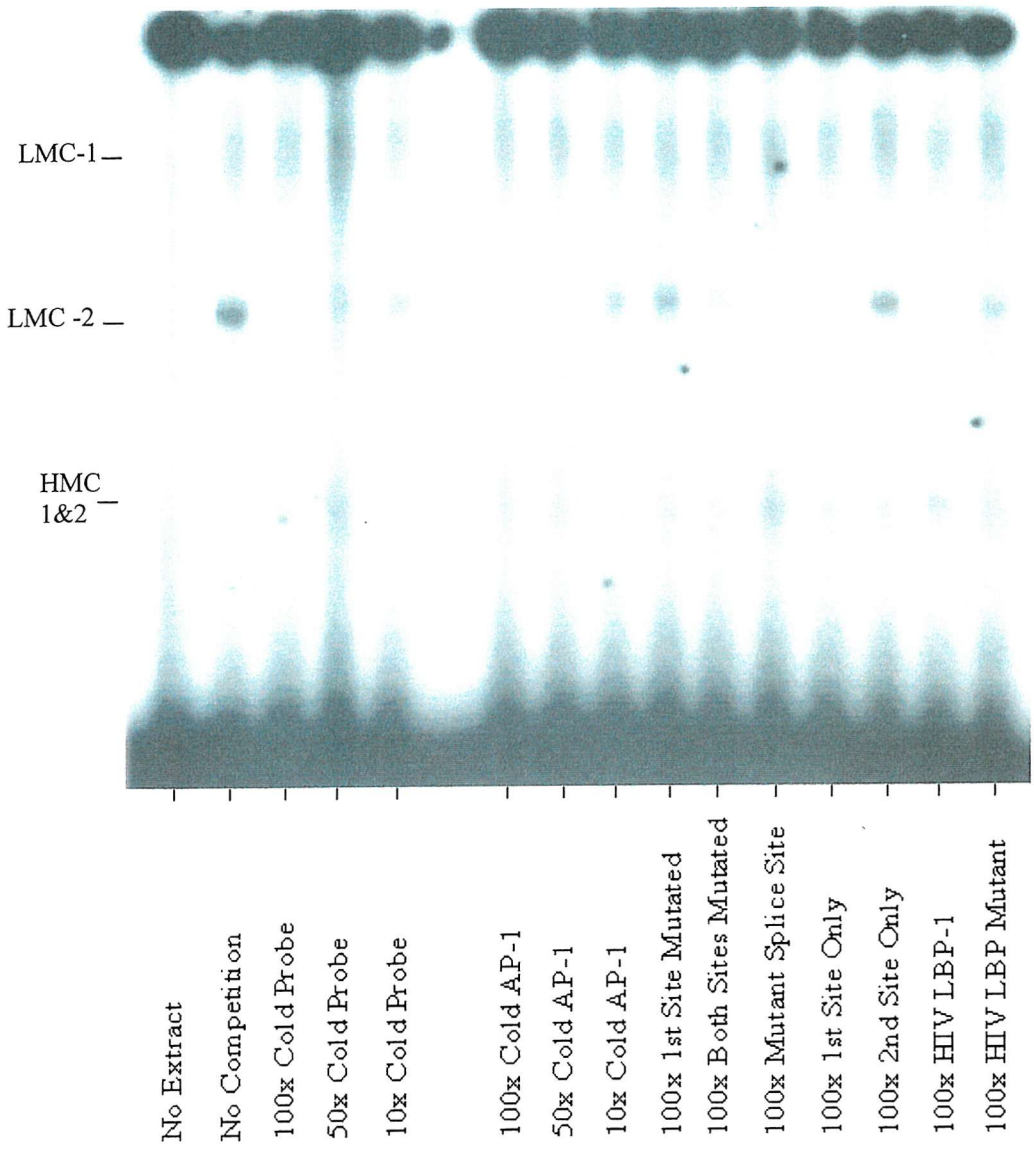

Figure 6.6.4 The characterisation of the protein DNA interaction for the TIMP-1 LBP-1 full-length probe. The protein DNA interaction was shown to be specific by competition with a titration of unlabelled full-length cold oligonucleotides. The complex specificity was also established by the addition of unlabelled alternative transcription factor, mutant and partial length double stranded oligonucleotides. Each of the competition oligonucleotides was titrated in place of the reaction water. All reactions were performed at a concentration of 144mM NaCl. 10μg of protein from crude nuclear MT11 Jurkat cell line extract was added in each reaction with 0.2ng of wild type TIMP-1 LBP-1 full-length probe.

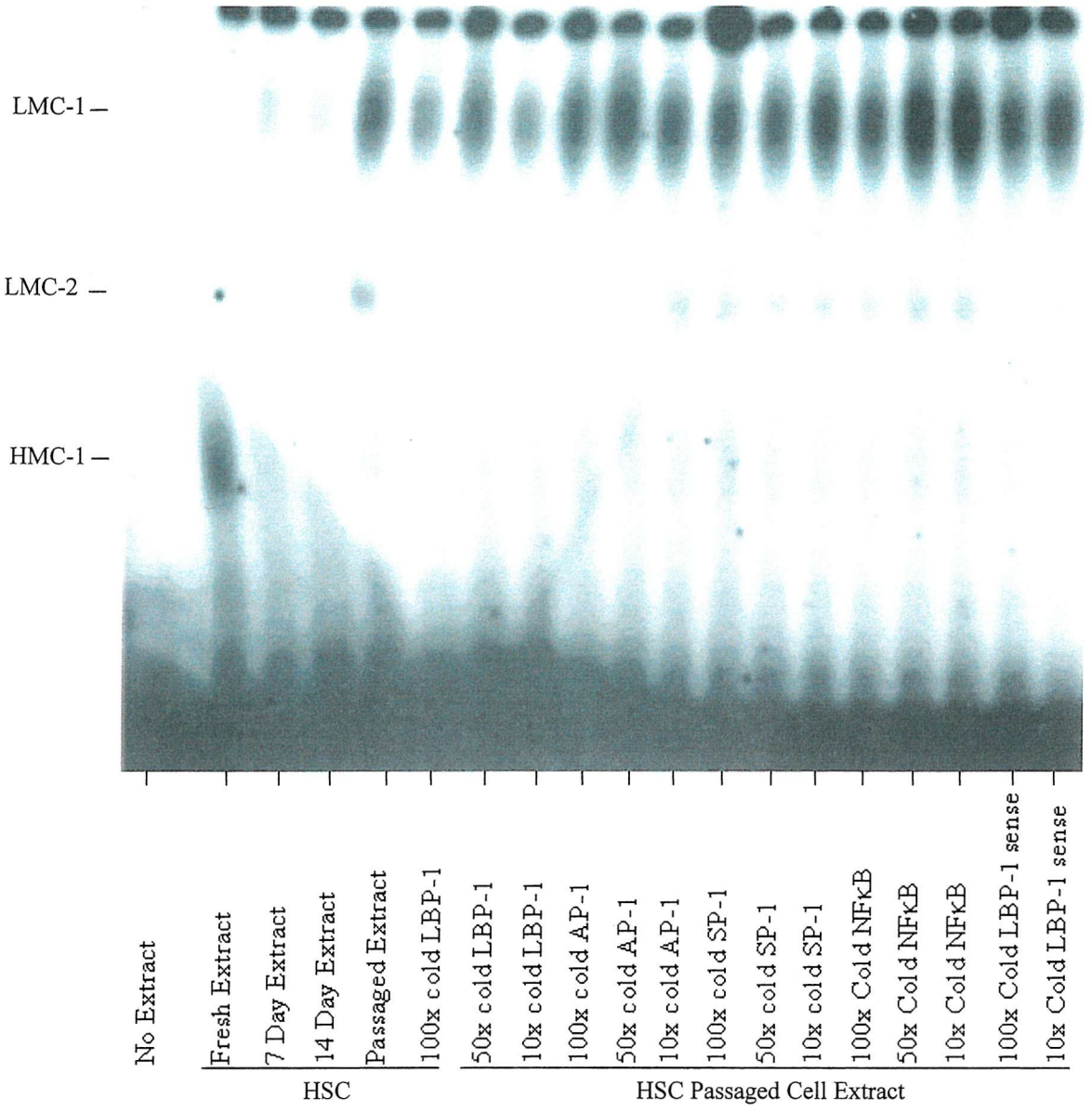

Figure 6.6.5. The characterisation of the DNA protein interactions for LBP-1 in the rat HSC cell. 10μg of crude extract from either rat HSC time course or passaged cells were added to each well with competition oligonucleotides prior to the addition of TIMP-1 LBP-1 double stranded probe, 0.2ng per reaction. The unlabelled cold titrated oligonucleotides were added in place of the reaction water. All reactions were performed at a concentration of 144mM NaCl.

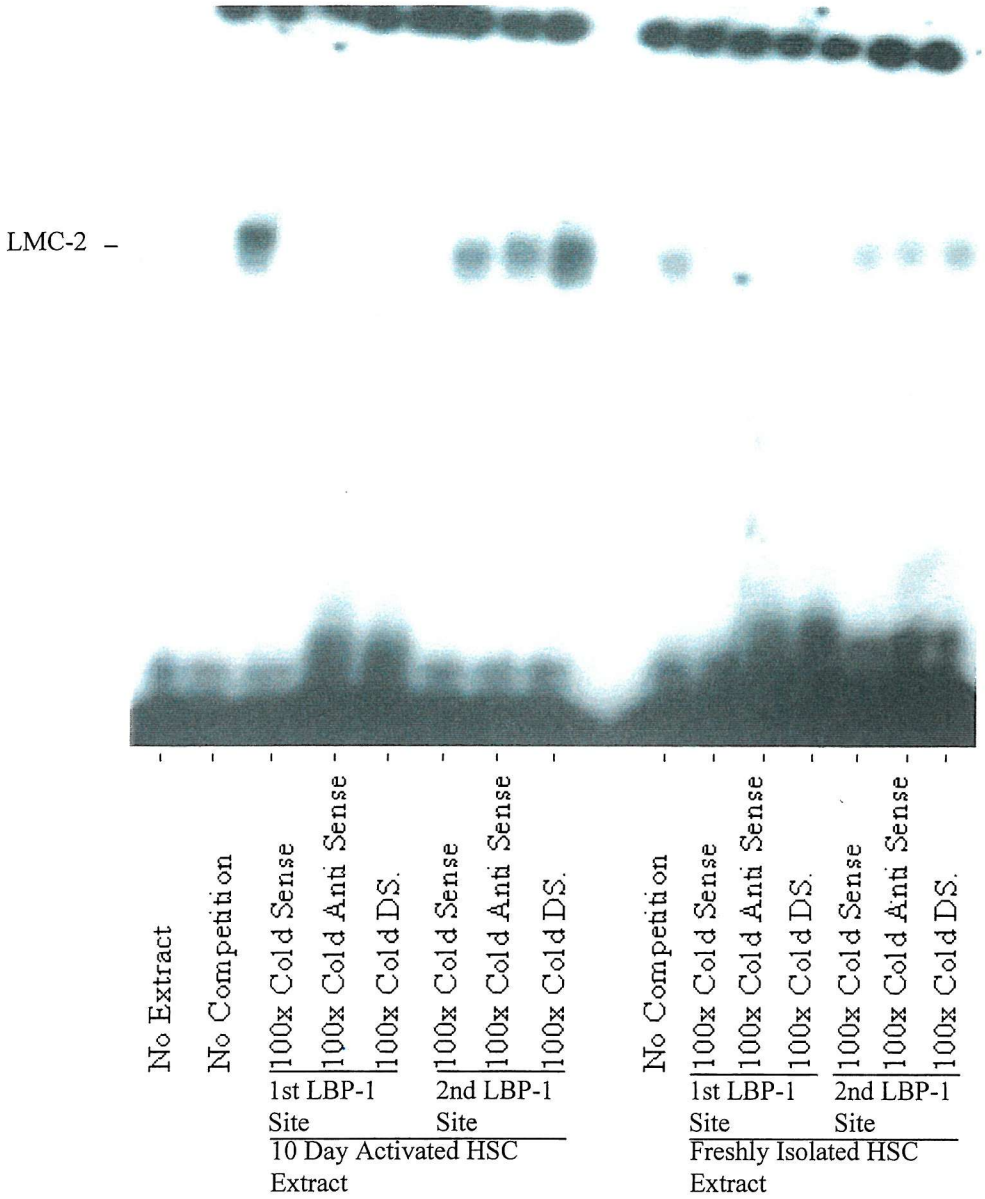

Figure 6.6.6. Characterisation of the single strand binding protein to LBP-1. The single strand protein DNA interaction specificity was demonstrated by competition with a titration of unlabelled first and second LBP-1 half sites against the full length TIMP-1 LBP-1 sense strand probe added at 0.2ng per reaction. Each oligonucleotide was used in a competition assay to establish binding in both strands individually and in the double stranded form. The unlabelled cold titrated oligonucleotides were added in place of the reaction water. All reactions were performed at a concentration of 144mM NaCl. 10μg of protein from crude nuclear extract was added in each reaction from either freshly isolated or activated HSC.

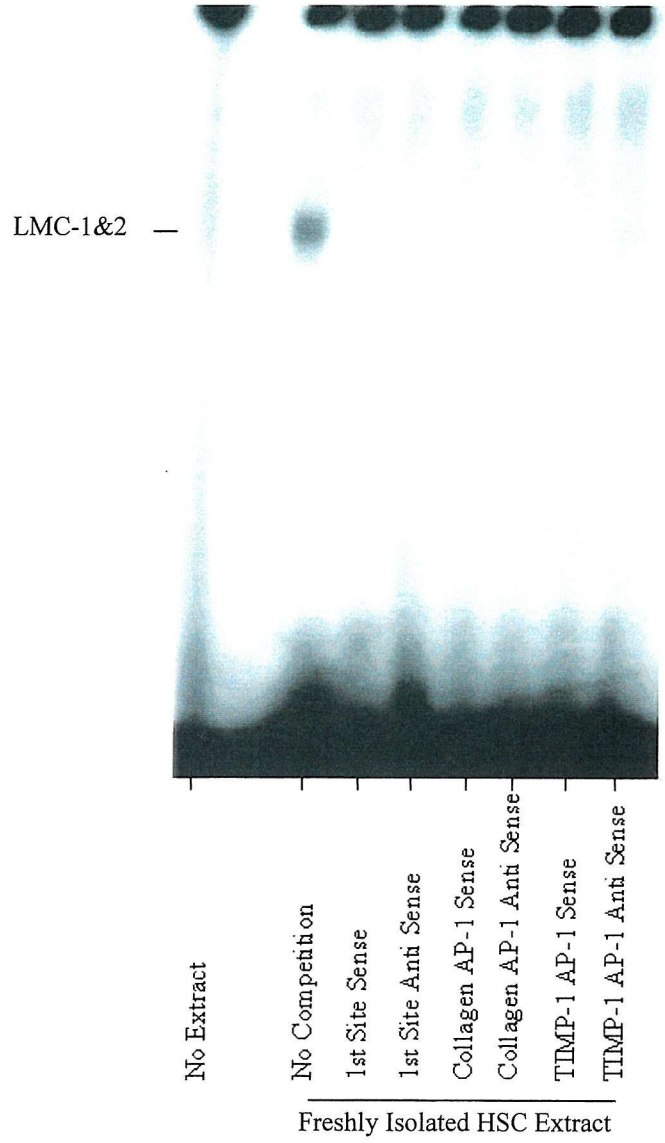

Figure 6.6.7. Characterisation of single stranded binding protein specificity with full length TIMP-1 LBP-1 sense strand probe added at 0.2ng per reaction. The unlabelled competition oligonucleotides were added in place of the reaction water at a concentration equal to 100x that of the probe. All reactions were performed at a concentration of 144mM NaCl. 10μg of protein from crude nuclear extract was added in each reaction from 10 day activated rat HSC.

6.7 Discussion

Work in the literature has suggested a role for the SP-1 transcription factor in the activated HSC (Rippe *et al.*, 1995; Miao *et al.*, 1999; Rippe *et al.*, 1999).

The results of the transfection studies for TIMP-1 5' and 3' SP-1 or GC-Box mutants indicated that the whole of the SP-1 site in the TIMP-1 minimal promoter is not functionally active in the HSC myofibroblast (Figure 6.3.1). The results indicate a significant reduction in activity upon the mutation of the 3' half of the SP-1 site, with no reduction of mutation into the 5' region. The reason for the lack of effect of a mutation in the 5' half of the SP-1 promoter is unknown. It may be that the 3' end is more important for protein interactions or that a different protein is binding. The transfections were repeated in NIH3T3 cells indicated a significant reduction for the 3' mutation (Figure 6.3.2.). The mutation of the 5' end resulted in a reduction that approached significance. It is probable that with more repetition the 5' mutation would also have been shown to significantly affect transcription and this will be investigated further at a later date.

A second transfection was performed, in which the NIH3T3 cells were co-transfected with 3', 5' SP-1 mutants or –111WT and either the PAC empty vector or SP-1 PAC, a SP-1 expression vector. This transfection has only been performed on a single occasion all be it in triplicate, but it did indicate that both the 3' and 5' mutations of the SP-1 site removed the TIMP-1 promoters responsiveness to the SP-1 protein. This lack of response by the mutated site to SP-1 over expression indicates that the putative TIMP-1 site is involved functionally in SP-1 regulation of TIMP-1. The data also suggest that the result seen in HSC cells may be due to the binding of another GC-Box binding protein, as both mutations prevented high level transcription.

To elucidate the protein interactions that may occur with the SP-1 site or GC-Box, a series of EMSA were performed using nuclear extracts from both rat HSC and NIH3T3 fibroblasts. A possible reason for the confusion in the department over the absence of SP-1 protein and DNA interactions is demonstrated in the first EMSA (Figure 6.4.1). As

it had previously been suggested, there is strong binding of complex directly following cell isolation but this is shown in both individuals to be almost absent in 7 Day activated cells, which are normally considered activated. However, with 10 days activation on plastic the levels of SP-1 expression returned to those seen in the freshly isolated extracts.

Competition EMSA were performed using nuclear extracts from both HSC and NIH3T3 cells. These indicated that all three complexes present were competed by the 50-fold excess of unlabelled TIMP-1 SP-1 probe (Figure 6.4.2). The addition of double stranded oligonucleotides corresponding to the 3' and 5' mutants, AP-2 consensus, TIMP-1 AP-2 and the consensus AP-1, did not compete with the SP-1 probe for protein binding. The 3' SP-1 mutant and AP-2 consensus did result in a slight decrease in complex intensity but this may be a result of loading differences.

Supershift assays were also performed on the extracts from the HSC and NIH3T3 cells to establish which proteins were interacting with the SP-1 site or GC-Box. The results of the supershift analysis using HSC extracts indicated that there was a protein specific blockade of complex formation (Figure 6.4.3). The antibodies shown to interact with the complexes formed were specific to SP-1, SP-3 and SP-4. The most dramatic effects were seen with the addition of the SP-4 specific antibody, which blocked the formation of all 3 complexes. The specific antibody for SP-3 completely blocked the formation of LMC-1 and SP-1 was shown to reduce LMC-1 & 2 (Figure 6.4.5).

In NIH3T3 supershift analysis identified the major factors to be SP-1 and SP-3 (Figure 6.4.4). The antibody specific to SP-3 completely blocked the formation of all three complexes and, as in the HSC, the SP-1 antibody significantly reduced LMC-1 and LMC-2. The reductions seen for the SP-2 antibody were only slight and most likely due to variation in loading (Figure 6.4.6).

The results of the Western blots for GC-Box binding proteins agree with those seen in the supershift analysis for both the HSC and NIH3T3 cells (Figure 6.4.7). While it is not possible to quantitatively compare one Western blot with another for the same or a

different protein, the results of the Western blots are dramatic enough that some observations can be drawn. The Western blots support the dominance of SP-1 and SP-3 over the other factors in the NIH3T3 cells. In the HSC, however, the blots again implicate SP-1 but suggest that there is less SP-3 present.

The result of the super shift analysis and Western blots together seem to suggest that the binding in the NIH3T3 cell is primarily SP-1 and SP-3 whereas in the HSC it is primarily SP-1 and SP-4, with some SP-3 involvement. The three transcription factors SP-1, SP-3 and SP-4 all bind GC-Boxes and have very similar binding affinities (Hagen *et al.*, 1994). The factors SP-1 and SP-4 are usually considered to be positive regulators of transcription and SP-3 a negative regulator (Hagen *et al.*, 1994; Majello *et al.*, 1994; Hagen *et al.*, 1995; Dennig *et al.*, 1996). There is some contradictory suggestions that SP-3 may also function as a positive regulator (Bakovic et al., 2000; Galvagni et al., 2001). There is also an indication that in some promoters, such as that for alcohol dehydrogenase, SP-4 can also act as an inhibitor. It is believed that the inhibition of SP-1 due to SP-3 and SP-4 occurs as a result of direct competition (Kwon *et al.*, 1999). The role of SP-3 and possibly SP-4 in the NIH3T3 and HSC respectively may therefore be as a brake on TIMP-1 transcription. This may explain the results in the NIH3T3 co-transfection with SP-1 over expression vector (Figure 6.3.3), which resulted in an increase of 400% in promoter activity in the wild type.

The role for SP-3 as an inhibitor of SP-1 is more widely excepted than that of SP-4. Although SP-4 is a positive regulator, unlike SP-1 it does not act synergistically with other SP-1 sites (Courey *et al.*, 1991; Sun *et al.*, 1994). The transactivation activity of SP-4 can however, be dramatically up regulated by the interaction of SP-1 that need not be bound to the DNA itself (Hagen *et al.*, 1994). The role of the SP-1 binding site synergy is an important consideration when looking at the result of the transfection study, as the minimal promoter has only been shown to contain one SP-1 binding site, although the full promoter region contains 8 (-2009/+977) (Clark *et al.*, 1997). The presence of only one site could prevent the synergistic up regulation of the promoter activity in both cell types. In the HSC, where SP-4 role is shown to be significant by supershift, the

interaction with SP-1 may be important for promoter activity (Clark *et al* 1997; Hagen *et al.*, 1994). This interaction may explain the results of the HSC supershift, in which the addition of SP-1 specific antibody reduced LCM-1 & 2 but the addition of SP-4 specific antibody removed all three complexes (Figure 6.4.3 and 6.4.5).

SP-4 has also been shown to bind other sites such as (GGCCGCGC), which may suggest that although both SP-1 and SP-4 bind to the SP-1 consensus sequence, ($^{T}/_{G}{}^{A}/_{G}$GGCG$^{T}/_{G}{}^{A}/_{G}{}^{A}/_{G}{}^{T}/_{C}$) they might not bind to the same area (Yamaguchi *et al.*, 1999). The difference in possible binding site may explain the lack of effect of the 5' SP-1 mutation on the activity of the TIMP-1 promoter in the HSC. As the NIH3T3 cells are dominated by SP-1 and the inhibitor SP-3, different binding positions would not be apparent (Figure 6.3.1-3).

Further investigations should be made into the functions of the SP-1 family of proteins, such as BTEB, which has been identified in the HSC and has been shown to have a role in the regulation of α1(I) collagen (Chen *et al.*, 2000). Future work should also look at larger promoter fragments, or work with the endogenous gene, to establish the effect of site synergy on the promoter. It would also be useful to repeat the transfection of the 3' and 5' SP-1 mutants into both the HSC and NIH3T3 cells to establish whether both mutations have an effect in the fibroblasts, but not in the HSC. An investigation should also be performed to establish the effects of the under and over expression of all of the SP-1 family members on the transcription of TIMP-1.

The LBP-1 sites situated at the 3' end of the minimal promoter have been previously identified as having a role in the TIMP-1 promoter function in fibroblasts (Clark *et al.*, 1997). The LBP-1 sites have also been implicated as being important in TIMP-1 regulation by truncation mutagenesis (Bahr *et al.*, 1997).

The results of the mutational study using vectors obtained via collaboration with Ian Clark (UEA Norwich) indicated that mutant Tm SMA 7 significantly reduced TIMP-1 promoter activity, indicating that these sites are in fact crucial. The lack of significance

of the other mutant constructs may well be due to the sampling method used, in which single transfections of each construct were made separately, on four separate occasions. The lack of significance has occurred as a result of inconsistency in the transfection of the wild type construct. This work ideally needs to be repeated with triplicate transfections of each construct, each time. When repeating the experiment it would also be a good idea to perform the co-transfection of Renilla as a better method of regulating transfection efficiency. The results would seem to suggest that with greater consistency, the mutants Tm SMA 2, 5, 7 and 8 might result in significant reductions in promoter activity. The mutation Tm SMA 2 & 7 represent mutations of both sites, while Tm SMA 5 is a mutation of the first site and Tm SMA 8 is the insertion of a linker between the sites. These results suggest that the first LBP-1 site and the spacing between the two sites may be important, although this cannot be proved at this time.

In conjunction with the promoter assay, a series of EMSA were performed using oligonucleotides obtained in collaboration with Ian Clark (UEA, Norwich) (Figure 6.6.1 and Appendix 1). The oligonucleotides were used to identify the binding of complexes to the LBP-1 region of the TIMP-1 promoter. The first EMSA was performed using crude nuclear extracts from 24hour-cultured HSC, a HSC time course and a series of cell lines including MT11 (a T-cell line) HeLa and RAW cells (a macrophage cell line) (Figure 6.6.2). Four DNA binding complexes were identified; two low mobility complexes (LMC-1 & 2), which were only very weakly visible in the cell line extracts, and another two complexes, HMC-1 & 2. The HMC-2 appeared in all the lanes and HMC-1 appeared in all lanes in which extract was present. The presence of HMC-2 in the extract free lanes indicates that its binding is not specific.

In order to establish which DNA binding complexes were LBP-1 specific the EMSA was repeated using extracts from RAW and MT11 cells, which had shown the presence of all four complexes (Figure 6.6.3). The nuclear extracts from the MT11 cells were also used to refine the reaction conditions for the purposes of identifying complex binding in HSC. A significant difference between the standard protocols used by our group and that of I.M. Clark was identified, in that the NaCl concentrations in the reaction buffers varied

between 84 and 184mM respectively. MT11 Jurkat cell nuclear extract was used in a NaCl titration, which indicated that optimum binding of the LMC-1 was achievable at 144mM NaCl. The salt concentration did not affect any of the other complexes. The results of the complex competition in the MT11 cells seemed to indicate the LMC-2 could be competed, but the complexes HMC-1 & 2 both appear to be non-specific.

In a second competition EMSA, binding of the complex in MT11 Jurkat cells suggested that LMC-2 was titratable by unlabelled full length LBP-1 and also by AP-1, suggesting that it was none specific (Figure 6.6.4.). However competition also identified that only the first site was involved in the binding of the complex, and competition could be achieved by oligonucleotides containing this site or by the site on its own. The second site, which contained an identical LBP-1 half-site (CCAGA), did not compete. The HIV consensus oligonucleotide, that also contained the LBP-1 half site, does compete, but the site mutant does not. The result of the EMSA also indicated that complexes LMC-1 and HMC-1 are not specific, as they are not competed by any of the oligonucleotides.

The contradictory data from the competition (Figure 6.6.4) led to further study with other transcription factor sites. This revealed that the formation of the LMC-2 complex could be competed by a titration of LBP-1 and AP-1 probes but not SP-1 or NFκB (Figure 6.6.5). The competition assay also identified that the binding of the LMC-2 could be competed by the sense unlabelled LBP-1 full-length oligonucleotide. The nuclear extract used for the competition assay was from passaged HSC, which had previously been shown to contain LMC-2. The complex LMC-2 was barely visible in the HSC time course, but the freshly isolated cells did contain large quantities of the non-specific HMC-1.

The identification of competition by a single-stranded LBP-1 sense oligonucleotide (Figure 6.6.5) suggested that this might be the target of the complex binding. An EMSA was performed using only the sense strand of the full length TIMP-1 probe (Figure 6.6.6). There was very strong binding to the probe in both 10 day and freshly isolated HSC extract. The role of the single stranded binding complex explained the problems

encountered when trying to obtain a strong signal, binding is limited only to the contaminated single strand probe. This explained the large variations between the different abilities of probes to form a complex, i.e. high percentage of annealing would lead to lower complex formation and therefore lower band intensity.

The use of a pure single strand probe identified binding of LMC-2 in HSC. This was seen in freshly isolated cells and much stronger in activated cells, of higher intensity than previously seen in cell lines. The ability of the cell line extract and passaged HSC extracts to form complex LMC-2 probably represents the high level of expression, as equal quantities of protein were loaded in each case. The LMC-2 binding was competed in both freshly isolated and 10 day activated HSC EMSA by sense and anti sense oligonucleotides, but only by the first half site. The competition that was previously shown (Figure 6.6.4 and 6.6.5) by the double stranded unlabelled probe is probably due to contaminating single stranded DNA. There was also no LMC-1 or HMC-1 present in the reactions, indicating that this had been non-specific binding to the double stranded oligonucleotide.

The competition of the single stranded binding complex LMC-2 was also demonstrated to be performed by both the sense and antisense strands of both the TIMP-1 AP-1-like binding site and also the AP-1 consensus. The AP-1 consensus double stranded oligonucleotide had previously been shown to compete the LMC-2 formation, in an EMSA using the double stranded full-length oligonucleotide, supporting the fact these complexes are the same.

The binding of LMC-1 was shown to be competed by either strand of the LBP-1 first half site, HIV LBP-1 half site, consensus AP-1 (Collagen I) and TIMP-1 AP-1. The binding of LMC-2 is not, however, competed by consensus oligonucleotides for SP-1, NFκB consensus sites or more importantly, by the sense and anti sense TIMP-1 second site oligonucleotides. There appears to be a contradiction suggesting that there is specific inhibition of complex formation when EMSA binding can be competed by either sense or anti sense of a number of different oligonucleotides. The lack of competition by the

second site appears strange, however, as the LBP-1 sites are identical only the flanking regions are altered. The sequences are also different from those seen in the AP-1 binding sites. The results of the CAT reporter assay reactions also seem to suggest that the first site may be functional.

The proteins bound to single stranded DNA in a sequence specific non-strand specific fashion, as has previously been identified in the literature for both AP-1 consensus and TIMP-1 AP-1 sites (Phillips *et al.*, 1999). The protein identified as binding to the AP-1 site may in fact be the same as the one identified in this study. There must be some homology between the sequences of the first LBP-1, consensus AP-1, TIMP-1 AP-1 and HIV sites, which is not present in the very similar sequence of the HIV mutant or second half site on either strand. It is possible that the same protein or proteins interact to bind either or both strands. This is supported, in theory at least, by the position that the TIMP-1 LBP-1 sites and many of the other functional LBP-1 and YY1 (see Section 1.22) sites appear in the promoter. These sites tend to appear either up or down stream, close to the transcription start site (see Figure 6.7.1). This could indicate that the proteins that bind to these regions may be involved in maintaining DNA separation in order to aid transcription.

Sequence	Position	Reference
CTCTCTGG	+5/+12 and+37/+44 HIV leader	Wu *et al.*, 1988
$^{A}/_{T}$CTGG	+3/+2, +8/+12, +40/+44 HIV LTR	Yoon *et al.*, 1994
CCATCAA AAGATGG	-40/-34 and –35/-29 Collagen I α1 BalBc/3T3 Fibroblasts.	Riquet *et al.*, In Press

Figure 6.7.1 The position of various LBP-1 binding sites, in other genes.

At present, it is not known which consensus site the single strand binding complexes are binding to. It is also unknown if the single stranded binding proteins are functional.

Recent work by other investigators has identified the strong interaction of YY1 with the murine α(2)I collagen promoter in hepatic stellate cells (Miao *et al.*,1999). YY1 is a possible candidate for interaction with the LBP-1 sites in TIMP-1 as it has a very poorly described, highly variable consensus binding site (see Figure 1.22.1).

The only real similarity between the TIMP-1 AP-1, consensus AP-1, HIV half site and the TIMP-1 LBP-1 half sites is the repetition of GA, which is not present in SP-1, NFκB and is shorter in the HIV mutant and second half site oligonucleotide (see Figure 6.7.2). A more defined well defined binding site could be described as Pu, Pu, $^{A}/_{T}GAG^{A}/_{T}$ (see Figure 6.7.2).

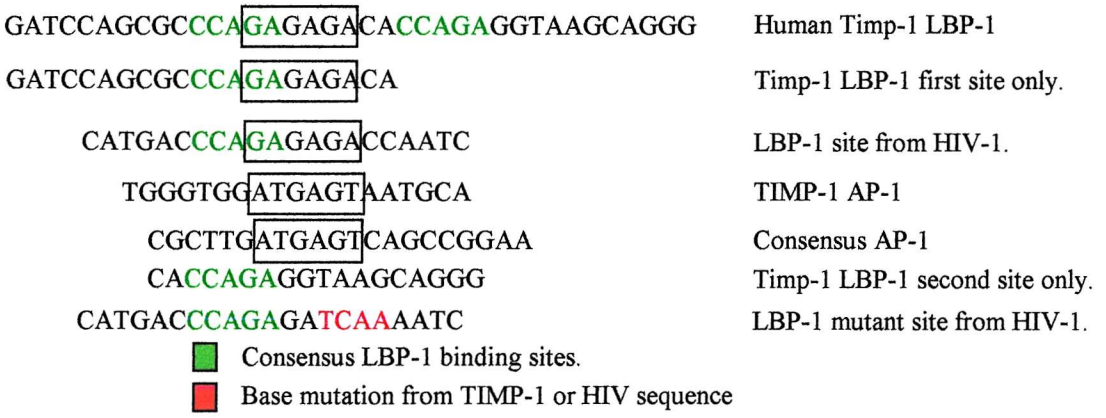

Figure 6.7.2 A comparison of the various oligonucleotides tested in competition assay of the single stranded binding protein to the first TIMP-1 LBP-1 site. The sequence localised by the black box indicates the area of possible protein interaction.

To continue this work it is necessary to repeat the transfection of the mutant constructs in order to reduce the errors and improve the data significance. To do this it would be necessary to perform the transfection on each occasion in triplicate for each construct and the co-transfection of Renilla expression construct would improve the transfection efficiency. It is also important to establish what the specific role of the single strand binding protein is and establish whether it has a functional role. Further work could also establish the consensus sequence to which the single stranded binding protein is interacting.

Chapter 7.
General Discussion

This research has focused on the role of various transcription factors and their binding sites in regulating the transcription of the TIMP-1 promoter.

Through the investigation of TIMP-1 transcription in the HSC it has been possible to identify that the AP-1 transcription factor-binding site of the TIMP-1 minimal promoter is crucial to high-level transcriptional activity. Previous studies have suggested that TIMP-1 in other cell types is regulated by the interaction of c-Jun and c-Fos. However it has been shown in this study that Jun D homodimers are the main positive regulators and the other endogenous factors, Fos B and Fra 2, were shown to be negative regulators of TIMP-1 transcription in the HSC.

This study has also shown that while there is an increase in IL-6 expression with HSC activation, the IL-6 gene is differentially regulated from that of the TIMP-1 gene. The AP-1 site in the IL-6 minimal promoter, which had been shown in other cell types to be a positive regulator, negatively regulated transcription in the HSC. The over expression of Jun D was shown to result in an increase in promoter activity but this was not mediated in the form of homodimers. These results together indicate that the activity of the IL-6 promoter is dependent on the formation and binding of a Jun D containing dimer with an as yet unknown partner or binding site such as an alternative AP-1, or a CRE site.

To identify whether the effects seen in the HSC were cell specific the TIMP-1 promoter investigations were repeated in NIH3T3 cells fibroblasts. The over expression of c-Jun and Jun B was shown to result in significant increases in TIMP-1 promoter activity, while the over expression of Jun D resulted in no change in promoter activity. The change seen in the activity of the transfected expression vectors following serum shock is believed to be due to an increase in protein kinase activity in the cell. The results of the over expression of FOS proteins in NIH3T3 cells differed from those seen in the HSC, indicating positive regulatory roles for c-Fos and Fra-1. The result for the JUN and FOS proteins in the NIH3T3 cells supported the classical regulation suggested for TIMP-1. The lack of activity of c-Fos in the HSC may well be due to the low level of c-Ets expression.

The *in vivo* work supported observations previously made in culture activated HSC indicating that there was an increase in Jun D expression with HSC activation. The results also suggested that there was a change in Jun D isoform with HSC activation and this may be a further level of TIMP-1 transcriptional regulation in HSC.

Using Jun $D^{-/-}$ gene knockout mice it was possible to demonstrate a significant reduction in liver fibrosis in the knockout mice when compared with the wild type following an 8-week CCl_4 liver injury study. The results of Taqman quantitative RT PCR indicated that there was less TIMP-1 and procollagen I mRNA in the knockouts than the wild type controls following liver injury.

The mutation of the putative SP-1 binding site indicated that there was a difference in the activity of the site in the HSC and NIH3T3 fibroblasts. The results indicated that the 3' end of the SP-1 site was required for high-level transcription of the TIMP-1 promoter in both HSC and the NIH3T3 cell, a mutation of the 5' end had no effect on promoter activity in the activated HSC. Investigation of the GC box binding proteins suggested that in the HSC and the NIH3T3 there were differences in the relative quantities of SP-1, SP-3 and SP-4 present.

The studies of the LBP-1 sites indicated that they were necessary for TIMP-1 transcription. The studies of the LBP-1 binding site by EMSA established that a complex binds to either strand of the first or 5' LBP-1 but does not bind to the second LBP-1 site. The complex also binds to either strand of the AP-1 consensus, TIMP-1 AP-1 and the HIV LBP-1 consensus. It is at present unknown whether this binding protein is functional and it is possible that this protein is the same as a previously identified protein in the literature, shown to bind to either strand of the TIMP-1 AP-1 site, in a fibroblast line.

A large amount of research in this study has been performed using reporter assays. These assays provide an artificial picture of the endogenous gene transcription or expression. It would have been better to analyse the results from this work by Western blot or Taqman

quantitative RT PCR. The need for the movement away from reporter assay methods is important for the investigation of transcription factor synergy in an entire promoter and with enhancers from elsewhere in the genome. It would have also been useful in this study to work in the endogenous gene, as nucleosomes play a fundamental role in the process of HSC activation. An endogenous method would also have been useful in the investigation of SP-1 as it is known to act synergistically with other SP-1 sites.

The reason for the use of reporter assays over other methods was that it was the best option available at the time. With transfection it is only possible to achieve at best about 10% transfection in the activated HSC. This level is not high enough to investigate the modulation of endogenous gene expression by conventional transfection, as any change would not be seen. It would have been better to use a viral system of infection, which could provide significantly larger transfection efficiency and allow the measurement of endogenous changes in transcription and expression. Unfortunately at the start of this work there was no viral expertise in the department and there was not such a broad range of viruses as expression vectors available.

Future work should use a viral transfection system and an endogenous assay, such as Taqman quantitative PCR, to study the effects of transcription factors on the endogenous genes. A recent development is the BacMam virus, which has been shown to have a high transfection efficiency of activated HSC. The BacMam virus is very easily manipulated by basic sub cloning and can also contain a DNA fragment of practically any size. The combination of the BacMam vector and the Invitrogen Gateway system using their conversion cassette would make this system even better. The Gateway system allows directional cloning of any DNA fragment via the highly efficient clonase recombination system. The Gateway BacMam vector could be used to quickly create a variety of transcription factor expression vectors from the plasmids presently available. By generating two versions of the Gateway BacMam vector with forward and reverse recombination sites it is possible to efficiently shuttle the insert from an expression vector into the other vector to form an antisense expression construct. There is also the added benefit of the BacMam system that there is a tetracycline regulated expression system

currently being tested in the department, allowing the transcription factor of interest to be modulated.

The future of the work in this thesis is in the use of viral gene transfer systems and endogenous gene assay. It would probably be useful to maintain some work with plasmids and reporter assays as they offer a quick method of screening without the need for the construction of a viral vector. The results could then be verified and the investigations furthered following the transfer of the cDNA to a viral vector from the plasmid.

In continuing this work it would be useful to look in greater depth at the roles of the various JUN and FOS family members as well as the members of the ATF family, which are not investigated in this thesis but were highlighted. These factors could be modulated by the use of viral vectors as previously mentioned to express AP-1 and ATF proteins or their antisense. There is also the possibility of using microinjection of expression or antisense plasmids, inhibitory transcription factor specific antibodies or antisense oligonucleotides. The investigation into the modulation of the JUN, FOS and ATF factors should not just concentrate on TIMP-1 and IL-6 but also look at other fibrotic markers MMPs, cytokines and matrix proteins. Using these systems of transcription factor modulation it would also be possible to investigate the various effects of these vectors on proliferation, apoptosis and the expression of other genes. The investigation of these various parameters could be performed by the use of time lapse photography, proteomics and gene chip technology. The use of microinjection may also be of particular use in the investigation of the role of the dynamic changes in AP-1 protein expression in the activation of the HSC.

Another area of research developing from the work already performed in the HSC and NIH3T3 is looking into the role of phosphorylation on the activation of the JUN and FOS proteins. The results so far suggest that AP-1 induced activity in NIH3T3 cells is dependent on JNK activity while HSC are independent of JNK. The results also indicated that the NIH3T3 cells were dependent on serum shock to activate the AP-1

binding proteins, but this was not necessary in the HSC. For these reasons it is necessary to establish the role of phosphorylation in TIMP-1 transcription in both cell types. Serum shock is known to be very nonspecific in its induction of kinase activity so initial work will concentrate on the use of other more specific inducers of protein kinase activity such as UV, TNFα, phorbol ester and Okadaic acid. The further classification of kinase activity could be achieved with specific inhibitors such as PD98059 and Curcumin. The various agonists and antagonists of the protein kinases could be used in conjunction with protein or antisense expression, for JNK, ERK, FRK and JAB1. The relative level of endogenous c-Jun and Jun D phosphorylation could be established through the use of a Phospho-Specific c-Jun antibody such as those available from Novagen. This Phospho-Specific antibody could be used to help establish if and how JUN proteins are phosphorated in the HSC. The investigations of JUN and FOS phosphorylation would not only concentrate on the endogenous phosphorylation that takes place but would also look at its effects on DNA protein interactions, AP-1 protein dynamics, IL-6 and TIMP-1 transcription, proliferation, apoptosis and activation itself.

The future of the investigation into SP-1 initially requires the repeat of some of the experiments already shown. It is necessary to improve the NIH3T3 EMSA and also to establish if the differences seen between the fibroblasts and HSC for the SP-1 site mutational analysis are significant. The further investigation or characterisation of the TIMP-1 minimal promoter putative SP-1 site could be performed by DNase I footprinting with cellular extracts from quiescent and activated HSC. Alternatively the endogenous DNA protein interactions could be studied using *in vivo* footprinting by pretreatment of the HSC with Dimethyl Sulphate and digestion of the genomic DNA with Piperidine. These footprinting methods could also be used to investigate the synergy of the SP-1 site in the TIMP-1 minimal promoter with the others present further upstream. It would also be useful to repeat the SP-1 expression vector and TIMP-1 reporter co-transfection both in HSC and also with the other SP-1 family members including ZF-9 and BTEB. Ideally, for all of these experiments, as mentioned earlier, it would be best if the reporter assays were replaced with endogenous analysis of gene transcription using viral transformation

and Taqman RT PCR. Taqman RT PCR could also prove useful in establishing the relative changes in the expression of the various SP-1 family binding proteins with time. The effects of the over expression and inhibition of the various SP-1 family proteins should also be established using expression and antisense viral vectors combined with proteomics and gene chip analysis. The use of proteomics and gene chip analysis in this way could identify the broader role of the SP-1 proteins in HSC activation and the expression of presently un-investigated genes. As with the study into the effects of phosphorylation, the effects on proliferation, activation and resistance to apoptosis should also be established for each of the SP-1 family proteins.

In continuing the work into the LBP-1 site it is necessary to repeat the transfection of the mutated reporter constructs using triplicate transfections and Renilla luciferase contransfection for transfection efficiency control. The EMSA analysis should be continued to further characterise the binding of the complex, concentrating on the consensus suggested by the previous work. The EMSA analysis could be used to establish a series of critical point mutations and corresponding mutations made to the TIMP-1 reporter construct. These TIMP-1 mutant reporters should be used to address the fundamental question of whether the single strand protein is functional. Assuming the protein is functional then it would have to be identified by a system such as Matchmaker-One-Hybrid system (Clontech).

The *in vivo* study is at present only just beginning and as such requires much more work. The present study lacks uninjured controls and as a result there is no base line in any of the experiments so it is not possible to establish if the results seen are reductions in the level of pathology or are normal. This study will be repeated in the future with more mice in each group and will also include uninjured mice as controls. The future study will also be performed for an increased duration to increase the amount of fibrosis and establish a more chronic phenotype.

In the future it would also be very useful to purify HSC from wild type and Jun $D^{-/-}$ gene knockout mice and compare the relative differences in proliferation, gene expression and

apoptosis in response NGF or cycloheximide. The investigation could be performed both with cells activated on plastic and cells purified from CCl_4 injured mice. The investigations into the effects on gene expression should not only look at TIMP-1, procollagen I, αSMA and other fibrotic markers as previously mentioned, but could also be expanded to look at broader cellular effects through the use of gene chip or proteomic technology. Following the identification of any phenotype in isolated cells, it should be attempted to reverse the phenotype by the reintroduction of Jun D expression via viral vector for the purposes of experimental control.

Using a viral mediated sytem it may be possible to specifically target the HSC with the viral vector mediated expression of antisense Jun D. Our collaborators are at present working to change the viral capsular proteins to target BacMam viruses to specific cell surface receptors. It is hoped that it may be possible to use an N-CAM, PDGF or TGFβ receptor targeted BacMam virus as a delivery system for the activated HSC. The targeted virus could contain a Jun D antisense expression vector under tetracycline dependent regulation. It is hoped that this viral delivery system could be used to reverse or prevent fibrosis. This plan obviously requires much more work and initially requires the success of the larger animal model. The recent establishment of a liver slice culture model in the department could be used in the early testing of the viral vectors.

It is hoped that Jun D targeting may be a method of gene or drug therapy to protect or reverse liver fibrosis. It is believed that targeting Jun D in the HSC will prove effective, as it does not only reduce TIMP-1 but also other fibrotic mediators as well. It is also hoped that the results of the manipulation of other transcription factors will be as successful as those of Jun D, providing a number of possible drug and therapy targets.

References

1. Adler V, Schaffer A, Kim J, Dolan L, Roni Z. UV radiation and heat shock mediate JNK activation via different pathways. J Biol Chem 1995 Nov 3;270(44):26071-26077.

2. Ahonen M, Baker AH, Kahari VM. Adenovirus-mediated gene delivery of tissue inhibitor of metalloproteinase-3 inhibits invasion and induces apoptosis in melanoma cells. Cancer Res. 1998 Jun1;58(11):2310-2315.

3. Airola K, Karonen T, Vaalamo M, Lehti K, Lohi J, Kariniemi AL, Keski-Oja J, Saarialho-Kere UK. Expression of collagenase-1 and –3 correlates with the level of invasion in malignant melanomas. Br J. Cancer 1999 May; 80 (5-6):733-743

4. Alcolado R, Arthur MJP, Iredale JP. Pathogenesis of liver fibrosis. Clin Sci. 1997 Feb;92(2):103-112.

5. Alexander Cm, Howard EW, Bissell MJ, Werb Z. Rescue of mammary epithelial cell apoptosis and entactin degradation by a tissue inhibitor of metalloproteinase-1 transgene. J Cell Biol. 1996 Dec;135(6 Pt 1):1669-1677.

6. Allegretto EA, Smeal T, Angel P, Spiegelman BM, Karin M. DNA-binding activity of Jun is increased through its interaction with Fos. J Cell Biochem 1990 Apr;42(4);193-206.

7. Anania FA, Womack L, Jiang M, Saxena NK. Aldehydes potentiate alpha(2)(I) collagen gene activity by JNK in activated stellate cells. Free Radic Biol Med. 2001 Apr 15;30(8):846-857.

8. Andus T, Gross V, Tran-Thi TA, Schreiber G, Nagashima M, Heinrich PC. The biosynthesis of acute phase proteins in primary cultures of rat hepatocytes. Eur J Biochem. 1983 Jul 1;133(3):561-571

9. Andus T, Ramadori G, Heinrich PC, Knittel T, Meyer zum Buschenfelde KH. Cultured Ito cells of rat liver express the α_2-macroglobulin gene. Eur J Biochem. 1987 Nov 2;168(3):641-646.

10. Angel P, Baumann I, Stein B, Delius H, Rahmsdorf HJ, Herrlich P. 12-O-tetradecanoyl-phorbol-13-acetate induction of the human collagenase gene is mediated by an inducible enhancer element located in the 5'-flanking region. Mol Cell Biol. 1987 Jun;7(6):2256-2266.

11. Angel P, Hattori K, Smeal T, Karin M. The Jun Proto-oncogene is positively autoregulated by its product, Jun/AP-1. Cell 1988 Dec2;55(5):875-885.

12. Arenson DM, Friedman SL, Bissell DM. Formation of extracellular matrix in normal rat liver: lipocytes a major source of proteoglycan. Gastroenterology 1988 Aug;95(2):441-447.

13. Armendariz-Borunda J, Simkevich CP, Roy N, Raghow R, Kang AH, Seyer JM. Activation of Ito cells involves regulation of AP-1 binding proteins and induction of type I collagen gene expression. Biochem J. 1994 Dec 15;304(Pt3):817-824.

14. Arthur MJP, Friedman SL, Roll FJ, Bissel Dm. Lipocytes from normal rat liver release a neutral metalloproteinase that degrades basement membrane (type IV) collagen. J Clin Invest. 1989 Oct;84(4):1076-1085.

15. Arthur MJP. Matrix degradation in the liver. Semin Liver Dis. 1990 Feb;10(1):47-55.

16. Arthur MJP, Jackson CJ, Friedman SL. Release of type IV collagenase/gelatinase by human lipocytes. Cells of the Hepatic Sinusoid 1991;3:161-163.

17. Arthur MJP. The role of matrix degradation in liver fibrosis. Molecular and Cell Biology of Liver Fibrosis Editors. Gressner and Ramadori. Kluwer Acedemic Publishers. 1992a.

18. Arthur MJP. The metalloproteinases. Cellular and molecular aspects of cirrhosis 1992b;216:235-244.

19. Arthur MJP, Stanley A, Iredale JP, Rafferty JA, Hambry RM, Friedman SL. Secretion of 72 kDa type IV collagenase/gelatinase by cultured human lipocytes. Biochem J. 1992c Nov 1;287(Pt3):701-707.

20. Arthur MJP. Degradation of matrix proteins in liver fibrosis. Path. Res. Pract. 1994 Oct;190(9-10):825-833.

21. Atkinson SJ, Crabbe T, Cowell S, Ward RV, Butler MJ, Sato H, Seiki M, Reynolds JJ, Murphy G. Intermolecular autolytic cleavage can contribute to the activation of progelatinase A by cell membranes. J Biol Chem. 1995 Dec 22;270(51):30479-30485.

22. Bachem MG, Meyer D, Melchior R, Sell K-M, Gressner AM. Activation of rat liver perisinusoid lipocytes by transforming growth factors derived from myofibroblastic cell types. J Clin Invest. 1992 Jan;89(1):19-27.

23. Bahr MJ, Clark IM, Iredale JP, Arthur MJP, Mann DA. Mapping of cis-acting regions of the human TIMP-1 promoter in freshly isolated and culture activated hepatic stellate cells. Cells of the Hepatic Sinusoid 1997;6:18-21.

24. Bahr MJ, Vincent KJ, Arthur MJP, Fowler AV, Smart DE, Wright MC, Clark IM, Benyon RC, Iredale JP, Mann DA. Control of the tissue inhibitor of metalloproteinases-1 promoter in culture-activated rat hepatic stellate cells: Regulation by activator protein-1 DNA binding proteins. Hepatology 1999 Mar;29(3):839-848.

25. Baker AH, Zaltzman AB, George SJ, Newby AC. Divergent effects of tissue inhibitor of metalloproteinase 1,-2,-3 over expression on rat vascular smooth muscle cell invasion, proliferation, and death in vitro. TIMP-3 promotes apoptosis. J Clin Invest. 1998 Mar 15,101(6):1478-1487.

26. Baker AH, George SJ, Zaltzman AB, Murphy G, Newby AC. Inhibition of invasion and induction of apoptotic cell death of cancer cell lines by overexpression of TIMP-3. Br J Cancer. 1999 Mar;79(9-10):1347-1355.

27. Bakiri L, Lallemand D, Bossy-Wetzel E, Yaniv M. Cell cycle-dependant variations in c-Jun and Jun B phosphorylation: a role in the control of cyclin D1 expression. EMBO J. 2000 May2;19(9):2056-2068.

28. Bakovic M, Waite KA, Vance DE. Functional significance of Sp1, Sp2, and Sp3 transcription factors in regulation of the murine CTP:phosphocholine cytidylyltransferase alpha promoter. J Lipid Res. 2000 Apr;41(4):583-594.

29. Baraona E, Abittan CS, Dohmen K, Moretti M, Pozzato G, Chayes ZW, Schaefer C, Lieber CS. Gender differences in pharmacokinetics of alcohol. Alcohol Clin Exp Res. 2001 Apr;25(4):502-507.

30. Barasch J, Yang J, Qiao J, Tempst P, Bromage H, Leung W, Oliver JA. Tissue inhibitor of metalloproteinase-2 stimulates mesenchymal growth and regulates epithelial branching during morphogenesis of the rat metanephros. J Clin Invest. 1999 May;103(9):1299-1307.

31. Batchelor WB, Robinson R, Strauss BH. The extracellular matrix in balloon arterial injury:a novel target for prevention. Prog Cardiovasc Dis. 1998 Jul-Aug;41(1):35-49.

32. Bautista AP. Impact of alcohol on the ability of Kupffer cells to produce chemokines and its role in alcoholic liver disease. J. Gastroenterol Hepatol. 2000Apr;15(4):349-356.

33. Benyon RC, Iredale JP, Goddard S,Winwood PJ, Aurthur MJP. Tissue inhibitor of metaloproteinase 1 and 2 is increased in fibrotic human liver. Gastroenterology 1996 Mar;110(3):821-831.

34. Bian J, Wang Y, Smith MR, Kim H, Jacobs C, Jackman J, Kung HF, Colburn NH, Sun Y. Suppression of in vivo tumour growth and induction of suspension cell death by tissue inhibitor of metalloproteinases (TIMP)-3. Carcinogenesis 1996 Sep;17(9):1805-1811.
35. Bissell DM, Arenson DM, Maher JJ, Roll FJ. Support of cultured-hepatocytes by laminin-rich-gel Evidence for a functionally significant subendothelial matrix in normal rat liver. J Clin Invest. 1987 Mar;79(3):801-812.

36. Blackwell TK, Weintraub H. Differences and similarities in DNA-binding preferences of MyoD and E2A protein complexes revealed by binding site selection. Science 1990 Nov 23;250(4984):1104-1110.

37. Blomhoff R, Wake K. Perisinusoidal stellate cells of the liver: important roles in retinol metabolism and fibrosis. FASEB J. 1991 Mar 1;5(3):271-277.

38. Bohmann D, Bos TJ, Admon A, Nishmura T, Vogt PK, Tjian R. Human protooncogene c-Jun encodes a DNA-binding protein with structural and functional-properties of transcription factor AP-1. Science 1987 Dec 4;238(4832):1386-1392.

39. Bond M, Murphy G, Bennett MR, Amour A, Knauper V, Newby AC, Baker AH. Localization of the death domain of tissue inhibitor of metalloproteinase-3 to the N terminus. Metalloproteinase inhibition is associated with pro-apoptotic activity. J Biol Chem. 2000 Dec 29;275(52):1358-1363.

40. Bortolotti F. Billariere's clinical gastroenterology. 1996 Balliere Tindall

41. Bosch J, Garcia-Pagan JC. Complications of cirrhosis. I. Portal hypertension. J Hepatol 2000;32(1 Suppl):141-156.

42. Brito JM, Borojevic R. Liver granulomas in schistosomiasis: mast cell-dependant induction of SCF expression in hepatic stellate cells is mediated by TNF-alpha. J Leukoc Biol. 1997 Sep;62(3):389-96.

43. Buck M, Kim DJ, Houglum K, Hassanein T, Chojkier M. c-Myb modulates transcription of the alpha-smooth muscle actin gene in activated hepatic stellate cells. Am J Physiol Gastrointest Liver Physiol 2000 Feb;278(2):G321-328.

44. Bugno M, Graeve L, Gatsios P, Koj A, Heinrich PC, Travis J, Kordula T. Indentification of the interleukin-6/oncostatin M response element ion the tissue inhibitor of metalloproteinase-1 (TIMP-1) promoter. Nucleic Acids Res. 1995 Dec 25;23(24):5041-5047.

45. Buratowski S, Hahn S, Guarente L, Sharp PA. Five intermediate complexes in transcription initiation by RNA polymerase II. Cell 1989 Feb 24;56(4):549-561.

46. Burley SK, Roeder RG. Biochemistry and structural biology of transcription factor IID (TFIID). Annu Rev Biochem. 1996;65:769-799.

47. Busch SJ, Sassone-Corsi P. Dimers, leucine zippers and DNA-binding domains. Trends Genet 1990 Feb;6(2):36-40.

48. Bushel P, Kim JH, Chang W, Catino JJ, Ruley HE, Kumar CC. Two serum response elements mediate transcriptional repression of human smooth muscle alpha-actin promter in ras-transformed cells. Oncogene 1995 Apr 6;10(7):1361-1370.

49. Buttice G, Quinones S, Kurkinen M. The AP-1 site is required for basal expression but is not necessary for TPA-response of the human stromelysin gene. Nucleic Acids Res. 1991 Jul 11;19(13):3723-3731.

50. Campbell CE, Flenniken AM, Skup D, Williams BRG. Identification of a serum- and phorbol ester-response element in the murine tissue inhibitor of metalloproteinase gene. J Biol Chem. 1991 Apr 15;266(11):7199-7206.

51. Cawston T. Matrix metalloproteinases and TIMPs: properties and implications for the rheumatic diseases. Mol Med Today 1998 Mar;4(3):130-137.

52. Chambers RS, Wang BQ, Burton ZF, Dahmus ME. The activity of COOH-terminal domain phosphatase is regulated by a docking site on RNA polymerase II and by the general transcription factors IIF and IIB. J Biol Chem. 1995 Jun 23;270(25):14962-14969.

53. Chamovitz DA, Segal D. JAB1/CSN5 and the COP9 signalosome. A complex situation. EMBO Rep 2001 Feb;2(2):96-101

54. Chandrasoma P, Taylor CR, Concise pathology, Second edition. 1995Appleton and Lange.

55. Chatton B, Bocco JL, Goetz J, Gaire M, Lutz Y, Kedinger C. Jun and Fos heterodimerize with ATFa, a member of the ATF/CRAB family and modulate its transcriptional activity. Oncogene 1994 Feb;9(2):375-385.

56. Chen A, Davis BH. UV irradiation activates JNK and increases alpha(I) collagen gene expression in rat hepatic stellate cells. J Biol Chem. 1999 Jan 1;274(1):158-164.

57. Chen A, Davis BH. The DNA binding protein BTEB mediates acetaldehyde-induced, jun N-terminal kinase-dependant alpha(I) collagen gene expression in rat hepatic stellate cells. Mol Cell Biol. 2000 Apr;20(8)2818-2826.

58. Chen CA, Okayama H. Calcuim phosphate-mediated gene transfer: a highly efficient transfection system for stably transforming cells with plasmid DNA. Biotechniques 1988 Jul;6(7):632-628.

59. Chiu R, Boyle WJ, Meek J, Smeal T, Hunter T, Karin M. The c-Fos protein interacts with the c-Jun/AP-1 to stimulate transcription of AP-1 response genes. Cell 1988 Aug 12;54(4):541-552.

60. Chung KC, Park JH, Kim CH, Ahn YS. Tumour necrosis factor-alpha and phorbol 12-myristate 13-acetate differentially modulate cytotoxic effect of nitric oxide generated by serum deprivation in neuronal PC12 cells. J. Neurochem. 1999 Apr;72(4):1482-1488.

61. Chytil M, Peterson BR, Erlanson DA, Verdine GL. The orientation of the AP-1 heterodimer on DNA strongly affects transcriptional potency. : Proc Natl Acad Sci U S A. 1998 Nov 24;95(24):14076-14081.

62. Claret FX, Hibi M, Dhut S, Toda T, Karin M.A new group of conserved co-activators that increase the specificity of AP-1 transcription factors. Nature 1996 Oct 3;383(6599):453-457.

63. Clark IM, Rowan AD, Edwards DR, Bech-Hansen T, Mann DA, Bahr MJ, Cawston TE. Transcriptional activity of the human tissue inhibitor of metalloproteinases 1 (TIMP-1) gene in fibroblasts involves elements in the promoter, exon 1 and intron 1. Biochem J. 1997 Jun 1;324(Pt2):611-617.

64. Cobb MH, Goldsmith EJ. How MAP kinases are regulated. J Biol Chem. 1995 Jun 23;270(25)14843-14846.

65. Colotta F, Polentarutti N, Sironi M, Mantovani A. Expression and involvement of c-Fos and c-Jun protooncogene in programmed cell death induced by growth factor deprivation in lymphoid cell lines. J Biol Chem. 1992 Sep 15;267(26):18278-18283.

66. Conaway RC, Conaway JW. General initiation factors for RNA polymerase II. Annu Rev Biochem 1993;62:161-190.

67. Courey AJ, Holtzman DA, Jackson SP, Tjian R. Synergistic activation by the glutamine-rich domains of human transcription factor SP-1. Cell 1989 Dec 1;59(5):827-836.

68. Crocker SJ, Morelli M, Wigle N, Nakabeppu Y, Robertson GS. D_1-receptor-related priming is attenuated by antisense-mediated 'knockdown" of FosB expression. Brain Res Mol Brain Res. 1998 Jan;53(1-2):69-77.

69. Dabbagh K, Laurent GJ, Shock A, Leoni P, Papakrivopoulou J, Chambers RC. Alpha-1-antitrypsin stimulates fibroblast proliferation and procollagen production and activates classical kinase signalling pathways. J Cell Physiol 2001 Jan;186(1):73-81.

70. Dean G, Young DA, Edwards DR, Clark IM. The human tissue inhibitor of metalloproteinase (TIMP)-1 gene contains repressive elements within the promoter and intron 1. J Biol Chem. 2000 Oct 20;(42):32664-32671.

71. De Bleser PJ, Niki T, Rogiers V, Geerts A. Transforming growth factor-beta gene expression in normal and fibrotic rat liver. Hepatology 1997 Oct;26(4):886-893.

72. Decker CJ, Parker R. A turnover pathway for both sable and unstable mRNAs in yeast: evidence for a requirement for deadenylation. Gene Dev 1993 Aug;7(8):1632-1643.

73. Degos F Hepatitis C and Alcohol. J. Hepatol 1999;31 Suppl 1:113-118.

74. de Groot RP, Karperien M, Pals C, Kruijer W. Charicterisation of the mouse Jun D promoter-high basal level activity due to an octamer motif. EMBO J. 1991 Sep;10(9):2523-2332.

75. Deng T, Karin M. c-Fos transcriptional activity stimulated by H-Ras-activated protein kinase distinct from JNK and ERK. Nature. 1994 Sep 8;371(6493):171-175.

76. Dennig J, Beato M, Suske G. An inhibitor domain in Sp3 regulates its glutamine-rich activation domains. EMBO. J 1996 Oct 15;15(20):5659-5667.

77. Dérijard B, Raingeaud J, Barrett T, Wu IH, Han J, Ulevitch RJ, Davis RJ: Independent human MAP kinase signal transduction pathways defined by MEK and MKK isoforms. Science 1995 Feb 3;267(5198):682-685.

78. Dignam JD, Lebovitz RM.and Roeder RG. Accurate transcription initiation by RNA polymerase-II in a soluble extract from isolate mammalian nuclei. Nucleic Acids. Res. 1983 Mar 11;11(5):1475-1489.

79. Doyle GAR, Saarialhokere, U.K. and Parks, W.C. Distinct mechanisms regulate TIMP-1 expression at different stages of phorbol ester-mediated differentiation of U937 cells. Biochemistry 1997 Mar 4;36(9):2492-2500.

80. Dooley S, Delvoux B, Lahme B, Mangasser-Stephan K, Gressner AM. Modulation of transforming growth factor beta response and signaling during transdifferentiation of rat hepatic stellate cells to myofibroblasts. Hepatology 2000 May;31(5):1094-1106.

81. d'Ortho MP, Will H, Atkinson S, Butler G, Messent A, Gavrilovic J, Smith B, Timpl R, Zardi L, Murphy G. Membrane-type matrix metalloproteinases 1 and 2 exhibit broad-spectrum proteolytic capacities comparable to many matrix metalloproteinases. Eur J Biochem. 1997 Dec 15;250(3):751-757.

82. Drapkin R, Reardon JT, Ansari A, Huang JC, Zawel L, Ahn K, Sancar A, Reinberg D. Dual role of TFIIH in DNA excision repair and in transcription by RNA polymerase II. Nature 1994 Apr 21;368(6473):769-772.

83. Drummond DR, Armstrong J, Colman A. The effect of capping and polyadenylation on the stability, movement and translation of synthetic messenger RNAs in Xenopus oocytes. Nucleic Acids Res 1985 Oct 25;13(20):7375-7394.

84. Duncan MR, Berman B. Stimulation of collagen and glycosaminoglycan production in cultured human adult dermal fibroblasts by recombinant human interleukin-6. J Invest Dermatol 1991 Oct;97(4):686-692.

85. Edwards DR, Roucheleau H, Sharma RR, Wills AJ, Cowie A, Hassell JA, Heath JK. Involvement of AP-1 and PEA3 binding sites in the regulation of murine tissue inhibitor of metalloproteinases-1 (TIMP-1) expression. Biochem et Biophy Acta. 1992 Nov 15;1171(1):41-55.

86. Eikelberg O, Pansky A, Mussmann R, Bihl M, Tamm M, Hildebrand P, Perruchoud AP, Roth M. Transforming growth factor-β1 induces interleukin-6 expression via activating protein-1 consisting of Jun D homodimers in primary human lung fibroblasts. J Biol Chem. 1999 Apr 30;274(18):12933-12938.

87. Elsharkawy AM. Wight MC, Hay RT, Arthur MJ, Hughes T, Bahr MJ, Degitz K, Mann DA. Persistanent activation of nuclear factor-kappaB in cultured rat hepatic stellate cells involves the induction of potentially novel Rel-like factors and prolonged changes in the expression of IkappaB family proteins. Hepatology 1999 Sep;30(3):761-769.

88. Enghild JJ, Salvesen G, Brew K, Nagas HE. Interaction of human rheumatoid synovial collagenase (matrix metalloproteinase 1) and stromelysin (Matrix metalloproteinase 3) with human α-2-macroglobulin and chicker ovostatin. J. Biol Chem. 1989 May 25;264(15):8779-8785.

89. Fabris P, Infantolino D, Biasin MR, Marchelle G, Venza E, Terribile Wiel Marin V, Benedetti P, Tositti G, Manfrin V, de Lalla F. High prevalence of HCV-RNA in the saliva cell fraction of patients with chronic hepatitis C but no evidence of HCV transmission amoung sexual partners. Infection 1999 Mar-Apr;27(2):86-91.

90. Faris M, Kokot N, Latinis K, Kasibhatla S, Green DR, Koretzky GA, Nel A. The c-Jun N-Terminal kinase cascade plays a role in stress-induced apoptosis in jurkat cells by up-regulating Fas ligand expression. J Immunol. 1998 Jun 1;160(1):134-144.

91. Fata JE, Leco KJ, Moorehead RA, Martin DC, Khokha R. TIMP-1 is important for epithelial proliferation and branching morphogenesis during mouse mammary development. Dev Biol. 1999 Jul 15;211(2):238-254.

92. Flanagan JR, Becker KG, Ennist DL, Gleason SL, Driggers PH, Levi BZ, Appella E, Ozato K. Cloning of a negative transcription factor that binds to the upstream conserved region of Moloney murine leukemia virus. Mol cell Biol. 1992 Jan;12(1):38-44

93. Fraley R, Subramani S, Berg P, Papahadjopoulos D. Introduction of liposome-encapsulated SV40 DNA into cells. J Biol Chem 1980 Nov 10;255(21):10431-10435.

94. Fridman R, Fuerst TR, Bird RE, Hoyhtya M, Oelkuct M, Kraus S, Komarek D, Liotta LA, Berman ML, Stetler-Stevenson WB. Domain structure of human 72-kDa gelatinase/type-IV collagenase. Characterization of proteolytic activity and identification of the tissue inhibitor of metalloproteinase-2 (TIMP-2) binding regions. J Biol Chem. 1992 Aug 5;267(22):15398-15405.

95. Friedman SL, Roll FJ, Boyles J, Bissell DM. Hepatic lipocytes: the principle collagen-producing cells of the normal rat liver. Proc Natl Acad Sci USA. 1985 Dec;82(24):8681-8685.

96. Friedman SL, Roll FJ, Boyles J, Arenson DM, Bissell DM. Maintenance of differentiated phenotype of cultured rat hepatic lipocytes by basement-membrane matrix. J Biol Chem. 1989 Jun 25; 264(18):10756-10762.

97. Friedman SL, Rockey DC, McGuire RF, Maher JJ, Boyles JK, Yamasaki G. Isolated hepatic lipocytes and kupffer cells from normal human liver: morphological and functional charicteristics in primary culture. Hepatology 1992 Feb;15(2):234-243.

98. Friedman SL. Cellular basis of hepatic fibrosis. N Engl J Med. 1993 Jun 24;328(25):1828-1835.

99. Friedman SL. Hepatic stellate cells. Prog Liver Dis. 1996;14;101-130.

100. Fuchs SY, Dolan L, Davis RJ, Ronai Z. Phosphorylation-dependant targeting of c-Jun ubiquitination by Jun N-kinase. Oncogene 1996 Oct 3;13(7):1531-1535.

101. Fuchs SY, Xie B, Adler V, Fried VA, Davis RJ, Ronai Z. c-Jun NH2-terminal kinases target the ubiquitination of their associated transcription factors. J Biol Chem. 1997 Dec 19;272(51):32163-32168.

102. Galvagni F, Capo S, Oliviero S. Sp1 and Sp3 physically interact and co-operate with GABP for the activation of the utrophin promoter. J Mol Biol. 2001 Mar 9;306(5):985-996.

103. Garcia JA, Wu FK, Mitsuyasu R, Gaynor RB. Interactions of cellular proteins involved in the transcriptional regulation of the human immunodeficiency virus. EMBO 1987 Dec 1;6(12):3761-3770.

104. Garcia-Trevijano ER, Iraburu MJ, Fontana L, Dominguez-Rosales JA, Auster A, Covarrubias-Pinedo A, Rojkind M. Transforming growth factor beta1 induces the expression of alpha1(1)procollagen mRNA by a hydrogen peroxide-C/EBPbeta-dependant mechanism in rat hepatic stellate cells. Hepatology 1999 Mar;29(3):960-970.

105. Gaudin P, Trocme C, Berthier S, Kieffer S, Boutonnat J, Lamy C, Surla A, Garin J, Morel F. TIMP-1/MMP-9 imbalance in an EBV-immortalized B lymphocyte cellular model: evidence for TIMP-1 multifunctional properties. Biochim Biophys Acta 2000 Dec 11;1499(1-2):19-33.

106. Geiger JH, Hahn S, Lee S, Sigler PB. Crystal structure of the yeast TFIIA/TBP/DNA complex. Science. 1996 May 10;272(5263):830-836.

107. Gewert DR, Coulombe B, Castelino M, Skup D, Williams BRG. Charicterisation and expression of a murine gene homologous to human EPA/TIMP: a virus-induced gene in the mouse. EMBO J. 1987 Mar;6(3):651-657.

108. Gille H, Sharrocks AD, Shaw PE. Phosphorylation of transcription factor p62TC by MAP kinase stimulates ternary complex formation at c-Fos promoter. Nature 1992 Jul 30;358(6385):414-417.

109. Glass CK, Rose DW, Rosenfield MG. Nuclear receptor coactivators. Curr Opin Cell Biol. 1997 Apr;9(2):222-232.

110. Goldberg GL, Wilhelm SM, Kronberger A, Bauer EA, Grant GA, Eisen AZ. Human fibroblast collagenase. Complete primary structure and homology to an oncogene transformation induced rat protein. J Biol Chem. 1986 May 15;261(14):4583-4591.

111. Gressner AM, Bachem MG. Cellular sources of noncollagenous matrix proteins: role of fat storing cells in fibrogenesis. Semin Liver Dis. 1990 Feb;10(1):30-46.

112. Gromis-Ruth FX, Maskos K, Betz M, Bergner A, Huber R, Suzuki K. Mechanisms of inhibition of the human matrix metalloproteinase stromelysin-1 by TIMP-1. Nature 1997 Sep 4;389(6646):77-81.

113. Gruber BL, Marchee MJ, Suzuki K, Schwartz LB, Okada Y, Nagase H, Ramamurthy NS. Synovial procollagenase activation by human mast cells tryptase dependence upon matrix metalloproteinase 3 activation. J Clin Invest. 1989 Nov;84(5):1657-1662.

114. Grunstein M. Histone acetylation in chromatin structure and transcription. Nature 1997 Sep 25;389(6649):349-352.

115. Guedez L, Courtemanch L, Stetler-Stevenson M. Tissue inhibitor of metalloproteinase (TIMP)-1 induces differentiation and an anti-apoptotic phenotype in germinal center B cells. Blood 1998 Aug 15;92(4):1342-1349.

116. Gutman A, Wasylyk B. The collagenase gene promoter contains a TPA and oncogene-responsive unit encompassing the PEA3 and AP-1 binding sites. EMBO J. 1990 Jul;9(7):2241-2246.

117. Hagen G, Muller S, Beato M, Suske G. Sp1-mediated transcriptional activation is repressed by Sp3. EMBO J. 1994 Aug 15;13(16):3843-3851.

118. Hagen G, Dennig J, Preiss A, Beato M, Suske G. Functional analyses of the transcription factor Sp4 reveal properties distinct from Sp1 and Sp3. J Biol Chem. 1995 Oct 20;270(42):24989-24994.

119. Hahn EG, Wick G, Pencev D, Timpl R. Distrobution of basement membrane proteins in normal and fibrotic human liver: collagen type IV, Laminin and Fibronectin. Gut 1980 Jan;21(1):63-71.

120. Hai T, Curran T. Cross-family dimerization of transcription factors Fos/Jun and ATF/CREB alters DNA binding specificity. Proc Natl Acad Sci USA. 1991 May 1;88(9):3720-3724.

121. Hama-Inada H, Nishimoto T, Ohtsubo M, Sato K, Kasai M. Simple and effective method of electrophoration for introduction of plasmid and cosmid DNAs to mammalian cells. Nucleic Acids Symp Ser. 1988;19:149-152.

122. Hammani K, Blakis A, Morsette D, Bowcock AM, Schmutte C, Henriet P, Declerck YA. Structure and characterization of the human tissue inhibitor of metalloproteinase-2 gene. J Biol Chem 1996 Oct 11;271(4):25498-25505.

123. Hancock RL. Generalizing the control process for embryonic genes. Med Hypotheses 1992 Apr;37(4):245-249.

124. Hariharan N, Kelley DE, Perry RP. δ, a transcription factor that binds to downstream elements in several polymerase II promoters, is a functionally versatile zinc finger protein. 1991 Nov 1;88(21):9799-9803.

125. Hartl M, Hutchins JT, Vogt PK. The chicken junD gene and its product. Oncogene 1991 Sep;6(9):1623-1631.

126. Hattori K, Angel P, Le Beau MM, Karin M. Structure and chromosomal localization of the functional intronless human JUN protooncogene. Proc Natl Acad Sci U S A 1988 Dec;85(23):9148-9152.

127. Hauber J, Cullen BR. Mutational analysis of the trans-activation-response region of the Human immunodeficiency virus type 1 long terminal repeat. J Virol 1988 Mar;62(3):673-679.

128. Hayakawa T, Yamashita K, Tanzawa K, Uchijima E, Iwata K. Growth-promoting activity of tissue inhibitor of metalloproteinase-1 (TIMP-1) for a wide range of cells. A possible new growth factor in serum. FEBS Lett 1992 Feb 17;298(1):29-32.

129. Hayakawa T, Yamashita K, Ohuchi E, Shinagawa A. Cell growth-promoting activity of tissue inhibitor of metalloproteinases-2 (TIMP-2). J Cell Sci. 1994 Sep;107(Pt 9):2373-2379.

130. He C, Wilhelm SM, Pentland AP. Marmer BL, Grant GA, Eisen AZ, Goldberg GI. Tissue cooperation in a proteolytic cascade activating human interstitial collagenase. Proc Natl Acad Sci USA. 1989 Apr;86(8):2632-2636.

131. He C. Molecular mechanisms of transcriptional activation of human gelatinase B by proximal promoter. Cancer Lett 1996 Sep 10;106(2):185-191.

132. Hellemans K, Grinko I, Rombouts K, Schuppan D, Geerts A. All-trans and 9-cis retinoic acid alter rat hepatic stellate cell phenotype differentially. Gut. 1999 Jul;45(1):134-42.

133. Hellerbrand, Wang SC, Tsukamoto H, Brenner DA, Rippe RA. Expression of intracellular adhesion molecule 1 by activated hepatic stellate cells. Hepatology 1996 Sep;24(3):670-676.

134. Hellerbrand C, Stefanovic B, Giordano F, Burchardt ER, Brenner DA. The role of TGF Beta-1 in initiating hepatic stellate cell activation. J Hepatol. 1999 Jan;30(1):77-87.

135. Herbst H, Wege T, Miliani S, Pellegrini G, Orzechowski HD, Bechstein WO, Neuhaus P, Gressner AM, Schuppan D. Tissue inhibitor of metalloproteinase-1 and –2 RNA expression in rat and human liver fibrosis. Am J Pathol 1997 May;150(5):1647-1659.

136. Hirt B. Selective extraction of polyoma DNA from infected mouse cell cultures. J Mol Biol 1967 Jun 14;26(2):365-369.

137. Holstege FC, Tantin D, Carey M, van der Vliet PC, Timmers HT. The requirement for the basal transcription factor IIE is determined by the helical stability of promoter DNA. EMBO J 1995 Feb 15;14(4):810-819

138. Houglum K, Badossa P, Chojkier M. TGF-beta and collagen-alpha 1 (I) gene expression are increased in hepatic acinar zone 1 of rats with iron overload. Am J Physiol. 1994 Nov;267(5 Pt 1):G908-13.

139. Houglum K, Buck M, Alcorn J, Contreras S, Bornstein P, Chojkier M. Two different cis-acting regulatory regions direct cell-specific transcription of the collagen alpha (I) gene in hepatic stellate cells and in skin and tendon fibroblasts. J Clin Invest. 1995 Nov;96(5):2269-2276.

140. Houglum K, Venkataramani A, Lyche K, Chojkier M. A pilot study of the effects of d-alpha-tocopherol on hepatic stellate cell activation in chronic hepatitis C. Gastroenterology. 1997 Oct;113(4):1069-1073.

141. Howard EW, Banda MJ. Binding of tissue inhibitor of metalloproteinase-2 to two distinct sites on human 72 kD gelatinase. J Biol Chem 1991a Sep 25;266(27):17972-17977.

142. Howard EW, Bullen EC, Banda MJ. Regulation of the autoactivation of human 72 kDa progelatinase by tissue inhibitor of metalloproteinase-2. J Biol Chem 1991b Jul 15;266(20):13064-13069.

143. Huang HC, Sundseth R, Hansen U. Transcription factor LSF binds two variant bipartite sites within the SV40 late promoter. Genes Dev 1990 Feb;4(2):287-298.

144. Huber R, Schlessinger D, Pilia G. Multiple Sp1 sites efficiently drive transcription of the TATA-less promoter of the human glypican 3 (GPC3) gene. Gene. 1998 Jul 3;214(1-2):35-44.

145. Ikeda H, Nagoshi S., Ohno A, Yanase M, Maekawa H, Fujiwara K. Activated rat stellate cells express c-met and respond to hepatocyte growth factor to enhance transforming growth factor beta 1 expression and DNA synthesis. Biochem Biophys Res Commun 1998 Sep 29;250(3):769-775.

146. Ikura Y, Morimoto H, Ogami M, Jomura H, Ikeoka N, Sakurai M. Expression of platelet-derived growth factor and its receptor in livers of patients with chronic liver disease. J. Gastroentrology 1997 Aug;32(4):496-501.

147. Imbalzano AN, Zaret KS, Kingston RE. Transcription factor (TF) IIB and TFIIA can independently increase the affinity of the TATA-binding protein for DNA. J Biol Chem. 1994 Mar 18;269(11):8280-8286.

148. Iraburu MJ, Dominguez-Rosales JA, Fontana L, Auster A, Garcia-Trevijano ER, Covarrubias-Pinedo A, Rivas-Estillia AM, Greenwel P, Rojkind M. Tumour necrosis factor alpha down-regulates expression of the alpha1(I) collagen gene in rat hepatic stellate cells through a p20C/EBPbeta- and C/EBPdelta-dependant mechanism. Hepatology. 2000 May;31(5):1086-1093.

149. Iredale JP, Murphy G, Hembry RM, Friedman SL, Arthur MJP. Human hepatic lipocytes synthesize tissue inhibitor of metalloproteinase-1: implications for the regulation of matrix degradation in liver. J Clin Invest. 1992 Jul;90(1):282-287.

150. Iredale JP, Winwood PJ, Choudhury Ak, HembryRM,Murphy G, Arthur MJP. Immunostaining for 95 kD and 72 kD type IV collagenase/gelatinase and tissue inhibitor of metalloproteinase-1 during C. Parvu-induced rat liver injury. Cells of Hepatic Sinusoid 1993;4:105-108.

151. Iredale JP, Benyon RC, Ferris WF, Cottrell B, Alcolado G, Murphy G, Arthur MJP. Tissue inhibitor of metalloproteinase-1 expression is up-regulated relative to interstitial collagenase in CCl_4 induced liver fibrosis and activated human hepatic lipocytes. Cells of the Hepatic Sinusoid 1995a;5:418-419.

152. Iredale JP, Goddard S, Murphy G, Benyon RC, Aurthur MJP. Tissue inhibitor of metalloproteinase-1 and interstitial collagenase expression in autoimmune chronic active hepatitis and activated human hepatic lipocytes. Clin Sci (colch). 1995b;89(1):75-81.

153. Iredale JP, Benyon RC, Aurthur MJP, Ferris W, Alcolado R, Winwood PJ, Clark N, et al. Tissue inhibitor of metalloproteinase-1 mRNA expression is enhanced relative to interstitial collagenase mRNA in experimental liver injury and fibrosis. Hepatology 1996 Jul;24(1):176-184.

154. Iredale JP, Benyon RC, Pickering J, McCullen M, Northrop M, Pawley S, Hovell C, Arthur MJ. Mechanisms of spontaneous resolution of rat liver fibrosis. Hepatic stellate cell apoptosis and reduced hepatic expression of metalloproteinase inhibitors. J Clin Invest. 1998 Aug 1;102(3):538-549.

155. Itoh Y, Takamura A, Ito N, Maru Y, Sato H, Suenaga N, Aoki T, Seiki M. Homophilic complex formation of MT1-MMP facilitates proMMP-2 activation on the cell surface and promotes tumour cell invasion. EMBO J 2001 Sep 3;20(17):4782-4793.

156. Jackson DA. Chromatin domains and nuclear compartments establishing sites of gene expression in eukaryotic nuclei. Mol Biol Rep 1997 Aug;24(3):209-220.

157. Jakobovits et al., A discrete element 3' of human immunodeficiency virus (HIV-1) and HIV-2 mRNA initiation sites mediates transcriptional activation by an HIV trans activator. Mol Cell Biol. 1988 Jun;8(6):2555-2561.

158. Johnson RS, van Lingen B, Papaioannou VE, Spiegelman BM. A null mutation at the c-jun locus causes embryonic lethality and retarded cell growth in culture. Genes Dev. 1993 Jul;7(7B):1309-1317.

159. Johnson R, Spiegelman B, Hanahan D, Wisdom R. Cellular transformation and malignancy induced by ras require c-Jun. Mol Cell Biol. 1996 Aug;16(8):4505-4511.

160. Kallunki T, Su B, Tsigelny I, Sluss HK, Derijard B, Moore G, Davis R, Karin M. JNK2 contains a specificity-determining region responsible for efficient c-Jun binding and phosphorylation. Genes Dev. 1994 Dec 15;8(24):2996-3007

161. Kallunki T, Deng T, Hidi M, Karin M: c-Jun can recuit JNK to phosphorylate dimerization partners via specific docking interactions. Cell 1996 Nov 29;87(5):925-939.

162. Karin M. The regulation of AP-1 activity by mitogen-activated protein kinases. J Biol Chem. 1995 Jul 14;270(28):16483-16486.

163. Karin M, Liu Z, Zandi E, Ap-1 function and regulation. Cur Opin Cell Biol. 1997 Apr;9(2):240-246.

164. Kawada N, Seki S, Kuroki T, Keneda K. Rock inhibitor Y-27632 attenuates stellate cell contraction and portal pressure increase induced by endothelin-1. Biochem Biophys Res Commun. 1999 Dec 20;2(2):296-300.

165. Kerppola TK. Fos and Jun bend the AP-1 site: Effects of probe geometry on the detection of protein-induced DNA bending. Proc Natl Acad Sci USA. 1996 Sep 17;93(19):10117-10122.

166. Kerr LD, Miller DB, Matrisian LM. TGF-beta 1 inhibition of transin/stromelysin gene expression is mediated through a Fos binding sequence. Cell 1990 Apr 20;61(2):267-278.

167. Kikuchi K, Kadono T, Furue M, Tamaki K. Tissue inhibitor of metalloproteinase 1 (TIMP-1) may be an autocrine growth factor in scleroderma firoblasts. J Invest Dermatol 1997 Mar;108(3):281-284.

168. Kim CH, Heath C, Bertuch A, Hansen U. Specific stimulation of simian virus 40 late transcription in vitro by a cellular factor binding the simian virus 40 21-base-pair repeat promoter element. Proc Natl Acad Sci USA. 1987 Sep;84(17):6025-6029.

169. Kim J, Shapiro DJ. In simple synthetic promoters YY1-induced DNA bending is important in transcription activation and repression. Nucleic Acids Res. 1996a Nov 1;24(21):4341-4348.

170. Kim J, de Haan G, Shapiro DJ. DNA bending between upstream activator sequences increases transcriptional synergy. Biochem Biophys Res Commun. 1996b Sep 24;226(3):638-644.

171. Kim Y, Ratuiu V, Choi SG, Lalazar A, Thesis G, Dang Q, Kim SJ, Friedman SL. Transcriptional activation of transforming growth factor β1 and its receptors by the Kruppel-like factor Zf9/core promoter-binding protein and SP1. J Biol Chem. 1998 Dec 11;273(50):33750-33758.

172. Kitabayashi I, Kawakami Z, Matsuoka T, Chiu R, Gachelin G, Yokoyama K. Two cis-regulatory elements that mediate different signaling pathways for serum-dependant activationof the Jun B gene. J Biol Chem. 1993 Jul 5;268(19):14482-14489.

173. Knittel T, Muller L, Saile B, Ramadori G, Effect of tumour necrosis factors-alpha on proliferation, activation and protein synthesis of rat hepatic stellate cells. J. Hepatol 1997 Dec;27(6):1067-1080.

174. Knittel T, Mehde M, Kohold D, Saile B, Dinter C, Ramadori G. Expression patterns of matrix metalloproteinases and their inhibitors in parenchymal and non-parenchymal cells of liver: regulation by TNF-alpha and TGF-beta1. J. Hepatol 1999a Jun;30(1):48-60.

175. Knittel T, Kobold D, Dudas J, Saile B, Ramadori. G. Role of the Ets-1 transcription factor during activation of rat hepatic stellate cells in culture. Am J Pathol 1999b Dec;155(6):1841-1848.

176. Knook DL, Sleyster EC. Separation of Kupffer and endothelial cells of the rat liver by centrifugal elutriation. Exp Cell Res 1976 May;99(2):444-449.

177.Kojima N, Sato M, Imai K, Miura M, Matano Y, Senoo H. Hepatic stellate cells (vitimin A-storing cells) change their structure by extracellular matrix components through a signal transduction system. Histochem Cell Biol. 1998 Aug;110(2):121-128.

178.Kojima S, Hayashi S, Shimokado K, Suzuki Y, Shimada J, Cripa MP, Friedman SL. Transcriptional activation of urokinase by the Kruppel-like factor Zf9/COPEB activates latent TGF-beta1 in vascular endothelial cells. Blood. 2000 Feb 15;95(4):1309-1316.

179.Korner K, Wolfraim LA, Lucibello FC, Muller R. Characterization of the TATA-less core promoter of the cell cycle-regulated cdc25C gene. Nucleic Acids Res. 1997 Dec 15;25(24):4933-4939.

180.Kovalovich K, DeAngelis RA, Li W, Furth EE, Ciliberto G, Taub R. Increased toxin-induced liver injury and fibrosis in interleukin-6-deficient mice. Hepatology 2000 Jan;31(1):149-159.

181.Kovary K, Bravo R. The Jun and Fos protein families are both required for cell-cycle progression in fibroblasts. Mol Cell Biol. 1991 Sep;11(9):4466-4472.

182.Kristensen DB, Kawada N, Imamura K, Miyamoto Y, Tateno C, Seki S, Kuroki T, Yoshizato K. Proteome analysis of rat hepatic stellate cells. Hepatology 2000 Aug;32(2):268-277.

183.Kumer P, Clark M. Clinical Medicine Third Edition. 1994 Balliere Tindall.

184.Kwon H-S, Kim M-S, Edenberg H-J, Hur M-W. SP3 and SP4 can repress transcription by competeting with SP-1 for core cis-elements on the human ADH5/FDH minimal promoter. J Biol Chem. 1999 Jan 1;274(1):20-28.

185.Kyriakis JM, Banerjee P, Nikolakaki E, Dai T, Rubie EA, Ahmad MF, Avruch J, Woodgett JR. The stress-activated protein kinase subfamily of c-Jun kinases. Nature 1994 May 12;369(6476):156-160.

186.Laimins LA, Khoury G, Gorman C, Howard B, Grus P. Host-specific activation of transcription by tandam repeats from simian virus 40 and Moloney murine sarcoma virus. Proc Natl Acad Sci USA 1982 Nov;79(21):6453-6457.

187.Lallemand D, Spyrou G, Yaniv M, Pfarr C. Varyations in Jun and Fos protein expression and AP-1 activity in cycling, resting and stimulated fibroblasts. Oncogene 1997,Feb 20;14(7):819-830.

188.Lang A, Schoonhovan R, Tuvia S, Brenner DA, Rippe RA. Nuclear factor kappaB in proliferation, and apoptosis in rat hepatic stellate cells. J Hepatol. 2000 Jul;33(1):49-58.

189.Lania L, Majello B, De Luca P. Transcriptional regulation by the Sp family proteins. Int J Biochem Cell Biol. 1997 Dec;29(12):1313-1323.

190.Lauricella-Lefebvre MA, Castronovo V, Sato H, Seiki M, French DL, Merville MP. Stimulation of the 92-kD type IV collagenase promoter and enzyme expression in human melanoma cells. Invasion Metastasis 1993;13(6):289-300.

191.Lee KS, Buck M, Houglum Chojkier M. Activation of hepatic stellate cells by TGF alpha and collagen type I is mediated by oxidative stress through c-Myb expression. J Clin Invest. 1995a Nov;96(5):2461-2468.

192.Lee S, Greenspan DS. Transcriptional promoter of the human α1 (V) collagen gene (COL5A1). Biochem J. 1995b Aug 15;310(Pt1):15-22.

193.Le-Niculescu H, Bonfoco E, Kasuya Y, Claret FX, Green DR, Karin M. Withdrawal of survival factors results in activation of the JNK pathway in neuronal cells leading to Fas ligand induction and cell death. Mol Cel Biol 1999 Jan;19(1):751-763.

194.Leo MA, Rosman AS, Lieber CS. Differential depletion of carotenoids and tocopherol in liver disease. Hepatology. 1993 Jun;17(6):977-986.

195.Leuther KK, Bushnell DA, Kornberg RD. Two-dimensional crystallography of TFIIB- and IIE-RNA polymerase II complexes: implications for start site selection and initiation complex formation. Cell 1996 May 31;85(5):773-779.

196.Levavasseur F, Loréal O,Liétard J, Théret N, L'Helgoualc'h A, Guillouzo A, Clement B. Basement membrane gene expression in the liver. J Hepatol. 1995;22 (Supplement 2):10-19.

197.Li B, Tournier C, Davis RJ, Flavell RA. Regulation of IL-4 expression by the transcription factor Jun B during T helper cell differentiation. EMBO J. 1999 Jan 15;18(2):420-432.

198.Li D, Friedman S. Liver fibrosis and the role of hepatic stellate cells: New insights and prospects for therapy. J. Gastroenterol Hepatol 1999 Jul;14(7):618-633.

199.Li G, Fridman R Tissue inhibitor of metalloproteinase-1 inhibits apoptosis of human breast epithelial cells. Cancer Res 1999 Dec 15;59(24):6267-6275.

200.Lim MS, Guedez L, Stetler-Stevenson WG, Stetler-Stevenson M. Tissue inhibitor of metalloproteinase-2 induces apoptosis in human T lymphocytes. Ann N Y Acad Sci 1999 Jun 30;878:522-523.

201.Logan SK, Garabadian MJ, Cambell CE, Werb Z. Synergistic transcription activation of the tissue inhibitor of metalloproteinases-1 promoter via functional interaction of AP-1 and Ets-1 transcription factors. J Biol Chem. 1996 Jan 12;271(2):774-782.

202.Loreal O, Levavasseur F, Rescan RY, Yamada Y, Guillouzo A, Clement B. Differential expression of laminin chains in hepatic lipocytes. FEBS Letters 1991 Sep 23;290(1-2):9-12.

203.Loreal O, Clement B, Schuppan D, Rescan PY, Rissel M, Guillouzo A. Distrodution asnd cellular origin of collagen VI during development and in cirrhosis. Gastroenterology. 1992 Mar;102(3):980-987.

204.Louis H, Van Laethem JL, Wu W, Quertinmont E, Degraef C, Van den Berg K, Demols A, Goldman M, Le Moine O, Geerts A, Deviere J. Interluekin-10 controls neutrophilic infiltration, hepatocyte proliferation and liver fibrosis induced by carbon tetrachloride in mice. Hepatology 1998 Dec;28(6):1607-1615.

205.Lukashev ME, Werb Z. ECM signaling: orchestrating cell behavior and misbehaviour. Trend Cell Biol. 1998 Nov;8(11):437-441.

206.McCabe LC, Banerjee C, Kundu R, Harrison JR, Dobner PR, Stein JL, Lian JB, Stein GS. Developmental expression and activities of specific Fos and Jun proteins are functionally related to osteoblast maturation:role of Fra-2 and Jun D during differentiation. Endocrinology 1996 Oct;137(10):4398-4408.

207.McGuire RF, Bissell DM, Boyles J, Roll JF. Role of extracellular matrix in regulating fenestrations of sinusoidal endothelial cells isolated from normal rat liver. Hepatology 1992 Jun;15(6):989-997.

208.Maher JJ, Friedman SL, Roll FJ, Bissell DM. Immunolocalization of laminin in normal rat liver and biosynthesis of laminin by hepatic lipocytes in primary culture. Gastroenterology. 1988 Apr;94(4):1053-1062.

209.Maher JJ, Lozier JS, Scott MK. Rat hepatic stellate cels produce cytokin-induced neutrophil chemoattractant in culture and in vivo. Am J Physiol. 1998 Oct;275(4 Pt 1):G847-53.

210.Maiotti M, Monteleone G, Tarantino U, Fasciglione GF, Marini S, Coletta M. Correlation between osteoarthritic cartilage damage and levels of proteinases and proteinase inhibitors in synovial fluid from the knee. Arthroscopy 2000 Jul-Aug;16(5):522-526.

211.Majello B, De Luca P, Lania L. Sp3 is a bifunctional transcription regulator with modular independent activation and repression domains. J Biol Chem. 1997 Feb 14;272(7):4021-4026.

212.Mak KM, Lieber CS. Lipocytes and transitional cells in alcoholic liver disease: a morphology study. Hepatology 1988 Sep-Oct;8(5):1027-1033.

213.Maki Y, Bos TJ Davis C, Starbuck M Vogt PK. Proc Natl Acad Sci USA. 1987 May; 84(9):2848-2852.

214.Malim MH, Fenrick R, Ballard DW, Hauber J, Bohnlein E, Cullen BR. Functional characterisation of a complex protein-DNA-binding domain located within the human immunodeficiency virus type 1 long terminal repeat leader region. J. Virol 1989 Aug;63(8):3213-3219

215.Mallat A. Hepatic stellate cells and intrahepatic modulation of portal pressure. Digestion 1998 Jul-Aug;59(4):416-419.

216.Mann DA, Smart DE. Transcriptional Regulation of hepatic stellate cell activation. Gut In Press

217.Marchenko GN, Ratnikov BI, Rozanov DV, Godzik A, Deryugina EI, Strongin AY. Characterisation of matrix metalloproteinase-2 a novel metalloproteinase widely expressed in cancer cells of epithelial origin. Biochem J.2001 Jun 15;356(Pt 3):705-718.

218.Margolis DM, Somasundaran M, Green MR. Human transcription factor YY1 represses human immunodeficiency virus type 1 transcription and virion production. J Virol 1994 Feb;68(2):905-910.

219.Marra F, Valente AJ, Pinzani M, Abboud HE. Cultured human liver fat-storing cells produce monocyte chemotactic protein-1. Regulation by proinflammatory cytokines. J Clin Invest. 1993 Oct;92(4):1674-1680.

220.Marra F, Gentilini A, Pinzani M, Choudhury GG, Parola M, Herbst H, Dianzani MU, Laffi G, Abboud HE, Gentilini P. Phosphatidylinositol 3-kinase is required for platelet-derived growth factor's actions on hepatic stellate cells. Gastroenterology 1997 Apr;112(4):1297-1306.

221.Marra F, DeFranco R, Grappone C, Milani S, Pastacaldi S, Pinzani M, Romanelli RG, Laffi G, Gentilini P. Increased expression of monocyte chemotactic protein-1 during qactive hepatic fibrogenesis:Correlation with monocyte infiltration. Am J Pathol 1998 Feb;152(2):423-430.

222.Marra F, Romanelli RG, Giannini C, Failli P, Pastacaldi S, Arrighi MC, Pinzani M, Laffi G, Montalto P, Gentilini P. Monocyte chemotactic protein-1 stimulates hepatic stellate cell migration. Hepatology 1999 Jan;29(1):140-148.

223..Martinez-Hernandez A. The hepatic extracellular matrix, II. Electron immunohistochemical studies in rats with CCl_4 induced cirrhosis. Lab Invest 1985 Aug;53(2):166-186.

224.Mast EE, Alter MJ, Margolis HS. Strategies to prevent and control hepatitis B and C virus infections: global perspective. Vaccine 1999 Mar;17(13-14):1720-1733.

225.Mathurin P, Deng QG, Keshavarzian A, Choudhary S, Holmes EW, TsukamotoH. Exacerbation of alcoholic liver injury by enteral endotoxin in rats. Hepatology 2000 Nov;32(5):1008-1017.

226.Matrisian LM. The Matrix-degrading metalloproteinases. Bioessays. 1992 Jul;14(7):455-463.

227. Mechta-Grigoriou F, Gerald D, Yaniv M. The mammalian Jun proteins: redundancy and specificity. Oncogene 2001 Apr30;20(19):2378-2389.

228. Mercer JF, Wake SA. An analysis of the rate of metallothionein mRNA poly(A)-shortening using RNA blot hybridization. Nucleic Acids Res 1985 Nov 25;13(22):7929-7943.

229. Meyer DH, Krull N, Dreher KL, Gressner AM. Biglycan and decorin gene expression in normal and fibrotic rat liver:cellular lacalization and regulatory factors. Hepatology. 1992 Jul;16(1):204-216.

230. Miao K, Potter JJ, Anania FA, RennieTankersley L, Mezey E. Identification of two repressor elements in the mouse alpha(2)(I) collagen promoter. Arch.Biochem.Biophy. 1999 Jan 1;361(1):7-16.

231. Milani S, Herbst H, Schuppan D, Eckhart GH, Harald S. In situ hybridization for procollagen types I, III, IV mRNA in normal and fibrotic rat liver: Evidence for predominant expression in nonparenchymal liver cells. Hepatology 1989 Jul; 10(1):84-92.

232. Milani S, Herbst H, Schuppan D, Grappone C, Pellegrini G, Pinzani M, Casini A, Calabro A, Ciancio G, Stefanini F, et al. Differential expression of matrix-metalloproteinase-1 and –2 genes in normal and fibrotic human liver. Am J Pathol 1994 Mar;144(3):528-537.

233. Minden A, Lin A, Smeal T, Derijard B, Cobb M, Davis R, Karin M. c-Jun N-terminal phosphorylation correlates with activation of the JNK subgroup but not the ERK subgroup of mitogen-activated protein kinases. Mol Cell Biol. 1994 Oct;14(10):6683-6688.

234. Minto Y, Hasumura Y. Takeuchi J. The role of fat storing cells in Dissé space fibrogenesis in alcoholic liver disease. Hepatology 1983 Jul-Aug;3(4):559-566.

235. Murawaki Y, Ikuta Y, Idobe Y, Kitamura Y, Kawasaki H. Tissue inhibitor of metalloproteinase-1 in the liver of patients with chronic liver disease. J. Hepatol 1997 Jun;26(6):1213-1219.

236. Murphy G, Cawson TE, Renolds JJ. An inhibitor of collagenase from human amniotic fluid. Purification, characterisation and action on metalloproteinases. Biochem J. 1981 Apr;195(1):167-170.

237. Murphy G. The regulation of connective tissue metalloproteinases by natural inhibitors. Progress in inflammation research and therapy. Agents Actions Suppl. 1991;35:69-76.

238. Murphy G. Docherty AJP. Hambrey RM, Reynolds JJ. Metaloproteinases and tissue damage. Br J Rheumatol. 1991:30 Suppl. 1, 25-31.

239. Murphy G, Atkinson S, Ward R, Gavrilovic J, Renolds JJ. The role of the plasminogen activators in the regulation of connective tissue metalloproteinase. Ann N Y Acad Sci. 1992a Dec 4; 667:1-12.

240. Murphy G.Docherty AJP. The matrix metalloproteinases and their inhibitors. Am J Respir Cell Biol 1992b Aug;7(2):120-125.

241. Nagase H, Jackson RC, Brinckerhoff CE, Vater CA, Harris EDJ. A precusor form of latent collagenase produced in a cell free system with mRNA from rabbit synovial cells. J Biol Chem. 1981 Dec 10;256(23):11951-11954.

242. Nagase H, Brinckerhoff CE, Vater CA, Harris ED. Biosynthesis and secreation of procollagenase by raddit synovial fibroblasts. Inhibition of procollagenase secreation by monensin and evidence for glycosallation of procollagenase. Biochem J. 1983 Aug 15;214(2):281-288.

243. Nagase H, Enghild JJ, Suzuki K, Salvesen G. Stepwise activation mechanisms of the precursor of matrix metalloproteinase 3 (stromelysin) by proteinase and (4-aminophenyl) mercuric acetate. Biochemistry 1990 Jun 19;29(24):5783-5789.

244. Nakabeppu Y, Nathans D. A naturally occurring truncated form of FosB that inhibits Fos/Jun transcriptional activity. Cell 1991 Feb 22;64(4):751-759.

245. Napoli J, Bishop GA, McCaughan GW. Increased intrahepatic messenger RNA expression of interleukines 2,6 and 8 in human cirrhosis. Gastroenterology 1994 Sep;107(3):789-798.

246. Natsume M, Tsuji H, Harada A, Akiyama M, Yano T, Ishikura H, Nakanishi I, Matsushima K, Kaneko S, Mukaida N. Attenuated liver fibrosis and depressed serum albumin levels in carbon tetrachloride-treated IL-6-deficient mice. J Leukoc Biol. 1999 Oct;66(4):601-608.

247. Nehls MC, Rippe RA, Veloz L, Brenner DA. Transcription factors nuclear factor 1 and Sp1 interact with the murine collagen α1 (1) promoter. Mol Cell Biol 1991 Aug;11(8):4065-4073.

248. Nekabeppu Y, Oda S, Sekiguchi M. Proliferative activation of quiescent Rat-1A cells by delta FosB. Mol Cell Biol. 1993 Jul;13(7):4157-4166.

249. Neubauer K, Knittel T, Aurisch S, Fellmer P, Ramadori G. Glial fibrillary acidic protein--a cell type specific marker for Ito cells in vivo and in vitro. J Hepatol. 1996 Jun;24(6):719-730.

250. Newby AC Zaltsman AB. Fibrous cap formation or destruction – the critical importance of vascular smooth muscle cell proliferation, migration and matrix formation. Cardiovasc Res 1999 Feb;41(2):345-360.

251. Nicolaides NC, Correa I, Casadevall C, Traveli S, Soprano KJ, Calabretta B. The Jun family members, c-Jun and Jun D, Transactivate the human c-Myb promoter via an AP-1 like element. J Biol Chem 1992 Sep 25;267(27):19665-19672.

252. Niemela O, Parkkila S, Juvonen RO, Viitala K, Gelboin HV, Pasanen M. Cytochromes P450 2A6, 2E1 and 3A and production of protein aldehyde adducts in the liver of patients with alcoholic and non-alcoholic liver disease. J Hepatol. 2000 Dec;33(6):893-901.

253. Nikolov DB, Burley SK. RNA polymerase II transcription initiation: a structural view. Proc Natl Acad Sci U S A 1997 Jan 7;94(1):15-22.

254. Nishizawa M, Goto N, Kawai S. An avain transforming retrovirus isolated from a nephroblastoma that carries the FOS-gene as the oncogene. J. Virol 1987 Dec;61(12):3733-3750.

255. Nouchi T, Tanaka Y, Tsukada T, Sato C, Marumo F. Appearance of alpha –smooth-muscle-actin positive cells in hepatic fibrosis. Liver 1991 Apr;12(2):100-105.

256. Ohkuma Y, Hashimoto S, Wang CK, Horikoshi M, Roeder RG. Analysis of the role of TFIIE in basal transcription and TFIIH-mediated carboxy-terminal domain phosphorylation through structure-function studies of TFIIE-alpha. Mol Cell Biol. 1995 Sep;15(9):4856-4866.

257. Okada A, Bellocq JP, Rouyer N, Chenard MP, Rio MC, Chambon P, Basset P. Membrane-type matrix metalloproteinase (MT-MMP) gene is expressed in stromal cells of human colon, breast, and head and neck carcinomas. Proc Natl Acad Sci U S A. 1995 Mar 28;92(7):2730-2734.

258. Okada Y, Gonoji Y, Naka K, Tomita K, Nakanishi I, Iwata K, Yamashita K, Hayakawa T: Matrix metalloproteinase-9 (92-kDa gelatinase/type-IV collagenase) from HT-1080 human fibrosarcoma cells – purification and activation of the precursor and enzymatic properties. J Biol Chem 1992 Oct 25;267(30):21712-21719.

259. Okanoue T, Burdige EJ, French SW. The role of the Ito cell in perivenular and intralobular fibrosis in alcoholic hepatitis: Arch. Pathol Lab Med. 1983 Sep;107(9):300-308.

260. Okazaki J, Maruyama K. Collagenase activity in experimental hepatic fibrosis. Nature 1974 Nov 1;252(5478):49-50.

261. Okazaki S, Ito T, Ui M, Watanabe T, Yoshimatsu K, Iba H. Two proteins translated by alternative usage of initiation codons in mRNA encoding a Jun D Transcriptional regulator. Biochem Biophys Res Commun 1998 Sep 18;250(2):347-353.

262. Okuno M, Moriwaki H, Imai S, Kawada N, Suzuki Y, Kojima S. Retinoids exacerbate rat liver fibrosis by inducing the activation of latent TGF-beta in liver stellate cells. Hepatology 1997 Oct;26(4):913-921.

263. Okuno M, Moriwaki h, Muto Y, Kojima S. Protease inhibitors suppress TGF-beta generation by hepatic stellate cells. J Hepatol. 1998 Dec;29(6):1031-1032.

264. Ogbourne S, Antalis TM. Transcriptional control and the role of silencers in transcriptional regulation in eukaryotes. Biochem J 1998 Apr 1;331(Pt 1):1-14.

265. Oyanagi Y, Takahashi T, Matsui S, Takahashi S, Boko S, Takahashi K, Furukawa K, Arai F, Asakura H. Enhanced expression of interleukin-6 in chronic hepatitis C. Liver 1999 Dec;19(6):464-472.

266. Paquet KJ, Kamphausen U. The carbon-tetrachloride-hepatotoxicity as a model of liver damage. First report: Long-time biochemical changes. Acta Hepatogastroenterol (Stuttg) 1975 Apr;22(2):84-88.

267. Paradis V, Kollinger M, Fabre M, Holstege A, Poynard T, Bedossa P. In situ detection of lipid peroxidation by-products in chronic liver diseases. Hepatology 1997a;26:135-142.

268. Paradis V, Mathurin P, Kollinger M, Imbert-Bismut F, Charlotte F, Piton A, Opolon P, Holstege A, Poynard T, Bedossa P. In situ detection of lipid peroxidation in chronic hepatitis C: Correlation with pathological features. J Clin Pathol 1997 May;50(5):401-406.

269. Paranjape SM, Rohinton T, Kamakaka, Kadonaga JT. Role of chromatin structure in the regulation of transcription by RNA polymerase II Annual Review Biochemistry 1994;63:265-29.

270. Park K, Atchison ML. Isolation of a candidate repressor/activator, NF-E1 (YY-1, delta), that binds to the immunoglobulin kappa 3' enhancer and the immunoglobulin heavy-chain mu E1 site. Proc Natl Acad Sci USA. 1991 Nov 1;88(21):9804-9808.

271. Parlesak A, Schafer C, Schutz T, Bode JC, Bode C. Increased intestinal permeability to macromolecules and endotoxemia in patients with chronic alcohol abuse in different stages of alcohol-induced liver disease. J Hepatol. 2000 May;32(5):742-747.

272. Parola M, Robino G, Marra F, Pinzani M, Bellomo G, Leonarduzzi G, Chiarugi P, Camandola S, Poli G, Waeg G. Gentilini P, Dianzani MU. HNE interacts directly with JNK isoforms in human hepatic stellate cells. J Clin Invest 1998 Dec1;102(11):1942-1950.

273. Patikoglou GA, Kim JL, Sun L, Yang SH, Kodadek T, Burley SK. TATA element recognition by the TATA box-binding protein has been conserved throughout evolution. Genes Dev 1999 Dec 15;13(24):3217-3230

274. Pei D, Weiss SJ. Furin-dependant intracellular activation of the human stromelysin-3 zymogen. Nature 1995 May 18;375(6528):244-247.

275. Perez-Tamayo R, Montfort I, Gonzalez E. Collagenolytic activity in experimental cirrhosis of the liver. Exp Mol Pathol 1987 Dec;47(3):300-308.

276. Phillips BW, Sharma R, Leco PA, Edwards DR. A sequence-selective single stranded DNA-binding protein regulates basal transcription of the murine tissue inhibitor of metalloproteinase-1 (TIMP-1) gene. J Biol Chem. 1999 Aug 6;274(32):22197-22207.

277. Pinzani M, Failli P, Ruocco C et al. Fat storing cells as liver-specific pericytes:spatial dynamics of agonist-stimulated intracellular calcium transients. J Clin Invest 1992 Aug;90(2):642-646.

278. Pinzani M, Milani S, Grappone C, Weber FL Jr, Gentilini P, Abboud HE. Expression of platelet-derived growth factor in a model of acute liver injury. Hepatology 1994 Mar;19(3):701-707.

279. Poulos JE, Weber JD, Bellezzo JM, Di Bisceglie AM, Britton BR, Baldassure JJ. Fibronectin and cytokines increase JNK, ERK, AP-1 activity, and transin gene expression in rat hepatic stellate cells. Am J Physiol. 1997 Oct;273(4 Pt 1):G804-811.

280. Prescott LF. Paracetamol, alcohol and liver. Br J Clin Pharmacol. 2000 Apr;49(4):291-301.

281. Price MA, Hill C, Treisman R. Integration of growth factor signals at the c-Fos serum response element. Philos Trans R Soc Lond B Biol Sci. 1996a Apr 29;351(1339):551-559.

282. Price MA, Cruzalegui FH, Triesman R. The p38 and ERK MAP kinase pathways cooperate to activate ternary complex and c-Fos transcription in response to UV light. EMBO J. 1996b Dec 2;15(23):6552-6563.

283. Purcell RH. The discovery of the hepatitis viruses. Gastroenterology 1993 Apr;104(4):955-963.

284. Puri PL, Sartorelli V, Yang X, Hamamori Y, Ogryzko VV Howard BH, Kedes L,Wang JYJ, Graessmann A, Nakatani Y, Levrero M. Different roles of p300 and PCAF acetyltransferases in muscle differentiation. Mol Cell. 1997 Dec;1(1):35-45.

285. Quantin B, Breathnach R. Eidermal growth-factors stimulates the transcription of the c-Jun proto-oncogene in rat fibroblasts. Nature 1988 Aug 11;334(6182):538-359.

286. Rajaram N, Kerppola TK. DNA bending by Fos-Jun and the orientation of heterodimer binding depend on the sequence of the AP-1 site. EMBO J 1997 May 15;16(10):2917-2925.

287. Ramadori G, Knittel T, Odenthal M, Schwogler S, Neubauer K, Meyer zum Bushchenfelde KH. Synthesis of cellular fibronectin by rat liver fat-storing (Ito) cells: regulation by cytokines. Gastroenterology. 1992 Oct;103(4):1313-1321.

288. Ratziu O, Lalazar A, Wong L, Dang Q, Collins C, Shaulian E, Jensen S, Friedman SL. Zf9, a Kruppel-like trancription factor up-regulated in vivo during early hepatic fibrosis. Proc Natl Acad Sci USA. 1998 Aug 4;95(16):9500-9505.

289. Rescan PY, Loreal O, Hassell JR, Yamada Y, Guillouso A, Clement B. Distribution and origin of the basement membrane component perlecan in rat liver and primary hepatocyte culture. Am J Pathol. 1993 Jan;142(1):199-208.

290. Rice JC, Allis CD. Histone methylation versus histone acetylation: new insights into epigenetic regulation. Curr Opin Cell Biol 2001 Jun;13(3):263-273.

291. Ried S, Jager C, Jeffers M, Vande Woude GF, Graeff H, Schmitt M, Lengyl. Activation mechanisms of the urokinase-type plasminogen activator promoter by hepatocyte growth factor/scatter factor. J Biol Chem. 1999 Jun 4;274(23):16377-16386.

292. Rippe RA, Almounajed G, Brenner DA. SP-1 binding activity increases in activated Ito cells. Hepatology 1995 Jul;22(1):241-251.

293.Rippe RA, Schrum LW, Stefanovic B, SolisHerruzo JA, Brenner DA. NF-kappa B inhibits expression of the alpha 1(I) collagen gene. DNA Cell Biol, 1999 Oct;18(10):751-761.

294.Robertson GS, Tetzlaff W, Bedard M, St-Jean M, Wigle N. c-Fos mediates antipsychotic-induced neurotensin gene expression in the rodent striatum. Neuroscience 1995 Jul;67(2):325-344.

295.Rockey DC, Boyles JK, Gabbiani G, Friedman SL. Rat hepatic lipocytes express smooth muscle actin upon activation invivo and in culture. J Submicrosc Cytol Pathol. 1992 Apr;24(2):193-203.

296.Rockey DC, Housset CN, Friedman SL. Activation dependant contractility of rat hepatic lipocytes in culture and invivo. J Clin Invest. 1993 Oct;92(4):1795-1804.

297.Rockey DC, Fouassier L, Chung JJ, Carayon A, Vallee P, Rey C, Housset C. Cellular localization of endothelin –1and production of liver injury in the rat: Potential for autocrine and paracrine effects on stellate cells. Hepatology 1998 Feb;27(2):472-80.

298.Roeb E, Graeve L, Hoffmann R, Decker K, Edwards DR, Heinrich PC. Regulation of tissue inhibitor of metalloproteinase-1 gene expression by cytokines and dexamethasone in rat hepatocyte primary cultures. Hepatology 1993 Dec;18(6):1437-1442.

299.Roeb E, Graeve L, Mullberg J, Matern S, Rose-John S. TIMP-1 protein expression is stimulated by IL-1 beta and IL-6 in primary rat hepatocytes. FEBS Lett 1994 Jul 25;349(1):45-49.

300.Roffler-Tarlov S, Jeremy J, Brown G, Tarlov E, Stolarov J, Chapman DL, Alexiou M, Papaioannou VE. Programmed cell death in the absence of c-Fos and c-Jun. Development 1996 Jun;122(1):1-9.

301.Rojkind M, Takahashi S, Giambrone MA. Collagenase and reversible hepatic fibrosis in rat. (Abstr.) Gastroentrology 1978;75:984.

302.Rojkind M, Giambrone M-A, Biempica L. Collagens types in normal and cirrhotic liver. Gastroenterology 1979 Apr;79(4):710-719.

303.Rolla R, Vay D, Mottaran E, Parodi M, Traverso N, Arico S, Sartori M, Bellomo G, Klassen LW, Thiele GM, Tuma DJ, Albano E. Detection of circulation antibodies against malondialdehyde-acetaldehyde adducts in patients with alcohol-induced liver disease. Hepatology 2000 Apr;31(4):878-884.

304.Roth S, Gong W, Gressner AM. Expression of different isoforms of TGF-beta and latent TGF-beta binding protein by rat Kupffer cells. J Hepatol. 1998 Dec;29(6):915-922.

305.Rutberg SE, Saez E, Lo S, Jang SI, Markova N, Spiegelmann BM, Yuspa SH. Opposing activities of c-Fos and Fra-2 on AP-1 regulated transcriptional activity in mouse keratinocytes induced to differentiate by calcium and phorbol esters. Oncogene 1997 Sept;15(11):1337-1346.

306.Ryder K, Nathans D. Induction of protooncogenes c-Jun by serum growth-factors. Proc Natl Acad Sci USA. 1988 Nov;85(22):8464-8467.

307.Ryseck RP, Hirai SI, Yaniv M, Bravo R. Transcription activation of c-Jun during the GO/G1 transition in mouse fibroblasts. Nature 1988 Aug 11;334(6182):535-537.

308.Ryseck RP, Bravo R. c-Jun, Jun B and Jun D differ in their binding affinities to AP-1 and CRE concensus sequences; effect of Fos proteins. Oncogene 1991 Apr;6(4):533-542.

309.Saika S, Kawash Y, Okada Y, Tanaka SI, Yamanaka O, Ohnishi Y, Ooshima A. Recombinant TIMP-1 and –2 enhance the proliferation of rabbit cormeal epithelial cells in vitro and the spreading of rabbit corneal epithelium in situ. Curr Eye Res 1998 Jan;17(1):47-52.

310. Sarbah SA, Younossi ZM. Hepatitis C: An update on the silent epidemic. J Clin Gastroenterol. 2000 Mar;30(2):125-143.

311. Sato H, Seiki M. Regulatory mechanism of 92 kDa type IV collagenase gene expression which is associated with invasiveness of tumor cells. Oncogene 1993 Feb;8(2):395-405.

312. Sato M, Kojima N, Miura M, Imai K, Senoo H. Induction of cellular processes containing collagenase and retinoid by integrin-binding to interstitial collagen in hepatic stellate cell culture. Cell Biol Int 1998;22(2):115-125.

313. Savagner P, Krebsbach PH, Hatano O, Miyashita T, Liedman J, Yamada Y. Collagen II promoter and enhancer interact synergistically through SP-1 and distinct nuclear factors. DNA Cell Biol 1995Jun;14(6):501-510.

314. Schaefer M, Hopkins RG, Failla ML, Gitlin JD. Hepatocyte-specific localization and copper-dependent trafficking of the Wilson's disease protein in the liver. Am J Physiol. 1999 Mar;276(3 Pt 1):G639-646.

315. Schaffner F, Popper H. Cappilarzation of hepatic sinusoids in man. Gastroenterology 1963;44:239-242.

316. Schmidt C, Fischer G, Kadner H, Genersch E, Kuhn K, Poschi E. Differential effects of DNA-binding proteins on bidirectional transcription from the common promoter region of human collage type IV genes COL4A1 and COL4A2. Biochim Biophys Acta 1993 Jul 18;1174(1):1-10.

317. Schreiber M, Kolbus A, Piu F, Szabowski A, Mohle-Steinlein U, Tian J, Karin M, Angel P, Wagner EF. Control of cell cycle progression by c-Jun is p53 dependant. Genes Dev. 1999 Mar 1;13(5):607-619.

318. Schuppan D, Herbst H, Miliani S. Matrix synthesis and molecular networks in hepatic fibrosis; In : Extracellular matrix, Zern MA, Reid LM, eds. New York: Marcel Dekker Inc., 1993:201-254.

319. Schwogler S, Odenthal M, Myer zum Bushenfelde KH, Ramadori G. Alternative splicing products of tenascin gene distinguish rat liver fat storing cells from arterial smooth muscle cells and skin fibroblasts. Biochem Biophys Res Commun. 1992 Jun 15;185(2):768-775.

320. Seitz M, Dayer JM. Enhanced production of tissue inhibitor of metalloproteinases by peripheral blood mononuclear cells of rheumatoid arthritis patients responding to methotrexate treatment.

321. Shatkin AJ, Manley JL. The ends of the affair: capping and polyadenylation. Nat Struct Biol 2000 Oct;7(10):838-842

322. Shi Y, Seto E, Chang LS, Shenk T. Transcriptional repression by YY1, a human GL1-Kruppel-related protein, and relief of repression by adenovirus E1A protein. Cell 1991 Oct 18;67(2):377-388.

323. Shimizu I, Mizobuchi Y, Yasuda M, Shiba M, Ma R-Y, Horie T, Liu F, Ito S. Inhibitory effect of oestrodiol on activation of rat hepatic stelate cells in vivo and in vitro. Gut 1999 Jan;44(1):127-136.

324. Shinoda C, Takaku S. Interleukin-1 beta, interleukin-6, and tissue inhibitor of metalloproteinase-1 in the synovial fluid of the temporomandibular joint with respect to cartilage distruction. Oral Dis 2000 Nov;6(6):383-390.

325. Shyu A-B, Greenberg ME, Belassco JG. The Fos transcript is targeted for rapid decay by two distinct mRNA degrading pathways. Genes Dev. 1989 Jan;3(1):60-72.

326. Shyu A-B, Belasco JG, Greenberg ME. Two distinct destabilization elements in the c-Fos message trigger deadenylation as a first step in rapid mRNA decay. Genes Development 1991 Feb;5(2):221-231.

327. Smart DE, Vincent KJ, Arthur MJP, Eickelberg O, Castellazzi M, Mann J, Mann DA. JunD regulates transcription of the tissue inhibitor of metalloproteinase-1 and IL-6 genes in activated stellate cells. J Biol Chem. 2001 Jun 29;276(26):24414-24421.

328. Smeal T, Angel P, Meek J, Karin M. Different requirements for formation of Jun:Jun and Jun:Fos complexes. Genes Dev 1989 Dec;3(12B):2091-2100.

329. Smeal T, Hibi M, Karin M. Altering the specificity of signal transduction cascades: positive regulation of c-Jun transcriptional activity by protein kinases A. EMBO J. 1994 Dec 15;13(24):6006-6010.

330. Smeyne RJ, Vendrell M, Hayward M, Baker SJ,Miaao GG, Schilling K, Robertson LM, Curren T, Mogan J. Continuous c-Fos expression precedes programmed cell death in vivo. Nature 1993 May 13;363(6425):166-169.

331. Soloway PD, Alexander CM, Werb Z, Jaenisch R. Targeted mutagenesis of Timp-1 reveals that lung tumour invasion is influenced by Timp-1 genotype of the tumour but not that of the host. Oncogene 1996 Dec 5;13(11):2307-14.

332. Sonobe MH, Yoshida T, Murakami M, Kameda T, Ida H. Fra-2 promoter can respond to serum stimulation through AP-1 complexes. Oncogene 1995 Feb 16;10(4):689-696.

333. Sprenger H, Kaufmann A, Garn H, Lahme B, Gemsa D, Gressner AM. Induction of neutrophil-attracting chemokines in transforming rat hepatic stellate cells. Gastroenterology 1997 Jul;113(1):277-285.

334. Springman EB, Angleton EL, Birkedal-Hansen H, Van Wart HE. Multiple modes of activation of latent human fibroblast collagenase: Evidence for the role of a Cys^{73} active-site zinc complex in latency and a "cysteine switch" mechanisms for activation. Proc Natl Acad Sci USA. 1990 Jan;87(1):364-368.

335. Stables J, Scott S, Brown S, Roelant C, Burns D, Lee MG, Rees S. Development of a dual glow-signal firefly and Renilla luciferase assay reagent for the analysis of G-protein coupled receptor signalling. J Recept Signal Transduct Res. 1999 Jan;19(1-4):395-410.

336. Stein B, Balwin AS, Ballard DW, Greene WC, Angle P, Herrlich P. Cross coupling of the NF-theta–B P65 and FOS JUN transcription factors produces potentiated biological function. EMBO J. 1993 Oct;12(10):3879-3891.

337. Sternlicht MD, Lochter A, Sympson CJ, Huey B, Rougier JP, Gray JW, Pinkle D, Bissell MJ, Werb Z. The stromal proteinase MMP3/stromelysin-1 promotes mammary carcinogenesis. Cell 1999 Jul 23;98(2):137-146.

338. Sun D, Hurley LH. Cooperative bending of the 21-base-pair repeats of the SV40 viral early promoter by human SP-1. Biochemistry 1994 Aug 16;33(32):9578-9587.

339. Surdej P, Riedl A, Jacobs-Lorena M. Regulation of mRNA stability in development. Ann Rev Genet 1994;28:263-282.

340. Sutherland JA, Cook A, Bannister AJ, Kouzarides T. Conserved motifs in Fos and Jun define a new class of activation domain. Genes Dev. 1992 Sep;6(9):1810-1819.

341. Su W, Jackson S, Tjian R, Echols H. DNA looping between sites for transcriptional activation: self-association of DNA-bound SP-1. Genes Dev. 1991 May;5(5):820-826.

342. Suzuki T, Okuno H, Yoshida T, Endo T, Nishina H, Ida H. Difference in transcriptional regulatory function between c-Fos and Fra-2. Nucleic Acids Res. 1991 Oct 25;19(20);5537-5542.

343. Svaren J, Horz W. Regulation of gene expression by nucleosomes. Curr Opin Genet Dev 1996 Apr;6(2):164-170.

344. Takahara T, Kojima T, Miyabayashi C, Inoue K, Sasaki H, Muragaki Y, Ooshima A. Collagen production in fat-storing after carbon tetrachloride intoxication in the rat: immunoelectronmicroscopic observation of type I, type III collagens, and prolyl hydroxylase. Lab Invest 1988 Oct;59(4):509-521.

345. Takahara T, Furui K, Yata Y, Jin B, Zhang LP, Nambu S, Sato H, Seiki M, Watanabe A. Dual expression of matrix metalloproteinase-2 and membrane-type matrix metalloproteinase in fibrotic human livers. Hepatology 1997 Dec;26(6):1521-1529.

346. Tamaki T, Ohnishi K, Hartl C, LeRoy EC, Trojanowska M. Characterization of a GC-rich region containing Sp1 binding site(s) as a constitutive resoponce element of the α2 (I) collagen gene in human fibroblasts. J Biol Chem 1995 Mar 3;270(9):4299-4304.

347. Tamai T, Seki T, Shiro T, Nakagawa T, Wakabayashi M, Imamura M, Nishimura A, Yamashiki N, Takasu M, Inoue K, Okamura A.Effects of alcohol consumption on histological changes in chronic hepatitis C: a clinicopathological study. Alcohol Clin Exp Res 2000 Apr;24 Suppl 4:106S-111S.

348. Tan S, Hunziker Y, Sargent DF, Richmond TJ. Crystal structure of a yeast TFIIA/TBP/DNA complex. Nature. 1996 May 9;381(6578):112-113.

349. Thepot D, Weitzman JB, Segretain D, Stinnakre MG, Babinet C, Yaniv M. Targeted disruption of the murine Jun D gene results in multiple defects in male reproductive function. Development 2000 Jan;127(1):143-153.

350. Thompson K, Maltby J, Fallowfield J, McAulay M, Millward-Sadler H, Sheron N. Iterluekin-10 expression and function in experimental murine liver inflammation and fibrosis. Hepatology 1998 Dec;28(6):1597-1606.

351. Thompson KC, Trowern A, Fowell A, Marathe M, Haycock C, Arthur MJ, Sheron N. Primary rat and mouse hepatic stellate cells ecpress the acrophage inhibitor cytokine interleukin-10 during the course of activation in vitro. Hepatology 1998 Dec;28(6):1518-1524.

352. Thurman RG. Sex-related liver injury due to alcohol involves activation of Kupffer cells by endotoxin. Can J. Gastroenterol. 2000 Nov; 14 (Suppl D):129D-135D.

353. Tiggelman AM, Boers W, Linthorst C, Brand HS, Sala M, Charmuleau RA. Interleukin-6 production by human liver (myo)fibroblasts in culture. Evidence for a regulatory role of LPS, IL-1 beta and TNF alpha.

354. Toda K, Umagai N, Tsuchimoto K, Inagaki H, Suzuki T, Oishi T, Atsukawa K, Saito H, Morizane T, Hibi T, Ishii H. Induction of hepatic stellate cell proliferation by LPS-stimulated peripheral blood mononuclear cells from patients with liver cirrhosis. J Gastroenterol 2000;35(3):214-220.

355. Tomoda K, Kubota Y, Kato J-Y. Degradation of the cyclin-dependant-kinase inhibitor $p27^{Kip1}$ is insigated by Jab1. Nature 1999 Mar 11;398(6723):160-165.

356. Treier M, Stwaszewski LM, Bohman D. Ubiquitin-dependant c-Jun degradation in vivo is mediated by the delta domain. Cell 1994 Sep 9;78(5):787-798.

357. Trim JE, Samra S, Arthur MJP, Wright MC, McAulay M, Beri R, Mann DA. Upstream tissue inhibitor of metalloproteinase-1 (TIMP-1) Element-1, a Novel and essential regulatory DNA motif in the human TIMP-1 gene promoter, directly interacts with a 30-kDa nuclear protein. J Biol Chem. 2000 Mar 3;275(9):6657-6663.

358. Trim N, Morgan S, Evans M, Issa R, Fine D, Afford S, Wilkins B, Iredale J. Hepatic stellate cells express the low affinity nerve growth factor receptor p75 and undergo apoptosis in response to nerve growth factor stimulation. Am J Pathol. 2000 Apri156(4):1235-1243.

359. Tsurumi C. Ishida N, Tamura T, Kakaizuka A, Nishida E, Ilumura E,Kishimoto T, Inagki M, Okazaki K, Sagata N et al. Degradation of c-Fos by the 26s proteosome is accelerated by c-Jun and multiple protein kinases. Mol Cell Biol. 1995 Oct;15(10):5682-5687.

360. Turner BM, Birley AJ, Lavender J. Histone H4 isoforms acetylated at specific lysines residues define individual chromosomes and chromatin domains in drosophila polytene nuclei. Cell. 1992 Apr 17;69(2):375-384.

361. Turner BM, O'Neil LP. Histone acetylation in chromatin and chromosomes. Semin Cell Biol. 1995 Aug;6(4):229-236.

362. Turner J, Crossley M. Mammalian Kruppel-like transcription factors: more than just a pretty finger. Trends Biochem Sci. 1999 Jun;24(6):236-240.

363. Ungefroren H, Krull NB. Transcriptional regulation of the human biglycan gene. J Biol Chem. 1996 Jun 28;271(26):15787-15795.

364. Valente P, Fassina G, Melchori A, Masiello L, Cilli M, Vacca A, Onisto M, Santi L, Stetler-Stevenson WG, Albini A. TIMP-2 over-expression reduces invasion and angiogenesis and protects B16F10 melanoma cells from apoptosis. Int J Cancer 1998 Jan 19;75(2):246-253.

365. Vandel L, Pfarr CM, Huguier S, Loiseau L, Sergeant A, Castellazzi M. Increased transforming activity of JunB and JunD by introduction of an heterologous homodimerization domain. Oncogene 1995 Feb 2;10(3):495-507.

366. Van Dyke MW, Roeder RG, Sawadogo M. Physical analysis of transcription preinitiation complex assembly on a class II gene promoter. Science 1988 Sep 9;241(4871):1335-1338.

367. Van Wart HE, Birkedal-Hansen H. The cysteine switch: A principle of regulation of metalloproteinase activity with potential applicability to the entire matrix metalloproteinase gene family. Proc Natl Acad Sci USA. 1990 Jan;87(1):5578-5582.

368. Verrijzer CP, Tjian R. TAFs mediate transcriptional activation and promoter selectivity. Trends Biochem Sci 1996 Sep;21(9):338-342.

369. Vincent KJ, Jones E, Arthur MJP, et al., Regulation of E-box binding during invivo and invitro activation of rat human hepatic stellate cells. Gut 2001 Nov;49(5):713-719.

370. Yoshida Y, Kurosawa N, Kanematsu T, Kojima N, Tsuji S. Genomic structure and promoter activity of the mouse polysialic acid synthase gene (mST8Sia II). Brain-specific expression from a TATA-less GC-rich sequence. J Biol Chem. 1996 Nov 22;271(47):30167-30173.

371. Vyas SK, Leyland H, Gentry J, Arthur MJ. Rat hepatic lipocytes synthesize and secrete transin (stromelysin) in early primary culture. Gastroenterology. 1995 Sep;109(3):889-898.

372. Wallrath LL. Unfolding the mysteries of heterochromatin. Curr Opin Genet Dev 1998 Apr;8(2):147-153.

373. Wang H, Xie Z, Scott R. Differentiation modulates the balance of positive and negative jun/AP-1 DNA binding activities to regulate cellular proliferative potential: different effects in nontransformed and transformed cells. J Cell Biol 1996a Nov;135(4):1151-1162.

374. Wang H, Xie Z, Scott R Jun D phosphorylation, and expression of AP-1 DNA binding activity modulated by serum growth factors in quiescent murine 3T3T cells. 1996b Dec 19; 13(12):2639-2647.

375. Wang SC, Ohata M, Schrum L, Rippe RA, Tsukamoto H. Expression of interleukin-10 by in vitro and in vivo activated hepatic stellate cells. J Biol Chem 1998 Jan 2;273(1):302-308.

376. Ward NS, Waxman AB, Homer RJ, Mantell LL, Einarsson O, Du Y, Elias JA. Interleukin-6 induced protection in hyperoxic acute lung injury. Am J Respir Cell Mol Biol 2000 May;22(5):535-542.

377. Ward RV, Arkinson SJ, Slocombe PM, Docherty AJP, Renolds JJ, Murphy G. Tissue inhibitor of metalloproteinase-2 inhibits the activation of 72kDa progelatinase by fibroblast membranes. Biochim Biophys Acta. 1991 Aug 30;1079(2):242-246.

378. Wasylyk C, Gutman A, Nicholson R, Wasylyk B. The c-Ets oncoprotein activates the stromelysin promoter through the same elements as several non-nuclear oncoproteins. EMBO J. 1991 May;10(5):1127-1134.

379. Weiner JA, Chen A, Davis BH. E-Box-binding repressor is down-regulation in hepatic stellate cells during up-regulation of mannose 6-phosphate/insulin-like growth factor-II receptor expression in early hepatic fibrogenesis. J Biol Chem. 1998 Jun 26;273(26):15913-15919.

380. Weiner JA, Chen A, Davis BH.Platet-derived growth factor is a principal inductive factor modulating mannose 6-phosphate/insulin-like growth factor receptor gene expression via a distal E-box in activated hepatic stellate cells. Biochem J. 2000 Jan 15;345 Pt 2:225-231.

381. Weitzman JB, Fiette L, Matsuo K, Yaniv M. Jun D protects cells from p53-dependant senescence and apoptosis. Moll Cell. 2000 Nov;6(5):1109-1119.

382. Werb Z, Burleigh MC, Barrett AJ. The interaction of alpha-2-macroglodulin with proteinases. Binding inhibition of mammmalian collagenases and other metal proteinases. Biochem J. 1974 May; 137(2):359-368.

383. Werb Z, Chin JR. Extracellular matrix remolding during morphogenesis. Ann N Y Acad Sci. 1998 Oct 23;857:110-118.

384. Whitmarsh AJ, Davis RJ. Transcription factor AP-1 regulation by mitogen-activated protein kinase signal transduction pathways. J Mol Med 1996 Oct;74(10):589-607.

385. Wick M, Haronen R, Mumberg D, Burger C, OlsenBR, Budarf ML, Apte SS, Müller R. Structure of the human TIMP-3 gene and its cell cycle-regulated promoter. Biochem J. 1995 October 15;311(Pt2):549-554.

386. Willimann TE, Trueb B. Identification of functional elements and reconstitution of the α1 (VI) collagen promoter. J Biol Chem 1994 Jan 7;269(1):332-338.

387. Wisdom R, Johnson RS, Moore C. c-Jun regulates cell cycle progression and apoptosis by distinct mechanisms. EMBO J. 1999;18(1):188-197.

388. Wolffe AP. Nucleosomes positioning and modification: chromatin structures that potentiate transcription. Trends Biochem Sci. 1994 Jun;19(6):240-244.

389. Wong L, Yamasaki G, Johnson RJ, Friedman SL. Induction of beta-platelet-derived growth factor receptor in rat hepatic lipocytes during cellular activation in vivo and in culture. J Clin Invest. 1994 Oct;94(4):1563-1569.

390. Wright MC, Issa R, Smart DE, Trim N, Murray GI, Primrose JN, Arthur MJP, Iredale JP, Mann DA. Gliotoxin stimulates the apoptosis of human and rat hepatic stellate cells and enhances the resolution of liver fibrosis in rats. Gastroenterology 2001 Sep;121(3):685-698.

391. Wu FK, Garcia JA, Harrich D, Gaynor RB. Purification of the human immunodeficiency virus types 1 enhancer and TAR binding proteins EBP-1 and UBP-1. EMBO 1988 Jul;7(7):2117-2130.

392. Wu J, Grunstein M. 25 years after the nucleosome model: chromatin modifications. Trends Biochem Sci 2000 Dec;25(12):619-623

393. Xu ZY, Liu CB, Francis DP, Purcell RH, Gun ZL, Duan SC, Chen RJ, Margolis HS, Huang CH, Maynard JE. Prevention of perinatal acquisition of hepatitis B virus carriage using vaccine: preliminary report of a randomized, double-blind placebo-controlled and comparative trial. Pediatrics 1985 Nov;76(5):713-718.

394. Yang M, Nomura H, Hu Y, Kaneko S, Kaneko H, Tanaka M, Nakashima K. Prolactin-induced expression of TATA-less cyclin D3 gene is mediated by Sp1 and AP2. Biochem Mol Biol Int. 1998 Jan;44(1):51-58.

395. Yen J, Wisdom RM, Tratner I, Verma IM. An alternative spliced form of FosB is a negative regulator of transcriptional activation and transformation by Fos proteins. Proc Natl Acad Sci USA. 1991 Jun 15;88(12):5077-5081.

396. Yoon JB, Li G, Roeder RG. Characterisation of a family of related cellular transcription factors which can modulate human immunodeficiency virus type 1 transcription in vitro. Mol Cell Biol. 1994 Mar;14(3):1776-1785.

397. Yoshiji H, Kuriyama S, Miyamoto Y, Thorgeirsson UP, Gomez DE, Kawata M, Yoshii J, Ikenaka Y, Noguchi R, Hirohisa T, Nakatani T, Thorgeirsson SS, Fukui H. Tissue inhibitor of metaloproteinase-1 promotes liver fibrosis development in transgenic mouse model. Hepatology 2000 Dec;32(6):1248-1254.

398. You Y, Chen C-YA, Shyu A-B. U-rich sequence-binding proteins (URBPs) interacting with a 20-nucleotide U-rich sequence in the 3' untranslated region of c-Fos mRNA may be involved in the first step of c-Fos mRNA degradation. Mol. Cell. Biol 1992 Jul;12(7):2931-2940.

399. Yun K, Wold B. Skeletal muscle determination and differentiation: story of a core regulatory network and its context. Curr Opin Cell Biol. 1996 Dec;8(6):877-889.

400. Zawel L, Reinberg D. Initiation of transcription by RNA polymerase II: a multi-step process. Prog Nucleic Acid Res Mol Biol. 1993;44:67-108.

401. Zawel L, Reinberg D. Common themes in assembly and function of eukaryotic transcription complexes. Annu Rev Biochem. 1995a;64:533-561.

402. Zawel L, Kumar KP, Reinberg D. Recycling of the general transcription factors during RNA polymerase II transcription. Genes Dev. 1995b Jun 15;9(12):1479-1490.

403. Ziff EB. Trancription factors: a new family gathers at the cAMP response site. Trends Genet 1990 Mar;6(3):69-72

404. Zuckerkandl E. Junk DNA and sectorial gene repression. Gene 1997 Dec 31;205(1-2):323-343.0

Appendix 1.
Oligonucleotides All listed 5'-3'

PCR Primers
TIMP-1 General Primers
TIMP-111 (5' Sense)
GTA GGT AAG CTT GGT GGG TGG ATG AGT AAT GCA
TIMP +86 (3' Anti Sense)
CAA GCT GCA GCC CAG CTC CGG TCC CTG CTG

TIMP-1 Minimal Promoter AP-1 PCR Mutagenesis
TIMP-111 (AP-15'M)
GTA GGT AAG CTT GGT GGG TGG AAA GGT AAT GCA

Anti Sense Oligonucleotides
All anti sense oligonucleotides were phosphorothioated at every base and desalted before PAGE purification. Oligonucleotides for Anti Sense work were obtained either as part of a collaboration with Zenica, or commercially from Sigma Genosys.

Jun D (Sense) (Ryseck *et al.*, 1991)
ATG GAA ACG CCC TTC TAT
Jun D (Anti Sense)
ATA GAA GGG CGT TTC CAT

Fos B (Sense) (Robertson *et al.*, 1995)
CCA GGG AAA TTG TTC AAG
Fos B (Anti Sense)
CTT GAA ACA TTT CCC TGG

Fra2 (Sense) (Robertson *et al.*, 1995)
CCC ACC GCG GAT CAT GTA CC
Fra2 (Anti Sense)
GGT ACA TGA TCC GCG GTG GG

Jun D Knockout Screening Oligonucleotides
For genomic PCR screening of Jun D knockout mice for tail tip DNA.
Lac Z A
GCA TCG AGC TGG GTA ATA AGC GTT GGC AAT
Lac Z B
GAC ACC AGA CCA ACT GGT AAT GGT AGC GAC

Jun D 1
TCG CTC TTG GCA ACA GCG GCC GCC ACC AGG
Jun D 2
GGC CGC TCA GCG CCT CCT CGC CAT AGA AGG

Taqman Primers and Probes
Mouse GAPDH
GAPDH Forward
GGC CTA CAT GGC CTC CAA
GAPDH Reverse
TCT CTC TTG CTC TCA GTA TCC TTG C
GAPDH Probe
AGA AAC CCT GGA CCA CCC AGC CC

Mouse Procollagen I

Procollagen 1 Forward
TTC ACC TAC AGC ACG CTT GTG
Procollagen 1 Reverse
GAT GAC TGT CTT GCC CCA AGT T
Procollagen 1 Probe
ATG GCT GCA CGA GTC ACA

Mouse α Smooth Muscle Actin

α Smooth Muscle Actin Forward
TCA GCG CCT CCA GTT CCT
α Smooth Muscle Actin Reverse
AAA AAA AAC CAC GAG TAA CAA ATC AA
α Smooth Muscle Actin Probe
TCC AAA TCA TTC CTG CCC A

Mouse TIMP-1

TIMP-1 Forward
GCA TGG ACA TTT ATT CTC CAC TGT
TIMP-1 Reverse
TCT CTA GGA GCC CCG ATC TG
TIMP-1 Probe
CAG CCC CTG CCG CCA TCA

TIMP-1 Minimal Promoter SP-1 Two-Step PCR Mutagenesis and EMSA Competition Assays

SP13M (Sense)
TGC CAC CCC CGT AGT TAG CGT G
SP13M (Anti Sense)
CAC GCT AAC TAC GGG GGT GGC A

SP15M (Sense)
TGC CAT TGA TGC CCC TAG CGT G
SP15M (Anti Sense)
CAC GCT AGG GGC ATC AAT GGC A

SP-1 (TIMP-1) Oligonucleotides for EMSA

SP-1TIMPS (Sense)
TGC CAC CCC CGC CCC TAG CGT G
SP-1TIMPAS (Anti Sense)
CAC GCT AGG GGC GGG GGT GGC A

SP-1 Consensus (Sense)
ATT CGA TCG GGG CGG GGC GAG
SP-1 Consensus (Anti Sense)
CTC GCC CCG CCC CGA TCG AAT

TIMP-1 AP-2 (Sense)
GCC CGG GGT GGC CCA GCA GG
TIMP-1 AP-2 (Anti Sense)
CCT GCT GGG CCA CCC CGG GC

AP-2 Consensus (Sense)
GAT CGA ACT GAC CGC CCG CGG CCC GT
AP-2 Consensus (Anti Sense)
AC GGG CCG CGG GCG GTC AGT TCG ATC

TIMP-1 AP-1 (Sense)
TGG GTG GAT GAG TAA TGC A
TIMP-1 AP-1 (Anti Sense)
TGC ATT ACT CAT CCA CCC A

AP-1 Consensus (Sense)
CGC TTG ATG AGT CAG CCG GAA
AP-1 Consensus (Anti Sense)
TTC CGG CTG ACT CAT CAA GCG

NFκB Concensus (Sense)
AGT TGA GGG GAC TTT CCC AGG C
NFκB Concensus (Anti Sense)
GCC TGG GAA AGT CCC CTC AAC T

LBP-1 Oligonucleotides for EMSA
These oligonucleotides were donated by I.M. Clark UEA. (Clark *et al.*, 1997)

Full Length LBP-1 like region from Human TIMP-1 (Sense)
GAT CCA GCG CCC AGA GAG ACA CCA GAG GTA AGC AGG G
Full Length LBP-1 like region from Human TIMP-1 (Anti Sense)
CCC TGC TTA CCT CTG GTG TCT CTC TGG GCG CTG GAT C

Mutation in first half site (Sense)
GAT CCA GCG CCA CTA GCG CCA CCA GAG GTA AGC AGG G
Mutation in first half site (Anti Sense)
CCC TGC TTA CCT CTG GTG GCG CTA GTG GCG CTG GAT C

Mutation in both sites (Sense)
GAT CCA GCG CCA CTA GCG CCA CAC TAG GTA AGC AGG G
Mutation in both sites (Anti Sense)
CCC TGC TTA CCT AGT GTG GCG CTA GTG GCG CTG GAT C

Mutation around splice site (Sense)
GAT CCA GCG CCC AGA GAG ACA CCA GAT TCA AGC AGG G
Mutation around splice site (Anti Sense)
CCC TGC TTG AAT CTG GTG TCT CTC TGG GCG CTG GAT C

First half site (Sense)
GAT CCA GCG CCC AGA GAG ACA
First half site (Anti Sense)
TGT CTC TCT GGG CGC TGG ATC

Second half site (Sense)
CAC CAG AGG TAA GCA GGG
Second half site (Anti Sense)
CCC TGC TTA CCT CTG GTG

LBP-1 binding sequence from HIV (Sense)
GTA CTG GGT CTC TCT GGT TAG
LBP-1 binding sequence from HIV (Anti Sense)
CTA ACC AGA GAG ACC CAG TAC

Mutant LBP-1 sequence from HIV binding –ve (Sense)
GTA CTG GGT CTC TAG TTT TAG
Mutant LBP-1 sequence from HIV binding –ve (Anti Sense)
CTA AAA CTA GAG ACC CAG TAC

Appendix 2 i & ii

Vectors. PBLCAT3 & pCMV2

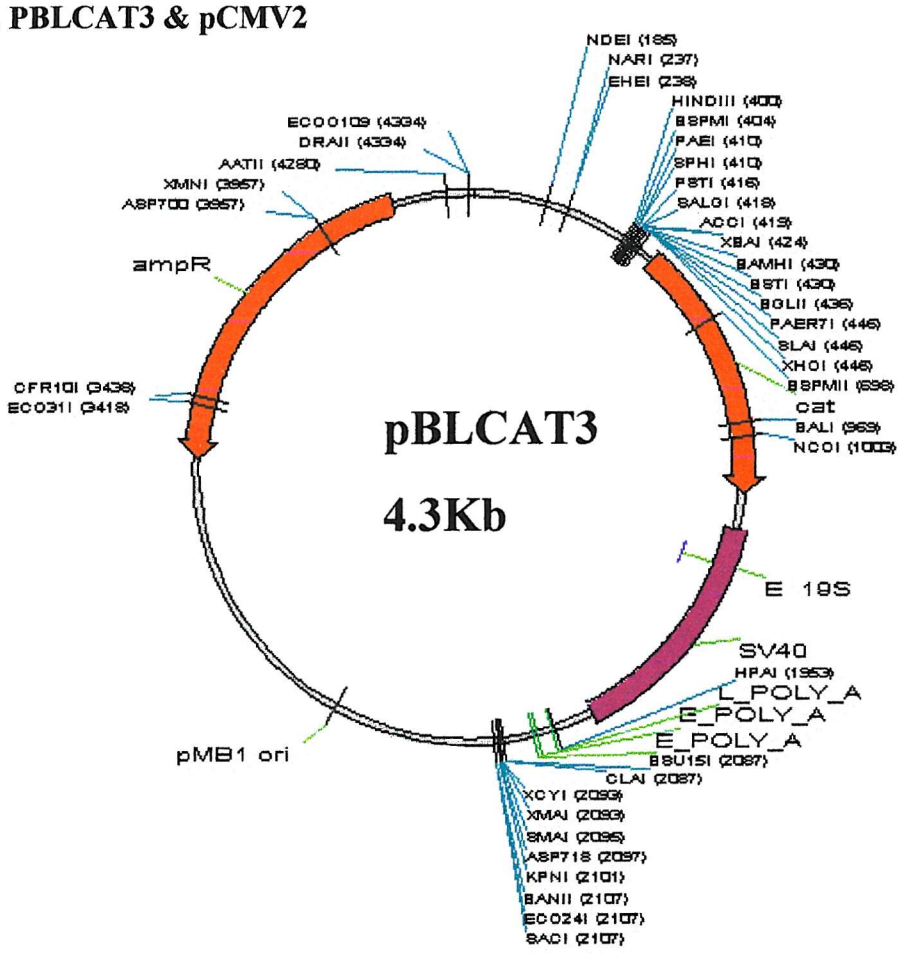

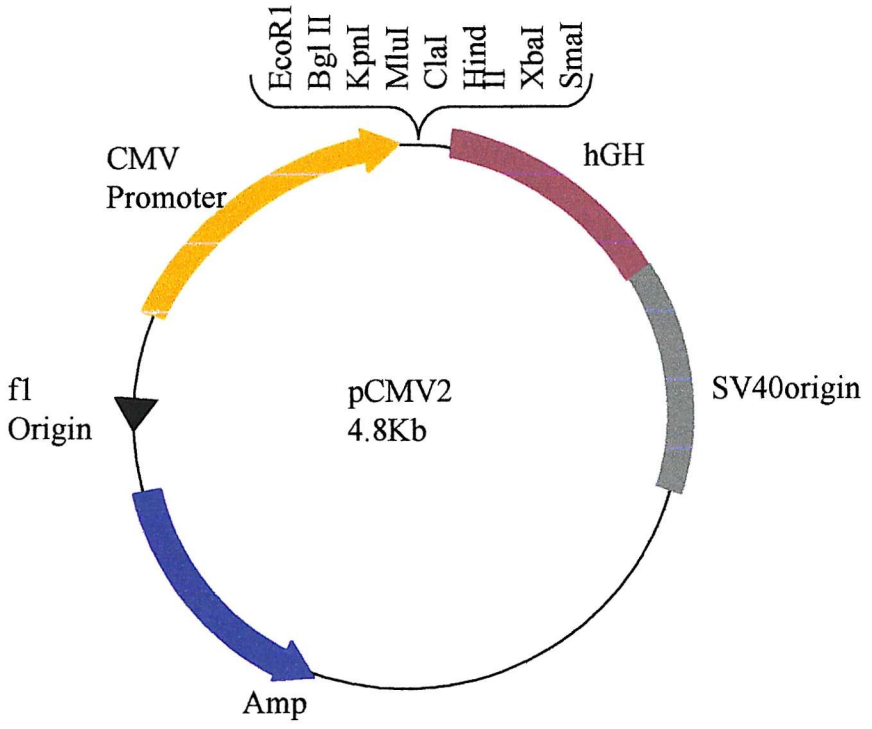

Appendix 2 iii & iv

Vectors. PDP7JUN/Eb1 & PcDNA3

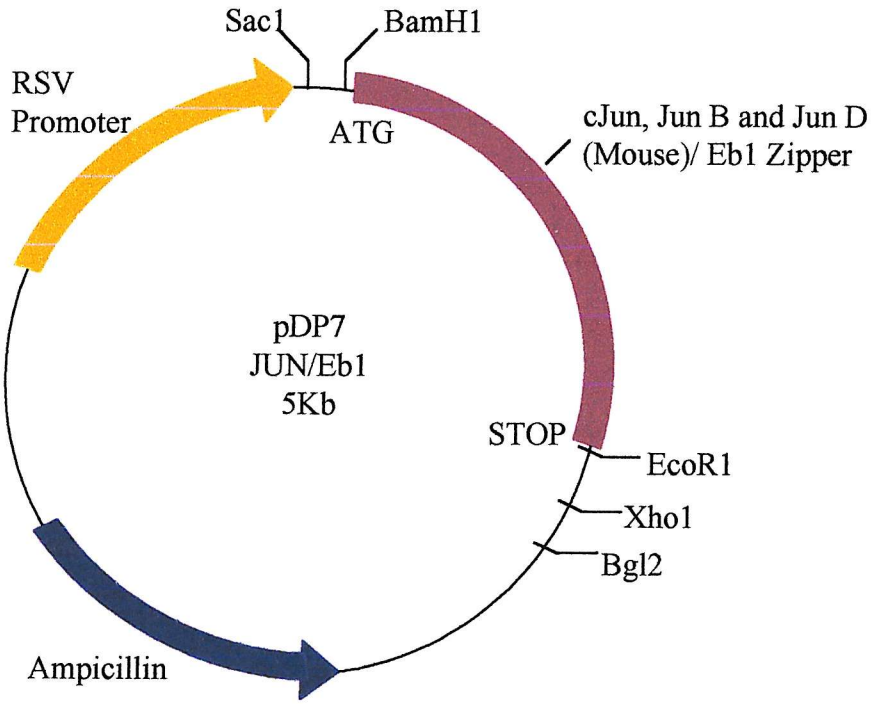

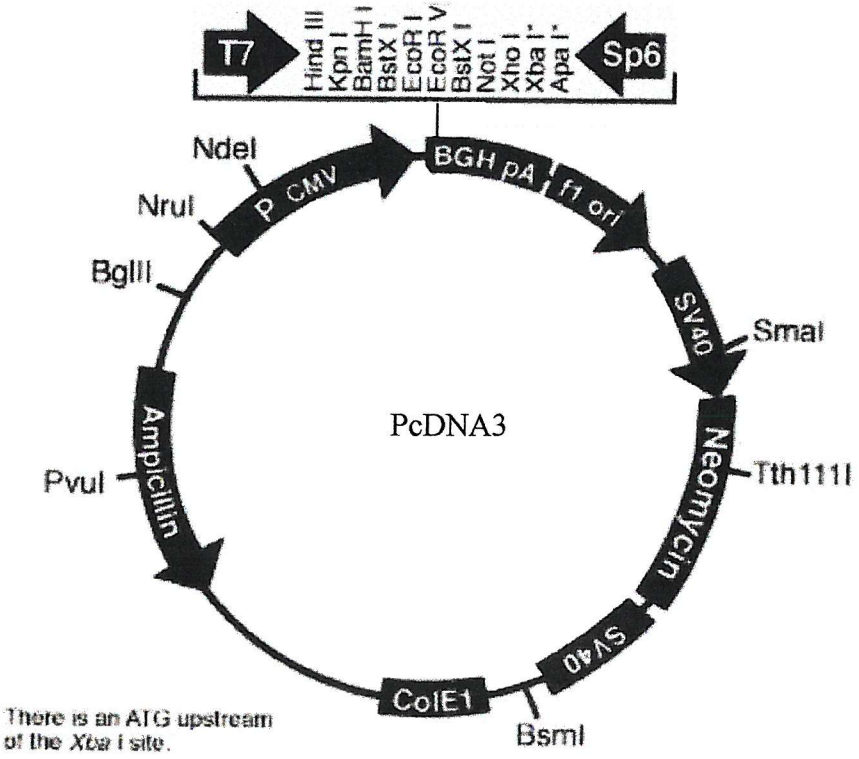

Appendix 2 v & vi

Vectors. sRSPA-HA-SAPKβ p54 KK→RR & pPacSP1

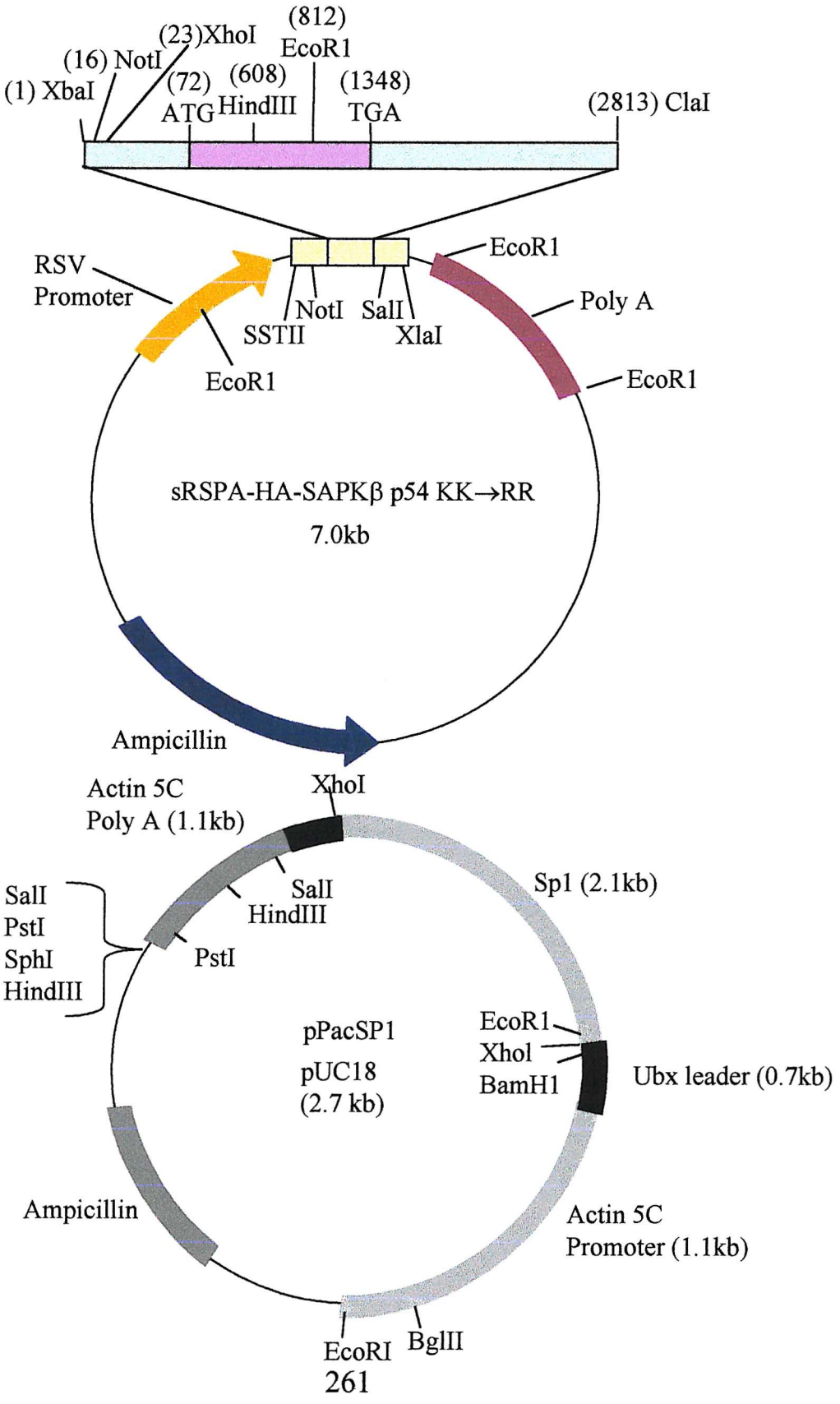

Appendix 3. Experimental Data

Transfected DNA	Experimental Data				Mean	SD	SE	T-test
-111WT	124.0	73.5	93.0	110.0	100	21.81	10.91	1.00E+00
PBLCAT3	12.5	5	3.29		6.93	4.9	2.83	2.00E-07
5' AP-1 Mutant	30.4	37.3	28.2	22.4	29.58	6.16	3.08	4.57E-07

Figure 3.2.1

Transfected DNA	Experimental Data				Mean	SD	SE	T-test
c-Jun	4.13	2.93	3.04	3.37	48.19	9.49	5.48	2.05E-02
Jun B	2.22	3.45	4.06	3.24	46.42	13.42	7.74	1.60E-02
Jun D	18.91	17.48	18.42	18.27	261.5	10.4	6	4.00E-04
-111WT (Control)	9.44	5.59	5.93	6.99	100	0	0	1.00E+00
PBLCAT3	0.61	0.35	0.38	0.45	6.39	2.04	1.17	4.76E-03

Figure 3.5.1

Transfected DNA	Experimental Data							Mean	SD	SE	T-test
c-Fos	64.5	84.4	88.1	13.5	13.5	150.2	55.61	67.12	47.49	17.92	1.20E-01
Fos B	79.9	28	127.6	20.8	20.8	31.99	76.25	55.05	40.7	15.36	3.00E-02
Fra1	98.9	40	38	91.2	91.2	99.12	90.22	78.38	27.15	10.25	8.00E-02
Fra2	26.7	50.1	16.6	104.7	104.7	5.95	29.98	48.39	40.75	15.38	2.00E-02
PCMV WT	100	100	100	100	100	100	100	100	0	0	1.00E+00
PCMV PBL	17.5	3.1	4.5	5.4	5.4	3.01	22.93	8.83	7.99	3.01	8.80E-08

Figure 3.6.1

Transfected Vector	Experimental Data			Mean	SD	SE	T-Test
-111WT (Control)	100	100	100	100	0	0	1.00E+00
RSV-B-Jun D	45.8	56.6	6.2	36.2	21.667	12.5	1.41E-02
PBLCAT3	37.7	22	2.4	20.7	14.44	8.33	1.62E-02

Figure 3.7.2

Transfected Vector	Experimental Data			Mean	%WT	SD	SE	T-test
JunD/Eb1-pDP7	29.34	27.45	23.01	26.6	358	43.74	25.24	2.40E-03
-111WT (Control)	9.46	7	5.83	7.43	100	0	0	1.00E+00
PBLCAT3	0.44	0.46	0.63	0.51	6.864	1.346	0.777	5.09E-03

Figure 3.7.3

Transfected DNA	Experimental Data			Mean	SD	SE	T-test
c-Jun EB1	197.49	216.59	210.15	208.08	9.72	5.61	1.06E-02
Jun B EB1	254.40	69.94	92.86	139.07	100.53	58.01	5.74E-01
-111WT	100.00	100.00	100.00	100.00	0.00	0.00	1.00E+00
PBLCAT3	2.95	1.73	1.76	2.15	0.69	0.40	2.20E-02

Figure 3.7.4

Transfected DNA	Experimental Data					Mean	SD	SE	T-test
Jun D AS	39.75	17.79	10.21	35.69	15.25	23.74	13.13	5.86	2.03E-04
Fra-2 AS	69.14	30.94	15.05	13.17	45.04	34.67	23.22	10.37	3.26E-03
Fos B AS			9.86	88.03	28.64	42.18	40.81	23.55	5.19E-01
-111WT (Control)	100.00	100.00	100.00	100.00	100.00	100.00	0.00	0.00	1.00E+00
PBLCAT3	29.63	13.26	6.92	21.62	1.35	14.56	11.31	5.05	7.20E-05

Figure 3.10.1

Transfected DNA	Experimental Data			Mean	SD	SE	T-test
JunD +-111WT	120.25	189.79	115.24	141.76	41.67	24.05	2.25E-01
Fra 2 + -111WT	43.79	46.67	63.17	51.21	10.46	6.03	1.50E-02
JunD + Fra 2 + -111WT	40.64	74.23	43.42	52.76	18.64	10.76	4.82E-02
PCMV + -111WT	100.00	100.00	100.00	100.00	0.00	0.00	1.00E+00
PCMV + PBLCAT3	2.87	2.65	2.40	2.64	0.23	0.13	1.92E-06

Figure 3.10.2

Transfected DNA	Experimental Data			Mean	SD	SE	T-test
Wild Type	100	100	100	100	0	0	1.00E+00
NF-kB	48.61	35.20	46.21	43.34	7.15	4.13	5.27E-03
NF-IL6	125.04	90.17	73.52	96.25	26.29	15.17	8.28E-01
NF-kB/ NF-IL6	29.45	10.19	10.83	16.82	10.94	6.31	5.72E-03
AP-1	230.67	197.97	183.04	203.90	24.36	14.06	1.78E-02
pGL3 Basic	3.10	2.62	1.32	2.35	0.92	0.53	2.96E-05

Figure 3.12.2

Transfected DNA	Experimental Data			Mean	SD	SE	T-test
IL6 (Control)	100.00	100.00	100.00	100.00	0.00	0.00	1.00E+00
Jun D	169.47	129.17	164.61	154.42	22.00	12.69	4.74E-02
RSV-B-JunD	44.05	42.49	19.88	35.47	13.53	7.81	1.43E-02
JunD / eb1	48.67	46.26	54.09	49.67	4.01	2.31	4.99E-02
pGL3 Basic	0.40	0.10	0.06	0.18	0.18	0.11	1.14E-06

Figure 3.12.3

Transfected DNA	Experimental Data			Mean	SD	SE	T-Test
c-Jun + WT	40.90	44.62	45.30	43.61	2.37	1.37	5.87E-04
Jun B + WT	11.26	13.87	11.83	12.32	1.37	0.79	8.14E-05
Jun D + WT	17.03	19.06	19.82	18.63	1.44	0.83	1.05E-04
PCMV + WT	100.00	100.00	100.00	100.00	0.00	0.00	1.00E+00
PCMV + PBL	7.21	13.49	8.90	9.87	3.25	1.88	4.33E-04

Figure 4.1.2

Transfected DNA	Experimental Data			Mean	SD	SE	T-Test
c-Jun + AP-1 Lux	27.61	21.25	54.72	34.53	17.77	10.26	4.71E-02
Jun B + AP-1 Lux	10.97	16.13	19.68	15.59	4.38	2.53	3.03E-02
Jun D + AP-1 Lux	18.57	15.53	19.84	17.98	2.22	1.28	3.58E-02
EB1 + AP-1 Lux	15.64	13.62	16.11	15.12	1.32	0.76	3.36E-02
PCMV + PGL Basic	8.75	10.48	7.00	8.75	1.74	1.00	2.79E-02
PCMV + AP-1 Lux	57.51	100.00	85.47	80.99	21.59	12.46	1.00E+00

Figure 4.1.4

Transfected DNA	Experimental data			Mean	SD	SE	T-test
c-Jun	312.50	253.49	345.10	303.70	46.44	26.79	1.69E-02
Jun B	220.00	188.37	152.94	187.10	33.55	19.36	4.61E-02
Jun D	102.50	104.65	64.71	90.62	22.47	12.96	5.45E-01
-111WT (Control)	100.00	100.00	100.00	100.00	0.00	0.00	1.00E+00
pBLCAT3	110.00	104.65	74.51	96.39	19.13	11.04	7.75E-01

Figure 4.2.1

Transfected DNA	Experimental Data			Mean	SD	SE	T-test
cJun/Eb1pDP7	375.30	471.15	348.91	398.45	64.32	37.12	1.51E-02
JunB/Eb1 pDP7	397.14	209.46	138.80	248.47	133.51	77.04	1.94E-01
JunD/Eb1pDP7	297.32	442.10	554.60	431.34	128.98	74.43	4.70E-02
-111WT (Control)	100.00	100.00	100.00	100.00	0.00	0.00	1.00E+00
pBLCAT3	8.77	8.84	9.38	8.99	0.33	0.19	4.41E-06

Figure 4.2.2

Transfected DNA	Experimental Data			Mean	SD	SE	T-test
c-Fos pCMV2	277.64	196.73	363.72	279.36	83.51	48.19	4.38E-02
FosB pCMV2	19.30	20.93	14.30	18.18	3.45	1.99	1.15E-02
Fra 1 pCMV2	209.58	87.76	294.04	197.13	103.70	59.84	2.45E-01
Fra 2 pCMV2	4.76	4.26	4.90	4.64	0.34	0.19	4.78E-02
-111WT (Control)	109.96	147.34	43.01	100.10	52.86	30.50	1.00E+00
pBLCAT3	3.13	2.93	2.42	2.83	0.37	0.21	8.59E-02

Figure 4.2.3

Transfected DNA	Experimental Data			Mean	%WT	SD	SE	T-test
Jun D + pCMV2 + WT	10.06	3.11	1.80	4.99	155.13	138.01	79.64	6.05E-01
Fra 2 + pCMV2 + WT	0.41	0.02	0.01	0.15	4.56	6.86	3.96	6.26E-04
Jun D + Fra 2 + WT	1.07	0.19	0.11	0.46	14.20	63.63	36.72	2.54E-02
pCMV2 + WT	7.25	1.52	0.88	3.22	100.00	11.55	6.66	1.00E+00
pCMV2 + pBLCAT3	0.40	0.10	0.11	0.20	6.32	5.30	3.06	1.18E-03

Figure 4.3.1

Transfected DNA	Experimental Data			Mean	%WT	SD	SE	T-test
JNK DOM NEG	1.15	1.72	1.03	1.30	51.79	14.67	8.46	1.82E-02
-111WT (Control)	2.11	2.91	2.51	2.51	100.00	15.85	9.15	1.00E+00
pBLCAT3	1.19	1.20	1.36	1.25	49.71	3.86	2.23	2.61E-02

Figure 4.4.1

Transfected DNA	Experimental Data			Mean	SD	SE	T-test
JNK	115.94	54.63	283.23	151.27	118.32	68.28	5.16E-01
-111WT (Control)	75.00	120.01	97.50	100.00	0.00	0.00	1.00E+00
pBLCAT3	10.80	11.48	12.16	11.48	0.68	0.39	2.20E-02

Figure 4.4.2

Transfected DNA	Experimental Data			Mean	SD	SE	T-test
-111WT (control)	100.00	100.00	100.00	100.00	0.00	0.00	1.00E+00
SP13'M	29.89	41.50	41.60	37.66	6.73	3.89	2.00E-03
SP15'M	126.68	80.00	118.20	108.29	24.87	14.37	6.22E-01
pBLCAT3	5.48	1.00	0.60	2.36	2.71	1.57	2.57E-04

Figure 6.3.1

Transfected DNA	Experimental Data			Mean	SD	SE	T-test
SP1 3'M	10.23	9.79	10.35	10.12	0.29	0.17	5.00E-03
SP1 5'M	47.00	27.19	16.20	30.13	15.61	9.02	5.70E-02
-111WT (Control)	51.36	45.84	60.80	52.67	7.56	4.37	1.00E+00
PBLCAT3	1.22	0.75	0.95	0.97	0.23	0.14	4.00E-03

Figure 6.3.2

Transfected DNA	Experimental Data			Mean	%WT	SD	SE	T-test
WT PAC	3.29	3.51	1.47	2.76	100.00	0.00	0.00	1.00E+00
WT SP-1	18.40	18.80	8.00	15.07	546.01	221.85	128.02	7.35E-02
3'M PAC	0.43	0.41	0.46	0.44	15.94	0.91	0.53	3.90E-05
3'M SP-1	0.47	0.46	0.39	0.44	15.94	1.58	0.91	1.18E-04
5'MPAC	0.35	1.05	0.91	0.77	27.90	13.42	7.74	1.14E-02
5'M SP-1	0.61	0.76	0.76	0.71	25.72	3.14	1.81	5.94E-04
pBLCAT3 PAC	0.36	0.39	0.36	0.37	13.41	0.63	0.36	1.75E-05

Figure 6.3.3

Transfected DNA	Experimental Data				Mean	SD	SE	T-test
Control	100.00	100.00	100.00	100.00	100.00	0.00	0.00	1.00E+00
TM SMA 2	8.80	2.09	100.96	149.09	65.24	71.83	35.92	4.04E-01
TM SMA 4	49.80	20.98	1313.46	1887.27	817.88	933.49	466.74	2.22E-01
TM SMA 5	18.00	2.94	209.62	272.73	125.82	135.80	67.90	7.29E-01
TM SMA 6	86.60	50.65	1707.69	1352.73	799.42	856.32	428.16	2.01E-01
TM SMA 7	9.20	2.09	48.08	78.18	34.39	35.51	17.75	3.44E-02
TM SMA 8	68.80	2.48	171.15	78.18	80.15	69.39	34.70	6.07E-01
PBLCAT3	6.80	2.16	35.58	69.09	28.41	30.89	15.44	1.89E-02

Figure 6.5.2

Appendix 4.

Antibodies

Primary Antibodies

Antibody	Supplier	Code	Origin
AP-1 FOS			
c-Fos	Autogen Bioclear (Santa Cruz)	4X (SC-52X)	Rabbit
FosB	Autogen Bioclear (Santa Cruz)	102X (SC-48X)	Rabbit
Fra-1	Autogen Bioclear (Santa Cruz)	N-17 (SC-183)	Rabbit
Fra-2	Autogen Bioclear (Santa Cruz)	Q-20 (SC-604)	Rabbit
AP-1 JUN			
c-Jun	Autogen Bioclear (Santa Cruz)	N (SC-045X)	Rabbit
Jun B	Autogen Bioclear (Santa Cruz)	210X (SC-073X)	Rabbit
Jun D	Autogen Bioclear (Santa Cruz)	329X (SC-74X)	Rabbit
AP-2α	Autogen Bioclear (Santa Cruz)	C-18X (SC-184X)	Rabbit
AP-2β	Autogen Bioclear (Santa Cruz)	H-87 (SC-8976X)	Rabbit
AP-2χ	Autogen Bioclear (Santa Cruz)	H-77X (SC-8977X)	Rabbit
β Actin	Sigma	A5441	Mouse
EB1	Marc Castellazzi (France) Collaboration		Rabbit
c-Ets-1 / Ets-2	Autogen Bioclear (Santa Cruz)	C-275 (SC-112)	Rabbit
GFAP	SIGMA	G-9269	Rabbit
JAB-1	Autogen Bioclear (Santa Cruz)	N-17 (SC-6371	Goat
αSMA	SIGMA	A2547	Mouse
SP-1	Autogen Bioclear (Santa Cruz)	PEP-2X (SC-59X)	Rabbit
SP-2	Autogen Bioclear (Santa Cruz)	K-20X (SC-643X)	Rabbit
SP-3	Autogen Bioclear (Santa Cruz)	D-20X (SC-644X)	Rabbit
SP-4	Autogen Bioclear (Santa Cruz)	V-20X (SC-645X)	Rabbit
TGFβ	R&D systems	100-B-001	Rabbit
ZF9	Autogen Bioclear (Santa Cruz)	R-173X (SC-7158X)	Rabbit

Secondary Antibodies

Antibody	Supplier	Code	Origin
Anti Rabbit IgG Whole Molecule HRP Conjugate	SIGMA	A6154	Goat
Anti Mouse IgG Whole Molecule HRP Conjugate	SIGMA	A9044	Rabbit
Anti Goat IgG Whole Molecule HRP Conjugate	SIGMA	A5420	Rabbit

Appendix 5.

Protein Sizes

Protein	Mass Predicted KDa^{-1}	Expressed KDa^{-1}
Aprotinin		6.5
BSA		66.2
cEts-1	50/55	52/48/42/39
cFos	41.6	55/62
cJun	35.7	39
FosB	36	52, 37 (Fos B2)
Fra1		29
Fra2		35
GFAP		56
Jab1		38
JunB	36	42
JunD	35	40-50
α2-Macroglodulin		725
Oncostatin M		28
αSMA		43
SP-1		95-106
SP-2	62	
SP-3		120
SP-4	96	
TIMP-1		28
ZF9		46

Appendix 6.

Human TIMP-1 Promoter

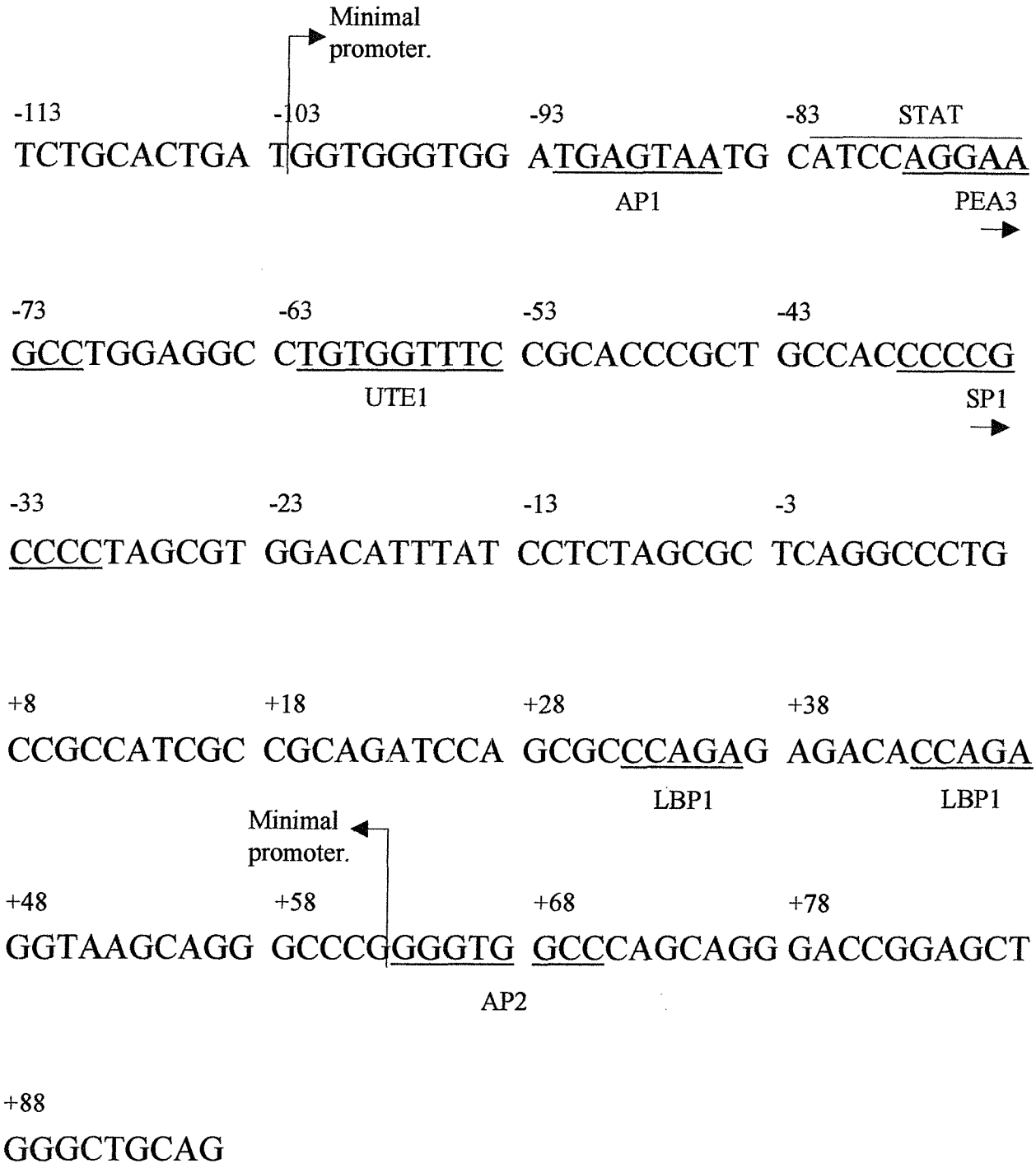

Appendix 7.

Human IL-6 Promoter

-347
AAACATAGCT TTAGCTTATT TTTTTTCTCT TTGTAAAACT
-307
TCGTGCATGA CTTCAGCTTT ACTCTTTGTC AAGACATGCC
-267 CRE
AAAGTGCTGA GTCACTAATA AAAGAAAAAA AGAAAGTAAA
-227 AP-1 NF-
IL-6
GGAAGAGTGG TTCTGCTTCT TAGCGCTAGC CTCAATGACG
-187
ACCTAAGCTG CACTTTTCCC CCTAGTTGTG TCTTGCGATG
-147
CTAAAGGACG TCACATTGCA CAATCTTAAT AAGGTTTCCA
-107 CRE
ATCAGCCCCA CCCGCTCTGG CCCCACCCTC ACCCTCCAAC
-67
AAAGATTTAT CAAATGTGGG ATTTTCCCAT GAGTCTCAAT
-27 NFκB AP-1
+1
ATTAGAGTCT CAACCCCCAA TAAATATAGG ACTGGAG**ATG**
+4 TATA
TCTGAGGCTC ATTCTGCCCT CGAGCCACCG GGAACGAAAG
+44
AGAAGCTCTA TCTCCCCTCC AGGAGCCCAG CT**ATG**AACTC

Base Pair mismatch with consensus binding site

Appendix 8i. Basic Polymerase Chain Reaction

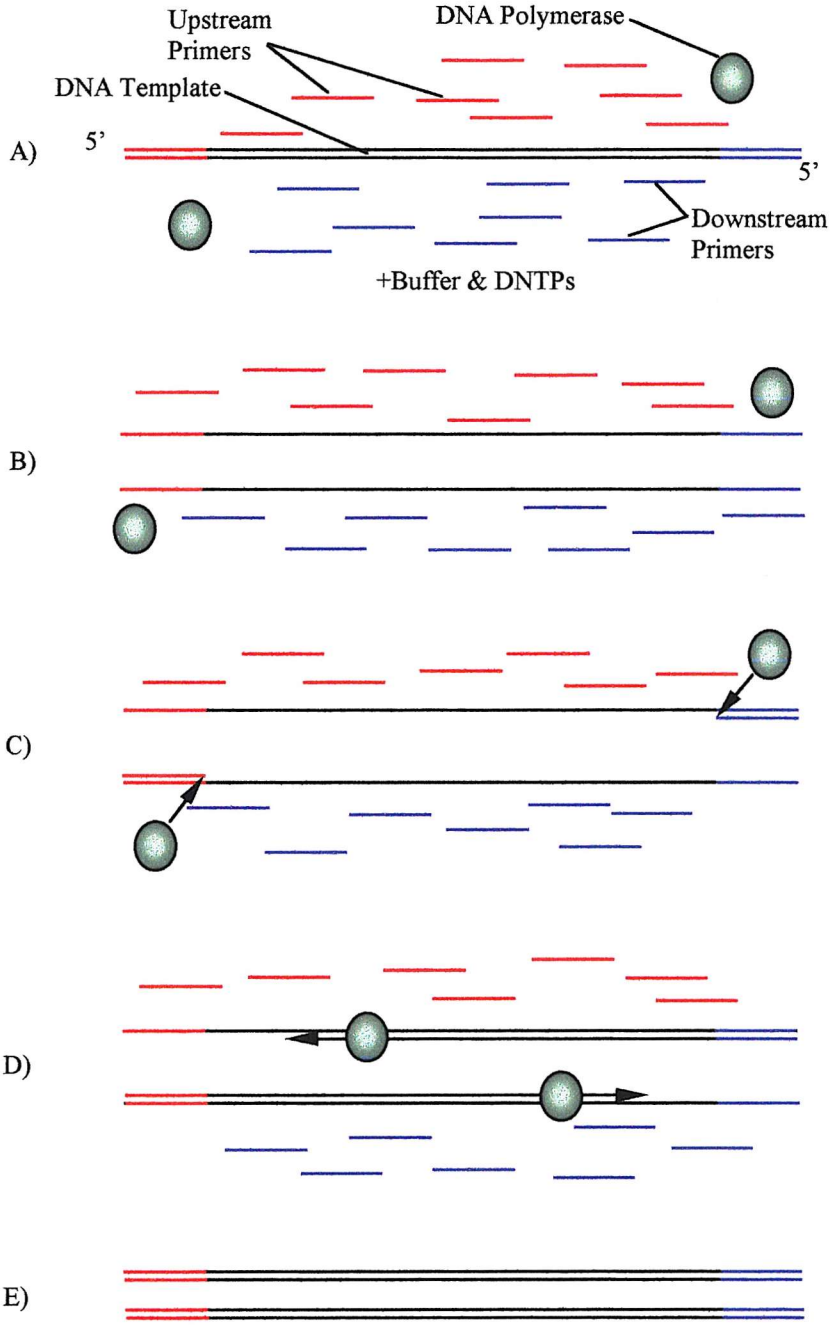

Basic Polymerase Chain Reaction (PCR) A) The reaction constituents. B) Denaturation, reaction mix is heated to 94^0C resulting in the melting of template DNA. C) Annealing, reaction is cooled to 50 to 65^0C allowing primers to specifically bind to recognised sites on the template DNA and polymerase enzymes binding to primers. D) Elongation, reaction is heated to 72^0C and polymerase enzymes incorporate DNTPs to the growing 3 prime end of the annealed primer according to the template strand. E) The final product is a template duplicate double stranded DNA. Further multiplication of the template DNA is achieved by repetitively cycling through stages B to D.

Appendix 8ii. One Step Mutational Polymerase Chain Reaction

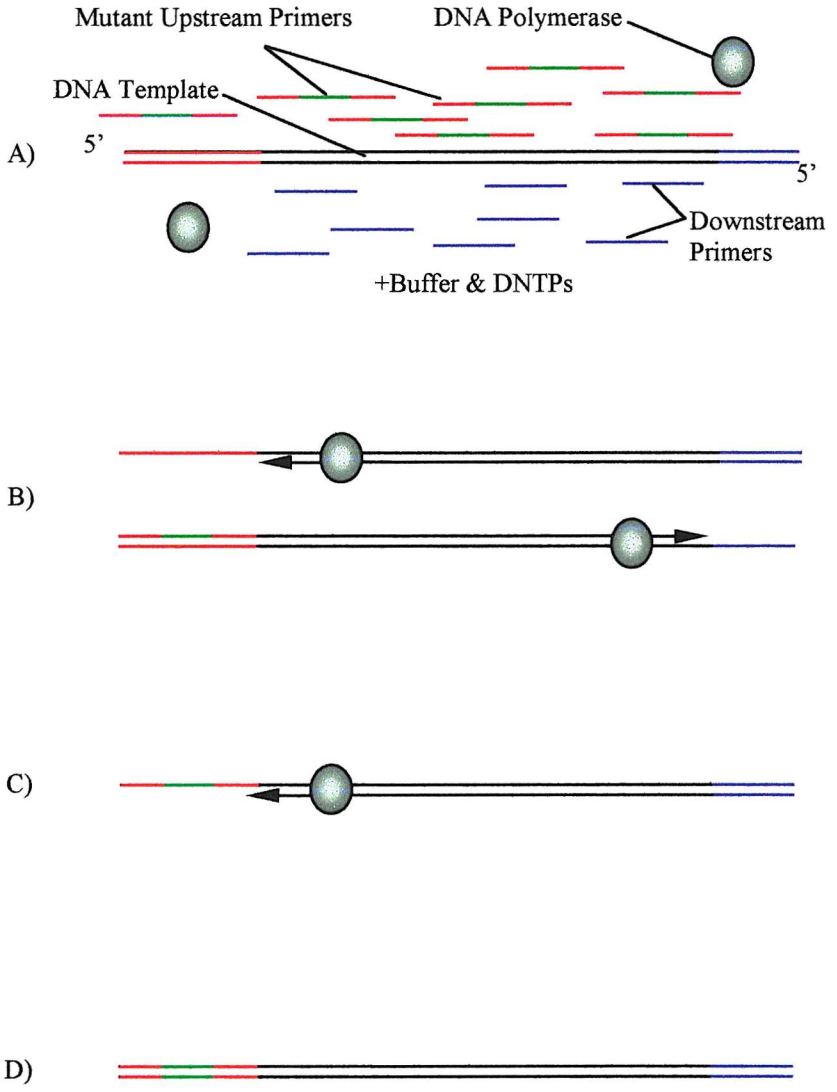

Mutational Polymerase Chain Reaction (PCR) A) The reaction constituents, which are the same as for normal PCR with the exception that one of the primers contains a sequence mutation. B) The primers are annealed and elongated in the same way as for normal PCR, generating in the first cycle a double stranded wild type and double stranded DNA with a specific mutation in the new strand. C) In the second cycle the wild type primer is annealed to the mutated DNA strand before being elongated. D) The product formed following 2 cycles is a double stranded specific mutant. The amount of mutant DNA is, as with normal PCR, increased by repeated cycling.

Appendix 8iii. Two Step Mutational Polymerase Chain Reaction

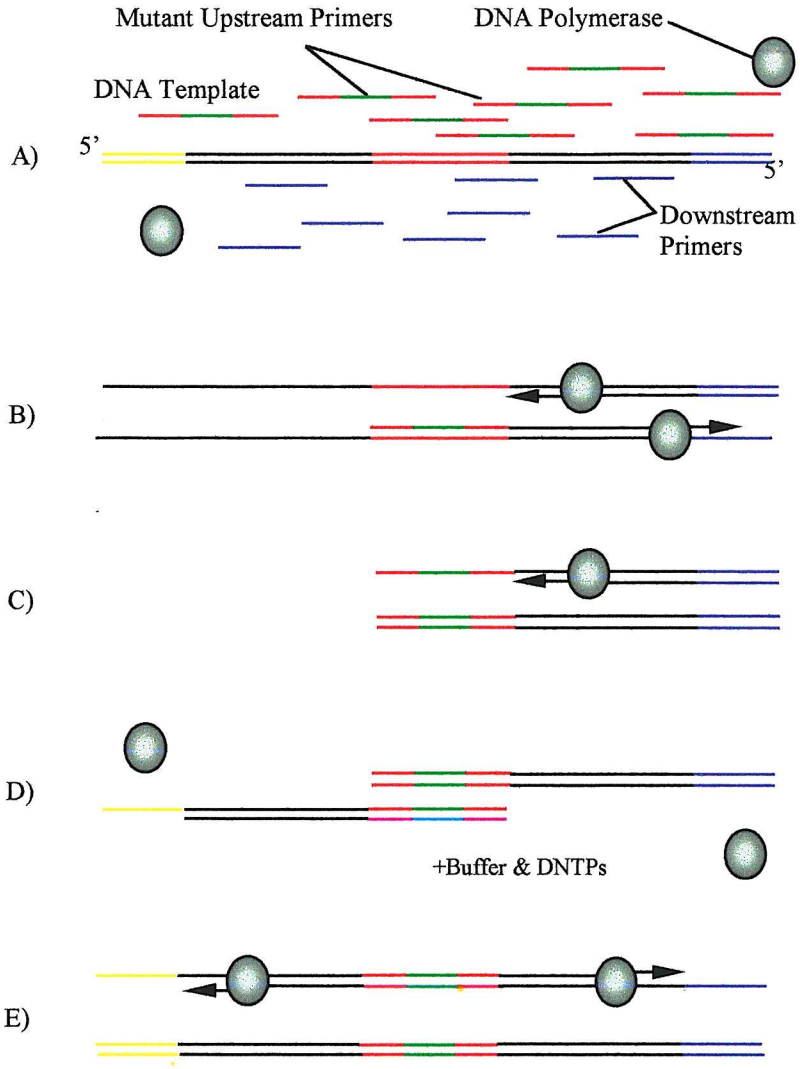

Two step mutational polymerase chain reaction for the generation of a centrally situated mutation. A) The reaction components used are similar to those of mutational PCR except the mutation and therefore the specific mutated primers are designed to a central region. Two primary reactions are performed each incorporating primers specific to one end of the template. B) The two separate first stage reactions undergo annealing and elongation as with normal PCR, generating a truncated single strand mutant DNA. C) The annealing and elongation of the downstream primer to the truncated mutated DNA template in subsequent cycles leads to the production of a double stranded truncation mutant. D) The gel purified fragments from the two preliminary reactions are combined in a second reaction with DNTPs in the absence of primers and template. E) The two fragments anneal with one another and are extended to create a full-length double stranded mutant DNA.